Régulation de l'activité de la NADPH oxydase des neutrophiles par des enzymes du métabolisme du glucose et l'hétérocomplexe S100A8/S100A9 : application à la polyarthrite rhumatoïde

Athan Baillet

UNIVERSITÉ DE GRENOBLE

THÈSE Pour obtenir le grade de

DOCTEUR DE L'UNIVERSITÉ DE GRENOBLE

Spécialité : **BIOLOGIE CELLULAIRE**

Arrêté ministériel : 7 août 2006

Présentée par

Athan BAILLET

Thèse codirigée par **Françoise MOREL** et **Philippe GAUDIN**

préparée au sein du **Laboratoire GREPI AGIM FRE3405 CNRS-UJF-EPHE** dans **l'École Doctorale Chimie et Sciences du Vivant**

Régulation de l'activité de la NADPH oxydase des neutrophiles par des enzymes du métabolisme du glucose et l'hétérocomplexe S100A8/A9

Application à l'étude de la Polyarthrite Rhumatoïde

Thèse soutenue publiquement le **9 décembre 2011** devant le jury composé de :

Pr. Daniel WENDLING PU-PH, CHU Besançon	(Président)
Pr. Marie-Anne GOUGEROT-POCIDALO PU-PH, CHU Paris Bichat	(Rapporteur)
Pr. Olivier VITTECOQ PU-PH, CHU Rouen	(Rapporteur)
Pr. Eric TSCHIRHART Professeur, Université du Luxembourg	(Membre)
Dr. Marie-Hélène PACLET MCU-PH, CHU Grenoble	(Membre)
Pr. Philippe GAUDIN PU-PH, CHU Grenoble	(Membre)
Pr. Françoise MOREL Professeur émérite UJF, Grenoble	(Membre)

Mes premiers remerciements vont au Pr. Françoise Morel qui m'a accueilli dans son laboratoire. J'ai appris beaucoup à vos côtés et pas seulement certains points de biochimie que je crains fort d'oublier avec les années. Je garderai intacte la mémoire de votre implacable passion du détail et votre talent dans l'organisation du quotidien du laboratoire. Je tacherai d'imiter dans mon exercice futur votre souci de faire son travail méticuleusement et avec sincérité.

Je tiens à exprimer ma très vive reconnaissance au Pr. Marie-Anne Gougerot-Pocidalo et au Pr. Olivier Vittecoq pour avoir accepté la charge d'être rapporteurs de ce travail. Leurs suggestions ont permis d'améliorer la qualité de cette thèse.
Je tiens à remercier le Pr. Daniel Wendling et le Pr. Eric Tschirhart pour l'intérêt qu'ils ont porté à ce travail en acceptant d'être membre du jury de thèse.

Je désire remercier le Pr. Philippe Gaudin pour son enthousiasme et la confiance qu'il a su m'accorder. Son soutien m'a permis d'investir toutes mes forces dans cette thèse. C'est un privilège rare. J'en mesure aujourd'hui la portée.
Je tiens également à remercier deux personnes qui m'ont encadré pendant ces quatre années au laboratoire. Un grand merci également au Dr. Marie-Hélène Paclet qui, avec une bonne humeur toujours égale et un sourire inaltérable, m'a supervisé pendant ces trois années de thèse. Sans sa disponibilité, le désert aride que constitue le monde de l'oxydase, pour un rhumatologue, aurait pu m'être fatal… Merci au Dr. Candice Trocmé qui m'a, durant mon stage de Master 2, initié aux techniques rudimentaires d'expérimentation scientifique ainsi qu'à l'approche protéomique. Merci Candice, pour ta patience et pour t'être adaptée aux difficultés qu'un clinicien peut éprouver devant un spectophotomètre, un spectromètre de masse ou une électrophorèse...
Merci à Sylvie Berthier, qui m'a transmis son intérêt pour les protéines S100. Sylvie, ton expertise théorique et expérimentale dans ce domaine a été capitale dans l'accomplissement de mon travail. J'ai également beaucoup apprécié de travailler en compagnie du Dr. Bernard Lardy dont l'enthousiasme est communicatif, mais également au côté de Françis Rousset et Marc-André Hograindleur.
Les discussions avec le Pr. Edgard Pick, le Pr. Elisabeth Ligeti et le Dr Jamel El Benna ont permis d'améliorer la qualité de notre travail. Je les remercie pour leur critique constructive de nos résultats.

Merci également au Pr. Robert Juvin et à l'ensemble du service de Rhumatologie du CHU de Grenoble qui m'ont permis de me consacrer entièrement à mon travail de thèse.

Bien entendu mes remerciements vont également à mes proches sans qui je n'aurais pas pu réaliser ce travail :

Merci à mes fils, Antoine et Amaury, sources inépuisables de motivation et de satisfaction. Un seul de vos sourires apaise toutes mes angoisses. Vous avez appris à être sages et à supporter les absences de votre père.

Merci à ma splendide épouse Cécile.

Grâce soit rendue à ma première lectrice, ma mère Christiane, que j'ai beaucoup mise à contribution et mon père Alain dont j'ai sollicité le talent de reprographiste. Merci à mon frère Axel. Même si tu n'es pas là aujourd'hui je pense à toi…

Merci à ma tante Yolande, indéfectible soutien.

Je remercie également mes plus proches amis avec qui je partage plus de 30 ans de complicité. Merci à vous Jérémy, Olivier et Joub.

La musique fut un exutoire ponctuel mais indispensable au maintien de ma motivation devant la paillasse. Merci aux membres du "*Bling Bling Band*", Hubert, Jérémy, Manhu et Franz pour ces intermèdes musicaux.

Enfin merci au laboratoire Abbott, à la Société Française de Rhumatologie (SFR) et à l'Association pour la Recherche en Pathologie Ostéo-Articulaire (ARPOA) pour leur soutien financier.

6PGDH	6-phosphogluconate déshydrogénase
AIR	"Auto-Inhibitory Region"
ACPA	"Anti-Citrullinated Protein/ peptide auto Anti-bodies"
AMPK	"5'adenosine monophosphate-activated protein kinase"
CRP	"C-Reactive Protein"
AIR	"Auto-Inhibitory Region"
ADN	Acide Désoxyribonucléique
ADP/ATP	Adénosine Diphosphate / Adénosine Triphosphate
Ca^{2+}	Ion calcium
CGD	"Chronic Granulomatous Disease"
DAMP	"Damage Associated Molecular Patterns"
DCFH-DA	"Dichlorofluorescin Diacetate"
DMF	Diméthylformamide
DSS	"Disuccinimidyl Suberate"
DUOX	"Dual oxidase"
EBV	"Epstein–Barr Virus"
ELISA	"Enzyme- Linked Immunosorbent Assay"
ERK	"Extracellular signal-Regulated Kinase"
FACS	"Fluorescence Activated Cell Sorter"
FAD	"Flavin Adenine Dinucleotide"
fMLP	N-formyl-Méthionyl-Leucyl-Phénylalanine
G6PDH	Glucose-6-phosphate déshydrogénase
G3PDH	Glycéraldéhyde-3-phosphate déshydrogénase
GDP/GTP	Guanosine diphosphate / Guanosine triphosphate
G-CSF	"Granulocyte-Colony Stimulating Factor"
GEF	"Guanine nucleotide Exchange Factor"
GM-CSF	"Granulocyte Macrophage-Colony Stimulating Factor"
GTPγS	Guanosine 5'-[gamma-thio]triphosphate
H2O2	Peroxyde d'hydrogène
HNP	"Human neutrophil peptide"
$HOCl^-$	Acide hypochloreux
HRPO	"Horse Radish Peroxidase"
Ig G	Immunoglobuline G
ICAM	"Intercellular Adhesion Molecule"
IL	Interleukine
JNK	"Jun N-terminal Kinase"
LAT	"Linker for Activation of T cells"
LDL	"Low Density Lipoprotein"
LFA1	"Lymphocyte Function-Associated antigen-1"
LPS	Lipopolysaccharide
mAb	"monoclonal Antibody"
MADCAM	"Mucosal vascular Cell-Adhesion Molecule"
MALDI-TOF	"Matrix Assisted Laser Desorption/Ionization -Time Of Flight"
MAPK	"Mitogen Activated Protein Kinase"
MIPα	"Macrophage Inflammatory Protein-1α"
MMP	"Matrix Metalloproteinase"
MPO	Myéloperoxydase
MTX	Méthotrexate
NADPH	Nicotinamide Adénine Dinucléotide Phosphate réduit
NDPK	Nucléoside diphosphate Kinase
$O_2^{\bullet-}$	Anion superoxyde
$^1O2$	Oxygène singulet
ONOO-	Peroxynitrite
$OH^{\bullet}$	Radical hydroxyle
PB1	"Phox and Bem1"
PAF	"Platelet Activating Factor"
PAK	"p21-Activated Kinase"
PAMP	"Pathogen Associated Molecular Patterns"
PFK	6-Phosphofructokinase
Phox	"Phagocyte Oxidase"
PI3-K	"Phosphatidylinositol-3-Kinase"
Pin1	Proline isomérase 1
PKC	Protéine-kinase C
PX	"Phox homology"
PLA_2	Phospholipase A_2
PMA	Phorbol 12-myristate 13-acétate
PMN	"Polymorphonuclear neutrophil"
PR	Polyarthrite Rhumatoïde
PRR	"Prolin Rich Region"
PRRs	"Pattern Recognition Receptors"
RANK	"Receptor Activator of NFκB"
RANKL	"Receptor Activator of NFκB Ligand"
RhoGDI	"Rho GDP dissociation inhibitor"
RhPso	Rhumatisme psoriasique
RLU	"Relative luminescence unit"
ROS	"Reactive Oxygen Species"
SA	Spondylarthrite Ankylosante
SELDI	Surface-Enhanced Laser Desorption/Ionization
SERCA	"Sarcoendoplasmique Reticulum Ca^{++}-ATPase"
STIM-1	"Stromal Interaction Molecule-1"
TCR	"T Cell Receptor"
TPR	"Tetratricopeptide Repeat"
VS	Vitesse de Sédimentation

INTRODUCTION BIBLIOGRAPHIQUE

1. La Polyarthrite Rhumatoïde (PR)

La PR est caractérisée par des arthralgies associées à des gonflements articulaires appelés synovites. L'évolution de cette affection se fait par poussées inflammatoires, à l'origine de la destruction articulaire et du handicap en l'absence d'une prise en charge efficace.

Bien que l'origine de la maladie demeure inconnue, les données récentes de la littérature incriminent les cellules de l'immunité innée dans le développement des lésions de la PR [Cedergren *et al.* 2007; Lefevre *et al.* 2009]. Comme la plupart des maladies auto-immunes, la PR est une pathologie multifactorielle, avec un terrain génétique particulier [Auger *et al.* 2005] impliquant des facteurs environnementaux tels que le tabac [Sugiyama *et al.* 2010] et la flore microbienne [Mikuls *et al.* 2009].

1.1. La PR, une maladie fréquente avec un impact médico-économique important

La PR constitue un véritable problème de santé publique, tant par le handicap occasionné par les lésions articulaires que par le coût du traitement sur l'économie de santé.

1.1.1. Données démographiques concernant la Polyarthrite Rhumatoïde

La PR est le rhumatisme inflammatoire chronique le plus fréquent. Elle touche 0,4 à 0,8% de la population caucasienne [Roux *et al.* 2007], soit environ 300000 à 500000 personnes en France, avec une incidence en légère diminution durant les 30 dernières années [Kaipiainen-Seppanen *et al.* 2006]. Elle atteint un homme pour 3 à 5 femmes [Kvien *et al.* 2006; Kwoh *et al.* 1996] mais cette différence de *sex ratio* s'atténue progressivement au-delà de 70 ans. La maladie peut se déclarer à tout âge bien qu'il existe une recrudescence de l'incidence entre 40 et 60 ans [Kaipiainen-Seppanen *et al.* 1996].

1.1.2. Impact de la Polyarthrite Rhumatoïde sur l'économie de santé

Les nouveaux traitements de la PR entraînent une dépense de santé conséquente, de 16000 à 20000 € / an, alors qu'un traitement de fond conventionnel engendre un coût 5 à 7 fois moins important [Nurmohamed *et al.* 2005]. Ainsi le montant total moyen de la maladie (coûts directs plus indirects) par patient varie de 3072 à 49786 € / an [Rat *et al.* 2004]. Les médicaments immuno-modulateurs et les thérapeutiques ciblées ont largement contribué à l'amélioration de la prise en charge des patients, permettant de diminuer l'activité de la maladie [Gartlehner *et al.* 2006], d'améliorer le handicap [Aletaha *et al.* 2008], la qualité de vie [Gartlehner *et al.* 2006] et de ralentir l'évolution de la destruction articulaire [Blumenauer *et al.* 2003; Gartlehner *et al.* 2006; Jones *et al.* 2003; Navarro-Sarabia *et al.* 2005]. Ces traitements ne sont pas dénués d'effets indésirables [Singh *et al.* 2009] parfois sévères

[Maxwell *et al.* 2009; Mertens *et al.* 2009] et génèrent un coût important sur les dépenses de santé [Chen *et al.* 2006b; Merkesdal *et al.* 2005].

1.2. La Polyarthrite Rhumatoïde, une maladie handicapante

1.2.1. L'arthrite, prototype de la réaction inflammatoire

Lors d'une aggression tissulaire, quelle qu'en soit la cause (infectieuse, tumorale, chimique, physique ou auto-immune), des molécules endogènes dispersées dans le milieu extra-cellulaire lors de la nécrose cellulaire ou des éléments microbiens polysaccharidiques, lipidiques et oligonucléotidiques recrutent rapidement les cellules de l'immunité innée. Ces composants moléculaires associés aux micro-organismes pathogènes (PAMP : "Pathogen Associated Molecular Patterns") ou aux molécules du soi dégradées (DAMP : "Damage Associated Molecular Patterns") constituent des signaux de danger détectés par des récepteurs (PRRs : "Pattern Recognition Receptors"). L'atteinte ostéo-articulaire de la PR résulte d'une réaction inflammatoire articulaire typique. Les cellules de l'immunité innée sont recrutées et activées dans un processus inflammatoire. Ainsi l'arthrite est caractérisée par une vasodilatation capillaire responsable d'un érythème, d'un gonflement articulaire, d'une chaleur et de douleurs pulsatiles associées à des réveils nocturnes avec pour conséquence une impotence fonctionnelle parfois très sévère.

Les mécanismes moléculaires et cellulaires en jeu sont communs à l'ensemble des réactions inflammatoires. La phase initiale vasculaire permet un recrutement cellulaire et une activation rapide au niveau du site inflammatoire. Elle nécessite la mobilisation d'effecteurs pré-formés contenus dans les granules des mastocytes et des polynucléaires neutrophiles (PMNs). La dégranulation du mastocyte permet de secréter immédiatement de puissants médiateurs vasodilatateurs (histamine, sérotonine et bradykinine) qui favorisent la domiciliation des cellules effectrices. Les granulations du PMN renferment des substances de défense comme les protéines du complément et la NADPH oxydase dédiée à la production de formes réactives de l'oxygène (ou ROS pour "reactive oxygen species"). Les métalloprotéases matricielles (ou MMPs pour "Matrix Metalloproteinases") favorisent la migration cellulaire. Dans le cas du PMN, la collagénase MMP-8 et la gélatinase MMP-9 dégradent respectivement les collagènes de type I et de type IV. Les protéases et les ROS peuvent aussi exercer des effets délétères par des dommages excessifs et incontrôlés de la matrice extra-cellulaire des tissus cibles. Après une deuxième phase d'amplification faisant intervenir des facteurs chimiotactiques de nature différente et des cytokines inflammatoires comme le "Tumor Necrosis Factor α"

(TNFα), l'interleukine1β (IL-1β) et l'IL-6, le macrophage permet la terminaison de la réaction inflammatoire par phagocytose et présente les peptides immunogènes afin d'initier une réponse immune adaptative.

1.2.2. L'arthrite, symptôme cardinal de la maladie

Une articulation est formée de deux extrémités, les épiphyses, reliées entre elles par un manchon rigide et étanche, la capsule articulaire. Les épiphyses et la capsule délimitent un espace clos, baigné par le liquide synovial. Les surfaces internes de cette cavité sont recouvertes soit par le cartilage coiffant l'os sous chondral soit par la membrane synoviale qui tapisse la capsule articulaire (**Figure 1**).

Figure 1. Schéma d'une coupe d'une articulation rhumatoïde

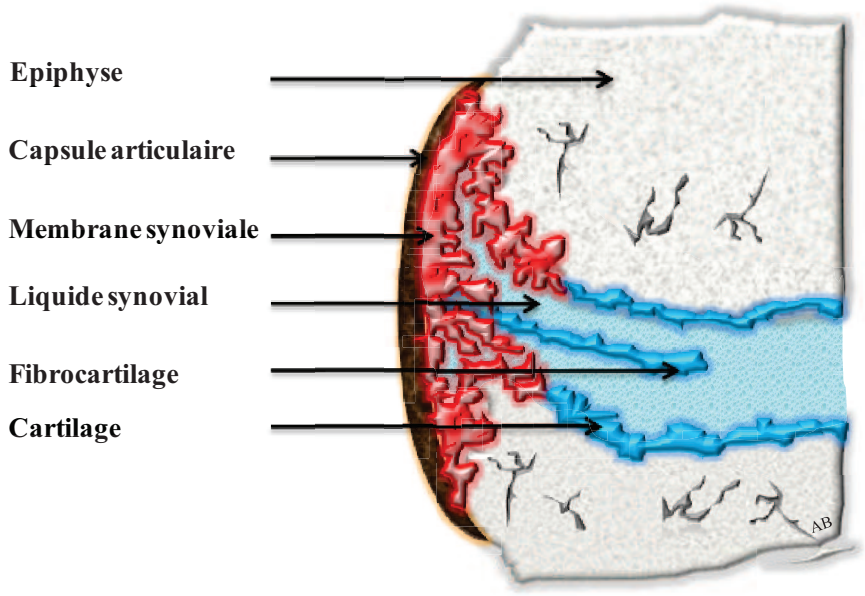

L'examen clinique d'un patient souffrant de PR est dominé par des douleurs articulaires, d'horaire "inflammatoire", associées à un gonflement des articulations (ou synovite) [Ritchie *et al.* 1968]. L'atteinte est le plus fréquemment bilatérale et symétrique ; elle concerne principalement les petites articulations du carpe, les articulations méta-carpo-phalangiennes et méta-tarso-phalangiennes. L'inflammation de la gaine des tendons (ou ténosynovite) est fréquente au niveau des muscles fléchisseurs de la main au stade initial de la maladie [Eshed *et al.* 2009]. On note le plus souvent une augmentation de la raideur articulaire en deuxième partie de nuit et le matin.

1.2.3. La destruction articulaire

Les destructions articulaires sont particulièrement importantes au stade précoce de la maladie, c'est pourquoi il est recommandé d'instaurer un traitement de fond, visant à contrôler les synovites et à prévenir les lésions articulaires, dès le début des symptômes. Les érosions osseuses et la destruction cartilagineuse (**Figure 2**) sont corrélées à un mauvais pronostic fonctionnel [Maillefert *et al.* 2003]. De plus les synovites itératives sont à l'origine de subluxations ou de luxations articulaires qui font le lit des ruptures tendineuses et des déformations. Ces complications grèvent considérablement le pronostic fonctionnel des patients après plusieurs années d'évolution.

Figure 2. L'atteinte clinique et radiologique de la PR

A.

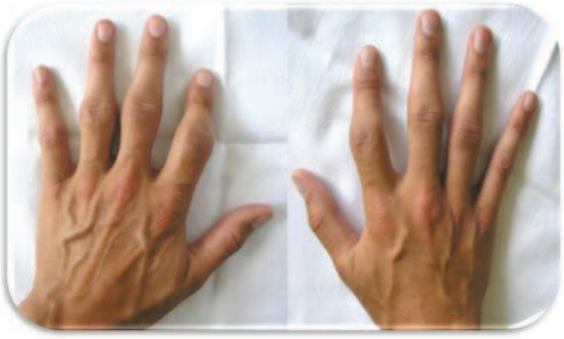

B.

A : Mains de face d'une patiente présentant une Polyarthrite Rhumatoïde.
B : Radiographie des deux mains de face de la même patiente.

1.2.4. Les atteintes extra-articulaires de la Polyarthrite Rhumatoïde

Chez 25% à 40% des patients, il existe des atteintes extra-articulaires [Carmona *et al.* 2003; Cimmino *et al.* 2000]. Les nodules rhumatoïdes siégeant surtout à la face postérieure de l'avant-bras et du coude sont, après quelques années d'évolution, présents dans environ 20% des cas [Carmona *et al.* 2003; Cimmino *et al.* 2000]. Un syndrome de Gougerot-Sjögren est constaté chez un patient sur six [Carmona *et al.* 2003; Cimmino *et al.* 2000]. Les atteintes

pulmonaires, principalement des bronchectasies, touchent environ 2,5% de la population souffrant de PR [Carmona *et al.* 2003].

La luxation antloïdo-axoidienne, pouvant entraîner une compression médullaire, complique environ 10% des PR. Elle est recherchée systématiquement afin de ne pas méconnaitre une compression médullaire cervicale. Les vascularites, l'amylose secondaire et le syndrome de Felty (associant une splénomégalie et une leuconeutropénie) sont des complications graves mais plus rares (≤1% des patients) qui surviennent volontiers dans des PR anciennes.

1.3. Difficultés diagnostiques de la PR

Le diagnostic de PR se fonde sur un faisceau d'arguments cliniques, biologiques et radiologiques [Haute Autorité de Santé 2007] après élimination des autres affections rhumatologiques [Aletaha *et al.* 2011]. Malgré les différents examens biologiques et radiologiques prescrits dans le bilan diagnostique de PR et la création d'algorithmes diagnostiques [Aletaha *et al.* 2011] et pronostiques [Visser *et al.* 2010], la recherche de nouveaux biomarqueurs diagnostiques, pronostiques et théragnostiques de la PR semble nécessaire pour améliorer la prise en charge des patients [Baillet *et al.* 2010; De Seny *et al.* 2005; De Seny *et al.* 2008].

1.3.1. Le bilan biologique

Il existe un syndrome inflammatoire associé à une positivité des anticorps anti-nucléaires (10-30 %) et du facteur rhumatoïde, anticorps de type IgM anti-gammaglobuline. Les résultats de ces examens ne sont toutefois pas assez discriminants pour le diagnostic de la PR contrairement aux anticorps anti-peptides citrullinées (ACPA pour "anti-citrullinated protein or peptide auto anti-bodies") dont la spécificité est excellente [Schellekens *et al.* 2000]. Cependant au stade initial la sensibilité des ACPA n'est que de 40 à 60% [Nishimura *et al.* 2007; Schellekens *et al.* 2000].

1.3.2. Le bilan radiologique

L'existence d'érosion osseuse sur les radiographies standard dans le cadre d'une polyarthrite débutante est fortement évocatrice d'une PR ou, au moins, d'une polyarthrite nécessitant l'instauration d'un traitement par méthotrexate [Aletaha *et al.* 2011]. L'échographie et l'imagerie par résonnance magnétique offrent une sensibilité supérieure [Baillet *et al.* 2011a] et permettent de faire le diagnostic avant l'apparition de lésions radiographiques. De nouveaux algorythmes diagnostiques [Aletaha *et al.* 2011] et pronostiques [Visser *et al.* 2010], intégrant les données de l'examen clinique et les résultats du bilan biologique et radiologique ont récemment été proposés.

2. Les synoviocytes et les PMNs : cellules clés de la physiopathologie de la PR

Bien que la physiopathologie de la PR soit encore mal connue, plusieurs phases, bien souvent intriquées, semblent caractériser l'évolution de la maladie. Bien avant le début des symptômes, il est probable qu'une inflammation aspécifique aboutisse à une rupture de la tolérance par émergence de protéines de danger, telles que les protéines S100A8/A9, et des peptides antigéniques au sein de la matrice extra-cellulaire de l'articulation. De nombreux types cellulaires incluant le monocyte/macrophage [Ma *et al.* 2005], le lymphocyte B [Gottenberg *et al.* 2009], le lymphocyte T [Skapenko *et al.* 2005], le chondrocyte [Yasuda 2006] et l'ostéoclaste [Gravallese 2002] sont impliqués dans l'étiopathogénèse de la maladie. Cependant un rôle primordial est désormais reconnu aux synoviocytes [Pap *et al.* 2000] et à leurs interactions avec les cellules infiltrantes phagocytaires [Kurz *et al.* 1999]. La jonction entre la membrane synoviale et le cartilage est une zone gâchette où débutent les premières lésions [Choy *et al.* 2001]. Des synoviocytes activés, au phénotype pseudo-tumoral, apparaissent dans cette zone critique bien avant le début des symptômes suggérant un rôle prépondérant de ce type cellulaire dans le développement et la chronicisation de la maladie [Lefevre *et al.* 2009; Noss *et al.* 2008; Perlman *et al.* 2010].

2.1. La synovite, lésion élémentaire de la Polyarthrite Rhumatoïde

Il existe de plus en plus d'arguments qui désignent la membrane synoviale et tout particulièrement la jonction pannus-cartilage comme une zone clé [Pap *et al.* 2000]. La synovite inflammatoire est la lésion élémentaire responsable de la destruction articulaire. Initialement, on note une augmentation du nombre de vaisseaux synoviaux avec un infiltrat composé de PMNs, de macrophages et de lymphocytes. Puis les cellules résidantes, les synoviocytes fibroblastiques, prolifèrent et deviennent hyperplasiques. Les synoviocytes, primitivement répartis en une fine couche bordante monocellulaire, se distribuent alors en plusieurs couches avec une hypertrophie des villosités synoviales et une multiplication des franges caractéristiques du pannus de la PR (**Figure 3**).

Figure 3. Histologie de la synovite rhumatoïde

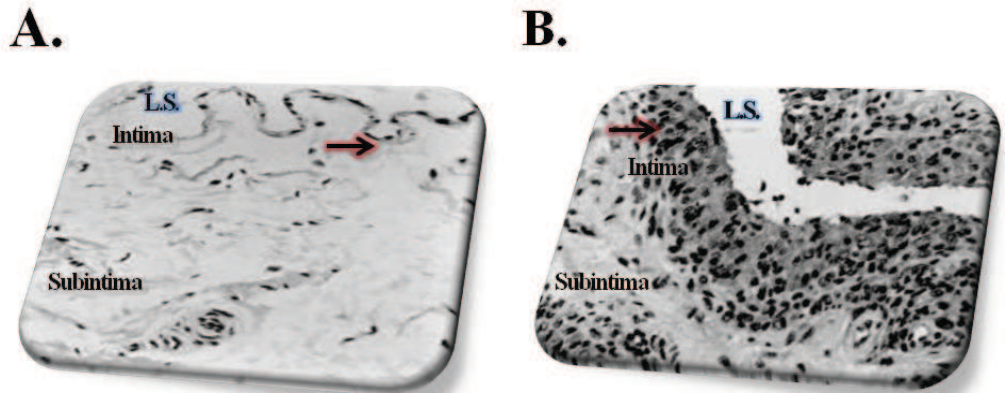

A : Répartition des synoviocytes fibroblastiques en une monocouche cellulaire (flèche) produisant le liquide synovial (L.S.) de la cavité articulaire.
B : Prolifération pseudotumorale des synoviocytes fibroblastiques rhumatoïdes de l'intima (flèche) et infiltation de cellules inflammatoires dans la subintima.

2.2. Les synoviocytes : cellules résidantes de la membrane synoviale

2.2.1. La membrane synoviale rhumatoïde

La membrane synoviale, d'origine mésenchymateuse, tapisse les bourses séreuses, les gaines tendineuses et toutes les surfaces articulaires à l'exception du cartilage, délimitant la cavité contenant le liquide synovial. Elle est organisée en replis et en franges qui augmentent la surface de contact avec le liquide synovial. La membrane synoviale est divisée en une couche profonde richement vascularisée et innervée recouvrant la capsule articulaire et en une couche superficielle, elle-même formée d'une couche bordante, composée d'une à deux assises de cellules, l'intima, et d'une zone plus profonde avec de nombreux capillaires sanguins, d'artérioles et de vaisseaux lymphatiques, la sub-intima.

La couche de cellules bordantes de la membrane synoviale est principalement formée de synoviocytes de 2 types. Les synoviocytes de type A ou macrophagiques, d'origine hématopoïétique [Shikichi *et al.* 1999], ont tendance à s'amasser dans les zones apicales des villosités, alors qu'ils sont plus rares dans les régions basales [Iwanaga *et al.* 2000; Shikichi *et al.* 1999]. Les synoviocytes macrophagiques assurent la phagocytose des débris contenus dans l'espace articulaire et présentent les peptides liés au Complexe Majeur d'Histocompatibilité de classe II [Kitamura *et al.* 2001]. Ce type cellulaire est donc directement partie prenante dans la destruction articulaire. Les synoviocytes macrophagiques sont incapables de proliférer *in vitro*, si bien qu'après quelques passages, le seul type cellulaire pouvant être cultivé est le synoviocyte fibroblastique [Hamilton *et al.* 1981].

Les synoviocytes fibroblastiques ou de type B sont responsables de la synthèse d'acide hyaluronique [Momberger *et al.* 2005] et de la plupart des constituants du liquide synovial tels que le collagène [Smith *et al.* 1998] et la fibronectine [Carsons *et al.* 1985] nécessaires à la

nutrition et à la lubrification du cartilage. Le rôle de la lubricine [Jay *et al.* 2011] dans la chondroprotection a récemment été souligné.

Ces deux types cellulaires ont des caractéristiques morphologiques, histochimiques et immuno-histologiques différentes [Barland *et al.* 1962].

2.2.2. Les transformations phénotypiques du synoviocyte fibroblastique rhumatoïde

La prolifération des synoviocytes fibroblastiques est une des caractéristiques qui définit la PR. Ces cellules jouent un rôle central dans la maladie [Lefevre *et al.* 2009]. L'acquisition singulière du phénotype pseudo-tumoral procède de plusieurs mécanismes dont certains déterminants ont récemment été caractérisés.

Le rôle des cytokines pro–inflammatoires, impliquées à la fois dans l'activation et la transformation phénotypique des synoviocytes rhumatoïdes, est mal cerné. En effet, il est expérimentalement difficile d'apporter la certitude qu'*in vivo* les cytokines pro-inflammatoires sont une cause de la transformation pseudo-tumorale et non pas la conséquence de l'activation cellulaire. L' IL-1β [Chevrel *et al.* 2002] et le TNFα [Imaizumi *et al.* 2009] augmentent la synthèse de cytokines par le synoviocyte rhumatoïde alors que l'IL-6 [Hashizume *et al.* 2009] permet la sécrétion du facteur angiogénique VEGF ("Vascular endothelial growth factor". L'IL-17 [Hot *et al.* 2011] ainsi que des facteurs de croissance "Fibroblast Growth Factor" (FGF [Muller-Ladner *et al.* 2007]), "Platelet Derived Growth Factor" (PDGF [Rosengren *et al.* 2010]) et "Transforming Growth Factor" (TGF-β [Warstat *et al.* 2011]) sont impliqués dans la synthèse de MMPs qui facilitent la migration et la dégradation de la matrice extracellulaire par le synoviocyte. Une hypothèse alternative est avancée pour expliquer le phénotype pseudo-tumoral des synoviocytes rhuamtoïdes. Li *et al.* suggèrent que les cytokines pro-inflammatoires pourraient maintenir les cellules souches mésenchymateuses du pannus rhumatoïde dans un état de synoviocytes dédifférenciés [Li *et al.* 2006a].

De plus, il existe une activation autocrine des cellules résidantes de l'articulation par des facteurs pro-métastatiques, S100A4 [Klingelhofer *et al.* 2007] et progranuline [Tang *et al.* 2011], qui accélèrent l'angiogénèse, la prolifération et la migration cellulaire. De plus, l'activation de proto-oncogène Fas, Bcl-2 et c-Myc [Matsumoto *et al.* 1996; Pap *et al.* 2004] tout comme le déficit d'expression de gènes suppresseurs de tumeur p53 [Cha *et al.* 2006] favorisent la prolifération et inhibent l'apoptose des synoviocytes [Matsumoto *et al.* 1996].

Enfin des modifications épigénétiques des synoviocytes fibroblastiques de PR ont été rapportées. L'hyper-acétylation génomique [Huber *et al.* 2007] contribue à l'activation de

facteurs de transcription pro-inflammatoires alors que l'hypo-méthylation de l'ADN [Karouzakis *et al.* 2009] en partie secondaire à l'expression de certains micro-ARN, miR-146a et miR-155 [Stanczyk *et al.* 2008] est à l'origine d'une activation du synoviocyte rhumatoïde.

2.2.3. Les synoviocytes rhumatoïdes, cellules "sentinelles"

Les synoviocytes fibroblastiques sont principalement dévolus à la synthèse de la matrice extra-cellulaire du tissu synovial et du liquide articulaire. De plus, ils sont engagés directement dans l'initiation et l'amplification de la réponse inflammatoire, notamment grâce à l'abondante expression de récepteurs de l'immunité innée [Ospelt *et al.* 2008]. Ainsi la voie des récepteurs "Toll like" (TLR), peut être activée par des molécules de danger comme les protéines S100A8/A9 [Vogl *et al.* 2007] ou par des produits de nécrose cellulaire [Ospelt *et al.* 2009]. Cette dualité fonctionnelle des synoviocytes fibroblastiques leur confère le rôle de sentinelle de l'articulation, garante de l'homéostasie de l'articulation dans un contexte physiologique et pathologique, en collaboration avec les synoviocytes macrophagiques [Smith *et al.* 1997; Xia *et al.* 1997]. L'activation de ce dernier type cellulaire, par des pathogènes ou des molécules de danger, est à l'origine d'une stimulation des synoviocytes de type fibroblastiques. Ce dialogue est un phénomène très précoce dans la physiopathologie de la PR, vraisemblablement à l'origine de l'émergence de néo-épitopes. Il s'ensuit une rupture de tolérance [Klimiuk *et al.* 1999] qui a pour conséquence une stimulation des lymphocytes T à l'origine de la réaction auto-immune. De plus les synoviocytes macrophagiques activés produisent du TGF-β qui est un facteur de croissance capital dans la polarisation de la réponse lymphocytaire Th17 [Yang *et al.* 2008]. Les synoviocytes fibroblastiques ainsi activés [Warstat *et al.* 2011] amplifient la réponse inflammatoire par la sécrétion de médiateurs pro-inflammatoires comme l'IL-1β [Chevrel *et al.* 2002], le TNFα et l'IL-6 (**Figure 4**).

Ces cellules jouent, en outre, un rôle central dans la protéolyse matricielle, de manière directe par leur invasion de la matrice extra-cellulaire et de manière indirecte en perturbant le fonctionnement des autres cellules résidantes chondrocytaires et ostéoclastiques. Les synoviocytes peuvent également stimuler les cellules de l'immunité innée et adaptative. En effet, elles sont capables d'interagir avec la plupart des cellules qui contribuent à la destruction du cartilage et à l'inflammation telles que les lymphocytes B [Reparon-Schuijt *et al.* 2000], les lymphocytes T [Benito-Miguel *et al.* 2009], mais aussi les monocytes/macrophages [Blue *et al.* 1993] et les neutrophiles [Filer *et al.* 2006].

Figure 4. Transformation phénotypique du synoviocyte fibroblastique rhumatoïde et sécrétion de molécules effectrices dans la Polyarthrite Rhumatoïde

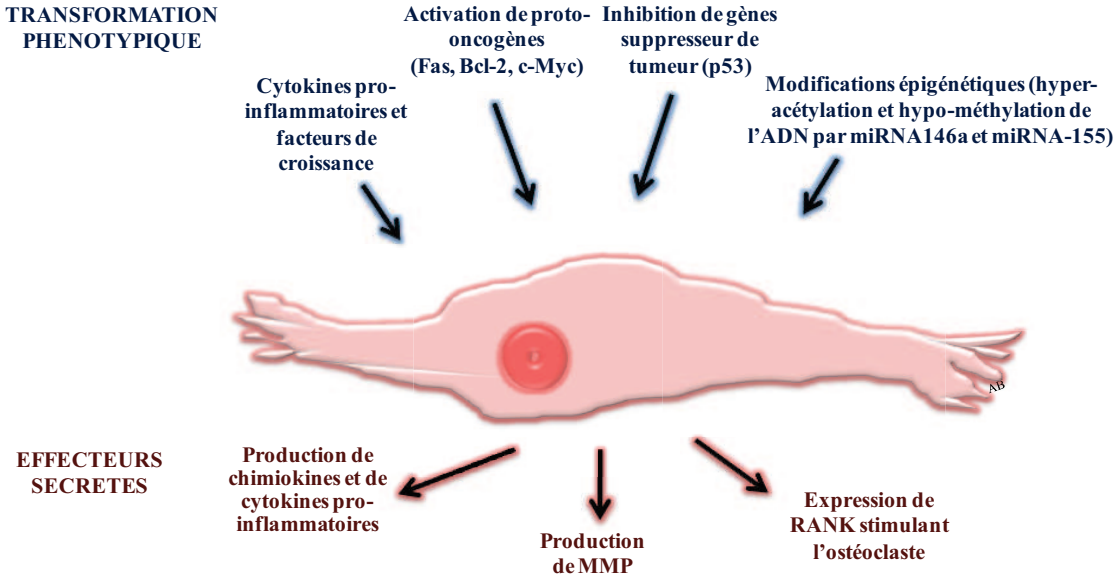

miRNA= "microRNA", MMP="Matrix Métalloproteinase", RANK="Receptor Activator of NF-κB".

2.2.4. Les molécules effectrices produites par les synoviocytes rhumatoïdes

L'activation du synoviocyte, secondaire à la stimulation par des cytokines pro-inflammatoires et à l'acquisition d'un phénotype pseudotumoral, entretient la réaction inflammatoire au sein de la membrane synoviale. Tout d'abord le synoviocyte produit des facteurs angiogéniques responsables d'une augmentation de la vascularisation du pannus [Pablos *et al.* 2003] puis il synthétise des chimiokines attirant les leucocytes au sein du pannus [Privat *et al.* 2001]. Il est vraisemblable que cette réaction inflammatoire initiale, qui implique les cellules résidantes, soit à l'origine de la formation de follicule lympho-plasmocytaire [Humby *et al.* 2009].

L'IL-6 produit par les synoviocytes fibroblastiques est un facteur majeur d'activation des lymphoctes B matures avant qu'ils ne se transforment en plasmocytes producteurs d'auto-anticorps anti-peptides citrullinés. L'interaction synoviocyte-lymphocyte T induit la stimulation [Singh *et al.* 2008] et la différenciation lymphocytaire vers un phénotype pro-inflammatoire [Benito-Miguel *et al.* 2009]. De plus, les synoviocytes fibroblastiques attirent les PMNs circulants par la production d'IL-8 [Gao *et al.* 1995]. Les deux types de synoviocytes fibroblastiques [Koch *et al.* 1992] et macrophagiques [Villiger *et al.* 1992] sont capables de produire la CCL-2, une chimiokine également appelée "monocyte-chemoattractant protein-1" (MCP-1) responsable du recrutement du monocyte et probablement du lymphocyte T au sein du pannus (**Figure 4**).

En outre, certaines MMPs membranaires sécrétées par les synoviocytes sont aptes à activer la gélatinase MMP-2 et la collagénase MMP-13 [Sato *et al.* 1994], amplifiant et entretenant la protéolyse matricielle. Les fragments de fibronectine et vitronectine ainsi générés activent également la sécrétion de différentes MMPs [Noss *et al.* 2008], brisant l'homéostasie en faveur d'un catabolisme matriciel (**Figure 5**). Il existe 4 inhibiteurs des MMPs : TIMPs1-4 ("tissu inhibitor of MMPs"). Bien que chacun des TIMPs puisse bloquer le site catalytique de l'ensemble des MMPs par son domaine N-terminal, il existe une certaine spécificité de chaque inhibiteur. Par exemple, la gélatinase MMP-2 est préférenciellement inhibée par les TIMPs 2-4 alors que la gélatinase MMP-9 a plus d'affinité pour le TIMP-1. Dans un modèle murin [Schurigt *et al.* 2005] et canin [Hegemann *et al.* 2003] de PR ainsi que chez les patients [Murphy *et al.* 2002], il existe un déséquilibre entre l'activité des MMPs et l'inhibition par les TIMPs au sein du pannus, à la faveur d'une majoration de l'activité protéolytique. C'est également le cas pour la cathepsine B, protéase à cystéine, dont l'activité catalytique n'est plus contôlée par la cystatin C [Hansen *et al.* 2000].

Enfin, de récentes données suggèrent que les synoviocytes de PR, à l'instar des métastases, empruntent la circulation systémique pour étendre le site inflammatoire à d'autres articulations [Lefevre *et al.* 2009].

Figure 5. Structure schématique de Métalloprotéases matricielles (MMPs)

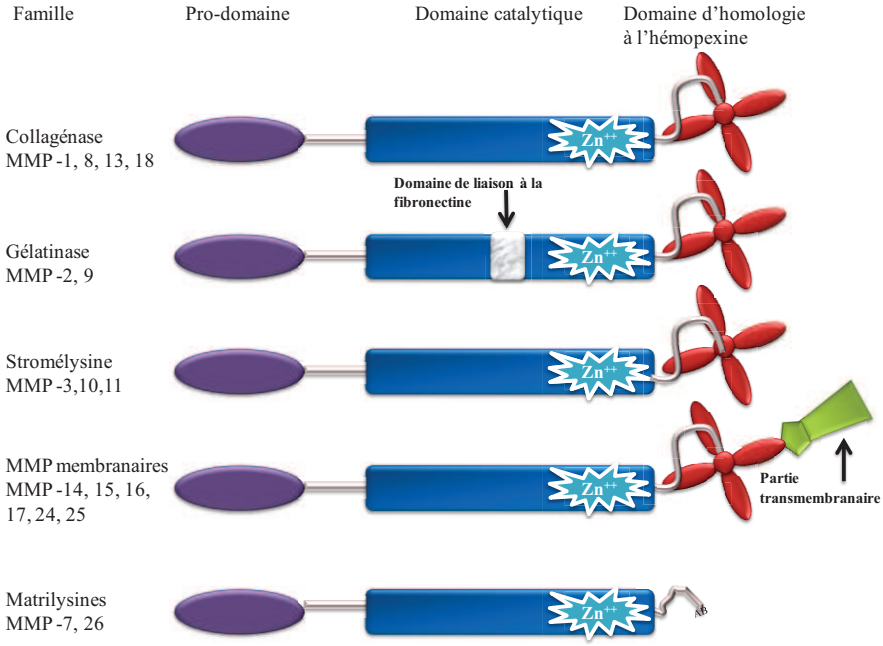

D'après [Preston 2002].

2.2.5. Les synoviocytes rhumatoïdes sont au cœur de la protéolyse matricielle

Les modifications phénotypiques du synoviocyte fibroblastique de PR lui confèrent la propriété d'adhérer sur le cartilage [Muller-Ladner *et al.* 1996], de proliférer de manière pseudo-tumorale [Lafyatis *et al.* 1989], de migrer dans le tissu synovial [Garcia-Vicuna *et al.* 2004; Gay *et al.* 1996] indépendamment de toute stimulation [Muller-Ladner *et al.* 1996].

De plus, les synoviocytes synthétisent des enzymes de dégradation de la matrice extra-cellulaire telles que la collagénase MMP-1 [Sorsa *et al.* 1992], la gélatinase MMP-2 [Clegg *et al.* 1999], l'agrécanase [Vankemmelbeke *et al.* 1999] et les stromélysines MMP-3 [Miyazawa *et al.* 1998] et MMP-10 [Tolboom *et al.* 2002].

Enfin, sous l'effet des proto-oncogènes des synoviocytes rhumatoïdes ou de cytokines pro-inflammatoires, des cathepsines [Cunnane *et al.* 1999; Hummel *et al.* 1998] sont sécrétées et dégradent les protéoglycanes ainsi que le collagène I, II, IX et XI [Trabandt *et al.* 1990]. Le synoviocyte de PR participe également à la destruction cartilagineuse [Steenvoorden *et al.* 2007a] en modifiant l'équilibre homéostasique du chondrocyte. D'une part, l'ostéoprotégérine produite par la membrane synoviale induit la synthèse de collagénase par le chondrocyte [Petrow *et al.* 2000]. D'autre part, L'IL-6 synthétisée par les synoviocytes de PR activés diminue les fonctions anaboliques du chondrocyte [Kurz *et al.* 1999], notamment la synthèse de protéoglycanes [Jikko *et al.* 1998].

Le récepteur RANK (Receptor Activator of NF-κB) de la superfamille des récepteurs au TNFα, est une voie majeure de l'activation de l'ostéoclaste [Teitelbaum 2000], cellule impliquée dans la résorption osseuse et les érosions des rhumatismes inflammatoires. Or le synoviocyte fibroblastique de PR exprime fortement le ligand de RANK, RANKL [Shigeyama *et al.* 2000]. L'ostéoclastogénèse est ainsi activée, expliquant les lésions osseuses constatées dans la PR [Ishida *et al.* 2009].

2.3. Les PMNs : cellules infiltrantes de l'articulation, chefs d'orchestre de la synovite

2.3.1. La granulopoïèse

Les polynucléaires neutrophiles, ou PMNs ("polymorphonucléaires neutrophiles"), comme tous les leucocytes dérivent de la cellule souche totipotente HPP-CFC ("High Proliferative Potential- Colony Forming Cell"). Le facteur de croissance GM-CSF ("Granulocyte Marophage-Colony Stimulating Factor") autorise la différenciation de la lignée myéloïde bipotente des granulocytes et des monocytes alors que le G-CSF ("Granulocyte-Colony Stimulating Factor") oriente vers le progéniteur granulocytaire. Durant la granulopoïèse de cette lignée, plusieurs types cellulaires vont se différencier : les myéloblastes, promyélocytes

et myélocytes, encore capables de proliférer, et les cellules terminales, incapables de mitose : les métamyélocytes et les PMNs. L'étude par radio-marquage a permis d'évaluer la durée de vie des cellules dans le sang périphérique (4 à 7h pour les PMNs) [Dresch *et al.* 1972] et la durée de la granulopoïèse (7 à 13j) au cours de laquelle vont apparaître successivement et à des stades très précis les granulations azurophiles ou primaires, spécifiques ou secondaires, riches en gélatinase et enfin les vésicules sécrétoires [Borregaard *et al.* 1997].

Figure 6. La granulopoïèse

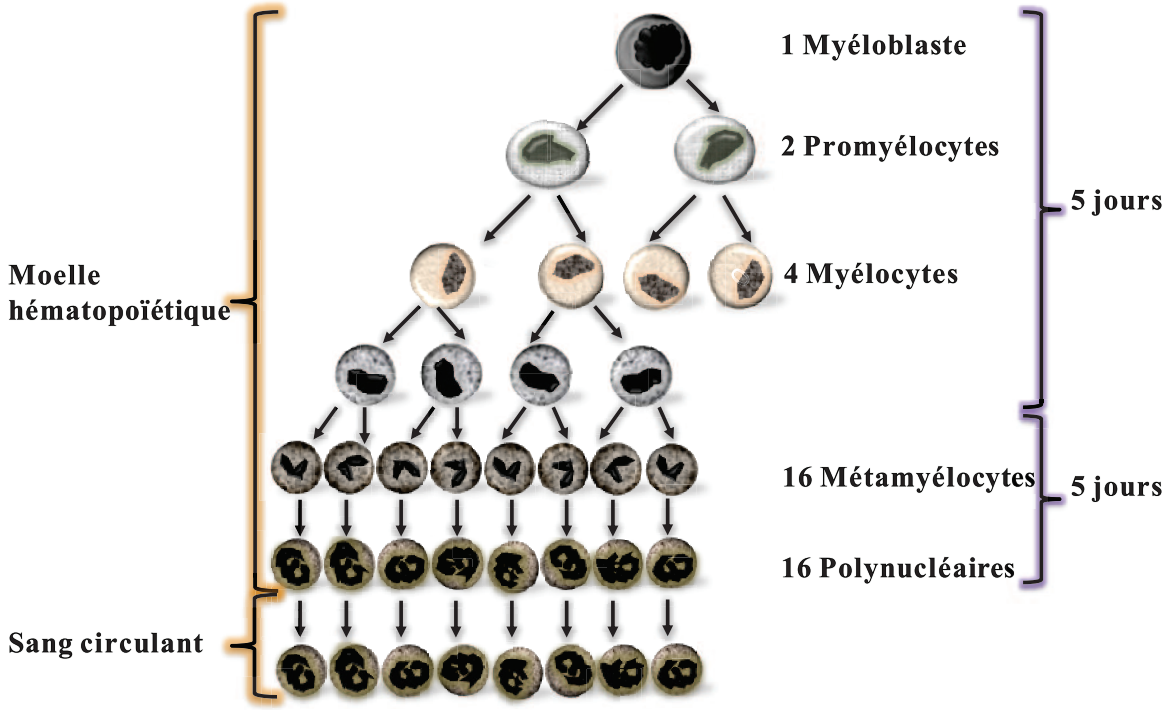

Le myéloblaste est une cellule peu représentée (0 à 2% des cellules d'un frottis médullaire). De forme quadrangulaire ou ovale, elle mesure 15 à 20 µm. Son noyau convexe contient une chromatine finement piquetée et de 1 à 3 nucléoles nettement délimités. Quelques granulations azurophiles immatures sont parfois visualisées dans son cytoplasme hyperbasophile. Le promyélocyte, plus volumineux, constitue 2 à 8% des cellules médullaires. Le début de condensation de la chromatine et l'apparition de nombreuses granulations azurophiles sont les stigmates de la maturation nucléo-cytoplasmique (**Figure 6**). La majorité de ces granules se répartit autour de l'appareil de Golgi. Ils sont pour la plupart sphériques et denses en microscopie électronique (environ 500 nm), mais certains sont oblongs et d'autres beaucoup plus petits. Au stade myélocyte (15 µm) la synthèse de ces granules cesse au profit de granules spécifiques contenant de la lactoferrine et de granules riches en gélatinase, d'environ 200 nm de diamètre. Le noyau devient convexe, la chromatine s'agrège en bloc, les

nucléoles disparaissent et le cytoplasme devient acidophile (**Figure 7**). Ces cellules représentent 12 à 20% des cellules médullaires. La dernière mitose de la lignée granuleuse du neutrophile intervient entre le stade myélocyte et métamyélocyte donnant naissance à une cellule qui ne diffère du myélocyte que par l'aspect réniforme du noyau, la condensation de la chromatine en blocs denses, la raréfaction des ribosomes et des mitochondries.

Figure 7. Les granules du PMN

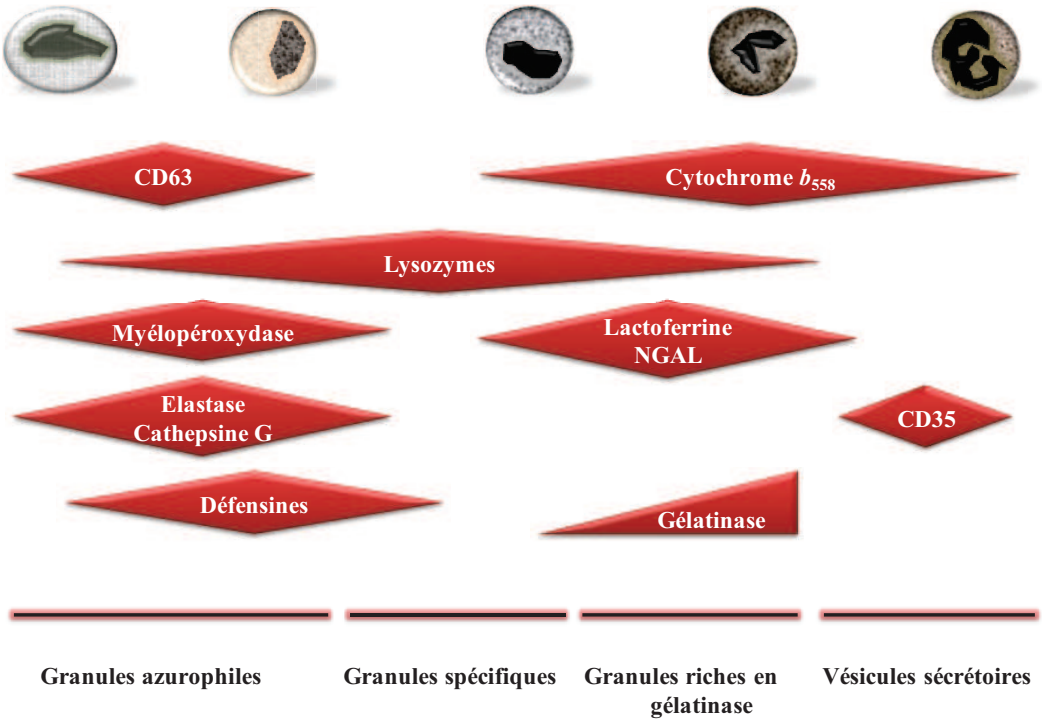

NGAL="Neutrophil gelatinase-associated lipocalin", CD="Cluster of differenciations". D'après [Borregaard et al. 1997].

2.3.2. Le PMN en condition physiologique

Au cours de la maturation nucléo-cytoplasmique, des PMNs médullaires (12 à 15µm) restent dans la moelle hématopoïétique pendant 5 jours, constituant une réserve médullaire, avant de rejoindre la circulation sanguine. Leur chromatine est condensée, leur noyau polylobé et leur cytoplasme contient différentes populations de granules (environ 200 à 300) : granules azurophiles, granules spécifiques, granules riches en gélatinase et vésicules sécrétoires [Damiano *et al.* 1988]. En condition physiologique, les PMNs constituent environ 70% des leucocytes circulants et demeurent peu de temps dans le sang périphérique [Moulding *et al.* 2001]. Environ 50 % des PMNs circulants forment une fraction marginale, faiblement liée à l'endothélium vasculaire par expression de L-sélectine.

2.3.3. Migration du PMN circulant sur le site inflammatoire

L'analyse de différents modèles murins de PR suggère que les PMNs sont les premières cellules infiltrant l'articulation [Chen *et al.* 2006a; Wipke *et al.* 2001]. Ils peuvent rester un à deux jours au niveau tissulaire avant de mourir par apoptose et d'être phagocytés par les macrophages. La migration transendothéliale des PMNs se fait selon plusieurs étapes successives pour parvenir sur le site inflammatoire. Dans un premier temps, le PMN circulant va être retenu contre la paroi vasculaire : c'est l'étape du roulement. L'adhérence labile entre les deux types cellulaires procède de l'expression de molécules d'adhésion de faible affinité de la famille des sélectines. La deuxième étape fait intervenir des molécules d'adhésion de la famille des intégrines qui vont asseoir l'adhérence du PMN sur l'endothélium (**Figure 8**). La cellule endothéliale participe activement en exposant des molécules d'adhérence E- et P-sélectines [Smith 1993] permettant au PMN de ralentir et de rouler sur la paroi vasculaire, puis en produisant de l'IL-8, du TNFα ou du GM-CSF. Ces médiateurs permettent le clivage des L-sélectines leucocytaires par des métalloprotéases, notamment ADAM-17 ("A Disintegrin And Metalloproteinase-17", [Li *et al.* 2006b]). Le PMN exprime alors VLA-4 ("Very Late Antigen-4" ; intégrine α4β1), LFA-1 ("Lymphocyte Function-Associated antigen-1"; intégrine αLβ2) et MAC-1 ("Macrophage Antigen-1"; intégrine αMβ2). La cellule ralentit puis adhère à l'endothélium, grâce l'expression endothéliale de nouvelles molécules [Diez-Fraile *et al.* 2002] ICAM-1 et -2 ("Intercellular Adhesion Molecule"), VCAM-1 ("Vascular Cell-Adhesion Molecule-1") et MADCAM-1 ("Mucosal vascular Cell-Adhesion Molecule-1").

Figure 8. Migration du PMN sur le site inflammatoire.

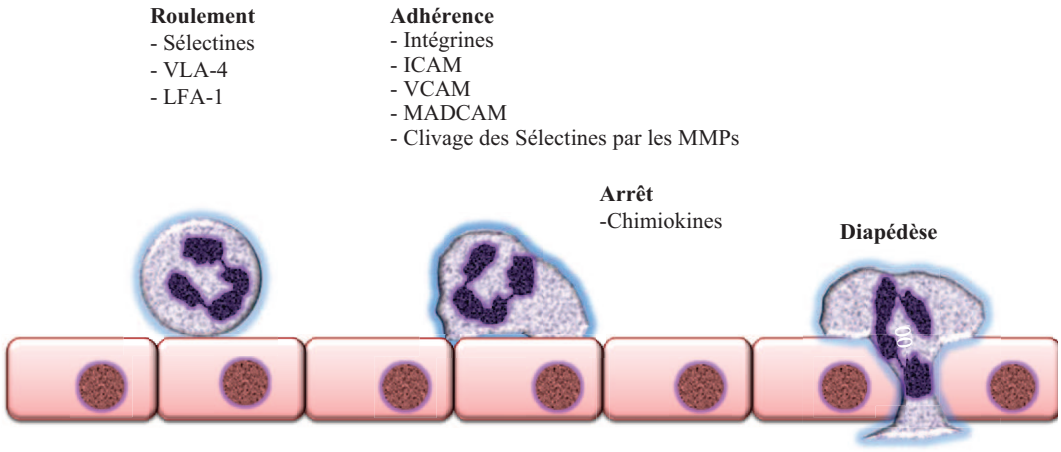

ICAM= "Intercellular Adhesion Molecule", LFA1="lymphocyte Function-associated Antigen-1", MADCAM= "Mucosal vascular Cell-Adhesion Molecule", MMP="Matrix Metalloproteinase", VLA-4= "Very Late Antigen-4", VCAM="Vascular Cell-Adhesion Molecule-1". D'après [Wright et al. 2010].

Il s'ensuit l'étape de la diapédèse au cours de la laquelle le PMN se glisse entre les cellules endothéliales puis traverse la membrane basale. Plusieurs protéases sont successivement secrétées. L'élastase participe au désassemblage des complexes cadhérines/caténines et dégage ainsi les jonctions inter-cellulaires alors que la gélatinase MMP-9 des PMNs dégrade la membrane basale. Ultérieurement la migration vers le site inflammatoire est médiée par un gradient de chimiokines. L'exposition à une concentration d'environ 10^{-9}M de fMLP (N-formyl-Méthionyl-Leucyl-Phénylalanine) ou à l'anaphylatoxine, fraction C5a du complément, induit la polarisation des chimiorécepteurs et la formation de pseudopodes riches en actine [Servant *et al.* 2000]. La chimiokine IL-8 [Gao *et al.* 1995] ainsi que certains médiateurs lipidiques tels que le PAF ("Platelet activating factor") et l'eicosanoïde LT-B4 (leucotriène B4) contribuent également à la migration du PMN. La fixation de ces chimiokines à leurs récepteurs à 7 domaines transmembranaires couplés aux protéines G hétérotrimériques [Haribabu *et al.* 2000] oriente la migration du PMN. A des concentrations plus élevées, de l'ordre de 10^{-7}M pour le fMLP, ces facteurs chimioattractifs activent le PMN, et en particulier la NADPH oxydase phagocytaire, lui permettant d'accomplir les tâches qui lui sont dédiées sur le site inflammatoire. Certains auteurs ont démontré l'implication des molécules de danger S100A9/A9 produites quasi-exclusivement par la lignée myéloïde, dans la migration et l'activation des PMNs dans des modèles murins d'arthrite [Ryckman *et al.* 2003a] et dans la goutte [Ryckman *et al.* 2004].

Figure 9. Mécanismes d'activation du PMN et production d'effecteurs dans la PR

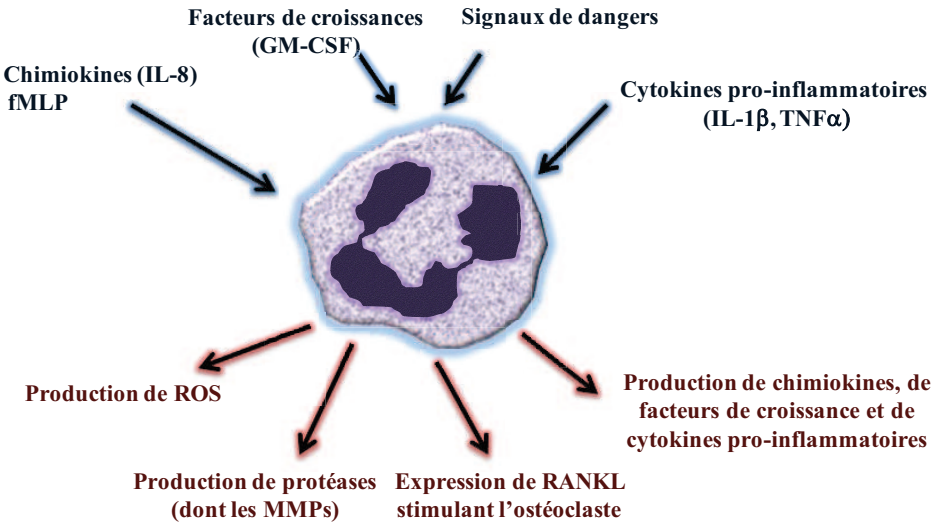

fMLP=N-formyl-Méthionyl-Leucyl-Phénylalanine, GM-CSF= "Granulocyte Macrophage – Colony Stimulating Factor", IL=Interleukine, MMP="Matrix Metalloproteinase", RANKL="Receptor Activator of NF-κB Ligand", TNF α="Tumor Necrosis Factor α", ROS="Reactive oxygen species".

2.3.4. Le PMN, phagocyte au rôle majeur dans la physiopathologie de la PR

Les PMNs constituent plus de 80% des leucocytes infiltrant le liquide synovial [Krey *et al.* 1979] lors d'une poussée de PR. Lors d'une stimulation, les neutrophiles gagnent le site inflammatoire en environ 30 min [Linderkamp *et al.* 1998]. Leur implication majeure dans la physiopathologie de la PR est supposée depuis longtemps [Mowat 1976] et suggérée expérimentalement par l'absence d'arthrite dans un modèle murin de PR dépourvu de PMN [Wipke *et al.* 2001]. De plus, ce type cellulaire est retrouvé dans cette zone gâchette constituée par la jonction pannus-cartilage, arguant pour une implication précoce dans le développement de la maladie [Mohr *et al.* 1981; Wittkowski *et al.* 2007]. En effet, le PMN intervient au premier plan dans plusieurs manifestations caractéristiques de la PR : la destruction cartilagineuse, les érosions osseuses et la synovite chronique (**Figure 9**).

L'élastase secrétée dans le liquide articulaire par les PMNs est responsable, *in vitro*, d'une dégradation du collagène III, IX, X et XI mais ne concerne pas le collagène de type II [Gadher *et al.* 1988]. De plus, le PMN semble diminuer la production de composants de la matrice par les cellules résidantes. Nuver-Zwart *et al.* montrent que le nombre de PMNs dans le liquide synovial de PR corrèle avec l'inhibition de la synthèse du protéoglycane [Nuver-Zwart *et al.* 1988]. *In vivo*, les protéases des neutrophiles participent à la destruction cartilagineuse dans des modèles murins d'arthrite [Joosten *et al.* 2009; Wipke *et al.* 2001].

Le neutrophile rhumatoïde est également capable d'augmenter la résorption osseuse en activant directement les ostéoclastes [52]. Les PMNs infiltrants expriment la protéine RANKL ("Receptor Activator of NFκB Ligand") [Poubelle *et al.* 2007] capable d'induire des érosions articulaires par stimulation de l'ostéoclaste [Chakravarti *et al.* 2009]. Le PMN contribue également à la pérennisation de l'inflammation en produisant des médiateurs pro-inflammatoires.

Bien que la production cytokinique du PMN soit quantitativement moins importante que celle du macrophage, l'importance de l'infiltration des neutrophiles dans le pannus et le liquide synovial contribue à l'empreinte cytokinique inflammatoire associée à la PR. Le PMN est capable de produire directement des cytokines pro-inflammatoires comme l'IL-1β [Lindemann *et al.* 1988], le TNFα [Djeu *et al.* 1990], l'interféron γ [Shirafuji *et al.* 1990] et des chimiokines tels que l'IL-8 [Cassatella *et al.* 1992] et MIP-1α ("Macrophage Inflammatory Protein-1α", [Kasama *et al.* 1994]). Certains facteurs de croissance sont également produits : le TGF-β [Fava *et al.* 1991], le GM-CSF [Kita *et al.* 1991]et le G-CSF

[Lindemann *et al.* 1989]. Enfin certaines protéases du neutrophile, la PR-3 (“proteinase-3“) et la caspase-1, sont responsables du clivage du pro- IL-1β en IL-1β bio-actif [Joosten *et al.* 2009].

3. Rôle des ROS dans l’étiopathogénie de la PR

La faible demi-vie des ROS (de l’odre de la milliseconde) et leur haute réactivité rendent difficile la démonstration directe de leur implication dans la physiopathologie de la PR. Cependant de nombreux arguments suggèrent un rôle central des ROS dans l’initiation et l’évolution de cette pathologie [Marklund 1982].

3.1. Les ROS : formes réactives de l’oxygène

3.1.1. La formation des ROS

Les formes réactives de l'oxygène (“Reactive Oxygen Species“, ROS) sont des espèces chimiques dérivées de l’oxygène que l’on peut séparer en deux groupes :

- Les radicaux oxygénés possédant un ou plusieurs électrons non appariés sur leur couche externe. Parmi eux, figurent l’anion superoxyde $O_2^{\bullet-}$, le radical hydroxyle $OH^{\bullet}$, monoxyde d’azote $NO^{\bullet}$ et le radical peroxyde ($ROO^{\bullet}$ où R est une chaîne carbonée).
- Les dérivés non radicalaires tels que le peroxyde d'hydrogène H_2O_2, le peroxynitrite $ONOO^-$, l’acide hypochlorique (HOCl), l’ozone O_3 et l’oxygène singulet $^1O_2$.

Plusieurs sources génératrices d’anions $O_2^{\bullet-}$ ont été rapportées. Elles restent modestes par rapport à la NADPH oxydase qui est le système majeur de production d’anions $O_2^{\bullet-}$. Environ 2% de l’oxygène subit une réduction monoélectronique au niveau de l’ubiquinone sans bénéficier de la réduction tétravalante de la chaine respiratoire de la membrane interne de la mitochondrie.

L’oxygène est réduit électron par électron en passant successivement par l’anion $O_2^{\bullet-}$, le peroxyde d’hydrogène et le radical hydroxyle et produit une molécule d’eau :

$$O_2 \xrightarrow{+e^-} O_2^{\bullet-} \xrightarrow{+e^- (+2H^+)} H_2O_2 \xrightarrow{+e^-} OH^{\bullet} \xrightarrow{+e^- (+H^+)} H_2O$$

D'autres sources potentielles d'anions $O_2^{\bullet-}$ ont été identifiées : le cytochrome P450, la lipooxygénase, la xanthine oxydoréductase, la gamma glutamyl transférase ainsi que la NO synthase découplée.

La NADPH oxydase phagocytaire catalyse la réduction monoélectronique de l'oxygène où le NADPH est le donneur d'électron selon la réaction suivante :

$$NADPH + 2O_2 \xrightarrow{\text{NADPH oxydase}} NADP^+ + H^+ + 2O_2^{\bullet-}$$

Figure 10. La famille des NADPH oxydases

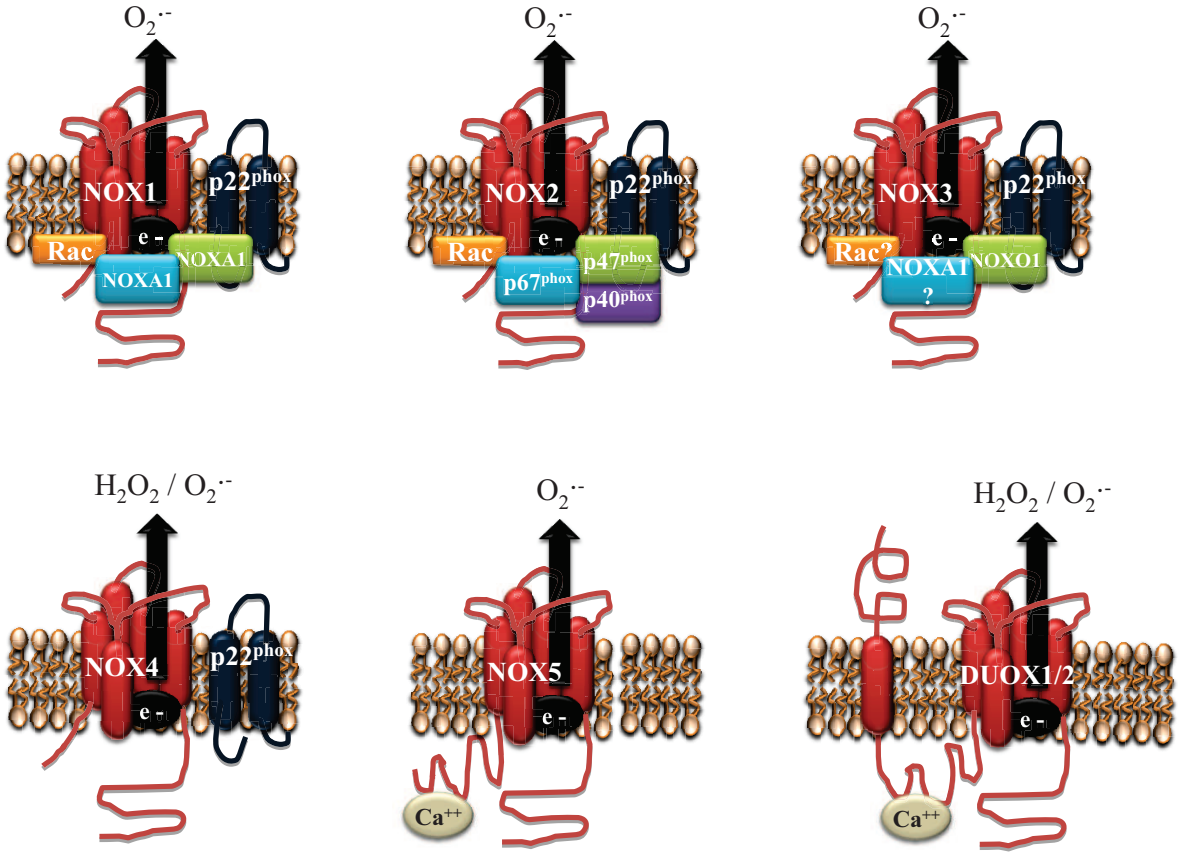

D'après[Bedard et al. 2007b].

Il existe 7 homologues (**Figure 10**) dans la famille des NADPH oxydase : NOX 1 à 5 et DUOX ("Dual oxidase") 1 et 2. NOX1, NOX2, NOX3 et NOX4 forment un dimère avec $p22^{phox}$ (phox pour "phagocytic oxidase"). De la même manière, les DUOX1 et 2 fonctionnent avec des partenaires assurant leur bonne maturation et leur adressage membranaire : les "DUOX activators" (DUOX A, la DUOX1 avec DUOX A1 et la DUOX2 avec DUOX A2). NOX1 a été la première isoenzyme de NOX2 caractérisée [Suh *et al.* 1999]. L'activité de NOX1, principalement présente dans l'épithélium du colon, les cellules

musculaires lisses vasculaires, les cellules endothéliales, l'utérus, la prostate et les ostéoclastes, est modulable par les facteurs NOXO1 et NOXA1 homologues respectifs de $p47^{phox}$ et $p67^{phox}$. L'activité de NOX3 pourrait également être stimulée par NOXO1 [Banfi et al, 2004]. L'expression de cette isoenzyme est restreinte à l'oreille interne. Contrairement aux autres membres de la famille des NADPH oxydases, NOX4 présente une activité constitutive même en l'absence de stimulus et ne semble pas activable [Martyn *et al.* 2006]. Toutefois, la "Polymerase Delta Interacting Protein-2" (poldip2) semble interagir avec NOX4 dans les cellules musculaires lisses. NOX5, dont l'activité ne requiert pas $p22^{phox}$, contient quatre domaines EF-hand de fixation du calcium sur sa partie N-terminale cytosolique [Banfi *et al.* 2001; Kawahara *et al.* 2005]. Les anions $O_2^{\bullet -}$, issus de la réduction monoélectronique de l'oxygène, sont des molécules instables. Ils semblent capables de traverser la membrane plasmique [Mao *et al.* 1992], mais exercent une toxicité directe limitée par leur dismutation en peroxyde d'hydrogène :

$$2\ O_2^{\bullet -} + 2H^+ \rightarrow O_2 + H_2O_2$$

Le peroxyde d'hydrogène est relativement stable. La toxicité de cette molécule provient de sa propension à générer le radical hydroxyle, hautement réactif, en présence de cations métalliques par la réaction de Fenton ou par réaction avec l'anion superoxyde dans la réaction d'Haber-Weiss [Wardman *et al.* 1996].

Réaction de Fenton :

$$H_2O_2 + Fe^{2+} \rightarrow OH^{\bullet} + Fe^{3+} + OH^-$$

Réaction d'Haber-Weiss :

$$H_2O_2 + O_2^{\bullet -} \rightarrow OH^{\bullet} + O_2 + OH^-$$

La myélopéroxydase, contenue dans les granules azurophiles, permet la formation de l'ion hypochlorite (ClO^-), oxydant très puissant au pouvoir bactéricide, à partir de peroxyde d'hydrogène et d'anion chlorure :

$$H_2O_2 + Cl^- \xrightarrow{\text{Myélopéroxydase}} ClO^- + O_2 + H_2O$$

L'acide hypochloreux (HOCl) peut réagir avec des amines et former des chloramines dont la la toxicité particulièrement grande résulte de sa durée de vie prolongée :

$HOCl + RNH2 \rightarrow RNHCl + H_2O$ (ou R est un groupe carbonné)

Enfin, l'association de H_2O_2 et OCl^- produit un oxygène singulet $^1O_2$:

$$H_2O_2 + ClO^- \rightarrow ClO^- + H_2O + {}^1O_2$$

3.1.2. La détoxification des ROS

Au dela d'un seuil, l'exposition aux ROS occasionne des lésions tissulaires. L'organisme possède des systèmes de régulation qui vont permettre l'élimination d'une part du peroxyde d'hydrogène par la catalase (EC 1.11.1.6) ou la glutathion peroxydase (EC 1.11.1.9) et d'autre part de l'anion $O_2^{\bullet -}$ par la superoxyde dismutase (SOD ; EC : 1.15.1.1) :

$$2H_2O_2 \xrightarrow{\text{catalase}} H_2O + O_2$$

$$H_2O_2 \xrightarrow[\text{Glutathions réduits (2 GSH)} \rightarrow \text{Glutathion oxydé (GS-SG)}]{\text{Glutathion peroxydase}} 2\ H_2O$$

Les SOD catalysent la réaction de dismutation de l'anion $O_2^{\bullet -}$ en peroxyde d'hydrogène :

$$2\ O_2^{\bullet -} + 2H+ \xrightarrow{\text{Superoxyde dismutase}} O_2 + H_2O_2$$

Il existe plusieurs isoenzymes de la SOD qui nécessitent différents cofacteurs. Le cytosol des cellules eucaryotes contient la SOD1, isoenzyme à cuivre-zinc [Afonso *et al.* 2006] alors que la SOD à manganèse est présente dans les mitochondries. La SOD3, extra-cellulaire, fonctionne également en présence de cuivre et de zinc [Stralin *et al.* 2000].

3.2. Les ROS sont engagées dans la physiopathologie de la PR

Les études épidémiologiques indiquent que la consommation de molécules anti-oxydantes réduit le risque de développer une PR. Dans une étude prospective d'une cohorte de près de 30000 femmes âgées de 55 à 69 ans, la consommation de vitamine C (acide ascorbique) ou de vitamine E (α-tocophérol) diminuait de 30% l'incidence d'une PR [Cerhan *et al.* 2003]. Ces résultats sont confortés par une étude finlandaise incluant 1419 patients adultes chez qui la probabilité de survenue d'une PR était inversement proportionnelle à la concentration plasmatique des anti-oxydants dosés dans l'essai (α-tocophérol, β-carotène et sélénium). De plus l'activité glutathion réductase, responsable de la synthèse du cofacteur de la glutathion peroxydase, le glutathion réduit, est augmentée chez les patients atteints de PR [Mulherin *et al.* 1996].

Par ailleurs il existe dans la PR une modification de l'équilibre entre les moyens de détoxification des ROS et les systèmes producteurs de ROS, en faveur de ces derniers. Le TNFα, dont la concentration est considérablement augmentée au sein du pannus rhumatoïde, est un puissant agent pré-activant la NADPH oxydase NOX2 des phagocytes [Dang *et al.* 2006]. Bien que l'IL-6 n'exerce pas cet effet pré-activateur de la NADPH oxydase du PMN [Elbim *et al.* 2006], cette cytokine induit une augmentation de la production de ROS par le synoviocyte fibroblastique [Sung *et al.* 2000]. De même le TNFα et l'IL-1β [Chenevier-Gobeaux *et al.* 2006] majorent l'activité NADPH oxydase des synoviocytes rhumatoïdes. De manière contemporaine à cette stimulation des systèmes producteurs de ROS, les médiateurs pro-inflammatoires inhibent les systèmes enzymatiques impliqués dans l'élimination des ROS. L'activité enzymatique de la SOD3, qui constitue le principal moyen de prise en charge des anions $O_2^{\bullet -}$ dans le liquide articulaire, est diminuée de moitié chez les patients souffrant de PR [Marklund 1982].

La présence de ROS dans le pannus rhumatoïde a pu être révélée par une augmentation des lésions qu'ils engendrent sur la matrice extra-cellulaire, les lipides, les protéines. L'examen du liquide articulaire et du tissu synovial de PR montre une dépolymérisation de l'acide hyaluronique [Grootveld *et al.* 1991] et de la chondroïtine sulfate [Rees *et al.* 2004] par l'anion superoxyde et l'hypochlorite. L'augmentation des résidus carbonyles traduit l'attaque radicalaire des protéines du liquide synovial de PR [Dalle-Donne *et al.* 2003] alors que l'élévation de la 8-oxo-7-déoxyguanosine dans les noyaux des lymphocytes et des PMNs circulants de PR est un stigmate des dégâts produits sur l'ADN. Il existe également des traces d'une peroxydation lipidique, accrue dans cette pathologie [Dai *et al.* 2000]. L'oxydation des

LDL ("Low Density Lipoprotein") entraîne une accumulation de ces lipides pro-inflammatoires sous l'intima vasculaire où ils sont ensuite phagocytés par les macrophages. Par ce mécanisme, les ROS participent à l'accélération de l'athérosclérose qui constitue la première cause de mortalité dans la PR [Avina-Zubieta *et al.* 2008].

3.3. Le rôle pro-inflammatoire des ROS dans les lésions de la PR

La production de ROS par les PMNs et les macrophages circulant [Ostrakhovitch *et al.* 2001] ou infiltrant [Cedergren *et al.* 2007; Eggleton *et al.* 1995] l'articulation de PR, le liquide articulaire ou la membrane synoviale de patient souffrant de PR, est nettement augmentée. La production massive au sein de l'articulation de cytokines TNFα et IL-8 est à l'origine d'une phosphorylation de $p47^{phox}$, participant à un état de pré-stimulation de la NADPH oxydase [El Benna *et al.* 2002], couramment dénommé "*priming*", qui autorise une production de ROS plus rapide et plus intense en réponse à un deuxième stimulus. Plusieurs résultats expérimentaux indiquent que l'augmentation de la production de ROS au sein du pannus rhumatoïde est un élément majeur dans l'étiopathogénèse de la réaction auto-immune et de la protéolyse matricielle [Kaur *et al.* 1996] à l'origine de la destruction articulaire de la PR [Allen *et al.* 1989; Blake *et al.* 1989; Merry *et al.* 1991].

Les ROS engendrent la dépolymérisation de l'acide hyaluronique de haut poids moléculaire (environ 10^6 kDa), en molécules de bas poids moléculaire (environ 0,2 x 10^6 kDa) aux propriétés pro-inflammatoires susceptibles de stimuler les récepteurs de l'immunité innée TLR-2 [Scheibner *et al.* 2006] et ainsi de promouvoir une réponse inflammatoire. Ces fragments, produits par la dépolymérisation de l'acide hyaluronique par les ROS, sont ainsi assimilables à de véritables signaux de danger à l'instar des polysaccharides bactériens et des nucléotides viraux [Matzinger 2002b]. De plus, la dépolymérisation de l'acide hyaluronique altère les propriétés rhéologiques du liquide articulaire. La diminution de viscosité du liquide articulaire de PR est responsable d'une modification de la répartition biomécanique des charges sur le cartilage articulaire, accélérant sa dégradation. Dans l'arthrose, l'injection intra-articulaire d'acide hyaluronique de haut poids moléculaire diminue la production d'IL-8 et de NO Synthase endothéliale en l'absence de stimulation cellulaire. Lors d'une stimulation par l'IL-1β, l'acide hyaluronique bloque la transcription de l'aggrécanase et du TNFα.

En plus de la diminution de viscosité du liquide articulaire, les ROS modifient la fonction chondrocytaire et contribuent à la dégradation cartilagineuse par un mécanisme direct de chondrolyse et un mécanisme indirect d'induction des protéases dégradant la matrice extra-cellulaire (**Figure 11**). La diminution de viabilité du chondrocyte, alors incapable de pallier la

dégradation physiologique de la matrice extra-cellulaire, est un phénomène important dans le développement des lésions cartilagineuses [Hashimoto *et al.* 1998]. La production d'anions $O_2^{\bullet -}$ et radicaux hydroxyles est responsable de l'apoptose des chondrocytes dans la PR, vraisemblablement en favorisant la formation du peroxynitrite $ONOO^-$ [Del Carlo *et al.* 2002]. De plus, la production de ROS conduit à une diminution de synthèse de la matrice extra-cellulaire par les cellules résidantes de l'articulation. Le peroxyde d'hydrogène H_2O_2 inhibe la synthèse de protéoglycane par le chondrocyte [Vincent *et al.* 1989] en freinant la glycolyse au niveau de la glycéraldéhyde-3-phosphate déshydrogénase [Baker *et al.* 1989]. Dans l'étude du modèle murin de souris invalidées pour le gène codant pour l' "Insuline Growth Factor" (IGF)-1, le $NO^{\bullet}$ diminue la sensibilité du chondrocyte à ce facteur de croissance. En outre, les ROS sont impliqués dans l'expression et l'activation de la collagénase pro-MMP-1 par la lignée chondrocytaire C20-A4 stimulée par l'IL1-β [Grange *et al.* 2006].

Certains auteurs ont d'ailleurs proposé de cibler la production de ROS pour diminuer l'inflammation et réduire l'importance de l'arthrite. Kröger *et al.* ont analysé l'impact du traitement par la N-acétyl-L-cystéine dans le modèle murin d'arthrite au collagène [Kroger *et al.* 1997]. Un traitement systémique par 50 mg/kg de cette molécule permettrait une diminution de l'inflammation articulaire de manière dose-dépendante, corrélant avec une baisse de production de ROS des monocytes et des PMNs murins. Un traitement par l'α-tocophérol, dans le modèle murin transgénique KRN/NOD [De Bandt *et al.* 2002] a permis de diminuer les destructions articulaires, alors que dans le modèle MRL/lpr, cet anti-oxydant fait chuter le taux sérique de cytokines pro-inflammatoires [Venkatraman *et al.* 1999]. Ces résultats prometteurs dans les modèles murins de rhumatismes inflammatoires ont du mal à être reproduits chez l'homme [Edmonds *et al.* 1997]. Le seul type d'alimentation ayant fait la preuve de son efficacité dans la PR est le régime crétois [Hagfors *et al.* 2003; Skoldstam *et al.* 2003], riche en anti-oxydants. Cependant, l'amélioration clinique ne semble pas corrélée avec l'augmentation du statut sérique en anti-oxydants.

Figure 11. Implication des ROS dans les lésions de la Polyarthrite Rhumatoïde

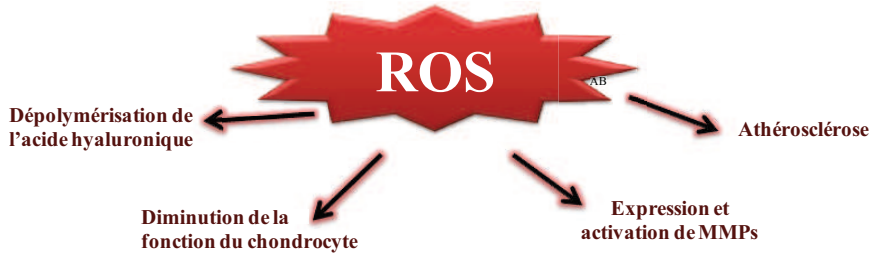

3.4. Rôles physiologiques et anti-inflammatoires de certains ROS

Le dogme des propriétés uniquement pro-inflammatoires des ROS est remis en question par l'analyse du phénotype des patients souffrant de granulomatose septique. Ces malades, chez qui la production de ROS par la NADPH oxydase des phagocytes est effondrée, montrent des signes d'hyper-inflammation et même d'auto-immunité.

Des arthralgies sont constatées chez 37% [Cale *et al.* 2007] des mères porteuses de l'allèle mutée du gène CYBB (chromosome Xp21) codant pour NOX2. De plus, la probabilité de développer des symptômes auto-immuns évocateurs de PR [Lee *et al.* 1994] et de lupus érythémateux disséminé [Winkelstein *et al.* 2000] est augmentée chez les patients atteints de granulomatose septique chronique (CGD pour "Chronic Granulomatous Disease", cf. paragraphe 4.2.).

L'étude du modèle murin de CGD suggère également un effet protecteur des ROS sur le développement des phénomènes auto-immuns et en précise les mécanismes cellulaires. Les souris déficientes en protéines NOX2 et $p47^{phox}$ présentent une réaction inflammatoire paradoxalement accrue après une injection de 50µg de lipopolysaccharide (LPS), par rapport aux souris C57BL/6J sauvages servant de contrôle. Chez les souris Ncf1, portant une mutation du gène de $p47^{phox}$, la susceptibilité de développer une arthrite induite par le collagène est augmentée parallèlement à l'effondrement de la production de ROS. Dans ce modèle murin, il est suggéré que la production physiologique de ROS module l'activité des lymphocytes T après contact avec la cellule présentatrice de l'antigène et induit l'apoptose de lymphocytes T auto-réactifs [Van der Veen *et al.* 2000]. Les mécanismes responsables sont probablement multiples et complexes. Une hypothèse est que la production physiologique de ROS module la "synapse immunologique" entre le lymphocyte T et la cellule présentatrice de l'antigène. Des lésions oxydatives du CD4 [Peterson *et al.* 1998] et des molécules impliquées dans la transduction du signal du TCR ("T Cell Receptor") comme la protéine LAT ("Linker for Activation of T cells" [Gringhuis *et al.* 2002]) ou ZAP-70 modulent la polarisation de la réponse du lymphocyte CD4+. De plus, les anions $O_2^{\bullet -}$ produits par NOX2 dans le phagosome des cellules dendritiques semblent essentiels pour l'alcalinisation du pH et un apprêtement antigénique optimal pour le lymphocyte CD8+ [Savina *et al.* 2006].

Bien que les produits de dégradations par les ROS de la matrice extra-cellulaire concourent à l'initiation et l'amplification de la réponse inflammatoire, ils peuvent également engendrer des modifications post-traductionnelles de molécules pro-inflammatoires, dont certains signaux de danger, prévenant l'expansion de l'inflammation. Les travaux de l'équipe de Carolyn Geczy supportent cette idée que l'oxydation des protéines S100A8/A9 par les ROS

leur confère des propriétés anti-inflammatoires. Contrairement aux protéines cytosoliques, maintenues dans un milieu fortement réducteur, la protéine S100A8 secrétée dans le milieu extra-cellulaire devenu oxydant par l'action des ROS est exposée à des nitrosylations. S100A8 nitrosylée est assimilable à une cytokine des PMNs et des monocytes. S100A8 nitrosylée retarde l'afflux des leucocytes de la microcirculation sur le site inflammatoire [Lim *et al.* 2008]. Cette commutation des propriétés chimiotactiques de S100A8 en fonction de son statut redox pourrait s'intégrer dans un mécanisme de résolution de l'inflammation. En effet, il est maintenant établi que les protéines cytosoliques S100A8/A9 sont des régulateurs positifs de l'activité oxydase [Berthier *et al.* 2003] et que leur production est dépendante des ROS [Grimbaldeston *et al.* 2003]. Les ROS, produits par les phagocytes stimulés, modifient l'équilibre redox du site inflammatoire favorisant l'émergence de molécules anti-inflammatoires telles que la S100A8 nitrosylée.

4. La NADPH oxydase des phagocytes : un système enzymatique multimérique

La NADPH oxydase (EC 1.6.99.6) est un complexe enzymatique multiprotéique formé d'un élément membranaire, le cytochrome b_{558} et de protéines cytosoliques $p40^{phox}$, $p47^{phox}$, $p67^{phox}$ s'assemblant selon une stœchiométrie 1 : 1 : 1 dans le cytosol de phagocytes activés [Lapouge *et al.* 2002]. Une protéine G monomérique appartient au complexe : Rac1 pour les monocytes ou Rac2 pour les PMNs. Une autre protéine G, Rap1A, colocalise avec le cytochrome b_{558} [Quinn *et al.* 1992] et semble, *in vitro*, en augmenter l'activité [Bokoch *et al.* 1991]. Cependant son rôle n'a pas encore été clairement élucidé.

4.1. La NADPH oxydase des phagocytes : un système de transport des électrons

En 1884, Mac Munn décrivait pour la première fois les propriétés spectrales de pigments, les cytochromes, et proposait une classification en fonction de leur signature spectrale dans l'ultra-violet à l'état réduit. Le cytochrome b_{558}, cœur catalytique de la NADPH oxydase des phagocytes, doit son nom à son spectre d'absorption comprenant une bande α à 558 nm. Il est formé par l'hétérocomplexe NOX2 (anciennement appelé $gp91^{phox}$) et $p22^{phox}$, assemblés selon une stœchiométrie 1:1 [Wallach *et al.* 1996], et par un groupe prosthétique ferro-protoporphyrine IX contenant un atome de fer. Dans les neutrophiles au repos, 20% du cytochrome b_{558} sont dans la membrane plasmique, les 80% restants étant retrouvés dans la membrane des granules spécifiques, des granules riches en gélatinase et dans la membrane des vésicules secrétoires. Après stimulation, on détecte le cytochrome b_{558} principalement dans la membrane plasmique [Borregaard *et al.* 1983].

4.2. La granumolatose septique chronique : modèle d'étude de la NADPH oxydase des phagocytes

La granulomatose septique chronique (CGD, "Chronic Granulomatous Disease") est une immunodéficience primaire d'origine génétique, affectant 1/250000 personnes. Elle est caractérisée par un déficit de microbicidie des phagocytes lié à un défaut d'activité de la NADPH oxydase. Elle occasionne des infections itératives fungiques et bactériennes graves. La forme la plus fréquente concerne la CGD à transmission liée à l'X. Dans ce cas, le cytochrome b_{558} est le plus souvent indétectable [Segal 1987]. On parle de CGD X^0. Mais le cytochrome b_{558} peut être présent en quantité réduite lors d'une $CGDX^-$ [Stasia *et al.* 2003] ou en proportion normale mais avec toutefois un déficit fonctionnel dans le cas de la $CGDX^+$ [Cross *et al.* 1995].

Les formes autosomales récessives touchant le gène codant pour $p47^{phox}$ représentent près de 20% des CGD alors que celles affectant l'expression de $p22^{phox}$ et $p67^{phox}$ comptent chacune pour moins de 5% de la population atteinte [Cross *et al.* 2000]. Un seul cas de CGD liée à une mutation du gène codant pour $p40^{phox}$ [Matute *et al.* 2009] a été rapporté.

4.3. NOX2, cœur catalytique du cytochrome b_{558}

4.3.1. Les différents sites de NOX2 impliqués dans le transport d'électron

NOX2 est une protéine de 570 acides aminés codée par le gène CYBB (chromosome Xp21.1) qui contient 13 exons [Royer-Pokora *et al.* 1986]. Le transcrit de 5kb est traduit en une protéine de 65 kDa (gp65) au niveau du réticulum endoplasmique [Porter *et al.* 1996]. Cette protéine sera massivement glycosylée sur 3 asparagines (Asn^{131}, Asn^{148}, Asn^{239}) dans l'appareil de Golgi [Yu *et al.* 1999]. La masse apparente de 91kDa, déterminée après migration électrophorétique, a donné son nom à la protéine mature. L'analyse de la structure primaire permet de prédire 6 passages transmembranaires et une queue cytosolique supportant les différents sites nécessaires au transfert d'électron depuis son substrat le NADPH jusqu'à l'oxygène (**Figure 12**). L'homologie de séquence avec les ferrédoxines NADP réductases indique 2 sites putatifs de liaison du FAD sur la queue cytosolique de NOX2 : ^{338}HPFTLSA^{342} et ^{354}IRIVGD^{359} [Taylor *et al.* 1993]. Il existe 4 sites potentiels de fixation du NADPH sur la partie C-terminale de NOX2. D'abord, on constate un motif riche en glycine ^{405}MLVGAGIGVTPF^{416} qui autorise des liaisons hydrogènes avec le pyrophosphate du NADPH, alors que le double motif Cys^{537}-Gly^{538} pourrait fixer le nicotinamide [Rosengren *et al.* 2010; Sumimoto *et al.* 1992]. Enfin deux autres motifs, ^{442}YWLCR^{446} et ^{504}GLKQ^{507}, sont susceptibles d'interagir par des liaisons faibles contractées avec le ribose ou l'adénine du

NADPH (**Figure 12**).

L'incubation de pseudo-neutrophiles PLB985 en présence d'inhibiteur de la synthèse de l'hème, le succinyl acétone, montre que l'incorporation de deux hèmes, au sein du noyau protoporphyrine, est indispensable à la stabilisation de NOX2 et à la formation de l'hétérodimère NOX2/p22^{phox} [Yu *et al.* 1997]. Quatre résidus histidines, situés sur le troisième (His^{101} et His^{115}) et le cinquième passage transmembranaire (His^{209} et His^{222}) de NOX 2, coordonnent l'atome de fer contenu dans chacun des 2 hèmes.

Figure 12. NOX2, cœur catalytique du cytochrome b_{558}

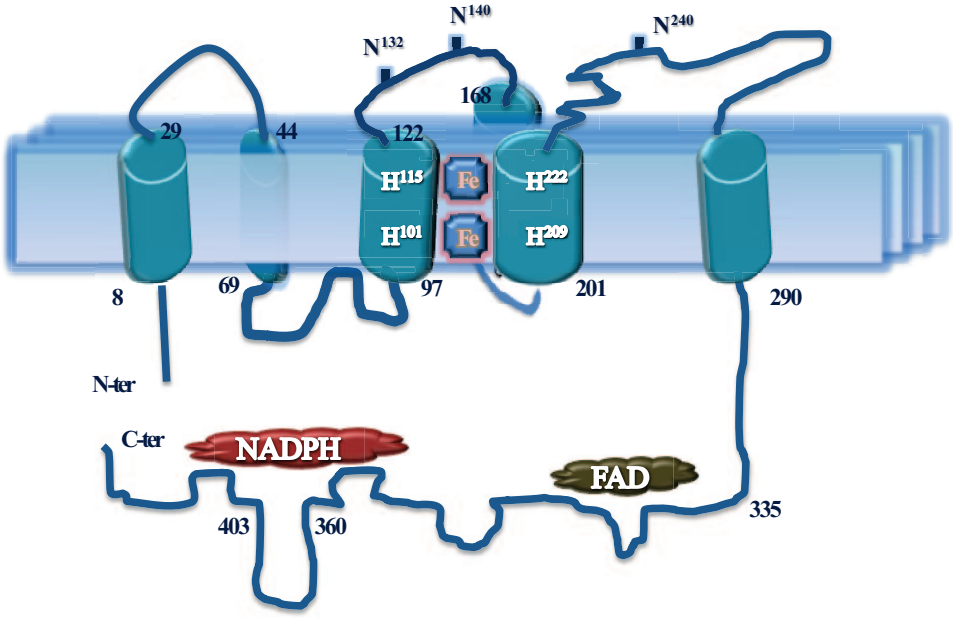

NOX2 est une protéine transmembranaire comprenant une partie C-terminale et N-terminale cytosoliques séparée par 6 hélices α. Les domaines de liaison au NADPH et au FAD sont figurés ainsi que les 4 Histidines des 3° et 5° passages transmembranaires permettant la coordination des noyaux hèmes contenant un atome de fer. Trois Asparagines sont glycosylées. D'après [Stasia et al. 2009] et [El-Benna et al. 2010].

4.3.2. Le processus de transport d'électron

Plusieurs étapes sont nécessaires au transfert des deux électrons du NADPH vers l'oxygène pour former les anions $O_2^{\bullet -}$. La première phase consiste en un transfert de deux électrons du NADPH vers le FAD. Un premier électron est délivré par le $FADH_2$ vers l'hème de plus bas potentiel redox qui le tranfère ensuite au deuxième hème. L'hème externe permet la production d'une première molécule d'anion $O_2^{\bullet -}$ par réduction monoélectronique de dioxygène (**Figure 13**). Puis un autre électron du FAD$^{\bullet}$ est transféré à une autre molécule d'oxygène *via* le premier puis le deuxième hème [Cross *et al.* 2004; Vignais 2002]. Des expériences de mutagénèse dirigée attestent que l'His^{338} joue un rôle capital dans la liaison du FAD au cytochrome b_{558} [Yoshida *et al.* 1998].

L'activité diaphorase, correspondant au transfert d'électron depuis le NADPH vers le FAD, est stimulable par la liaison de $p67^{phox}$ [Han *et al.* 2001] et de Rac [Nisimoto *et al.* 2004] sur NOX2.

Figure 13. Le processus de transport électronique du cytochrome b_{558}

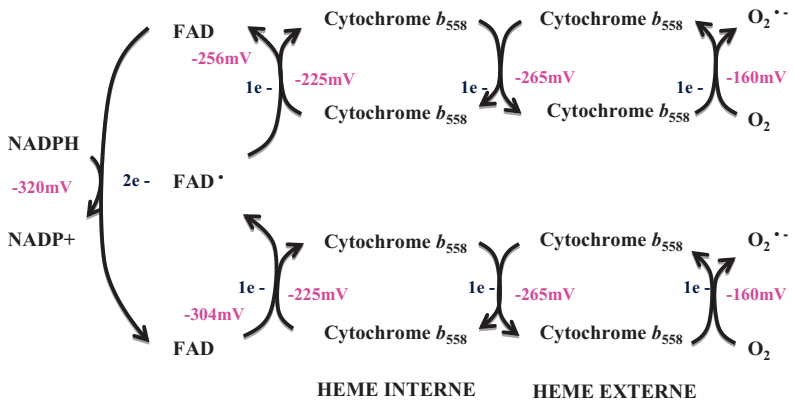

Les potentiels redox sont indiqués en rose. D'après [Vignais 2002] et [Cross et al. 2004].

4.4. $p22^{phox}$, partenaire de NOX2

L'analyse du génotype de patients atteints de CGD autosomale récessive a permis de caractériser le gène CYBA, formé de 6 exons, codant pour $p22^{phox}$. Il est situé sur le bras long du chromosome (16q24). La protéine $p22^{phox}$, contient 195 acides aminés (**Figure 14**).

Figure 14. Les domaines fonctionnels de $p22^{phox}$

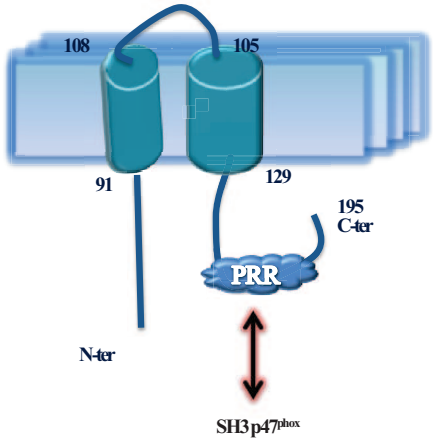

PRR="Prolin Rich Region", SH3="Src homology domain 3". D'après [El-Benna et al. 2010].

$P22^{phox}$ est essentielle à la maturation et à la stabilité de NOX2 [DeLeo *et al.* 2000] ainsi qu'à l'activation de l'oxydase. La protéine $p22^{phox}$ contient 2 passages transmembranaires et une région cytosolique riche en proline du côté C-terminal au niveau de laquelle se fixe la région SH3 ("Src homology domain 3") de $p47^{phox}$.

4.5. p67^{phox}, activateur du cytochrome b_{558}

La séquence primaire de p67^{phox} est composée de 526 acides aminés. Le gène NCF2 de 16 exons, codant pour cette protéine, est localisé sur le bras court du chromosome 1 (1q25) [Francke *et al.* 1990]. Plusieurs de ces domaines semblent indispensables à l'activation de l'oxydase. Du côté N-terminal, 4 motifs TPR ("Tetratricopeptide Repeat") confèrent à la protéine une structure compacte [Koga *et al.* 1999] et permettent l'interaction avec Rac selon une stœchiométrie 1 :1 [Ahmed *et al.* 1998; Lapouge *et al.* 2000]. Le domaine activateur indispensable à l'initiation du transfert d'électron [Han *et al.* 1998] est inclus entre les résidus 199 et 210. Le motif riche en proline (PRR, "Proline Rich Region"), porte le résidu Thr^{233} phosphorylable, et permet la liaison du domaine SH3 de p47^{phox}. Deux motifs SH3, au niveau des résidus 242-299 et 457-516 [Durand *et al.* 2010], sont impliqués dans la translocation de p67^{phox} via l'interaction avec le domaine PRR de p47^{phox} (**Figure 15**). Le domaine PB1 ("Phox and Bem1") de p67^{phox} engage des liaisons électrostatiques avec p40^{phox} [Ito *et al.* 2001; Nakamura *et al.* 1998]. Enfin, l'étude de la séquence primaire de p67^{phox} suggère l'existence de plusieurs sites putatifs de fixation du NADPH [Dang *et al.* 1999a; Dang *et al.* 2000; Smith *et al.* 1989] par des expériences d'affinité avec du NADPH dialdéhyde radioactif [Smith *et al.* 1996].

Figure 15. p67^{phox}, activateur de la NADPH oxydase

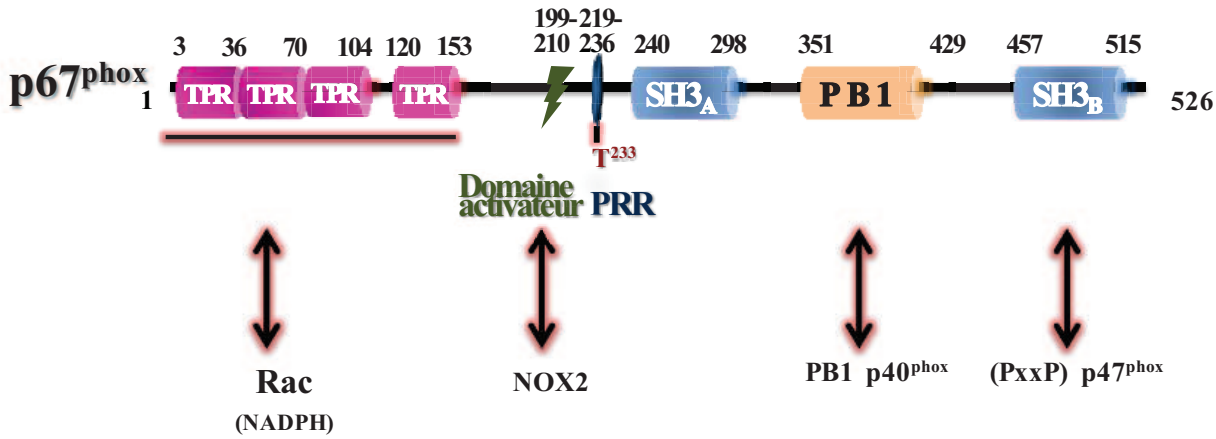

Domaines structuraux de p67^{phox} : PB1="Phox and Bem1", PRR="Proline Rich Region", TPR="Tetratricopepide Repeat", SH3="Src Homology domain 3", la Thr^{233} est figurée au niveau du site PRR. D'après [Groemping et al. 2005].

4.6. p47^{phox}, adaptateur du complexe NADPH oxydase

Le gène NCF1 est situé sur le bras long du chromosome 7 au locus 7q11.23 [Lomax *et al.* 1989]. Il code pour une protéine de 390 acides aminés orchestrant la translocation des facteurs cytosoliques [Heyworth *et al.* 1991]. Cependant la présence de p47^{phox} n'est pas nécessaire pour l'activation de l'oxydase dans un système acellulaire [Freeman *et al.* 1996; Koshkin *et al.* 1996]. Il existe quatre domaines fonctionnels importants [Groemping *et al.* 2005]. Deux domaines SH3 (résidus 156-215 et 226-285) sont impliqués dans les interactions avec p67^{phox} et p22^{phox} [Sumimoto *et al.* 1994] (**Figure 16**). La région riche en proline PRR (acides aminés 360-369) et le domaine auto-inhibiteur (AIR, "Auto-Inhibitory Region" : acides aminés 292-340) maintiennent, en l'absence de stimulation, la protéine p47^{phox} en conformation repliée par des interactions intra-moléculaires avec le tandem de domaines SH3 [Yuzawa *et al.* 2004]. Enfin le domaine PX, ("Phox homology") permet l'ancrage de p47^{phox} à la membrane plasmique par l'interaction avec les phosphoinositides membranaires [Kanai *et al.* 2001].

Figure 16. p47^{phox}, adaptateur de l'assemblage de la NADPH oxydase

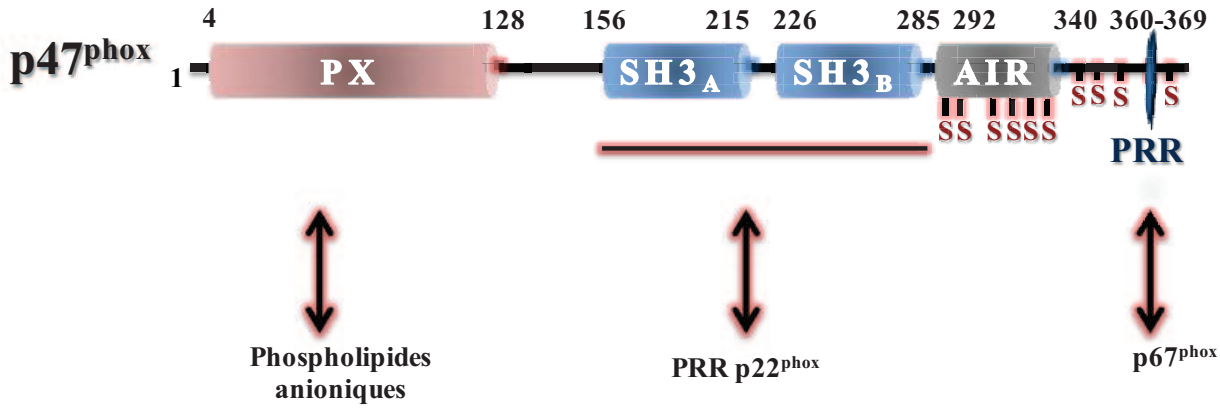

Domaines structuraux de p47^{phox} : PX="Phox homology", AIR="Auto-Inhibitory Region", PB1="Phox and Bem1", PRR="Proline Rich Region", SH3="Src Homology domain 3". Les sérines phosphorylables de la région C-terminale sont figurées. D'après [Groemping et al. 2005].

4.7. p40^{phox}, partenaire d'activation de la NADPH oxydase phagocytaire

La protéine p40^{phox} est composée de 339 acides aminés. Le gène de 10 exons codant pour cette protéine est localisé sur le bras long du chromosome 22 au locus 22q13.1. Trois domaines permettent une interaction avec les autres protéines de l'oxydase des phagocytes. Le domaine PB1 (acides aminés 237-329) est susceptible de lier les régions SH3 de p67^{phox} [Nakamura *et al.* 1998] mais pourrait engager des interactions intra-moléculaires avec le domaine C-terminal PX (acides aminés 24-143) liant spécifiquement le phosphatidylinositol-3-phosphate membranaire [Zhan *et al.* 1996]. Enfin un domaine SH3 (acides aminés 237-228)

est susceptible de lier le domaine PRR de $p22^{phox}$ [Tamura *et al.* 2007]. Au repos, le domaine PX C-terminal et PB1 N-terminal de $p40^{phox}$ engage une liaison intra-moléculaire, conférant à la protéine une conformation repliée [Ueyama *et al.* 2007] (**Figure 17**). Le rôle de $p40^{phox}$ dans l'activation de l'oxydase a longtemps été source de débat. La découverte d'un cas de granulomatose septique par mutation d'un acide aminé du domaine PX ($p40^{phoxR105Q/-}$) [Matute *et al.* 2009]) ainsi que la mise au point de modèles murins invalidés pour $p40^{phox}$ [Chessa *et al.* 2010] ont permis de souligner le rôle activateur de cette molécule dans l'assemblable du complexe oxydase.

Figure 17. $p40^{phox}$, partenaire d'activation de la NADPH oxydase phagocytaire

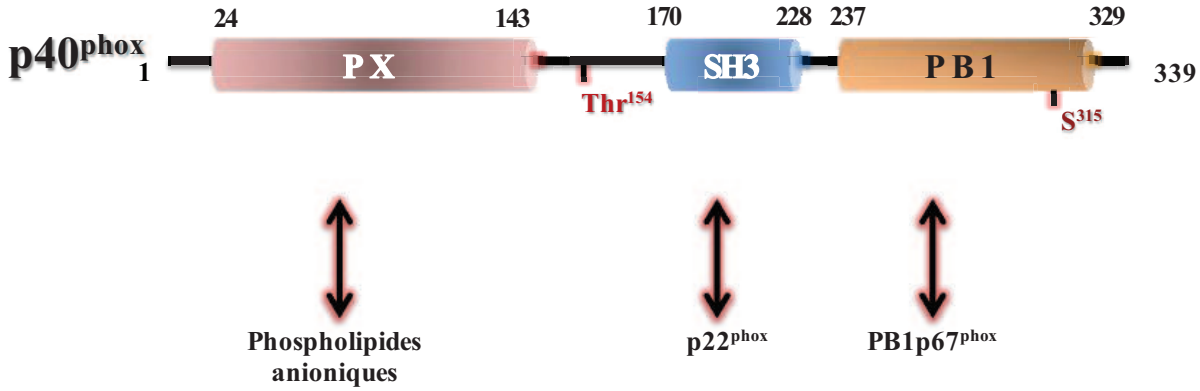

Domaines structuraux de $p40^{phox}$: PX="Phox homology", PB1="Phox and Bem1", PRR="Proline Rich Region", SH3="Src Homology domain 3". Les sites de phosphorylation Thr^{154} et de la Ser^{315} sont figurés. D'après [Groemping et al. 2005].

4.8. La protéine G monomérique Rac

Les protéines Rac sont des petites protéines G monomériques, à activité GTPase. Les trois isoenzymes Rac1, Rac2 et Rac3 appartiennent à la sous-famille Rho des protéines Ras. La protéine Rac3 est exprimée, chez l'homme, dans le cœur, le placenta et le pancréas ainsi que dans des lignées cellulaires de leucémie myéloïde, de carcinome mammaire, [Haataja *et al.* 1997]. L'expression de Rac1 est ubiquitaire alors que celle de Rac2 est restreinte à la lignée myéloïde. Ces 2 isoformes, de 192 acides aminés, présentent 92% d'homologie [Didsbury *et al.* 1989]. Dans le neutrophile humain, c'est Rac2 dont le locus est situé sur le chromosome 22 (22q13.1) qui est la forme prédominante permettant d'activer la NADPH oxydase [Knaus *et al.* 1991]. Du coté N-terminal, il existe deux domaines d'amorçage dont la conformation dépend de la liaison au GDP ou au GTP. L'association avec la protéine cytosolique RhoGDI ("Rho GDP dissociation inhibitor") permet le maintien de Rac2 sous une forme inactive liée au GDP. Après la dissociation de RhoGDI [Geiszt *et al.* 2001], Rac2 peut lier et hydrolyser le

GTP. Le changement de conformation qui s'ensuit permet à Rac de lier $p67^{phox}$ [Nisimoto et al, 1997]. Le domaine impliqué dans l'interaction avec NOX2 est compris entre les résidus 124 et 135. La translocation de Rac à la membrane plasmique est réalisée de manière indépendante de $p47^{phox}$ et $p67^{phox}$ [Kwong *et al.* 1993]. Le domaine C-terminal polybasique et une queue géranylgéranyl permettent d'ancrer Rac à la membrane plasmique (**Figure 18**).

Figure 18. Rac, la petite proteine G monomérique

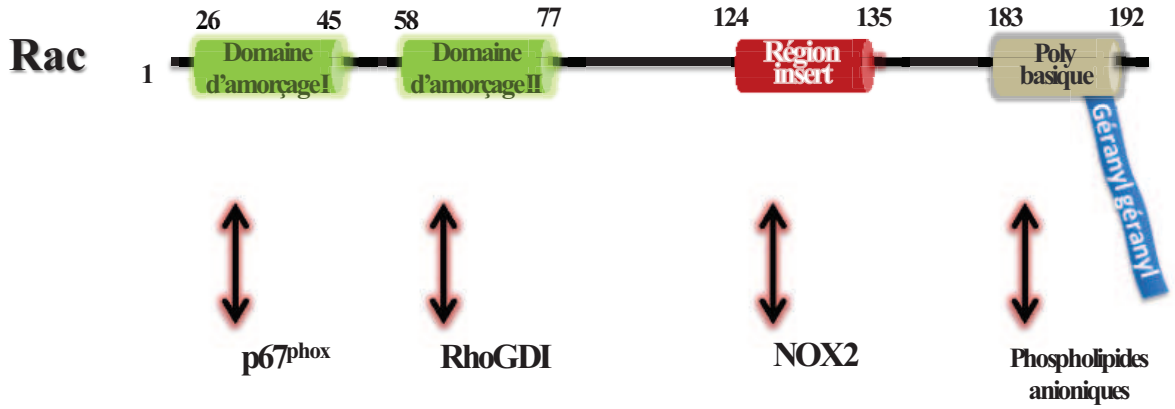

5. Mécanismes d'activation de la NADPH oxydase des phagocytes

La production transitoire et considérable de ROS par le PMN nécessite une étroite régulation. De nombreux mécanismes contrôlent l'initiation, la maintenance et la terminaison de l'explosion oxydative.

L'ensemble des facteurs du complexe NADPH oxydase doit être assemblé pour que le cytochrome b_{558} adopte une conformation active nécessaire à une production de ROS optimale. La phosphorylation des facteurs cytosoliques de la NADPH oxydase, et en particulier de $p47^{phox}$, permet de développer des interactions protéines-protéines ou protéines lipides impliquées dans l'assemblage et l'activation du complexe.

Lorsqu'il existe un défaut d'assemblage du complexe NADPH oxydase, l'activation n'est pas correcte. La substitution de l'Ile^{152} proche du domaine SH3 de $p47^{phox}$ par une alanine ne modifie pas la migration à la membrane des facteurs cytosoliques. Cependant cette mutation engendre une diminution de l'activité NADPH oxydase en affectant l'interaction entre les différentes protéines du complexe NADPH oxydase [Taura *et al.* 2009].

L'activité NADPH oxydase diffère en fonction de la compartimentation subcellulaire et de la répartition en microdomaines. En outre, l'activité catalytique est modulée par des phosphorylations de NOX2, par la disponibilité en substrat, par le cytosquelette, par l'acide arachidonique, par le flux de calcium et par des régulateurs allostériques coopératifs.

Une attention toute particulière s'est récemment portée sur les mécanismes de terminaison de l'explosion oxydative du neutrophile. Ainsi, la phosphorylation du résidu Ser^{379} de $p47^{phox}$ cause la dissociation de l'hétérocomplexe $p47^{phox}/p67^{phox}$ et contribue à l'arrêt de l'activité oxydase [Mizuki *et al.* 2005]. Toutefois, nous n'examinerons pas les évènements relatifs à l'interruption de l'activité enzymatique pour nous focaliser sur les mécanismes moléculaires de l'activation.

5.1. Pré-activation de la NADPH oxydase

Lorsqu'on incube des phagocytes avec de faibles concentrations de cytokines, telles que le TNFα, la chimiokine IL-8, le facteur de croissance GM-CSF [Elbim *et al.* 1994] et G-CSF [Khwaja *et al.* 1992] ainsi que le LPS [Ward *et al.* 2000], la NADPH oxydase NOX2 est pré-activée (**Tableau 1**). La production de réponse à une deuxième stimulation est potentialisée.

Tableau 1. Tableau synoptique des études de la pré-activation de NOX2

Etudes	*Stimulus pré-activateur*	*Durée*	*Stimulus activateur*	*Lignée cellulaire*	Mesure de production de ROS	*Résultats*
Khwaja *et al.* 1992	TNFα 5-500U/ml GM-CSF 0,05-1ng/ml GCSF10ng/ml	45min	fMLP 1µM C5a 10ng/ml	PMNs humains	Cytométrie en flux DCFH-DA	*- Pré-activation avec TNFα et GM-CSF* *-Pré-activation modeste avec G-CSF*
Elbim et al. 1994	TNFα 100U/l GM-CSF 100U/l IL-8 50ng/ml IL-6 100U/l IL-1β 100U/l	30min	fMLP 1µM	PMNs humains	Cytométrie en flux DCFH-DA	*- Pré-activation avec TNFα et GM-CSF > IL-8* *- Pas de pré-activation avec IL-6, IL1α et IL-1β*
Dang *et al.* 1999b	GMCSF 500pM	20min	fMLP 0,1µM	PMNs humains	Réduction cytochrome *c* sensible à la SOD	*- Pré-activation par phosphorylation de $p47^{phox}$ impliquant PI3-Kinase facilite la translocation à la membrane après stimulation par le fMLP*
Cadwallader *et al.* 2002	TNFα 200U/ml GM-CSF 100ng/ml PAF 1µg/ml	30min 10min	fMLP 100nM	PMNs humains	Réduction cytochrome *c* sensible à la SOD	*- Pré-activation par le TNFα et GM-CSF corréleé à une augmentation de l'activité PI3-Kinase*
Ward et al. 2000	TNFα 200U/ml LPS 100 ng/ml	10min	- fMLP 0,1µM - *S. aureus* 10^8/ml	PMNs humains	Cytométrie en flux DCFH-DA Réduction cytochrome *c* sensible à la SOD	*- Pré-activation par mobilisation du cytochome b_{558} à la membrane plasmique dépendante de p38 MAPK*
Dang *et al.* 2006	TNFα 10ng/ml GM-CSF 12ng/ml	20min	fMLP 0,1µM	-PMNs humains -PMNs du liquide synovial dePR	Réduction cytochrome *c* sensible à la SOD Chimiluminescence (luminol)	*- Pré-activation par TNFα et GM-CSF entraîne la phosphorylation du résidu Ser^{345} de $p47^{phox}$ par p38 MAPK* *- PMNs du liquide synovial de PR sont pré-activés*
Boussetta *et al.* 2010	TNFα 20ng/ml	20min	fMLP 0,1µM	PMNs humains	Chimiluminescence (luminol)	*- Liaison de Pin1 à Ser^{345} de $p47^{phox}$, induisant un changemant de conformation qui favorise une phosphorylation ultérieure par la PKC*
Brechard *et al.* 2005	IL-8 10nM	10 min	fMLP 1µM	HL60	Fluorométrie (Amplex red)	*- Pré-activation par l'IL-8 est en partie médiée par l'élévation de la concentration intra-cellulaire en Ca^{++}*

C5a=fraction 5a du complément (anaphylatoxine), DCFH-DA="Dichlorofluorescin diacetate", IL=Interleukine, fMLP=N-formyl-Méthionyl-Leucyl-Phénylalanine, GCSF= "Granulocyte-Colony Stimulating Factor", GMCSF="Granulocyte Macrophage-Colony Stimulating Factor", PAF="Platelet Activating Factor" PI3-Kinase="phosphatidylinositol 3-kinase", PKC= Protéine-Kinase C, Pin1=proline isomérase1, PMN="Polymorphonuclear neutrophil", S. aureus=Staphylococcus aureus, SOD=Superoxyde Dismutase, TNFα="Tumor Necrosis Factor α".

Plusieurs mécanismes sont évoqués pour expliquer cet amorçage. La phosphorylation partielle de $p47^{phox}$ semble un évènement important dans ce mécanisme [Dang *et al.* 1999b]. En réponse à une stimulation par le TNFα, la proline isomérase Pin-1, interagit avec la Ser^{345} de $p47^{phox}$, phosphorylée par les p38 ou ERK1/2 MAP-Kinases induisant un changement de conformation qui favorise une phosphorylation ultérieure par la PKC [Boussetta *et al.* 2010] (**Figure 19**). Il est vraisemblable que d'autres mécanismes favorisent cette pré-activation de la NADPH oxydase. Lors d'une stimulation par des doses suboptimales de TNFα, l'expression des récepteurs au fMLP est augmentée [McColl *et al.* 1990] et la concentration de cytochome b_{558} est accrue à la membrane classique par le recrutement des granules [Ward *et al.* 2000]. Dans les HL-60 différenciés en pseudo-neutrophiles, la pré-stimulation par IL-8 entraîne un afflux de calcium responsable de l'augmentation de production de ROS par NOX2 en réponse au fMLP [Brechard *et al.* 2005].

Figure 19. Phosphorylation de $p47^{phox}$ lors de la pré-activation et l'activation de la NADPH oxydase

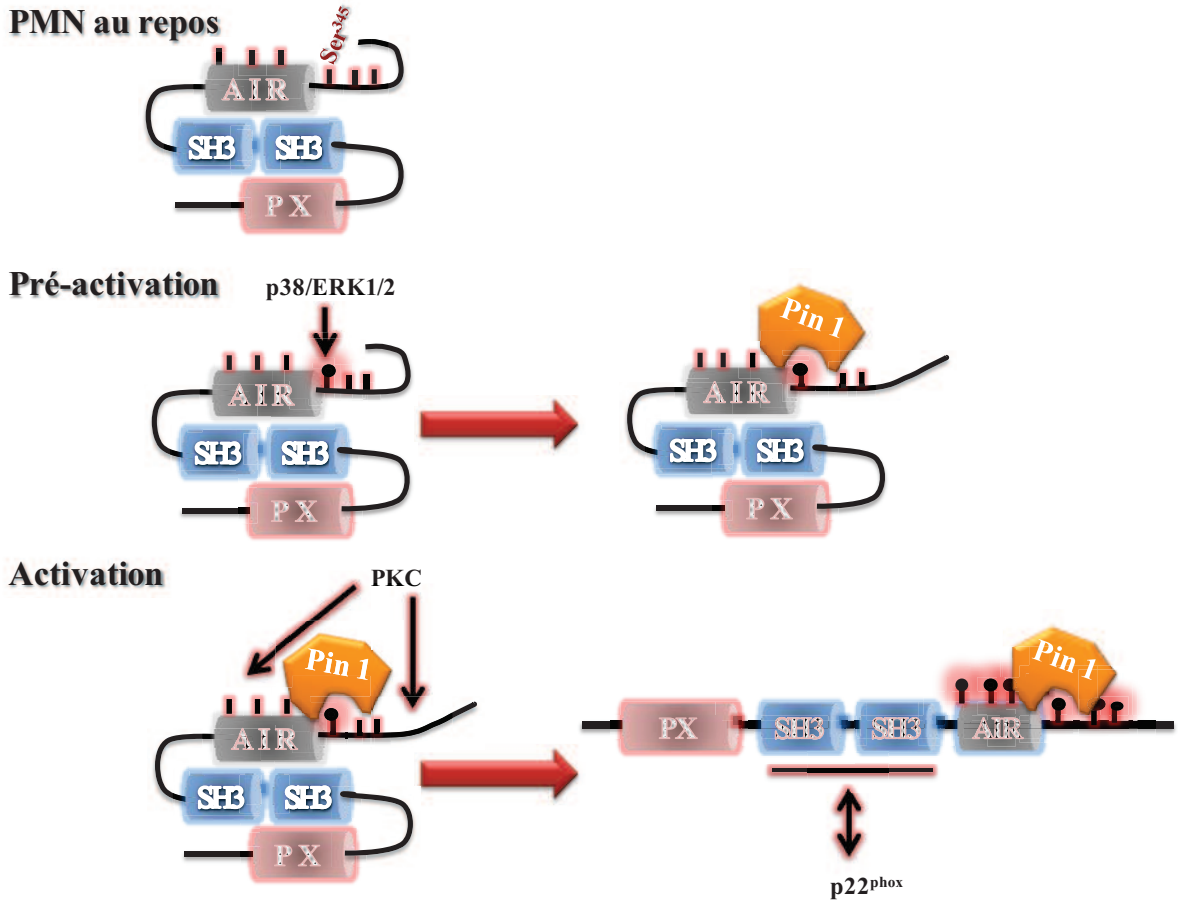

AIR="Auto-Inhibitory Region", PX="Phox homology", Pin1=Proline Isomérase 1, PB1="Phox and Bem1", p38/ERK1/2="p38 and ERK1/2 MAP-Kinases", PKC=Protéine-Kinase C, PRR="Proline Rich Region"; SH3="Src Homology domain 3". Les sérines phosphorylables de la région C-terminale sont figurées. D'après [Boussetta et al. 2010].

5.2. Assemblage du complexe NADPH oxydase

Au cours de l'explosion oxydative du PMN, $p47^{phox}$ orchestre le transfert vers la membrane plasmique de l'élément activateur, $p67^{phox}$. L'ensemble des facteurs cytosoliques est concerné directement ou indirectement par des phosphorylations faisant intervenir de nombreuses protéines-kinases. Ces modifications post-traductionnelles génèrent des interactions protéines-protéines ou protéines-lipides, responsables de la translocation et la stabilisation du complexe protéique à la membrane plasmique.

5.2.1. Kinases impliquées dans la phosphorylation de la NADPH oxydase

5.2.1.1. Protéines-kinases C

La PKC (EC 2.7.11.13) est une famille d'une dizaine de sérines/thréonines-kinases. On distingue les PKC classiques (isoenzymes α, βI, βII et γ) qui requièrent du Ca^{++}, du diacylglycérol produit par la phospholipase C et un phospholipide membranaire tel que la phosphatidylsérine pour son activation. Les isoenzymes δ, ε, η et θ constituent le groupe des nouvelles PKC. Leur fonctionnement ne nécessite pas de Ca^{++}. Les PKC atypiques (isoenzymes Mζ, ι, λ) n'ont besoin ni de Ca^{++} ni de diacylglycérol. Dans le PMN, les trois classes de PKC sont présentes avec une prédominance de la PKCβ [Dekker *et al.* 2000]. Le PMA (Phorbol 12-myristate 13-acétate) est un puissant activateur des PKC classiques [Castagna *et al.* 1982]. La PKCβ est impliquée dans la phosphorylation de $p47^{phox}$ [Reeves *et al.* 1999], l'assemblage et l'activation du complexe NADPH oxydase [Curnutte *et al.* 1994]. Les PKCζ et PKCδ semblent également engagées lors de la transduction du signal après stimulation par, respectivement, le fMLP [Dang *et al.* 2001] et le zymosan [Zhao *et al.* 2005]. Plusieurs expériences *in vitro* suggèrent que certaines enzymes du métabolisme du glucose constituent un substrat pour les PKC [Kitamura *et al.* 1988]. Cependant les phosphorylations générées par la PKC ne modifient pas toujours l'activité biologique d'une protéine. En effet, l'isoenzyme cardiaque de la phosphofructokinase 2 (PFK2) peut-être phosphorylée sur la Ser^{466} sans induire de modification de l'activité enzymatique [Rider *et al.* 1992a].

5.2.1.2. Protéines-kinases A

La PKA est une sérine/thréonine-kinase (EC 2.7.11.11) dont l'activité varie en fonction du niveau d'AMP cyclique (AMPc) dans la cellule. Cette kinase est donc sous la dépendance de l'adénylate cyclase couplée aux protéines G. La fixation de l'AMPc permet la dissociation des 2 sous-unités régulatrices et l'activation des 2 sous-unités catalytiques de la PKA. Cette

enzyme participe aux mécanismes de phosphorylation du métabolisme du glucose *via* la phosphorylation de la PFK2. En effet, de nombreuses études *in vitro* établissent que la PFK2 est un bon substrat pour la PKA [Deprez *et al.* 1997; Kitamura *et al.* 1988; Rider *et al.* 1992a]. Les phosphorylations de la PFK2 engendrées par la PKA portent sur la Ser^{466} et la Ser^{483}. Elle sont primordiales pour développer l'activité kinase de la PFK2 [Rider *et al.* 1992b]. Ainsi, chez la levure, la phosphorylation de la PFK2 par PKA multiplie par 5 son activité enzymatique [Dihazi *et al.* 2003]. La PKA peut phosphoryler $p47^{phox}$ [Kramer *et al.* 1988]. Les sites impliqués sont la Ser^{320} et une ou plusieurs autres sérines (Ser^{328} , Ser^{359} et Ser^{370} [El Benna *et al.* 1996a]). L'effet sur l'activité NADPH oxydase de ces phosphorylations est contradictoire [Hwang *et al.* 2003; Kramer *et al.* 1988; Park *et al.* 1992]. Une phosphodiestérase, activée par la PKA, convertit l'AMPc en AMP. Ce rétrocontrôle négatif explique que, selon les études, l'activité de la PKA est corrélée à une augmentation ou une diminution [Bengis-Garber *et al.* 1996; Fukuishi *et al.* 1997] de l'activité NADPH oxydase. La stimulation de PMNs humains par le fMLP induit une augmentation d'AMPc de façon très rapide et brève, ce qui suggère une stimulation très précoce et transitoire de la PKA lors de l'activation de la NADPH oxydase [Smolen *et al.* 1980]. La PKA ne doit pas être confondue avec la protéine-kinase dépendante de l'AMP-activée ("5' adenosine monophosphate-activated protein kinase" ou AMPK), qui, bien que de nature similaire, peut avoir des effets opposés [Hallows *et al.* 2009].

5.2.1.3. MAP ("Mitogen-activated protein")-kinases

Les MAP-Kinases (EC 2.7.11.24) sont des sérines/thréonines-kinases qui sont activées par une MAP-kinase kinase (ou MEK), elle-même phosphorylée par une MAP-kinase kinase kinase (ou MEKK). Cette famille est composée des ERK1/2 et des p38 MAP-kinases impliquées dans l'activations de l'oxydase [El Benna *et al.* 1996b] et de JNK ("Jun N-terminal kinase") MAP-Kinase.

5.2.1.4. PI3-kinases (phosphatidylinositol 3-kinases)

Les PI3-Kinases (EC 2.7.1.137) sont des hétérodimères constitués d'une sous-unité catalytique et d'une sous unité régulatrice. Ils transfèrent un phosphate de l'ATP sur le carbone 3' de l'inositol des phosphatidylinositols membranaires. Les PI3-Kinases catalysent donc la formation du phosphatidylinositol-3-phosphate, du phosphatidylinositol-3,5-diphosphate ainsi que du phosphatidylinositol-3,4,5-triphosphate qui sont des messagers secondaires essentiels à l'activation du complexe NADPH oxydase [Brown *et al.* 2003]

notamment par la stimulation des protéines kinases B (PKB/Akt). Dans le PMN, la PI3-Kinase p85/100 et la PI3-Kinase γ sont présentes [Stephens *et al.* 1994]. Cette dernière est activée très précocement lors de la stimulation du PMN par le fMLP [Naccache *et al.* 2000]. Les PI3-Kinases sont des protagonistes fondamentaux de la transduction du signal de cette chimiokine [Leopoldt *et al.* 1998]

5.2.1.5. Protéines-kinases B/ Akt

PKB/Akt est une famille de sérines/thréonines-kinases (EC 2.7.11.1). Son nom lui fut attribué par analogie avec l'oncogène viral "Akt-8". Les isoenzymes Akt1, Akt2 ont des fonctions très différentes, alors qu'Akt3 semble impliquée dans des phénomènes aussi divers que la carcinogénèse [Sharma *et al.* 2009] et la génèse des mitochondries au niveau cérébral [Wright *et al.* 2008]. Akt1 est plus volontiers impliquée dans la signalisation anti-apoptotique et dans la croissance tissulaire alors qu'Akt2 est une molécule majeure de la voie de signalisation de l'insuline. Les souris invalidées pour le gène Akt-2 développent un diabète par résistance à l'insuline [Garofalo *et al.* 2003]. *In vitro,* Akt peut phosphoryler les résidus Ser^{466} et Ser^{485} de la PFK2 [Deprez *et al.* 1997]. Ces résidus sont critiques dans l'activation de la PFK2 cardiaque [Pozuelo Rubio *et al.* 2003]. Cependant des expériences de dominants négatifs ciblant Akt apportent la démonstration que cette kinase est faiblement impliquée dans la phosphorylation de la PFK2 en réponse à l'insuline dans la lignée de tumeur embryonnaire rénale HEK-293 (Human Embryonic Kidney) [Bertrand *et al.* 1999]. *In vivo*, l'activation de la PFK2 cardiaque ne semble pas non plus sous la dépendance d'Akt [Mora *et al.* 2003]. L'inhibition de l'activité d'Akt diminue la production de ROS par la NADPH oxydase des PMNs humains en réponse au fMLP [Chen *et al.* 2003]. Des expériences de radiomarquages au ^{32}P établissent que $p47^{phox}$ est un substrat d'Akt. Récemment, une nouvelle voie de la stimulation impliquant Akt a été décrite par Patel *et al*. Dans le cytosol de pseudo-neutrophiles HL-60 stimulés par le fMLP, les auteurs ont constaté la co-immunoprécipitation des protéines phosphorylées Akt, ERK ½-Kinase et phospholipase D2. La phosphorylation d'ERK2 par Akt1, démontrée en milieu acellulaire, active la phospholipase D [Patel *et al.* 2010]. L'utilisation d'oligonucléotide anti-sens ciblant Akt confirme que la voie de signalisation impliquant Akt puis ERK et la phospholipase D, participe à l'activation de l'oxydase par le fMLP *via* le recrutement à la membrane de $p47^{phox}$ et $p67^{phox}$.

5.2.2. Phosphorylation du cytochrome b_{558}

Les modifications post-traductionnelles de $p22^{phox}$ et NOX2 modulent à la fois l'interaction avec les facteurs cytosoliques et l'activité enzymatique (cf paragraphe 5.4.1.) La phosphorylation de la sous-unité $p22^{phox}$, décrite de longue date [Garcia *et al.* 1988], concerne notamment le résidu Thr^{147}. Elle semble favoriser l'ancrage de $p47^{phox}$ à la membrane plasmique [Lewis *et al.* 2010]. La phosphorylation de la queue cytosolique C-terminale de NOX2, médiée par la PKC, favorise l'interaction avec $p47^{phox}$, $p67^{phox}$ et Rac2 [Raad *et al.* 2009].

5.2.3. Phosphorylation de $p47^{phox}$

Au cours de l'activation du neutrophile, $p47^{phox}$ est massivement phosphorylée [Faust *et al.* 1995] sur un dizaine de sérines [El Benna *et al.* 1994a]. L'importance relative et l'ordre chronologique des phosphorylations de chacun de ces sites, appartenant aux domaines C-terminaux AIR et PR, sont encore mal définis. Il semble cependant que les Ser^{359} et Ser^{370} soient les premières impliquées [Johnson *et al.* 1998]. De nombreuses kinases ciblent $p47^{phox}$ dans la lignée myéloïde : PKC [Fontayne *et al.* 2002], p38 et ERK1/2 MAP-Kinases [Dang *et al.* 2006] ainsi qu'Akt [Didichenko *et al.* 1996]. Une étude cristallographique suggère que les changements de charge apportés par les groupes phosphates brisent les interactions intra-moléculaires responsables de la conformation auto-inhibée de $p47^{phox}$. L'ordre chronologique dans lequel les sérines de $p47^{phox}$ sont phosphorylées pourrait influencer l'assemblage du complexe NADPH oxydase, mais demeure encore peu étudié.

5.2.4. Phosphorylation de $p67^{phox}$

Bien que $p67^{phox}$ soit également phosphorylée lors de la stimulation du PMN [El Benna *et al.* 1997; Forbes *et al.* 1999], le rôle des phosphorylations n'est pas clair. A l'instar de $p47^{phox}$, $p67^{phox}$ possède probablement, à l'état de repos, une structure auto-inhibée qui se relâche au cours de l'activation [Durand *et al.* 2010]. Des expériences de mutagénèse suggèrent que la Thr^{233} est le site principal de phosphorylation par les MAP-Kinases. Plusieurs kinases peuvent être impliquées : *in vitro* la kinase activée par p21 (PAK, "p21-activated kinase" [Ahmed *et al.* 1998]) et *in vivo* certaines MAP-Kinases : p38 et ERK2 MAP-Kinases [Dang *et al.* 2003]. Dans le PMN humain, il existe une phosphorylation basale de $p67^{phox}$. Lors d'une stimulation par le PMA, l'activation de MEK1/2 sous la dépendance d'un récepteur tyrosine-kinase et l'inhibition des sérines/thréonines phosphatases de type 1 et de type 2A permettent la phosphorylation des mêmes $p67^{phox}$ [Dang *et al.* 2011].

5.2.5. Phosphorylation de $p40^{phox}$

Certaines kinases de la famille PKC ont comme substrat $p40^{phox}$ [Bouin *et al.* 1998; Lopes *et al.* 2004]. L'impact de la phosphorylation de la Thr^{154} et de la Ser^{315} sur l'activation de la NADPH oxydase est encore contradictoire [Chessa *et al.* 2010; Lopes *et al.* 2004].

5.2.6. Activation de Rac par phosphorylation de RhoGDI

La protéine RhoGDI est phosphorylable sur les résidus Ser^{101} et Ser^{174} par différents types de kinases. Il s'ensuit une dissociation de RhoGDI et de Rac. La protéine Rac peut alors fixer et hydrolyser le GTP avant d'être transférée à la membrane plasmique [DerMardirossian *et al.* 2004].

5.2.7. Interactions protéines-protéines

Les domaines SH3 de $p47^{phox}$ permettent l'ancrage à la membrane plasmique grâce à la liaison avec la région PRR de $p22^{phox}$. $P47^{phox}$ positionne également $p67^{phox}$ sur NOX2. Les interactions entre Rac et les autres facteurs cytosoliques sont plus controversées. Pick *et al.* proposent que Rac2, à l'instar de $p47^{phox}$, assure le positionnement de $p67^{phox}$ par rapport à NOX2. L'implication des phosphorylations dans le changement de conformation et dans la liaison du site TPR de $p67^{phox}$ avec le domaine GTPase de Rac n'est pas encore clairement établie. De même, l'interaction directe entre Rac et le cytochrome b_{558} reste discutée [Sarfstein *et al.* 2004]. Bokoch *et al.* suggèrent une implication directe de Rac dans le transfert d'électron [Diebold *et al.* 2001].

5.2.8. Interactions protéines-lipides

La liaison des facteurs cytosoliques de la NADPH oxydase aux phospholipides membranaires peut procéder d'une interaction électrostatique aspécifique ou par la reconnaissance spécifique d'une structure lipidique [Lemmon 2008]. La fixation des phospholipides anioniques (phosphatidylsérine et acide phosphatidique) ou des phosphatidylinositides membranaires par le domaine PX de $p47^{phox}$ et $p40^{phox}$, permet de stabiliser la liaison avec le cytochrome b_{558}. Le domaine C-terminal polybasique de Rac développe des liaisons avec les phospholipides anioniques [Ugolev *et al.* 2006]. Son site d'attache de la queue géranylgéranyl (CAAX) permet d'ancrer Rac à la membrane plasmique

5.3. Régulation par compartimentation membranaire

Les lipides membranaires du neutrophile sont répartis de manière hétérogène, faisant émerger des microdomaines plus ou moins flexibles au sein de la membrane plasmique [Nebl *et al.* 2002]. Les radeaux lipidiques et les cavéoles sont des régions de 50 à 300nm, riches en cholestérol et en sphingolipides (**Figure 20**). Ils constituent des plateformes membranaires rigides permettant des interactions privilégiées pour l'activité de certaines protéines, notamment des enzymes du métabolisme du glucose qui sont transférées à la membrane plasmique lors de leur activation [Lloyd *et al.* 2001]. Lors de l'explosion oxydative du PMN, les facteurs cytosoliques de la NADPH oxydase colocalisent dans ces radeaux lipidiques [Shao *et al.* 2003; Vilhardt *et al.* 2004]. Ces microdomaines semblent impliqués dans l'initiation de l'activité NADPH oxydase en favorisant les interactions entre les facteurs cytosoliques et le cytochrome b_{558} [Shao *et al.* 2003]. Par conséquence, les PMNs de souris invalidées pour le gène de la cavéoline ont une production de ROS nettement diminuée, [Hu *et al.* 2008] en réponse au fMLP.

Figure 20. Schéma d'un radeau lipidique

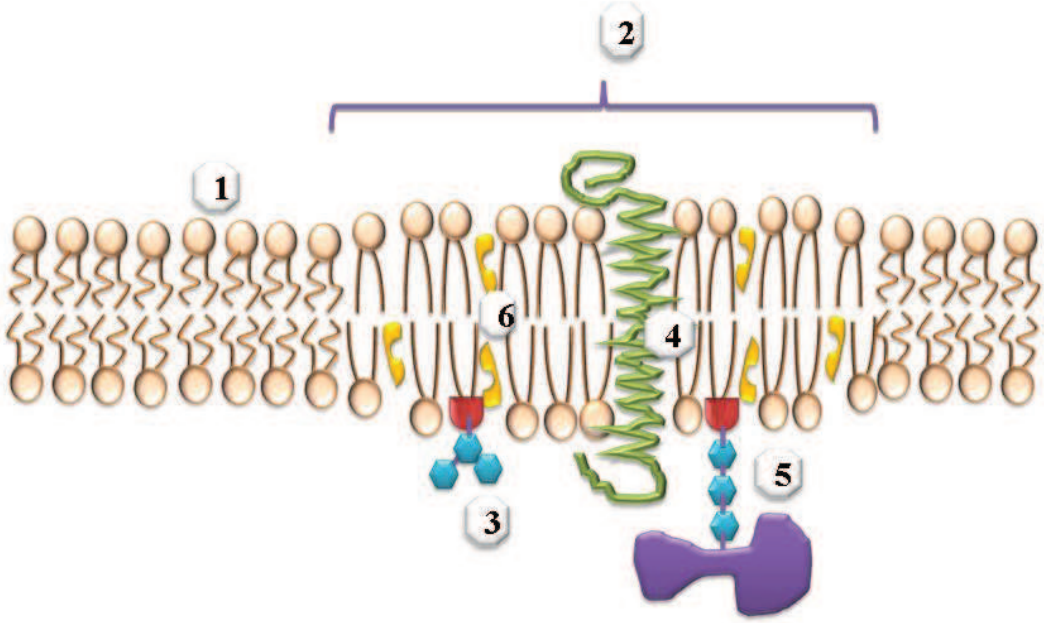

1. Membrane cellulaire sans radeau lipidique 2. Radeau lipidique 3. Glycolipide 4. Protéines transmembranaires 5. Bras GPI (glycosyl phosphatid linositol).

5.4. **Régulation de l'activité catalytique de la NADPH oxydase des phagocytes**

5.4.1. Phosphorylation du cytochrome b_{558}

Le marquage, par l'isotope ^{32}P, de PMNs humains stimulés suggère que la protéine NOX2 est phosphorylé. *In vitro*, la phosphorylation de la queue cytosolique C-terminale, médiée par PKC, augmente l'activité diaphorase, c'est-à-dire le transfert d'électron entre le NADPH et le FAD [Raad *et al.* 2009]. La phosphorylation de $p22^{phox}$ est corrélée à une augmentation de l'activité NADPH oxydase par des mécanismes dépendants et indépendants de la phospholipase D qui hydrolyse les phospholipides membranaires en acide phosphatidique. La PKC semble également impliquée dans cette phosphorylation de $p22^{phox}$ [Regier *et al.* 2000].

5.4.2. Régulation par allostérie

La cinétique enzymatique de la NADPH oxydase n'est pas michaélienne. La liaison de $p67^{phox}$ sur le cytochrome $b_{558,}$ à distance du site catalytique, génère une modification conformationnelle de l'hémoprotéine [Paclet *et al.* 2007; Paclet *et al.* 2000] nécessaire au transfert d'électron. La structure oligomérique, requise pour considérer l'existence d'une régulation allostérique, est suggérée pour l'isoenzyme NOX5 de la NADPH oxydase [Kawahara *et al.* 2011].

5.4.3. Implication du cytosquelette dans l'activation de NOX2

Plusieurs arguments corroborent l'implication du cytosquelette dans l'activation de NOX2. Les régions SH3 des facteurs cytosoliques $p67^{phox}$ et $p47^{phox}$ sont des motifs d'interaction classiquement décrits avec le cytosquelette [Hamaguchi *et al.* 1987]. Lors de l'activation de l'oxydase par le PMA, les facteurs cytosoliques $p47^{phox}$ et $p67^{phox}$ phosphorylés sont retrouvés dans la fraction insoluble contenant le cytosquelette, qui est obtenue après traitement par Triton X-100 (1% v/v) et ultracentrifugation [Nauseef *et al.* 1991]. Le groupe d'Anthony Segal montre par microscopie confocale et chromatographie d'affinité que le domaine PX de $p40^{phox}$, impliqué dans la liaison des structures lipidiques, est également responsable de l'interaction avec l'actine F [Shao *et al.* 2010]. L'analyse protéomique par MALDI-TOF du complexe NADPH oxydase, purifié à partir de cytosol et de membranes de PMNs activés, illustre l'interaction entre le complexe NADPH oxydase et d'autres protéines du cytosquelette liant l'actine telles que la coronine et la moésine [Paclet *et al.* 2007]. La mobilisation du cytosquelette semble indispensable à l'activité de NOX2 par le fMLP [Dahinden *et al.* 1983]. Les cellules adhérentes comme celles dont l'actine a été dépolymérisée par l'action de la

cytochalasine B, ont une activité prolongée [Dahinden *et al.* 1983]. La cytochalasine B gêne la désensibilisation, par internalisation, des récepteurs membranaires impliqués dans l'activation de l'oxydase du PMN [Jesaitis *et al.* 1985], mais pas du monocyte [Johansson *et al.* 1995]. Dans le PMN, la dépolymérisation de l'actine conduit à une accumulation de diacylglycérol [Bengtsson *et al.* 1991]. L'élévation de la concentration de ce messager secondaire induirait donc une activation de NOX2 *via* la stimulation de la PKC [Bengtsson *et al.* 2006].

5.4.4. Disponibilité en substrat

Lors de l'explosion respiratoire du PMN, la consommation d'oxygène est peu influencée par la concentration de glucose extra-cellulaire [Sbarra *et al.* 1959]. En condition physiologique, la pression partielle tissulaire en O_2, relativement constante, se situe à des taux très faibles par rapport à la valeur atmosphérique. En conséquence, l'apport en oxygène n'a qu'un faible impact sur la production de ROS par la NADPH oxydase [Gabig *et al.* 1979]. Le Km de cette enzyme pour le NADPH est d'environ 30µM [Burritt *et al.* 2003; McPhail *et al.* 1985; Nisimoto *et al.* 1999; Suzuki *et al.* 1980]. Bien que la concentration cytoplasmique de NADPH demeure relativement constante dans le neutrophile, vers 50 µM [DeChatelet *et al.* 1974], la concentration de substrat influence significativement l'activité NADPH oxydase [Petheo *et al.* 2005]. L'étude du courant électrique induit par l'activité oxydase de membrane de polynucléaires éosinophiles humains indique que la concentration de NADPH modifie le transfert d'électron en partie par modulation du potentiel de membrane [Petheo *et al.* 2005].

5.4.4.1. Métabolisme du glucose dans le PMN

L'étude du complexe NADPH oxydase, isolé sous forme constitutivement active, suggère que deux enzymes du métabolisme du glucose : la 6-phosphogluconate déshydrogénase (6PGDH) et la 6-phosphofructokinase 2 (PFK2) sont co-purifiées avec les autres partenaires du complexe NADPH oxydase [Paclet *et al.* 2007]. Les activités enzymatiques de la 6PGDH, enzyme de la voie des pentoses phosphates, et de la PFK2, enzyme régulant la glycolyse, sont impliquées dans la production de NADPH, substrat de NOX2 et de l'ATP (**Figures 21**) alors disponible pour la phosphorylation des composants de l'oxydase et pour la Nucléoside diphosphate Kinase (NDPK). Cette dernière enzyme pourrait, secondairement, activer Rac en catalysant la synthèse de GTP à partir de l'ATP [Mizrahi *et al.* 2005].

Figures 21. La 6-phosphogluconate déshydrogénase et la 6-phosphofructokinase 2, enzymes du métabolisme du glucose

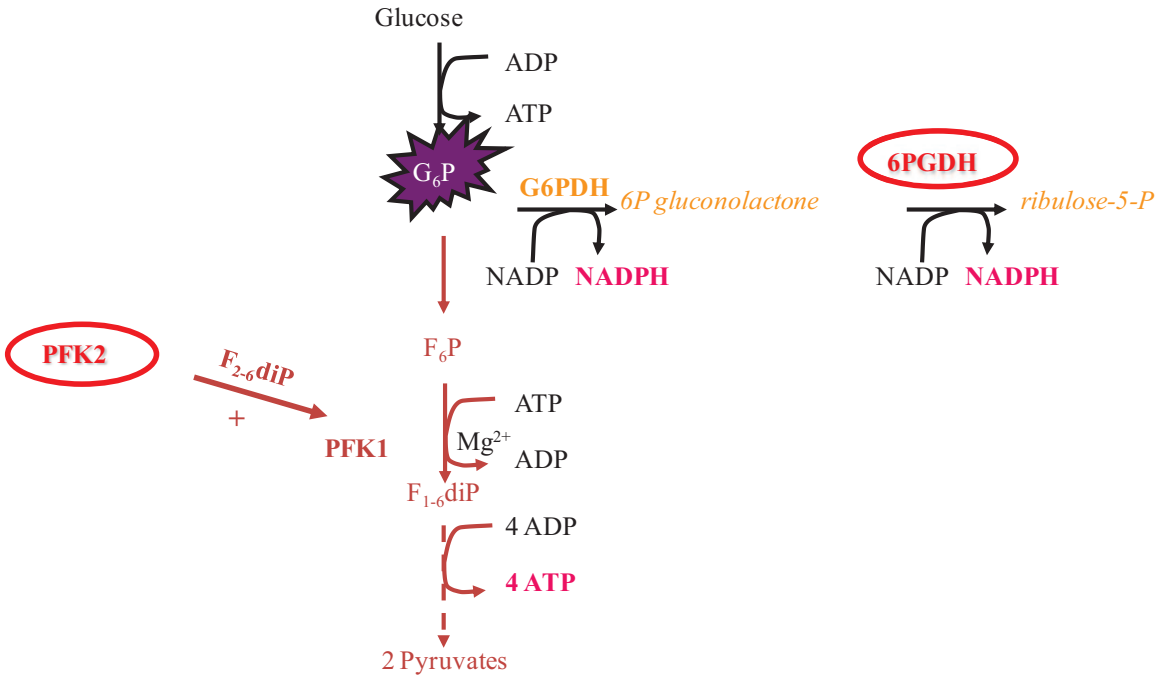

ADP/ATP=Adénosine Diphosphate/ Adénosine Triphosphate, F6P=Fructose-6-phosphate, F1-6P=Fructose-1,6-diphosphate, G6PDH=Glucose-6-phosphate déshydrogénase, G6P=Glucose-6-phosphate, NADPH=Nicotinamide Adénine Dinucleotide Phosphate, PFK=Phosphofructokinase, 6PGDH=6-phosphogluconate déshydrogénase.

5.4.4.2. La voie des pentoses phosphates

La voie des pentoses phosphates, autrement dénommée "shunt" des hexoses monophosphates, permet la synthèse du ribose-5-phosphate, précurseur des acides nucléiques nécessaires à la synthèse d'ADN et d'ARN, ainsi que la réduction du NADP+ en NADPH, substrat des NADPH oxydases et de la glutathion réductase qui permet le maintien du statut redox cytosolique. Lorsque les besoins cellulaires portent sur le NADPH, l'excès de ribose-5-phosphate produit par cette voie peut être utilisé par la glycolyse (**Figure 22**). Cette voie métabolique ne consomme, ni ne produit d'ATP. Le favisme ou déficit en glucose-6-phosphate déshydrogénase (G6PDH), première enzyme de la voie des pentoses phosphates, est le déficit enzymatique le plus répandu. Il provoque une hémolyse lors de l'ingestion d'aliment contenant des substances oxydantes comme les fèves, ou de médicaments fragilisant la membrane plasmique tels que la salazopyrine [Wijnands *et al.* 1991] et certains anti-paludéens [Alving *et al.* 1956]. Les patients chez qui la concentration du NADPH est diminuée par déficit sévère en G6PDH, présentent des infections itératives. Comme dans la CGD, les PMN de patients présentant un déficit sévère en G6GDH ont une bactéricidie altérée [Asghar *et al.* 1998; Baehner *et al.* 1972]

Figure 22. Schéma de la voie des pentoses phosphates

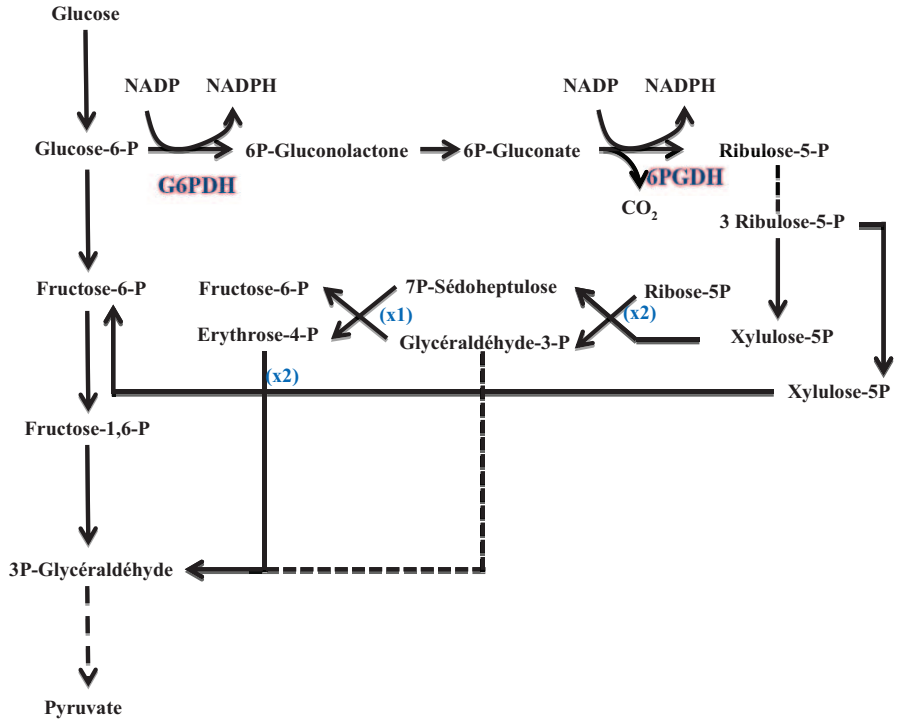

6PGDH=6-phosphogluconate déshydrogénase, Erythrose-4P=Erythrose-4-phosphate, Fructose-6-P=Fructose-6-phosphate, Fructose-1,6-P=Fructose-1,6-diphosphate, Glucose-6P=Glucose-6-phosphate, G6PDH=Glucose-6-phosphate déshydrogénase, 6P-Gluconolactone=6-phosphoglucunolactone ,6P-Gluconate=6-phosphogluconate, 3P-glycéraldéhyde=Glycéraldéhyde-3-phosphate, NADPH=Nicotinamide Adénine Dinucléotide Phosphate, Ribulose-5P=Ribulose-5-phosphate, Ribose-5-P=Ribose-5-phosphate, 7P-Sédoheptulose= Sédoheptulose-7-phosphate.

5.4.4.3. Les étapes de la voie des pentoses phosphates

La voie des pentoses phosphates se divise en 2 phases. La première partie permet la production de NADPH et d'un pentose : c'est la phase oxydative (**Figure 22**). La glucose-6-phosphate déshydrogénase oxyde le glucose-6-phosphate en 6-phosphoglucunolactone qui sera hydrolysé en 6-phosphogluconate par la glucunolactonase. La 6PGDH catalyse une décarboxylation pour aboutir au premier pentose, le ribulose-5-phosphate. Dans la phase non oxydative, le ribulose-5-phosphate est le substrat, d'une part de la ribose-5-phosphate isomérase produisant le ribose-5-phosphate, et d'autre part de la ribulose épimérase conduisant au xylulose-5-phosphate. Ces deux pentoses peuvent être pris en charge dans la glycolyse après la formation du fructose-6-phosphate et du glycéraldéhyde-3-phosphate par une succession de conversions faisant intervenir des aldolases et des cétolases.

5.4.4.4. La 6-phosphogluconate déshydrogénase

La 6PGDH (EC 1.1.1.44.) dont le locus est porté sur le chromosome 1 (1p36), est une enzyme limitante dans la voie des pentoses phosphates. C'est un homodimère d'environ 470 acides aminés possédant une séquence hautement conservée [Reizer *et al.* 1991]. Chaque monomère

de 52 kDa [Pearse *et al.* 1974] contenant une hélice α, catalyse indépendamment la synthèse du 6-phosphogluconate en ribulose-5-phosphate en 2 étapes irréversibles [Adams *et al.* 1983]. Le 6-phosphogluconate est tout d'abord oxydé en un produit instable qui est ensuite décarboxylé en ribulose-5-phosphate, isomère du ribose-5-phosphate. Contrairement à la plupart des carboxylases, la décarboxylation oxydative médiée par la 6PGDH ne requiert pas de dicathion métallique. Elle permet la réduction du NADP, son cofacteur, en NADPH. Les déficits génétiques concernant la 6PGDH sont rares. Ils se traduisent par des anémies hémolytiques [Scialom *et al.* 1966]. De manière surprenante, l'étude de deux patients montre que le déficit en 6PGDH s'accompagne d'une augmentation de 1,6-fructose diphosphate, normalement produit par la catalyse de la Phosphofructokinase 1 [Vives Corrons *et al.* 1996]. Les auteurs suggèrent que l'accumulation de ce métabolite de la glycolyse, lors du déficit en 6PGDH, est liée à un blocage de l'activité glycéraldéhyde-3-phosphate déshydrogénase (G3PDH).

5.4.4.5. La glycolyse génère l'ATP dans le PMN

Quelques mitochondries sont présentes dans le PMN [Maianski *et al.* 2004]. Elle sont importantes dans la programmation de l'apoptose [Maianski *et al.* 2002] mais elles sont incapables de produire de l'ATP. Par conséquence, dans le PMN, la production énergétique sous forme d'ATP est entièrement dépendante de la glycolyse.

Figure 23. Schéma de la glycolyse

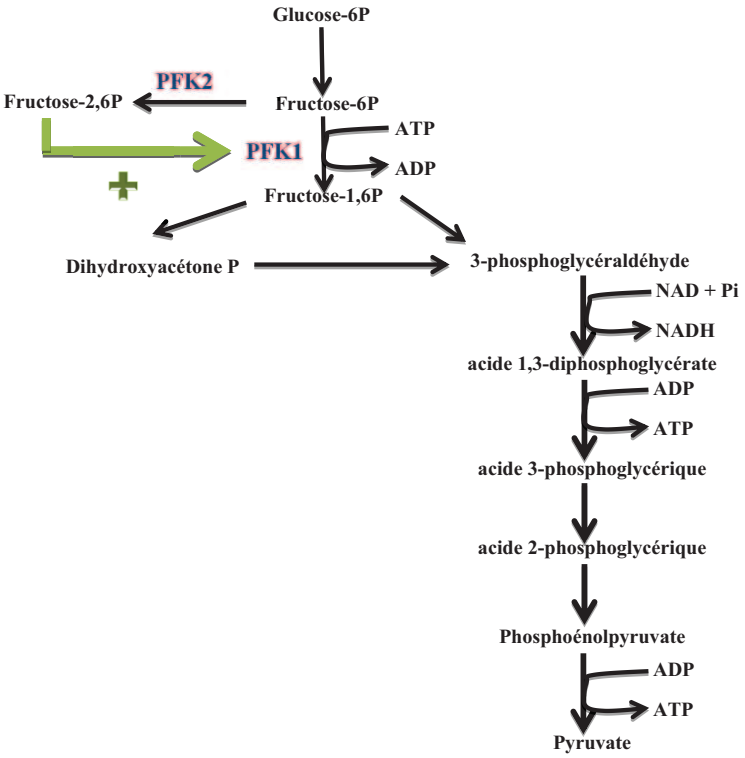

ADP/ATP= Adénosine diphosphate. Adénosine triphosphate déshydrogénase, G3PDH= glycéraldéhyde-3-phosphate déshydrogénase, PFK=phosphofructokinase .

5.4.4.6. Etapes de la glycolyse

La glycolyse se déroule dans le cytosol (**Figure 23**). Elle consiste en l'oxydation progressive d'un hexose, le glucose, en deux molécules de pyruvates, avec une production de 2 molécules d'ATP et de NADH. Cette voie est régulée à son entrée par l'activité hexokinase. La phosphofructokinase 1 (PFK1) catalyse la phosphorylation irréversible du fructose-6-phosphate en fructose-1,6-diphosphate en présence de Mg^{++}. Cette enzyme allostérique est finement régulée par la concentration d'ATP libre et le citrate mais c'est le fructose 2,6-diphosphate, produit par la PFK2, qui est le véritable régulateur allostérique physiologique de la PFK1.

5.4.4.7. La 6-phosphofructokinase 2 régule la glycolyse

La PFK2 (E.C.2.7.1.105) est une enzyme bifonctionnelle comportant un site catalytique kinase et un site phosphatase. Quatre gènes différents PFKB1, PFKB2, PFKB3 et PFKB4 codent respectivement pour les isoenzymes hépatiques, cardiaques, cérébrales et testiculaires. L'isoenzyme hépatique est la plus étudiée. Elle possède une activité phosphatase prépondérante. L'isoenzyme retrouvée dans le complexe oxydase, isolé à partir de membranes et de cytosols de PMNs activés, est l'isoenzyme cardiaque dont le locus est situé sur le chromosome 1 (1q13). C'est un homodimère d'environ 100 kDa qui se singularise par une partie C-terminale comprenant deux sites de phosphorylation pour la PKA. A la faveur d'une phosphorylation, l'activité kinase de l'isoenzyme cardiaque de la PFK2 est stimulée. Il s'ensuit une augmentation de la production de fructose 2,6-diphosphate, régulateur allostérique qui augmente l'affinité de PFK1 pour le fructose-6-phosphate et stimule ainsi la glycolyse.

5.4.5. Acide arachidonique

In vitro, l'acide arachidonique augmente l'activité NADPH oxydase des phagocytes [Doussière *et al.* 1999]. Rachel Lévy et al. montrent, à l'aide de PLB985 différenciés en pseudo-neutrophiles déficients en phospholipase A_2 (PLA_2) cytosolique, l'implication *in vivo* de l'acide arachidonique dans l'activité diaphorase [Pessach *et al.* 2001] et NADPH oxydase [Dana *et al.* 1998].

La PLA_2 cytosolique (EC 3.1.1.4) hydrolyse les phospholipides pour produire de l'acide arachidonique [Clark *et al.* 1990]. Cette enzyme possède deux domaines fonctionnellement distincts : une région N-terminale dont la liaison aux phospholipides dépend du calcium et une région catalytique C-terminale dont le fonctionnement ne dépend pas du calcium

[Nalefski *et al.* 1994]. Des expériences de marquage radio-actif membranaire de macrophages murins RAW 264.7 indiquent qu'après l'activation, dépendante du calcium, de la PLA_2 cytosolique, cette enzyme produit de l'acide arachidonique à partir des phospholipides membranaires [Channon *et al.* 1990]. Après stimulation du PMN par le PMA ou le zymosan, la PLA_2 cytosolique lie $p47^{phox}$ [Shmelzer *et al.* 2008].

Plusieurs mécanismes sont avancés pour expliquer la stimulation de l'activité NADPH oxydase par l'acide arachidonique. En se liant au cytochrome $b_{558,}$, l'acide arachidonique peut induire un changement conformationnel de l'hémoprotéine qui déclenche l'activation de la NADPH oxydase [Doussière *et al.* 1999; Doussière *et al.* 1996; Foubert *et al.* 2002]. De plus, cet agent amphiphile peut entraîner la rupture des liaisons intra-moléculaires auto-inhibitrices de $p47^{phox}$ facilitant l'interaction avec $p22^{phox}$ [Shiose *et al.* 2000].

Les phospholipides membranaires sont également le substrat d'autres phospholipases qui permettent la production de messagers secondaires. La phospholipase C (EC 3.1.4.3) clive la fonction ester liant le glycérol et le phosphate. Elle permet la synthèse de diacylglycérol qui active la protéine-kinase C et de phosphatidylinositol par lequel le domaine SH3 des facteurs cytosoliques se fixent à la membrane plasmique [Kanai *et al.* 2001]. L'acide phosphatidique, produit par la phospholipase D, participe à l'activation de la NADPH oxydase par le biais de la phosphorylation de $p22^{phox}$ et du transfert à la membrane plamique de $p67^{phox}$ et $p47^{phox}$ [Regier *et al.* 2000].

5.4.6. Rôle du flux calcique dans l'activation de NOX2

L'implication du calcium dans l'activation de NOX2 est connue depuis longtemps [Pozzan *et al.* 1983]. La chélation du calcium extra-cellulaire diminue la production d'anion $O_2^{\bullet -}$ chez les PMNs stimulés par le fMLP. Cette chimiokine provoque très précocement un influx de calcium lors de la stimulation des PMNs [Heyworth *et al.* 1990], selon un phénomène classiquement appelé "entrée capacitative" ou SOCE ("Store-Operated Calcium Entry"). La stimulation de récepteurs au fMLP induit une activation de la phospholipase Cβ (PLCβ) responsable d'une production d'inositol triphosphate (**Figure 24**). La liaison de ce messager secondaire sur son récepteur vidange le réticulum endoplasmique de sa réserve de calcium. L'effondrement de la concentration de calcium dans le réticulum endoplasmique va être détecté par STIM-1 ("Stromal Interaction Molecule 1"). Cette protéine transmembranaire permet l'activation des canaux calciques SOCs et ainsi l'entrée de calcium à travers la membrane plasmique. Le rétablissemement des stocks calciques du réticulum endoplasmique dépend des pompes SERCA ("Sarcoendoplasmique Reticulum Ca^{++}-ATPase") [Zhang *et al.*

2005]. Dans les cellules stimulées par le fMLP, l'influx de calcium à travers la membrane plasmique peut également être médié par la conversion de NADP+ en ADP ribose cyclique (cADP) par l'ADP ribosyl cyclase [Brechard *et al.* 2006]. Suite à l'influx calcique, plusieurs médiateurs concourent à l'activation du complexe NADPH oxydase. Dans la lignée myéloïde HL-60, une stimulation par le fMLP permet le recrutement de la PKCβ, qui phosphoryle $p47^{phox}$ et favorise la translocation des facteurs cytosoliques. Plusieurs isoformes de la PLA_2 cytosolique sont également induites par le calcium. La production d'acide arachidonique par la PLA_2 cytosolique et son transport par les protéines S100A8/A9, conduit à l'activation de l'oxydase, par un mécanisme régulé par le calcium. Dans la lignée myéloïde PLB985 [Shmelzer *et al.* 2003], la PLA_2 cytosolique activée migre à la membrane. L'acide arachidonique produit par son activité enzymatique est véhiculé par les protéines S100A8/A9. [Bouzidi *et al.* 2004; Kerkhoff *et al.* 2005]. Or la fixation du calcium est essentielle à la formation de l'hétérocomplexe S100A8/A9 puis à sa translocation à la membrane plasmique après phosphorylation de la Thr^{113} de S100A9 par les MAP-Kinases [Schenten *et al.* 2011]. Enfin, l'influx calcique semble également réguler le recrutement de Rac à la membrane plasmique [Valentin *et al.* 2001]. Une chélation du calcium extra-cellulaire prévient la translocation de Rac dans les HL-60 stimulés par le fMLP.

Figure 24. Entrée capacitive de calcium

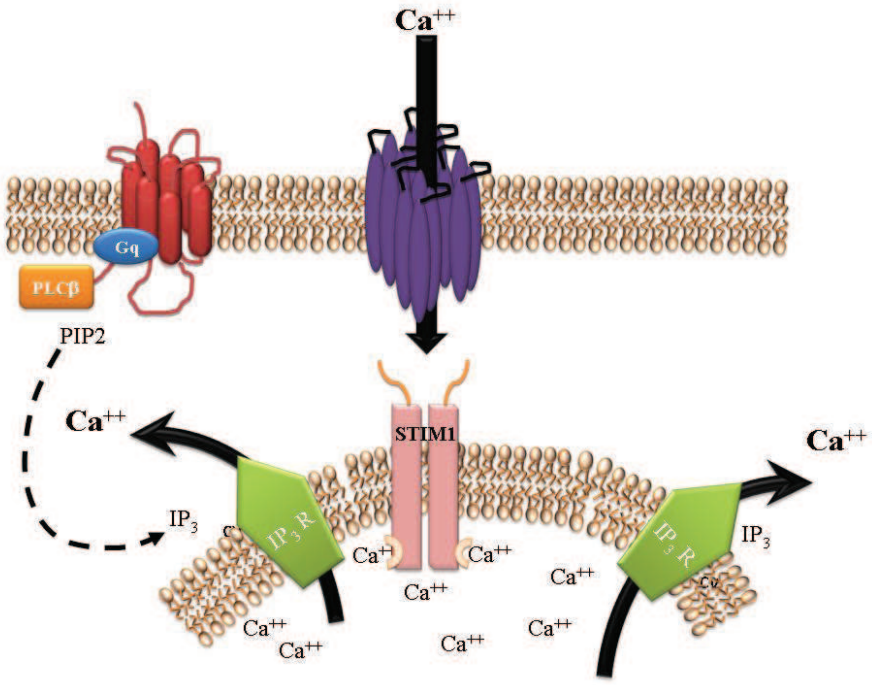

IP3R= Récepteur à l'inositide triphosphate, PLCβ=Phospholipase Cβ, STIM-1="Stromal Interaction Molecule-1", PIP2= Phosphatidylinositol 4,5-diphosphate, IP3= phosphatidylinositol 3,4,5-trisphosphate. D'après [Brechard et al. 2008].

5.5. S100A8/A9, nouveaux partenaires d'activation de NOX2

5.5.4. Structure des protéines S100

Les protéines S100 tirent leur nom de leur parfaite solubilité dans une solution de sulfate d'ammonium à 100% de saturation. Les 21 membres de cette famille [Ravasi *et al.* 2004] ont en commun 2 motifs EF-Hand leur conférant la capacité de lier deux molécules de calcium. Une région variable charnière relie ces deux parties (**Figure 25**). L'affinité du site de fixation pour le calcium côté C-terminal est supérieure au site de fixation côté N-terminal [Donato 2001]. La protéine S100A8 (également dénommée calgranuline A ou MRP8 pour "Myeloid Related Protein") et la protéine S100A9 (MRP14 ou calgranuline B) peuvent également lier une molécule de zinc avec une forte affinité [Donato 1999] sur un site en C-terminal His-X-X-X-His différent du site de fixation de calcium. L'étude structurale après cristallisation de l'hétérotétramère de protéines S100A8 et S100A9 révèle que le zinc se fixe à l'interface des deux partenaires [Korndorfer *et al.* 2007]. Les gènes codant pour les S100 humaines sont tous situés sur le chromosome 1 (1q21) [Kerkhoff *et al.* 1998] sauf celui de S100B dont le locus appartient au chromosome 21. La protéine S100A12 (92 acides aminés soit environ 10400 Da) constitue environ 5% du contenu protéique cytosolique du PMN. S100A8 est composée de 93 acides aminés soit une masse d'environ 10880 Da, alors que S100A9 est formée de 114 acides aminés pour une masse d'environ 13800 Da. Les protéines S100A8, S100A9 représentent 40 % des protéines du cytosol du PMN et seulement 2 à 5% des protéines cytosoliques du monocyte [Morel *et al.* 1994; Ryckman *et al.* 2003b]. Ces protéines sont le plus fréquemment retrouvées sous la forme d'un hétérodimère S100A8/A9 [Hunter *et al.* 1998], bien que la formation de trimère [Teigelkamp *et al.* 1991] ou tétramère [Strupat *et al.* 2000] soit également possible.

Il existe deux isoformes de S100A9 produites à partir d'un même ARN messager [Van den Bos *et al.* 1996]. La forme tronquée, S100A9*, est plus courte de 4 acides aminés en N-Ter. Chaque isoforme de S100A9 peut être phosphorylé sur la Thr^{113} par la p38 MAPK lors d'une stimulation du PMN [Bengis-Garber *et al.* 1993; Schenten *et al.* 2011]. D'autres modifications post traductionnelles incluant des méthylations et des acétylations peuvent intervenir modifiant les propriétés de ces protéines. Le cytosol est un milieu réducteur mettant en jeu des systèmes redox tels que la thiorédoxine réductase et des enzymes dépendant du glutathion alors que le milieu extra-cellulaire est fortement oxydant [Ellgaard *et al.* 2003], si bien que les protéines S100A8 et S100A9 sont fortement exposées aux oxydations lorsqu'elles sont sécrétées dans le milieu extra-cellulaire.

S100A8 et S100A9 ne possèdent pas la séquence signal qui leur autorise une sécrétion dans le milieu extra-cellulaire par la voie classique du Réticulum endoplasmique-Golgi. Elles sont secrétées par une voie dépendante de la protéine-kinase PKC mettant en jeu les microtubules [Rammes *et al.* 1997]. Lors de la nécrose des phagocytes, ces protéines sont également déversées dans le milieu extra-cellulaire constituant des signaux de danger [Matzinger 2002a] capables d'initier, d'amplifier et de pérenniser la réaction inflammatoire via les récepteurs de l'immunité innée TLR-4 (Toll-like receptor 4) [Vogl *et al.* 2007].

Figure 25. Structure des protéines S100A8 et S100A9

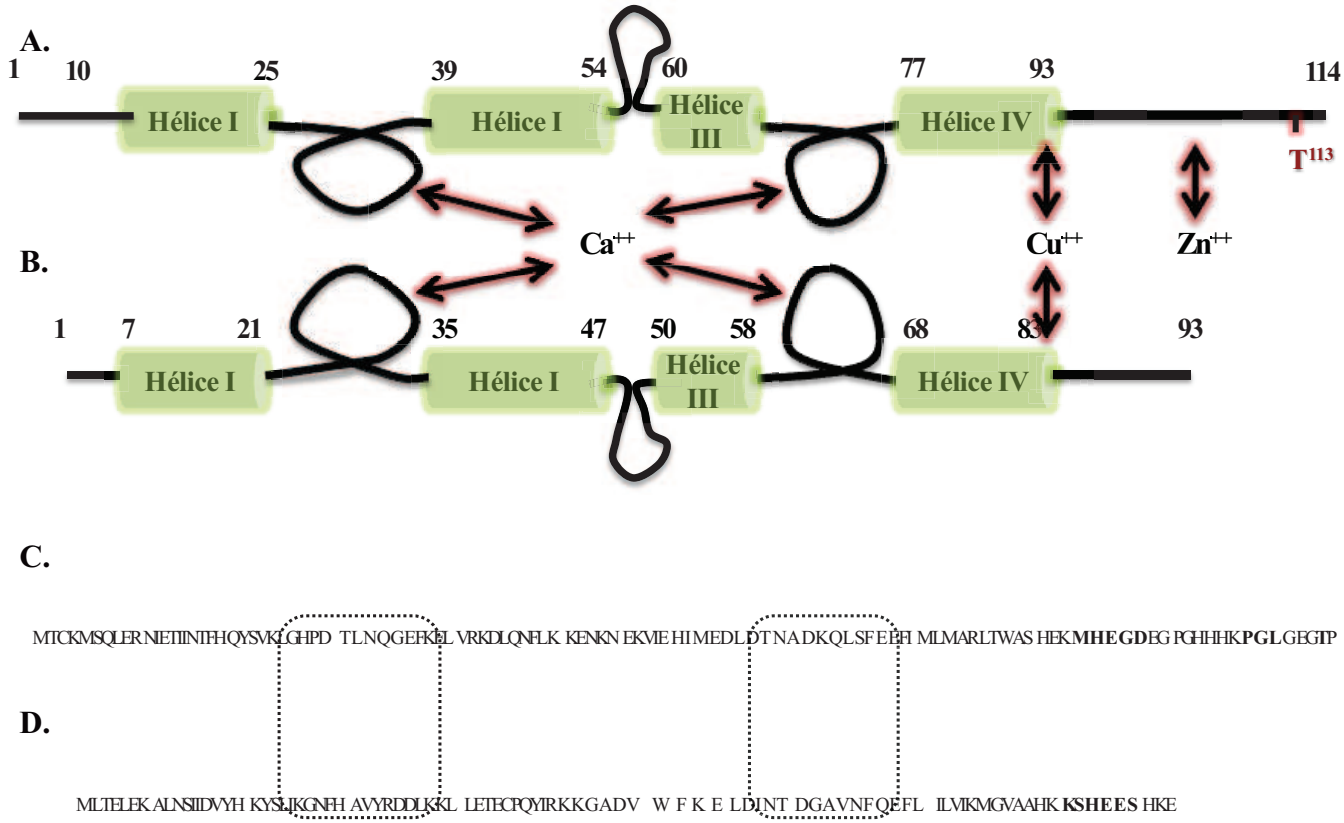

*Domaines fonctionnels de S100A9 (**A**) et S100A8(**B**) et séquences de S100A9(**C**) et S100A8 (**D**).*

5.5.5. Rôle des protéines S100A8 et S100A9 dans la stimulation des cellules myéloïdes

Un nombre grandissant de publications est venu récemment préciser le rôle intra-cellulaire des protéines S100A8 et S100A9. Cependant les fonctions de ces protéines semblent encore bien mal décrites au regard de leur abondance dans le cytosol du PMN. Il semble toutefois qu'elles soient impliquées dans plusieurs aspects de la maturation et de la stimulation du PMN. Tout d'abord, elles sont engagées dans la différenciation de la lignée myéloïde. Leur expression est limitée à certains stades de développement [Kerkhoff *et al.* 2002] du monocyte. S100A9 bloque la différenciation du macrophage [Cheng *et al.* 2008] et restreint l'expansion

des cellules dendritiques myéloïdes par l'induction de cellules myéloïdes suppressives. Chez les souris invalidées pour le gène codant pour S100A9, l'expression de S100A8 est détectable au niveau du transcrit mais ne l'est plus au niveau de la protéine. L'étude du cytosquelette des PMNs de ces souris S100A9$^{-/-}$, chez qui l'expression de l'hétérocomplexe S100A8/A9 est *quasi* nulle, montre que ces 2 partenaires sont impliqués dans la polymérisation de la tubuline. L'hétérocomplexe S100A8/A9 est impliqué dans le réarrangement du cytosquelette nécessaire à la diapédèse et à la migration du PMN sur le site inflammatoire [Vogl *et al.* 2004]. La phosphorylation de la Thr^{113} de S100A9, par la p38 MAPK, prévient la polymérisation de la tubuline.

5.5.6. Arguments expérimentaux de l'implication de S100A8/A9 dans l'activation de l'oxydase

Plusieurs études *in vivo* et in *vitro* convergent pour prouver que S100A8/A9 est un régulateur positif de l'oxydase. Tout d'abord, il semble qu'au cours de l'activation du neutrophile, l'hétérocomplexe est transféré à la membrane avec les facteurs cytosoliques de NOX2. La fixation d'anticorps polyclonaux anti-p67^{phox} à une matrice de protéine A-Sepharose a permis d'objectiver la co-immunoprécipitation de p67^{phox}, p47^{phox} et de S100A8/A9 dans le cytosol de neutrophiles bovins [Doussière *et al.* 2002].

Ces résultats sont confirmés par l'analyse protéomique par MALDI-TOF (Matrix-Assisted Laser Desorption/Ionization) du complexe d'activation cytosolique purifié à partir de cytosol de PMNs humains activés sur une matrice d'affinité sur laquelle ont été fixés des anticorps polyclonaux anti-p47^{phox}. L'hétérocomplexe S100A8/A9 est co-purifié dans les fractions d'élution contenant les facteurs cytosoliques p67^{phox}, p47^{phox} et p40^{phox} [Berthier *et al.* 2003].

De plus l'activité NADPH oxydase des PMNs de souris S100A9$^{-/-}$ et de cellules NB4 différenciées en pseudo-neutrophiles chez qui l'expression de S100A9 a été réprimée, est nettement diminuée [Kerkhoff *et al.* 2005]. La transfection du gène de S100A8 et de S100A9 dans les lymphocytes B immortalisés par le virus Epstein Barr (EBV) permet d'augmenter l'activité oxydase [Berthier *et al.* 2003]. Enfin, dans un système acellulaire contenant des anticorps dirigés contre S100A9, il existe une chute de l'activité oxydase [Kerkhoff *et al.* 2005].

5.5.7. Mécanismes moléculaires de l'activation de NOX2 par S100A8/A9

Les mécanismes moléculaires par lesquels l'hétérodimère S100A8/A9 est impliqué dans l'assemblage et l'activation du complexe NADPH oxydase sont multiples et variés. Le transport de l'acide arachidonique par l'hétérocomplexe S100A8/A9 est dépendant du

calcium [Sopalla *et al.* 2002]. Le site de fixation de l'acide arachidonique situé sur la partie C-terminale (His^{103}-His^{105}) est spécifique de S100A9 et n'est pas conservé chez les autres membres de la famille S100. Lors de la translocation à la membrane de S100A8/A9, l'acide arachidonique peut lier le cytochrome b_{558} et en modifier la conformation afin de le rendre pleinement actif [Doussière *et al.* 1999]. En outre, S100A8/A9 augmente l'affinité du cytochrome b_{558} pour $p67^{phox}$ de façon synergique avec $p47^{phox}$ [Berthier *et al.* 2003]. Des liens privilégiés de S100A8 avec $p67^{phox}$ ont été rapportés [Kerkhoff *et al.* 2005]. La fixation coopérative de S100A8/A9 sur le cytochrome b_{558} pourrait procéder d'une régulation allostérique de NOX2 [Berthier *et al.* 2003; Paclet *et al.* 2007] telle que l'ont définie Monod, Wyman et Changeux [Monod *et al.* 1965].

La voie de signalisation impliquée dans la migration de S100A8/A9 à la membrane plasmique a récemment été décrite. Schenten *et al.* montrent dans la lignée myéloïde HL-60 que la translocation est secondaire à une augmentation de la concentration cytosolique de calcium [Schenten *et al.* 2010] régulée par une Sphingosine-kinase [Schenten *et al.* 2011]. La phosphorylation de S100A9 par p38 MAPK est régulée par la PLA_2 et constitue une condition *sine qua none* à l'activation de NOX2 par S100A8/A9 [Schenten *et al.* 2010].

6. L'hétérocomplexe S100A8/A9 au cœur de la physiopathologie de la PR

6.1. S100A8/A9, médiateurs de l'inflammation

Les protéines S100A8 et S100A9 semblent jouer un rôle capital dans la phase aiguë de l'inflammation. Dans un modèle murin d'arthrite aiguë, l'inhibition de la protéine S100A8 empêche le recrutement de polynucléaires neutrophiles et le développement de l'arthrite [Ryckman *et al.* 2003a]. L'implication de ces médiateurs de l'inflammation dépasse le champ de la rhumatologie puisqu'une surexpression de l'une ou l'autre des protéines S100 a été rapportée dans les maladies inflammatoires de l'intestin, la glomérulonéphrite lupique, la mucoviscidose ou le développement tumoral. Ces protéines étant sécrétées localement par les neutrophiles activés, elles constituent des marqueurs inflammatoires plus sensibles que les protéines de la phase aiguë de l'inflammation à synthèse hépatique.

6.2. Protéines S100, marqueurs diagnostiques de la PR

Quelques études, utilisant diverses techniques de dosage, ont rapporté une élévation de la concentration des protéines S100A8, S100A9 dans le sérum et le tissu synovial de patients atteints de PR **(Tableau 2)** par rapport à un groupe témoin constitué de patients arthrosiques [De Seny *et al.* 2005].

6.3. Protéines S100, marqueurs pronostiques dans la PR

Le rôle des protéines S100A8 et S100A9 dans les destructions articulaires a été mis en évidence dans des modèles murins d'arthrites chroniques [Van Lent *et al.* 2008a]. Chez l'homme, une concentration plasmatique élevée de protéines S100A8 et S100A9 est corrélée à la sévérité clinique de la PR, aux lésions radiologiques [Hammer *et al.* 2008] et donc au pronostic fonctionnel du patient souffrant de PR. Dans le cadre de l'arthrite juvénile idiopathique, la concentration des protéines S100A8 et S100A9 est corrélée au handicap. Après instauration du traitement de fond, l'expression des protéines S100A8, S100A9 et S100A12 diminue rapidement chez les patients répondeurs pouvant permettre un suivi de la réponse aux traitements.

Tableau 2. Expression des protéines S100 dans les rhumatismes inflammatoires

Auteur	Technique	Milieu biologique	Patients	*Principaux résultats*
De Seny *et al.* 2005	SELDI	Sérum	16 patients sains, 34 PR, 14 arthroses	*Identification de S100A8, surexprimée dans le sérum de patients souffrant de PR par rapport aux sujets sains*
Liao *et al.* 2004	Chromatographie en 2 dimensions	Sérum	15 PR érosives et 15 PR peu érosives	*S100A8, S100A9 et S100A12 sont surexprimées dans le sérum des patients atteints de PR érosive*
Hammer *et al.* 2007	ELISA (S100A8/A9)	Sérum	145 PR	*La concentration sérique de l'hétérocomplexe S100A8/A9 :* *- est corrélée à la CRP et à la VS* *- est un facteur indépendant d'évolution radiologique péjorative (score de Sharp modifié)*
Wulffraat *et al.* 2003	ELISA (S100A8/A9)	Sérum	12 arthrites juvéniles idiopathiques	*La concentration de l'hétérocomplexe S100A8/A9 :* *- est corrélée au score fonctionnel (CHAQ)* *- diminue après traitement* *- augmente avant une rechute* *- n'est pas prédictive d'un syndrome d'activation macrophagique*
Foell *et al.* 2003	ELISA S100A12 Immuno-histochimie	Sérum, Liquide synovial et membrane synoviale	42 (RhPso, PR, SA) et 2 patients sains	*S100A12 est surexprimée dans la membrane synoviale de PR, SA et RhPso* *La production de S100A12 diminue dans la membrane synoviale après initiation du MTX*
Foell *et al*. 2004	ELISA S100A12	Sérum	124 arthrites juvéniles idiopathiques	*La concentration de S100A12 :* *- diminue après traitement* *- est prédictive d'une poussée inflammatoire*

CHAQ=Child Health Assemement Questionnaire, CRP="C-Reactive Proteine", ELISA=Enzyme- Linked Immunosorbent Assay, MTX=Méthotrexate, PR=Polyarthrite Rhumatoïde, RhPso=Rhumatisme psoriasique, SA=Spondylarthrite Ankylosante, SELDI-TOF=Surface-Enhanced Laser Desorption/Ionization, VS=Vitesse de Sédimentation.

6.4. S100A8/A9, acteurs étiopathogéniques de la PR

Le dosage de plusieurs membres de la famille des S100 pourrait s'intégrer dans la stratégie diagnostique des rhumatismes inflammatoires (**Tableau 2**). Outre les études situant ces protéines comme biomarqueurs de la PR, des données fondamentales impliquent les protéines S100 dans les mécanismes physiopathologiques de la PR [Baillet 2010].

Premièrement, les protéines S100A8 et S100A9 semblent avoir un rôle capital à la phase aiguë de l'inflammation notamment par l'induction de cytokines de type Th1 (TNFα, IL1-β) et par le recrutement de cellules inflammatoires. Ce sont également des chimiokines qui permettent le recrutement des PMNs sur le site inflammatoire [Ryckman *et al.* 2003a]. Deuxièmement, le rôle des protéines S100A8 et S100A9 dans les destructions articulaires a été mis en évidence dans des modèles murins d'arthrites chroniques [Van Lent *et al.* 2008a]. Troisièmement, les protéines S100A8 et S100A9 potentialisent la production d'anions $O_2^{\bullet -}$ par le complexe NADPH oxydase phagocytaire (**Annexe 2**, [Berthier *et al.* 2009; Berthier *et al.* 2003]). Elles favorisent donc la production de dérivés radicalaires de l'oxygène par les cellules infiltrant le pannus (neutrophiles, monocytes, lymphocytes…) ou les cellules résidantes de la membrane synoviale. Quatrièmement, des études *in vitro* montrent que la stimulation des récepteurs RAGE, récepteur de S100A12, dans les synoviocytes de PR pourrait contribuer à leur phénotype pseudotumoral [Steenvoorden *et al.* 2007b]. S100A8 et S100A9 régulent l'activité télomérase, favorisant la prolifération cellulaire et la formation de métastases pulmonaires [Hiratsuka *et al.* 2006]. Enfin, les protéines S100A8 et S100A9 sont impliquées dans le stress endothélial et la formation de la plaque d'athérome [McCormick *et al.* 2005]. Leurs concentrations *in situ* et systémiques s'élèvent lors d'un syndrome coronarien aigu plus précocement que la troponine et la myoglobine. La sensibilité des protéines S100A8/S100A9 est comparable à celle des marqueurs classiques de nécrose du myocarde [Altwegg *et al.* 2007].

PRESENTATION

DU TRAVAIL

La NADPH oxydase des phagocytes, est formée d'un centre catalytique membranaire, le cytochrome b_{558}, sur lequel viennent s'associer des protéines cytosoliques régulatrices. L'activité catalytique de cette enzyme est finement régulée et les éléments de ce complexe protéique sont différemment exprimés selon le type cellulaire. Ainsi, dans le PMN et le lymphocyte B immortilisé par le virus EBV, l'activité NADPH oxydase varie tant au plan quantitatif qu'au plan qualitatif (**Figure 26**).

Figure 26. Activité NADPH oxydase dans le PMN et le lymphocyte B-EBV

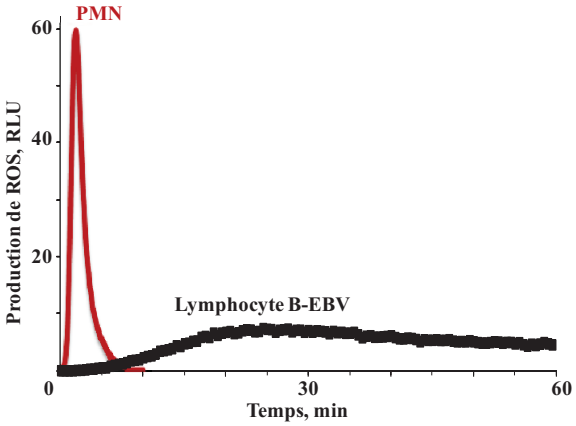

$2x10^5$ PMNs et $1x10^6$ lymphocytes B, immortalisés par le virus EBV, ont été incubés dans du PBS contenant 0,9mM de $CaCl_2$, 0,5mM de $MgCl_2$, 20mM de glucose, 20µM de luminol et 10U/m de HRPO ("Horse Radish Peroxidase"). La production d'$O_2^{\bullet-}$ a été mesurée par chimiluminescence après stimulation par 130nM de PMA. RLU="Relative Luminescence Unit", ROS=Formes réactives de l'oxygène. D'après [Berthier et al. 2009].

Les mécanismes moléculaires de la régulation de l'activité catalytique de la NADPH oxydase reposent sur la phosphorylation des facteurs cytosoliques et du cytochrome b_{558}, la concentration en substrat, la présence d'effecteurs allostériques et l'éventuelle microcompartimentation des différents constituants.

Dans notre travail, nous nous sommes intéressés à certains de ces mécanismes de régulation de l'activité NADPH oxydase phagocytaire. Compte tenu de l'importance de la stimulation du PMN dans le processus inflammatoire et les destructions articulaires de la PR, notre objectif, à terme, est de mieux comprendre le rôle de l'activation de la NADPH oxydase phagocytaire dans cette pathologie.

L'étude du complexe NADPH oxydase, isolé constitutivement actif, a révélé la présence de deux enzymes impliquées dans la régulation du métabolisme du glucose. Il s'agit de la PFK2 (6-phosphofructokinase 2) et de la 6PGDH (6-phosphogluconate déshydrogénase) [Paclet *et al.* 2007]. De plus, l'étude des protéines cytosoliques retenues sur une matrice d'affinité ciblant $p47^{phox}$, a établi que les protéines S100A8 et S100A9 sont associées au complexe de facteurs cytosoliques [Berthier *et al.* 2003]. L'hétérocomplexe S100A8/A9, augmente l'activité de la NADPH oxydase phagocytaire et induit un changement conformationnel du cytochrome b_{558}.

Au regard de ces résultats expérimentaux, nous nous sommes posé les questions suivantes :

- Les enzymes 6PGDH et PFK2 exercent-t-elles une régulation spécifique de l'activité catalytique de NOX2 ? Autrement dit, l'interaction entre NOX2 et ces protéines est-elle fortuite ou traduit-elle de nouveaux mécanismes de régulation de l'activité NADPH oxydase des phagocytes ?

- Quels sont les domaines impliqués dans l'interaction entre l'hétérocomplexe S100A8/A9 et le cytochrome b_{558} ?

- Sur un plan plus appliqué, la signature protéique de la PR contient-elle des stigmates de l'activation du PMN ? Peut-on discriminer des biomarqueurs spécifiques de la PR ?

Nous avons tenté de répondre à ces questions par des stratégies variées :

- Dans un premier temps, nous avons évalué l'impact de la 6PGDH et de la PFK2 sur l'activité oxydase, *ex vivo* et *in vitro*, par transfection d'ARN interférants. L'étude de l'association entre ces enzymes et les protéines régulatrices de NOX2 a été menée par co-immunoprécipitation et microscopie confocale.

- Dans un deuxième temps, les domaines de S100A8/A9 engagés d'une part dans la liaison au cytochrome b_{558} et d'autre part dans l'activation de l'oxydase ont été étudiés à l'aide de protéines recombinantes tronquées.

- Dans un troisième temps, nous avons comparé le protéome du liquide synovial rhumatoïde à celui de d'autres pathologies inflammatoires ainsi qu'à celui de patients arthrosiques. Puis, nous avons analysé dans quelle mesure l'activation du PMN influençait l'empreinte protéomique du liquide articulaire de patients souffrant de PR.

TRAVAUX DE RECHERCHE

CHAPITRE I

Régulation de l'activité NADPH oxydase des phagocytes par les enzymes du métabolisme du glucose

Articles 1 et 2

Partie 1 : La 6-phosphogluconate déshydrogénase et la 6-phosphofructokinase 2 : partenaires de régulation de la NADPH oxydase des phagocytes

La NADPH oxydase des phagocytes est un complexe protéique de transfert d'électrons composé d'un élément redox, le cytochrome b_{558} membranaire formé de NOX2/gp91^{phox} et son partenaire p22^{phox}, auquel s'associent des facteurs cytosoliques d'activation, p67^{phox}, p47^{phox}, p40^{phox} et Rac 1/2. L'assemblage de ces facteurs au niveau membranaire sur le cytochrome b_{558} qui est une hémoprotéine, conditionne l'activation de l'oxydase c'est-à-dire le transfert d'électrons depuis NADPH jusqu'à l'oxygène qui est réduit en $O2^{\bullet -}$. NOX2 est l'oxydase du système, son partenaire p22^{phox} stabilise l'hétérodimère, NOX2/p22^{phox}.Il est directement impliqué dans la maturation de NOX2 et constitue aussi le point d'ancrage de p47^{phox} au moment de l'assemblage des différents composants. Dans cet assemblage, p67^{phox} est déterminant : son interaction avec le cytochrome b_{558}, initie le changement de conformation de l'hémoprotéine et l'activation de l'oxydase.

Le complexe de la NADPH oxydase a été isolé pour la première fois, à partir de PMNs stimulés, sous une forme constitutivement active [Paclet *et al.* 2007].
L'étude de la fraction contenant le complexe protéique purifié, par spectrométrie de masse MALDI-TOF, révèle la présence de deux enzymes impliquées dans la régulation du métabolisme du glucose. Il s'agit de la PFK2 (6-phosphofructokinase 2) et de la 6PGDH (6-phosphogluconate déshydrogénase).

L'objectif de notre travail a été de comprendre le rôle de la 6PGDH et de la PFK2 dans l'activation du complexe de la NADPH oxydase des phagocytes, mais aussi de se poser la question de la spécificité de ces deux nouveaux partenaires dans le mécanisme de régulation.

1. La 6-phosphogluconate déshydrogénase, 6PGDH

La 6PGDH est l'une des deux enzymes majeures de la voie des pentoses phosphates. Dans les neutrophiles, cette voie devient prépondérante compte tenu des besoins en NADPH pour le fonctionnement de la NADPH oxydase.

Dans notre premier article nous montrons que :

- *La diminution d'expression de la 6PGDH est corrélée à une diminution de l'activité NADPH oxydase des PLB985 in vivo, ainsi que dans un système acellulaire reconstitué à*

partir de membrane et de cytosol de cellules dans lesquelles l'expression de la 6PGDH a été diminuée par transfection d'ARN interférants.

- La 6PGDH co-immunoprécipite avec les facteurs cytosoliques régulateurs de la NADPH oxydase phagocytaire, $p67^{phox}$, $p47^{phox}$ et $p40^{phox}$ dans le cytosol de PMNs activés par le PMA.

- Après stimulation par le PMA, la 6PGDH migre à la membrane plasmique où elle co-localise avec $p67^{phox}$.

- La 6PGDH module la quantité de NADPH et augmente l'affinité de la NADPH oxydase pour son substrat.

2. La phosphofructokinase-2, PFK2

La PFK2 est l'enzyme qui intervient dans la synthèse du fructose-2,6-diphosphate, activateur allostérique physiologique de la phosphofructokinase-1. La PFK1 est un point de régulation majeur de la vitesse de la glycolyse. Dans les neutrophiles, la glycolyse joue un rôle essentiel pour la synthèse de l'ATP compte tenu de l'absence de mitochondries fonctionnelles. La PFK2 est régulée par phosphorylation qui, selon les cellules ou les tissus, conduit à un état actif ou inactif de l'enzyme (isoenzymes).

Dans ce deuxième article nous montrons que :

- L'activité NADPH oxydase des PLB985 est plus faible lorsque la phosphorylation de la PFK2 est diminuée par des inhibiteurs de la Protéine-kinase A et de Akt. De même, la diminution d'expression de la PFK2 est corrélée à une diminution de l'activité NADPH oxydase des PLB985 in vivo, ainsi que dans un système acellulaire reconstitué à partir de membrane et de cytosol de cellules transfectées par ARN interférants.

- Dans le cytosol de PLB985 stimulés par le PMA, la PFK2 co-immunoprécipite avec les facteurs cytosoliques régulateurs de la NADPH phagocytaire $p67^{phox}$, $p47^{phox}$ et $p40^{phox}$ mais ne semble pas interagir avec Rac.

- La PFK2 est détectée au niveau des radeaux lipidiques riches en cholestérol où elle co-localise avec NOX2 et la Nucléoside diphosphate Kinase (NDPK) dans les cellules activées.

- La PFK2 augmente la production d'ATP. L'inhibition de l'expression de la PFK2 est responsable d'une diminution de la phosphorylation de $p47^{phox}$ sur les résidus Ser^{328} et Ser^{315}.

En conclusion, la 6PGDH et la PFK2 sont deux nouveaux régulateurs de la NADPH oxydase phagocytaire. Lors de la stimulation des neutrophiles, ces enzymes du métabolisme du glucose migrent à la membrane et semblent s'associer aux autres facteurs cytosoliques de la NADPH oxydase phagocytaire. La 6PGDH augmente l'affinité de NOX2 pour son substrat ainsi que la concentration cytosolique de NADPH. La PFK2 stimule la production d'ATP disponible d'une part pour la phosphorylation de $p47^{phox}$ et d'autre part pour la NDPK. Cette dernière enzyme pourrait secondairement activer Rac en catalysant la synthèse de GTP à partir de l'ATP.

J'ai contribué à ce travail en cultivant et en transfectant les PLB985 différenciés en pseudo-neutrophiles. J'ai analysé l'impact de la déplétion en 6PGDH et PFK2, sur l'activité NADPH oxydase des PLB985, et en mesurant la concentration cytosolique de NADPH et d'ATP. J'ai également étudié la répartition subcellulaire des protéines d'intérêt en microscopie confocale et les interactions protéines-protéines par co-immunoprécipitation.

Article 1 : **Baillet A.**, Xu R., Grichine A., Berthier S., Morel F., and Paclet M.H. (2011), Coupling of 6-phosphogluconate dehydrogenase with NADPH oxidase in neutrophils: NOX2 activity regulation by NADPH availability. *FASEB J* 25 2333-43.

Article 2 : **Baillet A.**, Hograindleur MA., El Benna J., Berthier S., Morel F., and Paclet M.H. 6-phosphofructo-2-kinase modulates neutrophil NADPH oxidase activity through Adenosine triphosphate availability. Soumis à *Jounal of Biological Chemistry*.

Article 1

Coupling of 6-phosphogluconate dehydrogenase with NADPH oxidase in neutrophils: NOX2 activity regulation by NADPH availability.

The FASEB Journal article fj.10-173807. Published online March 28, 2011.

Coupling of 6-phosphogluconate dehydrogenase with NADPH oxidase in neutrophils: Nox2 activity regulation by NADPH availability

Athan Baillet,*,†,1 Rang Xu,*,1 Alexei Grichine,§ Sylvie Berthier,*,‡ Françoise Morel,* and Marie-Hélène Paclet*,‡,2

*Groupe de Recherche et d'Etude du Processus Inflammatoire (GREPI), Techniques de l'Ingénierie Médicale et de la Complexité–Informatique, Mathématiques et Applications de Grenoble (TIMC-IMAG) Unité Mixte de Recherche (UMR) 5525 Centre National de la Recherche Scientifique (CNRS), Université Joseph Fourier (UJF), †Clinic of Rheumatology, and ‡Laboratory Biochimie des Enzymes et des Protéines, Institut de Biologie et Pathologie, Centre Hospitalier Universitaire (CHU), Grenoble, France; and §Platform Optical Microscopy–Cell Imaging, UJF, Institut National de la Santé et de la Recherche Médicale (INSERM) U823, Institut Albert Bonniot, La Tronche, France

ABSTRACT **It is well known that activation of the phagocyte NADPH oxidase requires the association of cytosolic proteins (p67-phox, p47-phox, p40-phox, and Rac) with the membrane cytochrome b_{558}, leading to its conformation change. Recently, the phagocyte NADPH oxidase complex was isolated in a constitutively active form. In this complex, 6-phosphogluconate dehydrogenase (6PGDH), an enzyme involved in the production of intracellular NADPH, was identified. This protein was absent from the oxidase complex isolated from B lymphocytes, suggesting a specific interaction with the neutrophil NADPH oxidase. To clarify the implication of 6PGDH in the NADPH oxidase activity, a siRNA approach was conducted in neutrophil-like PLB985 cells. NADPH oxidase activity of siRNA-transfected cells was shown to be decreased. Similar results were obtained *in vitro*, after reconstitution of oxidase activity with subcellular fractions isolated from siRNA-transfected cells. Interestingly, the Michaelis constant (K_m) of Nox2 for NADPH increases in 6PGDH-depleted cells. Moreover, 6PGDH coimmunoprecipitated with oxidase cytosolic factors from cytosol of stimulated cells. Data suggested that the affinity of Nox2 for NADPH is increased in the presence of 6PGDH on cell stimulation. The present work proposes a new way of NADPH oxidase activity regulation by modulating Nox2 affinity for NADPH.—Baillet, A., Xu, R., Grichine, A., Berthier, S., Morel, F., Paclet, M.-H. Coupling of 6-phosphogluconate dehydrogenase with NADPH oxidase in neutrophils: Nox2 activity regulation by NADPH availability. *FASEB J.* 25, 000–000 (2011). www.fasebj.org**

Key Words: phox · siRNA transfection · cytochrome b_{558}

The phagocyte NADPH oxidase (*phox*) is an enzymatic complex that, on cell activation, produces huge amounts of superoxide anions that participate in bacterial killing. Its activity is dependent on the assembly of cytosolic regulatory factors (p67-phox, p47-phox, p40-phox, and Rac1 or Rac2) on the membrane cytochrome b_{558} formed by 2 subunits, Nox2 (gp91-phox) and p22-phox (1–4). A defect in NADPH oxidase activity is illustrated in chronic granulomatous disease (CGD), characterized by severe and recurrent infections due to the incapacity of phagocytes to kill invading microbes. CGD is caused by mutations in any one of the 4 genes encoding the major oxidase subunits: Nox2, p22-phox, p47-phox, and p67-phox (5–6).

NADPH oxidase catalyzes an electron transfer from Nox2-bound NADPH through FAD and hemes to molecular oxygen in order to form superoxide anions $O_2^{\cdot -}$. Activation of NADPH oxidase requires a large and continuous supply of cytosolic NADPH, the substrate of the reaction. In cells, NADPH used in reductive biosynthesis reactions is produced by the pentose phosphate pathway (PPP). PPP is strictly dependent on the presence of glucose. Neutrophil stimulation is correlated to activation of both glucose metabolism and PPP (7, 8). The first step of the PPP is mediated by glucose-6-phosphate dehydrogenase, which converts glucose 6-phosphate, produced by glucose phosphorylation, into 6-phosphogluconolactone, with the release of a molecule of NADPH. 6-Phosphogluconolactone is transformed into 6-phosphogluconate by gluconolactonase. 6-Phosphogluconate dehydrogenase (6PGDH), a homodimer formed by two 52-kDa monomers, catalyzes the second oxidative step of PPP and converts 6-phos-

[1] These authors contributed equally to this work.

[2] Correspondence: GREPI TIMC-IMAG UMR 5525 CNRS/UJF, CHU Albert Michallon, 6ème étage Unité E, BP 217, 38043 Grenoble Cedex 9, France. E-mail: mhpaclet@chu-grenoble.fr

doi: 10.1096/fj.10-173807

This article includes supplemental data. Please visit *http://www.fasebj.org* to obtain this information.

phogluconate into ribose 5-phosphate, with the release of a second molecule of NADPH.

In a previous study, we isolated the whole NADPH oxidase complex in a constitutive active form (9) and identified the presence of 6PGDH associated with the neutrophil oxidase complex. 6PGDH was not found in the complex prepared with cytosol from EBV-B lymphocytes, suggesting a specific association with the enzyme in neutrophils and/or another source of NADPH in EBV-B cells. As neutrophil NADPH oxidase activity is strongly higher than that of EBV-B lymphocytes (10–12), we postulated that 6PGDH might be a regulatory element of NADPH oxidase activity in phagocytic cells.

In the present study, we analyzed the involvement of 6PGDH in the regulation of phagocyte NADPH oxidase activity by using a 6PGDH gene-silencing approach in neutrophil-like cells. Results clearly demonstrated that 6PGDH depletion was correlated with NADPH oxidase activity reduction but also with an affinity decrease of NADPH oxidase for NADPH. Coimmunoprecipitation analysis and confocal microscopy study showed a coupling of 6PGDH with NADPH oxidase only in activated cells, suggesting a cell-stimulation-dependent interaction of 6PGDH with NADPH oxidase. On the basis of the present data, 6PGDH might be a new target for therapeutic molecules in order to modulate NADPH oxidase activity in neutrophils.

MATERIALS AND METHODS

Materials

Chemical reagents used in this study and their sources were the following: diisopropyl fluorophosphate (DFP; Acros Organics, Noisy-Le-Grand, France); ECL Western blotting detection reagents, Sephacryl S-300 HR, DEAE Sepharose CL-6B, CM Sepharose CL-6B, and octyl Sepharose CL-4B (Amersham Pharmacia Biotech, Uppsala, Sweden); heparin-agarose and PMA (Sigma Chemicals, St. Louis, MO, USA); *n*-octyl glucoside (Roche Diagnostics, Meylan, France); monoclonal antibody directed against 6PGDH (clone 1G12; Abnova, Heidelberg, Germany); AllStars Negative Control siRNA coupled to Alexa Fluor 488 (Qiagen, Courtaboeuf, France.

PLB985 cell line and neutrophils

Neutrophils from buffy coats were isolated according to previous methods (13). PLB985 cells (14) were grown in RPMI 1640 medium supplemented with 2 mM glutamine, 10% (v/v) FBS, 100 U/ml penicillin, and 100 μg/ml streptomycin at 37°C and in 5% CO_2 atmosphere. For granulocytic differentiation, PLB985 cells (5×10^5 cells/ml) were treated with 0.5% (v/v) DMF for 1–6 d (14).

Measurement of NADPH oxidase activity in PLB985 cells

Undifferentiated and granulocyte-differentiated PLB985 cells (2.5×10^5 cells in 50 μl PBS) were suspended with 200 μl PBS containing 0.9 mM $CaCl_2$, 0.5 mM $MgCl_2$, 20 mM glucose, 20 μM luminol, and 10 U/ml horseradish peroxidase. Superoxide production was measured by chemiluminescence after adding PMA (130 nM; ref. 15). Photon emission was recorded at 37°C for 30 min with a Luminoscan (Labsystem, Pontoise, France).

Isolation of oxidase complex

Oxidase complex was isolated as described previously (9). Purified neutrophils and d 6 differentiated PLB985 cells were suspended at 10^8 cells/ml in PBS supplemented with 0.9 mM $CaCl_2$ and 0.5 mM $MgCl_2$. Cells were incubated at 37°C in presence of 5 μM cytochalasin B for 15 min and then activated with 810 nM PMA for 10 min. This step is required to obtain an activated cytochrome b_{558} conformation able to bind cytosolic regulatory proteins and also to remove granule proteases. In some experiments, neutrophils and PLB985 cells were not stimulated. Membrane proteins from stimulated neutrophils were prepared as previously reported (16) and solubilized using 68 mM *n*-octyl glucoside for 20 min at 4°C. After centrifugation at 2×10^5 *g*, the solubilized extract was submitted to ion exchange chromatography, formed by a mixture (1:1:1, v/v/v) of CM-Sepharose, DEAE Sepharose, and *N*-amino octyl-Sepharose, combined with heparin-agarose affinity chromatography, as described previously (9). Once cytochrome b_{558} was bound to heparin-agarose, the purification buffer (containing 100 mM HEPES, pH 7.2; 100 mM KCl; 10 mM NaCl; 1 mM EDTA; 0.1 mM DTT; 20% v/v glycerol; 0.1% w/v Triton X-100; and a mixture of protease inhibitors, 10 μM Nα-p-tosyl-L-lysine chloromethyl ketone, 1.8 μM leupeptin, and 1.5 μM pepstatin) was replaced by the same buffer containing 40 mM *n*-octyl-glucoside instead of Triton X-100. Then cytosol, either from resting (unstimulated control) or stimulated neutrophils, or from PLB985 cells (25 mg), was deposited on the heparin-agarose matrix. Once the absorbance at 280 nm was null, cytochrome b_{558} and the associated proteins were eluted using a NaCl gradient (0–0.5 M). Elution of cytochrome b_{558} was followed by measuring the reduced-minus-oxidized difference spectrum. Oxidase activity of the fractions containing cytochrome b_{558} was determined. Fractions with a high oxidase activity were pooled and applied to a Sephacryl S-300 column equilibrated in the purification buffer. After filtration, the heme-containing fractions were analyzed by Western blot, and their oxidase activity was measured. Cytochrome b_{558} was quantified by reduced-minus-oxidized difference spectra and by measuring the difference of absorbance between the Soret band at 426 nm and the valley at ~410–411 nm. The absorption coefficient used was 106 $mM^{-1} \cdot cm^{-1}$ at 426 nm (17).

Measurement of NADPH oxidase activity

Oxidase activity of the purified oxidase complex

NADPH oxidase activity was measured after mixing purified oxidase complex (0.2 pmol cytochrome b_{558}/assay) with 10 μM FAD, 40 μM GTPγS, and 5 mM $MgCl_2$ in a final volume of 100 μl PBS, and adding 150 μM NADPH (final concentrations). Activity was measured in absence of any stimulation (amphiphile agent) (9).

Oxidase activity reconstituted with membrane and cytosolic fractions

Crude membrane and cytosolic fractions were prepared as described previously (16). Membranes (7.5 μg protein) were incubated with cytosol (75 μg protein) in presence of 40 μM GTPγS and 5 mM $MgCl_2$ in a final volume of 100 μl. An optimum amount of arachidonic acid (40 to 100 nmol) was used for activation (18). After 10 min incubation at 25°C, the

medium was transferred to a photometric curve. The reaction was initiated by adding NADPH (0 to 750 μM).

Reconstituted oxidase activity was assessed by measuring the superoxide-dismutase-sensitive portion of ferricytochrome-*c* reduction recorded at 550 nm (ε_{550}=21.1 $mM^{-1} \cdot cm^{-1}$).

Transfection of differentiated PLB985 cells with 6PGDH siRNA

After 2 d of differentiation, PLB985 cells were collected and adjusted at the concentration of 2×10^7 cells/ml in the electroporation solution (RPMI 1640 containing 7 mM Na_2HPO_4 and 272 mM sucrose). Transfection conditions were set up by using increasing concentrations of an Alexa Fluor 488-labeled negative control siRNA. Cells (0.8×10^6 cells in 400 μl) were electroporated in presence of 0 to 300 nM of Alexa Fluor 488-labeled negative control siRNA during 40 ms at 250 V by using the ECM 830 electroporation system (BTX, Holliston, MA, USA). Transfection efficiency was estimated 5 h after transfection by measuring the fluorescence of Alexa Fluor 488 by flow cytometry. Inhibition of 6PGDH expression by using 4 different specific siRNAs (1 to 4) was evaluated 24 to 72 h after electroporation in the presence of 200 nM specific siRNA.

Flow cytometry analysis of transfection efficiency

PLB cells transfected with Alexa Fluor 488-labeled negative control siRNA were washed twice in PBS buffer and resuspended in 500 μl PBS containing 0.2% (w/v) BSA (5×10^5 cells). Fluorescence intensity (FL1) of the Alexa Fluor 488-labeled negative control siRNA was measured on a FACScalibur cytometer (Becton Dickinson, Le Pont-De-Claix, France; ref. 19).

RT-PCR analysis of 6PGDH expression

Total RNA from transfected PLB985 cells (1×10^7 cells) was extracted using TRIzol reagent (Invitrogen, Carlsbad, CA, USA), according to the manufacturer's instructions, at 24, 48, and 72 h after transfection. RNA concentrations were determined spectrophotometrically at 260 nm. Reverse transcription reactions were performed by using 5 μg of RNA with 20 U of AMV reverse transcriptase. All PCRs were processed with 35 cycles using 2.5 μl cDNA, 2.5 U of *Taq* polymerase and primers: ATTCTCAAGTTCCAAGACACCG (forward) and GTGGTAAAACAGGGCATGGGA (reverse). cDNA integrity and quantity were checked by amplification of a housekeeping gene actin using commercial primers.

Immunoprecipitation with anti-6PGDH antibody

Cytosol from resting and PMA-stimulated neutrophils (645 μg in 150 μl PBS buffer) was incubated with 5 μg of either anti-6PGDH mAb or an irrelevant mAb for 4 h at 4°C. Then 4 mg protein A-Sepharose CL-4B was added for a further 1-h incubation. After centrifugation at 14,000 *g* for 5 min at 4°C, the protein A-Sepharose beads were washed 3 times successively with PBS containing 1% (v/v) Triton X-100, PBS with 0.5 M NaCl, and finally PBS alone. Solubilization of the immunoprecipitate was carried out in the Laemmli sample buffer (20) for SDS/PAGE and immunoblotting.

Confocal microscopy

PMA-stimulated or unstimulated differentiated (d 6) PLB985 cells (2×10^5 cells in 50 μl PBS) were incubated on 0.01% (w/v) poly-L-lysine-coated round glass coverslips for 15 min at 37°C (21). After 2 washes with PBS, cells were fixed with 4% (w/v) paraformaldehyde for 10 min at room temperature. Coverslips were rinsed twice with PBS, and paraformaldehyde fluorescence was quenched by 50 mM NH_4Cl for 10 min at room temperature. After 2 washes with PBS, cells were permeabilized with 0.1% (w/v) Triton X-100 for 5 min at room temperature. After 2 washes with PBS, cells were first incubated for 1 h at room temperature with 50 μl of mouse monoclonal Ig specific of 6PGDH or irrelevant (1 μg in 50 μl PBS containing 1% w/v BSA) and with 50 μl of rabbit polyclonal Ig specific of p67-phox or irrelevant (1 μg in 50 μl PBS containing 1% w/v BSA). The cells were washed 3 times for 10 min with PBS containing 1% (w/v) BSA prior to a 1-h incubation with 100 μl of Alexa Fluor 488 donkey anti-mouse antibody (1:250 in PBS containing 1% w/v BSA) and with 100 μl of Alexa Fluor 546 donkey anti-rabbit antibody (1:250 in PBS containing 1% w/v BSA). After 2 washes with PBS, cell nuclei were stained with 40 μl Hoechst 33258 (0.5 μg/ml). Samples were then mounted in 10 μl DABCO solution, sealed, and stored at 4°C in the dark. Fixed cells were imaged at room temperature using the inverted confocal and 2-photon laser-scanning microscope (LSM 510 NLO; Carl Zeiss, Oberkochen, Germany) equipped with a ×40/1.3 Plan-Neofluar oil-immersion objective. The pinhole adjustment to 1 Airy unit resulted in <0.7-μm optical slice at 488-nm excitation wavelength. The image plane was chosen to be near the equator of the cell body and nucleus. The Alexa Fluor 488 fluorescence was selected with an NFT490 dichroic beamsplitter and LP505 long-pass filter (Zeiss). The Hoechst 33258 fluorescence was excited by 2-photon absorption of the 720-nm radiation of fs Ti:Sa laser (Tsunami; Spectra-Physics, Darmstadt, Germany) and selected with a 390- to 465-nm emission bandpass filter. No significant photobleaching was induced during image acquisition in either detection channel.

Polyclonal antibodies

Rabbit polyclonal antibodies were raised against polypeptides corresponding to the C-terminal region of p47-phox (residues 371–390), p67-phox (residues 511–526), p40-phox (residues 325–339), gp91-phox (residues 562–569), p22-phox (residues 184–195), and to the internal region shared by Rac1 and Rac2 (residues 123–145) (18, 22). Immunoglobulins were purified from rabbit antisera on 1 ml protein A-Sepharose.

SDS-PAGE and Western blot analysis

The proteins were fractionated by 10 or 11% SDS-PAGE (20) and electrotransferred to nitrocellulose, as described previously (23). Immunodetection was performed using rabbit polyclonal antibodies raised against p47-phox, p67-phox, p40-phox, gp91-phox, or p22-phox (dilution 1:1000). The immune complexes were detected with goat anti-rabbit secondary antibody combined with peroxidase. The bound peroxidase activity was detected using ECL reagents. Densitometry analysis of Western blot was performed by using Scion Image software (Scion Corp., Frederick, MD, USA).

Statistical analysis

Data are expressed as means ± SD. Statistical analysis was performed using the unpaired *t* test. The results are reported when significantly different (P<0.05) from the controls.

RESULTS

Isolation of the NADPH oxidase complex from PLB985 cells

In a previous work, we isolated the whole NADPH oxidase complex from neutrophils and B lymphocytes in a constitutively active form able to transfer electrons without stimulation in presence of NADPH (9). Analysis of proteins associated with the oxidase factors performed by MALDI-TOF mass spectrometry showed the presence of 6PGDH in the neutrophil complex but not in that prepared with EBV-B lymphocyte cytosol (9), even if the cytosolic concentration of 6PGDH was similar in PMN and B lymphocyte cytosol (data not shown). Considering only purified neutrophil oxidase complexes, the constitutive oxidase activity was either maximum (129 mol $O_2^{\cdot-}$·s^{-1}·mol heme b^{-1}; **Fig. 1*A*,** Cx1) or intermediate (~56 mol $O_2^{\cdot-}$·s^{-1}·mol heme b^{-1}, Fig. 1*A*, Cx2) depending on the purification. Interestingly, for both neutrophil complexes (Cx1 and Cx2, Fig. 1*A*), constitutive oxidase activity was correlated to the intensity of the band identified as 6PGDH (Fig. 1*A*, black arrow, high activity and intermediate activity respectively). There was no significant difference in NADPH oxidase constituents between complex with low and high constitutive activity as shown by Fig. 1*B*, even if the amount of p67-phox was 16% higher in the more active complex. To investigate the specificity of the association of 6PGDH with the neutrophil NADPH oxidase complex, a siRNA transfection approach was considered. This approach was performed in PLB985 cells, which can be differentiated in neutrophil-like cells and which are easily transfected. First, DMF-differentiated cells were collected from d 0 to 6 of differentiation in order to evaluate the expression of both NADPH oxidase cytosolic factors and 6PGDH. The expression of cytosolic regulatory proteins p67-phox and p40-phox was strongly up-regulated during differentiation, especially after 3 d of differentiation (**Fig. 2**). The expression of p47-phox was also increased, but the rise occurred early (d 1 of differentiation) and was weaker (Fig. 2). In contrast, the level of Rac and 6PGDH was unchanged during differentiation, indicating that the differentiation process did not affect the expression of both proteins (Fig. 2*A*).

In parallel, the NADPH oxidase activity was measured in intact PLB985 cells after PMA stimulation. Results clearly showed a regular increase of the superoxide anion production during the differentiation process until 4 d, where the activity seemed to be stable (Fig. 2*B*). There was no link between 6PGDH expression and NADPH oxidase activity during differentiation, as observed after densitometry analysis of Fig. 2*A* (data not shown); in contrast, there was a good correlation between the increase in p47-phox expression and the increase in NADPH oxidase activity during differentiation (Fig. 2*B*, inset).

According to these results, cells were collected at d 6 of differentiation in order to isolate the oxidase complex formed with neutrophil cytochrome b_{558} and PLB985 cell cytosol.

The NADPH oxidase complex was isolated as described previously (9). Briefly, membranes isolated from PMA-stimulated PMN were solubilized in octylglucoside, loaded on an ion exchange column (formed by a mixture of CM-Sepharose, DEAE-Sepharose, and *n*-octyl-Sepharose). The flowthrough was then loaded to a heparin-agarose matrix. Contaminant proteins

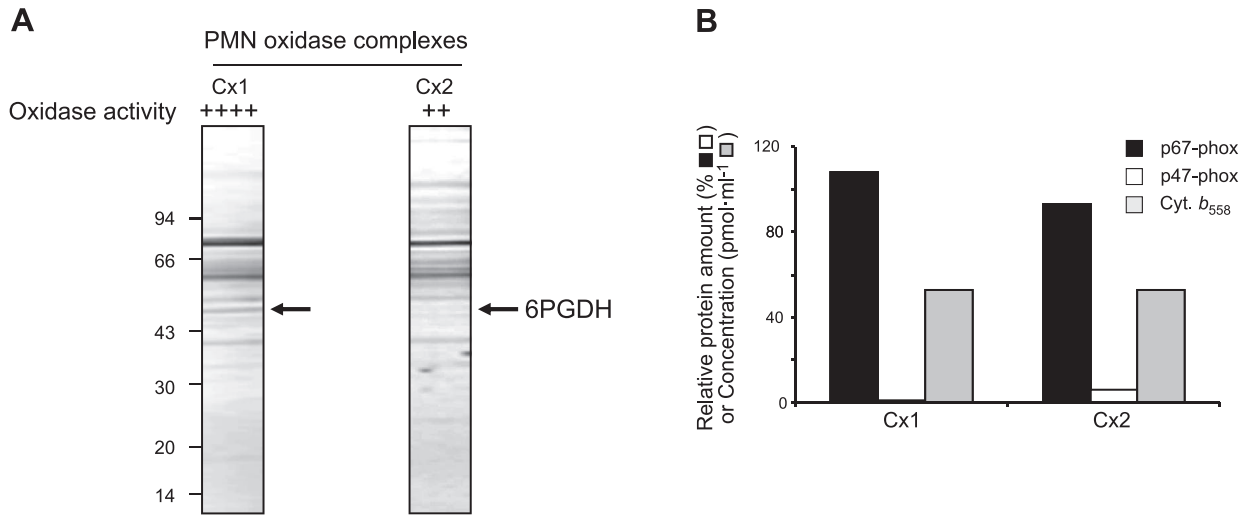

Figure 1. Analysis of constitutively active NADPH oxidase complexes isolated from neutrophils. Constitutively active NADPH oxidase complexes were isolated from PMA-stimulated subcellular fractions as described in Materials and Methods and by Paclet *et al.* (9). *A*) Isolated complexes were submitted to SDS-PAGE. Left panel: *phox* complex (Cx1) displaying a constitutive activity of 129 mol $O_2^{\cdot-} \cdot s^{-1} \cdot$ mol heme b^{-1}. Right panel: *phox* complex (Cx2) displaying a constitutive activity of 56 mol $O_2^{\cdot-} \cdot s^{-1} \cdot$ mol heme b^{-1}. Band indicated by arrow was identified as 6PGDH by MALDI-TOF mass spectrometry analysis (9). *B*) Quantification of NADPH oxidase constituents in constitutively active neutrophil oxidase complexes. Amount of p67-phox and p47-phox present in 1 ml oxidase complex was determined by densitometry analysis of Cx1 and Cx2 Western blots and expressed as a percentage of p67-phox or p47-phox present in 110 μg neutrophil cytosol.

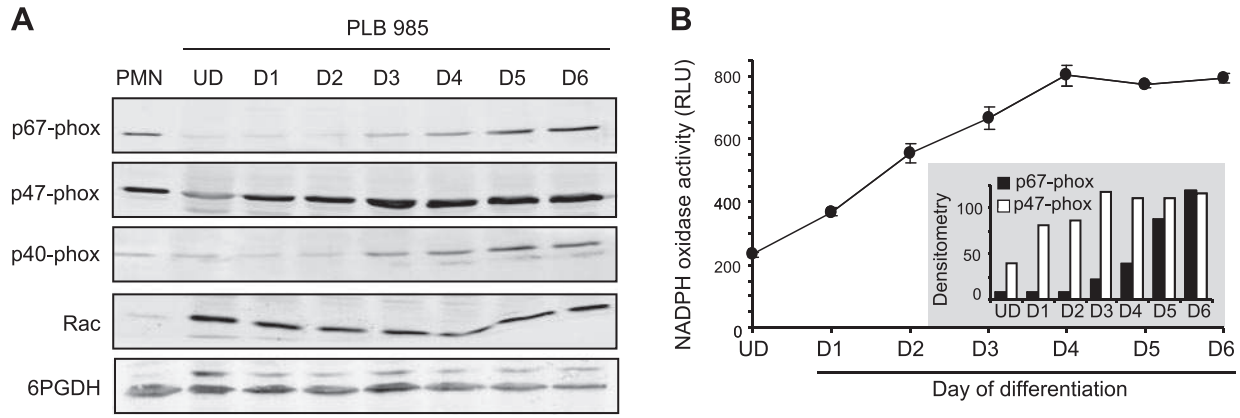

Figure 2. Expression of NADPH oxidase cytosolic factors and 6PGDH, and superoxide anion production during PLB985 cell differentiation. PLB985 cells were differentiated into granulocytic cells by DMF treatment. Cells were harvested each day from d 0 to 6 during granulocytic differentiation and analyzed for expression of oxidase components and NADPH oxidase activity. *A*) Immunoblot analysis of differentiated PLB985 cell cytosol probed with antibody for p67-phox, p47-phox, p40-phox, Rac, and 6PGDH. Samples were collected at the indicated times during DMF-induced granulocytic differentiation, and expression of the proteins was compared to that of blood neutrophils (PMN). Lanes D0–D6 were loaded with 50 μg protein. Control PMN cytosol lane was loaded with 10 μg protein. UD, undifferentiated. Western blots were probed with specific polyclonal antibodies, as described in Materials and Methods. Experiment is representative of 3 independent experiments. *B*) NADPH oxidase activity in intact cells was measured after PMA stimulation by chemiluminescence and luminol as substrate. NADPH oxidase activity was expressed in relative luminescent unit (RLU). Data represent the average of 3 independent experiments. Inset: densitometry analysis of Western blot in panel *A,* illustrating the expression of p67-phox and p47-phox during PLB985 cell differentiation.

present in the membrane-soluble extract were extensively washed with the purification buffer (containing 0.1% w/v Triton X-100 and a mixture of protease inhibitors), while cytochrome b_{558} bound to the heparin-agarose matrix. Then cytosol from either resting or PMA-stimulated PLB985 cells was deposited onto the heparin-bound cytochrome b_{558} to allow interactions between cytosolic proteins and cytochrome b_{558}. Cytochrome b_{558} and associated proteins were eluted with a NaCl gradient (0–0.5 M) and further purified on Sephacryl S300 gel filtration. Cytochrome b_{558} elution was followed by measuring the reduced-minus-oxidized differential absorption spectrum of the cytochrome b_{558} and by Western blot (**Fig. 3*A***). The presence of cytosolic factors and 6PGDH in the cytochrome b_{558}-containing fractions was analyzed by Western blot (Fig. 3*A*). As observed for neutrophil complexes (9), Rac was never immunodetected in PLB985 complex (Fig. 3*A*). The absence of detection is probably due to the low detection threshold of Rac with polyclonal antibodies (~10 pmol recombinant protein).

NADPH oxidase activity of eluted fractions presenting a cytochrome b_{558} spectrum was measured by the SOD-sensitive cytochrome *c* reduction assay in presence of NADPH and FAD, but without addition of anionic amphiphile as activator. As previously reported for the oxidase complex isolated from neutrophils (9), some cytochrome b_{558}-containing fractions were able to "constitutively" produce superoxide anions in presence of NADPH, with a turnover ranging from 43 to 58 mol $O_2^{\cdot -} \cdot s^{-1} \cdot$ mol heme b^{-1} depending on the fraction. The fraction with the maximum turnover was called PLB985 complex (Fig. 3, Cx). The activity profile was linked to the presence of p67-phox in the fractions (Fig. 3*B*), as previously shown for neutrophil oxidase complexes (9). Interestingly, the constitutive NADPH oxidase activity was dependent on the activation state of the cytosol used for the preparation (Fig. 3*B*, inset), as previously shown for the neutrophil complex (9): one explanation might be that modifications of cytosolic factors on cell stimulation are required for the interaction with heparin-bound cytochrome b_{558}.

Inhibition of 6PGDH expression by siRNA transfection

To evaluate the involvement of the 6PGDH in the NADPH oxidase activity regulation, d 2 differentiated PLB985 cells were transfected with 4 different 6PGDH-targeting siRNAs. First, transfection conditions were set up with a fluorescent negative control siRNA. Cells were electroporated with increasing concentrations of control siRNA in order to determine the optimal concentration for the best transfection efficiency. The fluorescence was measured by FACS, 6 h after electroporation. Results indicated significant transfection efficiency (>50%) with 200 and 300 nM siRNA (**Fig. 4**). For further experiments of 6PGDH siRNA transfection, electroporation was performed in the presence of 200 nM siRNA. Total RNA of transfected cells was isolated 24 to 72 h after transfection in order to evaluate the effect on the 6PGDH expression inhibition. 6PGDH mRNA expression level was analyzed by semiquantitative PCR and showed a ~30 to 70% decrease depending on the 6PGDH-targeting siRNA used (**Fig. 5*A; C***, inset). The decrease was similar between 24 and 72 h of transfection. The decrease of 6PGDH expression at the protein level was confirmed by Western blot analysis performed on cytosolic fractions isolated from transfected cells. Among the 4 siRNAs tested, siRNA1 and

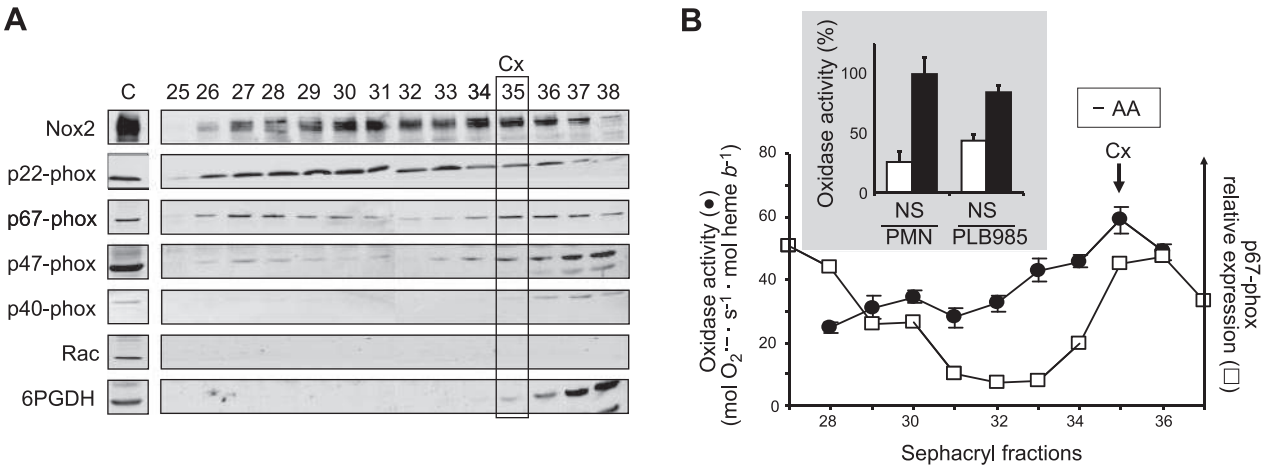

Figure 3. Purification and oxidase activity of a heterologous NADPH oxidase complex composed by neutrophil cytochrome b_{558} and cytosolic *phox* proteins from differentiated-PLB985 cells. *A*) Western blot analysis of Sephacryl elution fractions (45 μl/lane). Cytosolic *phox* proteins p67-phox, p47-phox, p40-phox, and Rac were immunodetected using specific polyclonal antibodies, while 6PGDH was detected by using a monoclonal antibody. Differentiated PLB985 cytosol (lane C; 50 μg) was used as a control. Immune complexes were detected by ECL. Fraction with the higher NADPH oxidase turnover was called PLB985 cell complex (Cx). Results are representative of ≥3 independent experiments. *B*) Constitutive NADPH oxidase activity of Sephacryl elution fractions in the absence of amphiphile agent (solid circles) and densitometry analysis of p67-phox in Sephacryl elution fractions (open squares). Superoxide anion production was measured in the absence of arachidonic acid (−AA) by incubating cytochrome b_{558}-containing fraction (0.2 pmol heme/assay) with 150 μM NADPH in the presence of 10 μM FAD, 40 μM GTPγS, and 5 mM $MgCl_2$, and by measuring the SOD-sensitive cytochrome *c* reduction at 550 nm. Results are presented as the average of ≥3 experiments. Relative amount of p67-phox was determined by densitometry analysis of Western blots. Inset: oxidase turnover of Sephacryl purified fractions derived from PMA-stimulated (S) or nonstimulated (N) PMN or differentiated PLB985 cells.

siRNA2 were the more efficient to reduce the expression of 6PGDH (Fig. 5*B; C*, inset). Intracellular NADPH concentration was estimated in 6PGDH-depleted cells (cells transfected with siRNA1 or siRNA2) and compared to that of untransfected cells. There was a strong decrease in intracellular NADPH concentration after 6PGDH-targeting siRNA transfection, suggesting that the decrease in 6PGDH expression was correlated to a decrease in intracellular 6PGDH activity (Supplemental Fig. S1).

Inhibition of NADPH oxidase activity in 6PGDH-depleted cells

To evaluate the effect of 6PGDH depletion on NADPH oxidase activity in intact cells, the activity was measured by chemiluminescence after PMA stimulation. The histogram in Fig. 5*C* indicated a decrease of NADPH oxidase activity in the range of 5 to 20%, depending on the siRNA used and on the experiment. The two siRNAs (siRNA1 and siRNA2) that produced the greatest NADPH oxidase activity inhibition (Fig. 5*C*) were also the ones that produced the greatest reduction of mRNA and protein (Fig. 5*C*, inset).

These results suggested a link between the decrease in 6PGDH expression and the decrease in NADPH oxidase activity in intact cells.

As NADPH concentration was decreased in 6PGDH-transfected cells (Supplemental Fig. S1), the effect of NADPH supplementation was evaluated on the NADPH oxidase activity reconstituted *in vitro* with cytosolic and

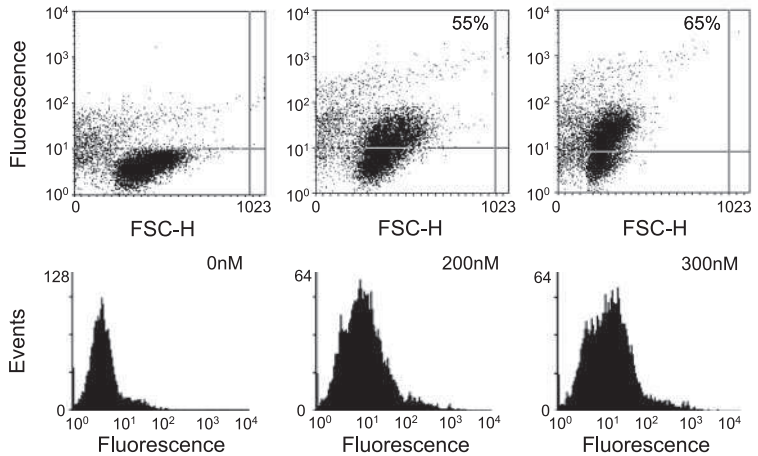

Figure 4. Determination of transfection conditions by using increasing concentrations of an Alexa Fluor 488-labeled negative control siRNA. Cells (0.8×10^6 cells in 400 μl) were electroporated in the presence of 0 to 300 nM of Alexa Fluor 488-labeled negative control siRNA during 40 ms at 250 V by using the ECM 830 electroporation system (BTX). Transfection efficiency was estimated 5 after transfection by measuring the fluorescence of Alexa Fluor 488 by flow cytometry.

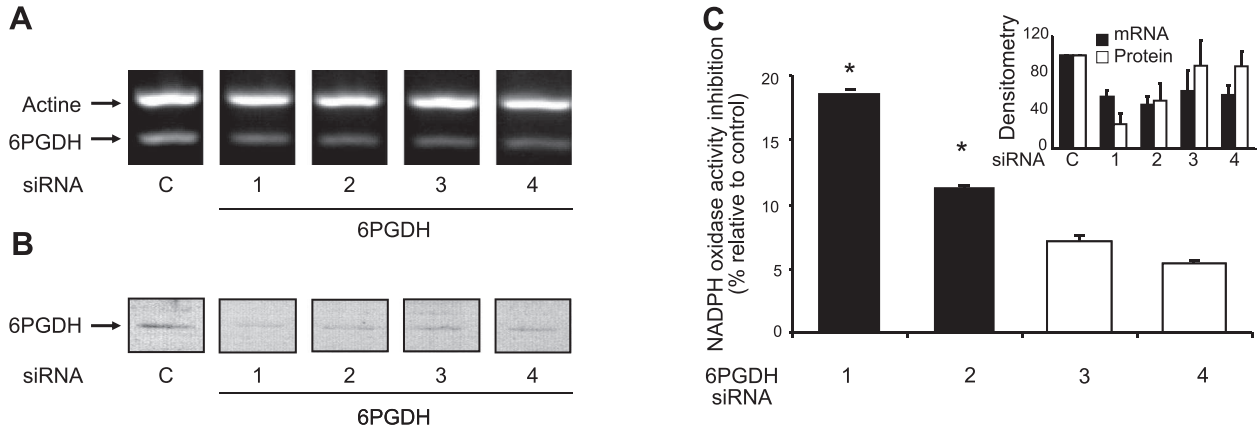

Figure 5. Effect of 6PGDH depletion on NADPH oxidase activity of PLB985 cells. *A*) Agararose gel assay of 6PGDH mRNA expression in PLB985 cells transfected with 6PGDH-targeting siRNA. RNA was extracted from control (lane C) or 6PGDH-targeting siRNA1–4-transfected PLB985 cells (lanes 1–4), and reverse-transcripted to cDNA as described in Material and Methods. Actine was used as a positive control of each RT-PCR. *B*) Western blot immunodetection of 6PGDH in cellular lysates (10^5 cells equivalent) of PLB985 cells transfected with either control or 6PGDH-targeting siRNA1–4 with a specific polyclonal antibody. *C*) Effect of 6PGDH depletion on NADPH oxidase activity of intact cells. PLB985 cells (10^5 cells) were stimulated with PMA (130 nM), and the NADPH oxidase activity was measured by chemiluminescence. Results are representative of ≥3 independent experiments and are expressed as percentage of inhibition of the activity obtained with control siRNA-transfected PLB985 cells (100% corresponded to 712±70 RLU). Inset: relative expression of 6PGDH mRNA (solid bars) and protein (open bars) measured by densitometry analysis of agarose gels (*A*) and Western blots (*B*). Results are expressed as averages ± SD of 2 or 3 independent experiments. $^*P < 0.05$ *vs.* control cells.

membrane fractions isolated from transfected cells. Results presented in **Fig. 6*A*** showed that NADPH oxidase activity reconstituted with neutrophil membranes and cytosol isolated from 6PGDH-siRNA-transfected PLB985 cells was strongly decreased (~50%) as compared to that obtained with cytosol from mock-siRNA-transfected PLB985 cells. As the reconstituted medium contained exogenous NADPH, these results suggested a specific role of 6PGDH in the activation process. Similar experiments were performed in the presence of a large excess of NADPH (750 instead of 150 μM). As shown on Fig. 6*B*, increasing NADPH concentration in the reconstitution medium restored a normal NADPH oxidase activity. Inhibition of 6PGDH expression seemed to increase the amount of NADPH required to get the control NADPH oxidase activity. To go further in the study, the Michaelis constant (K_m value) of the enzyme for NADPH was determined by

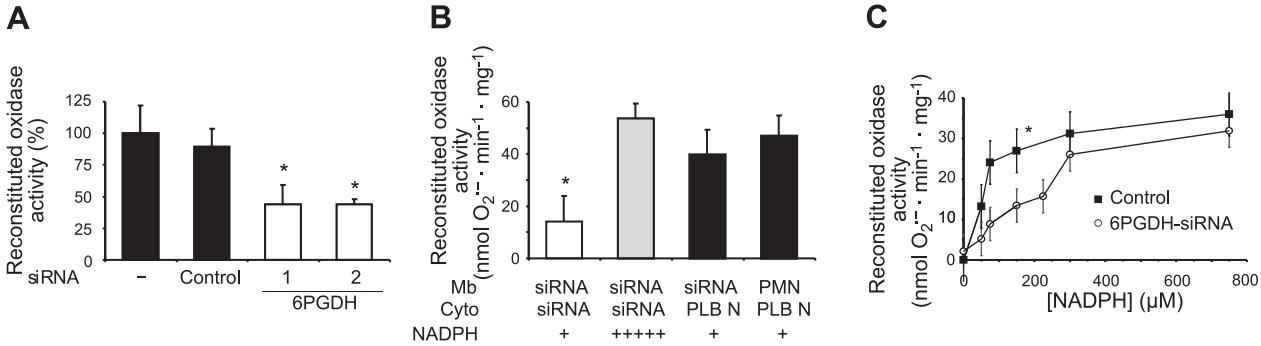

Figure 6. Effect of 6PGDH depletion on NADPH oxidase activity reconstituted in a cell-free assay. NADPH oxidase activity was reconstituted after incubation of a membrane fraction (7.5 μg) with a cytosol fraction (75 μg) in the presence of 40 μM GTPγS, 5 mM $MgCl_2$, and an optimal amount of arachidonic acid. Superoxide anion production was measured after the addition of NADPH by the SOD-sensitive portion of the cytochrome *c* reduction recorded at 550 nm. *A*) NADPH oxidase activity reconstituted with neutrophil membrane and cytosol isolated from PLB985 cells electroporated either in the absence of siRNA (−), or in the presence of PLB985 cells transfected with control siRNA (control), 6PGDH-targeting siRNA1 (bar 1), or 6PGDH-targeting siRNA2 (bar 2) in the presence of 150 μM NADPH. Activity was expressed as a percentage of that measured with cytosol of electroporated PLB985 cells (100% corresponded to 53±12 nmol $O_2^{\cdot-}$·min^{-1}·mg membrane $protein^{-1}$). $^*P < 0.05$ *vs.* control. *B*) NADPH oxidase activity reconstituted with membranes isolated from PMN or 6PGDH-targeting siRNA1 and cytosol isolated from control (N) or 6PGDH-targeting siRNA1 PLB985 cells, in presence of 150 μM (+) or 750 μM (+++++) NADPH. $^*P < 0.05$ *vs.* untransfected cells. *C*) NADPH oxidase activity reconstituted after incubation of membrane and cytosol fractions isolated from either control PLB985 cells (control) or 6PGDH-targeting siRNA transfected cells (6PGDH-siRNA) in presence of increasing concentrations of NADPH (0–750 μM). $^*P < 0.05$ *vs.* corresponding 6PGDH-siRNA. Results are expressed as the average ± SD of ≥3 different experiments.

measuring oxidase activity reconstituted in the presence of increasing concentration of NADPH (from 0 to 750 μM) with control subcellular fractions or fractions isolated from 6PGDH-siRNA-transfected cells (Fig. 6*C*). Results indicated that V_{max} was unchanged in 6PGDH-depleted cells, while K_m was increased from 50 to 200 μM after 6PGDH deletion. These data argue in favor of a role of 6PGDH in increasing the affinity of NADPH oxidase Nox2 for the substrate NADPH.

Association of 6PGDH with the neutrophil NADPH oxidase

To find an explanation for this effect, association of 6PGDH with the oxidase cytosolic factors was investigated. Immunoprecipitation experiments were performed with a specific 6PGDH monoclonal antibody on cytosol isolated from resting or stimulated neutrophils. Interestingly, p67-phox, p47-phox, and p40-phox coprecipitated with 6PGDH but only in cytosol from PMA-stimulated neutrophils, respectively (**Fig. 7** and data not shown) suggesting a cell-stimulation-dependent association of 6PGDH with NADPH oxidase. The specificity of this interaction was controlled by the negative result obtained by using an irrelevant antibody. Rac was never found associated with 6PGDH (data not shown).

6PGDH localization was then analyzed at the cellular level. In resting PLB985 cells, 6PGDH was distributed all around the cytosol (**Fig. 8** top panel). After PMA stimulation, 6PGDH was concentrated close to the plasma membrane and colocalized with the cytosolic factor p67-phox (Fig. 8, bottom panel).

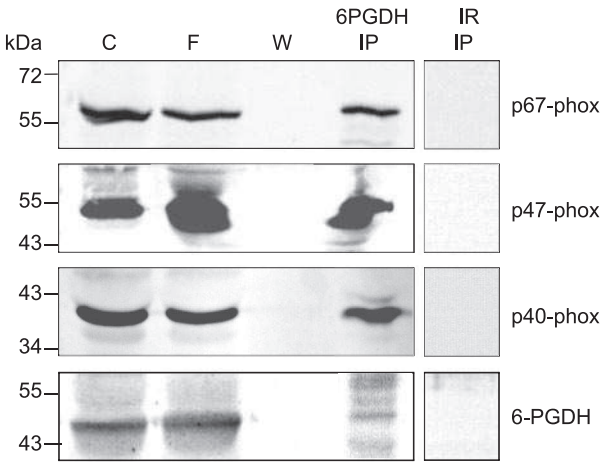

Figure 7. Coimmunoprecipitation of NADPH oxidase cytosolic factors with 6PGDH in cytosol from stimulated PMN. 6PGDH was immunoprecipitated from cytosol isolated from PMA-stimulated PMN (860 μg) with 5 μg of either specific or irrelevant (IR) antibody. Immunoprecipitates (IP) were collected and analyzed by Western blot for the presence of 6PGDH and cytosolic factors p67-phox, p47-phox, and p40-phox. Cytosol before immunoprecipitation (lane C; 50 μg), cytosol after immunoprecipitation (lane F; 50 μg) and wash (lane W) fractions were also analyzed. Results are representative of ≥2 independent experiments.

DISCUSSION

In this work, we showed that 6PGDH is a new partner of the neutrophil NADPH oxidase complex. It is associated with the constitutively active *phox* complex isolated from neutrophils but not from that isolated from B lymphocytes. 6PGDH coimmunoprecipitates with cytosolic oxidase factors and colocalizes with p67-phox on cell stimulation. Depletion of 6PGDH by specific-siRNA treatment leads to a decrease of NADPH oxidase activity in PMA-stimulated cells and to a decrease in Nox2 affinity for NADPH.

In cells, the PPP has 2 major functions: production of ribulose 5-phosphate required for nucleotide synthesis and production of NADPH, an important electron donor involved in biosynthesis reactions and in cell protection against oxidative stress (24). NADPH is the substrate of NADPH oxidase whose activity in phagocytic cells is initiated in response to inflammatory stimuli. On activation, neutrophils release a huge amount of superoxide anions in only few minutes (~10 nmol $O_2^{\cdot -}\cdot min^{-1}\cdot 10^6$ PMN^{-1}). This activity requires a high rate of NADPH consumption (5 nmol NADPH/min for 10^6 PMN) and NADPH is mainly produced in neutrophils by the action of 2 enzymes of the PPP: glucose 6-phosphate dehydrogenase and 6PGDH. It has been shown in a previous study by RET emission spectrophotometry that glucose 6-phosphate dehydrogenase and 6PGDH form a complex within resting neutrophils localized at the cell periphery (25). However, only 6PGDH was found associated with the neutrophil NADPH oxidase complex (9). The absence of glucose 6-phosphate dehydrogenase in the active oxidase complex could be explained by a weak association between 6PGDH and glucose 6-phosphate dehydrogenase that was broken during the purification process or by a strong and specific interaction of 6PGDH with the NADPH oxidase complex. Silencing 6PGDH by a specific-siRNA approach to deplete cells in 6PGDH led to a 5 to 20% decrease in the NADPH oxidase activity measured *ex vivo*, confirming a link between 6PGDH activity and superoxide anion production. As the final product of the reaction catalyzed by 6PGDH is NADPH, we expected to restore the deficient NADPH oxidase activity by adding exogenous NADPH in a cell-free assay. Surprisingly, the reduced oxidase activity was maintained after reconstitution of NADPH oxidase activity with neutrophil membrane and cytosol isolated from siRNA-treated PLB985 cells in the presence of 150 μM exogenous NADPH, the usual NADPH concentration used for this assay (22). Adding a large excess of NADPH (750 μM) was able to restore a control oxidase activity. Determining K_m of Nox2 for NADPH in control cells *vs.* 6PGDH-depleted cells showed that 6PGDH depletion leads to an increase of K_m, suggesting a role of 6PGDH in modulating Nox2 affinity for the substrate NADPH.

Enzyme microcompartmentation has been demonstrated in several metabolic pathways, such as glycolysis and the tricarboxylic acid cycle, allowing products of

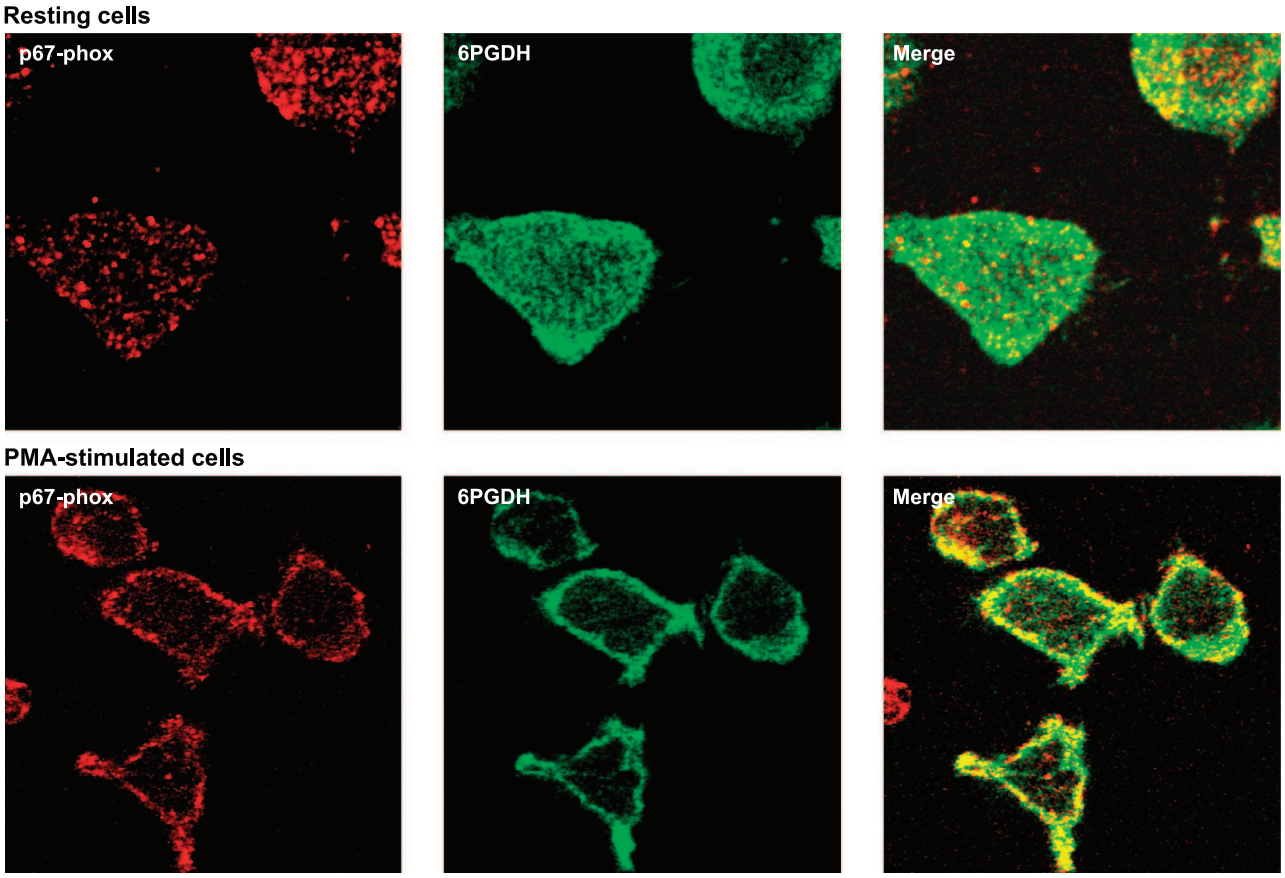

Figure 8. Colocalization of 6PGDH and p67-phox in PMA-stimulated differentiated PLB985 cells. Immunodetection of 6PGDH in resting and PMA-stimulated PLB985 cells by confocal microscopy. Differentiated PLB985 cells were incubated with PMA (130 nM) or DMSO for 10 min at 37°C. Resting and stimulated cells (2×10^5 cells) were then fixed, permeabilized, and labeled with both anti-6PGDH monoclonal antibody and anti-p67-phox polyclonal antibody (5 μg) for 1 h at room temperature, as described in Materials and Methods. An Alexa Fluor 488 secondary antibody was used to detect anti-6PGDH mAb binding; an Alexa Fluor 546 secondary antibody was used to detect p67-phox antibody binding. Fluorescence images were recorded.

the first enzymatic reaction to be directly passed to the next enzyme of the pathway without being released into the medium (26). In particular, coupling enzymes of the PPP (glucose 6-phosphate dehydrogenase and 6PGDH) with peripheral glycolytic cellular metabolism was shown to increase the efficiency of NADPH production, at least under conditions of normal glucose concentrations (25). This cellular microcompartmentation seems to be an important way of enzyme activity regulation by controlling NADPH availability in cellular processes. This mechanism is illustrated in neutrophils from pregnant women who have been reported to have depressed reactive oxygen species production in response to inflammatory stimulus (27). A key factor limiting superoxide anion production in neutrophils in pregnancy appears to be the translocation of 6PGDH from the cell periphery to the microtubule-organizing center. Spatial and temporal NADPH availability seems to provide a supplemental level in Nox2 activity regulation (27). The hypothesis of interactions between 6PGDH and NADPH oxidase components was supported by specific coimmunoprecipitation of 6PGDH with oxidase cytosolic factors, p67-phox, p47-phox, and p40-phox in cytosol of activated cells only. Moreover, the presence of 6PGDH in the isolated active *phox* complex (Figs. 3 and **9**) and its membrane localization after PMA stimulation is in favor of a translocation of 6PGDH along with NADPH oxidase regulatory cytosolic factors on neutrophil activation.

One hypothesis may be proposed in order to explain the implication of 6PGDH in NADPH oxidase activity regulation: interaction of 6PGDH with NADPH oxidase cytosolic components on cell stimulation allows a cotranslocation of these proteins to the membrane cytochrome b_{558}. This cotranslocation results in the increase of Nox2 affinity for NADPH, probably by a modification of the NADPH binding site conformation in order to facilitate the substrate binding to the enzyme active site. This modification could be due directly to the presence of 6PGDH or indirectly to the effect of 6PGDH on another component of the NADPH oxidase complex. It is well accepted that Nox2 is the catalytic element of the phagocyte NADPH oxidase and that it binds NADPH. However, a number of reports have investigated the binding of NADPH to p67-phox (28–32); among these studies, several presented evidence that native and recombinant purified p67-phox might be a NADPH binding component and that it was able to mediate a slow electron

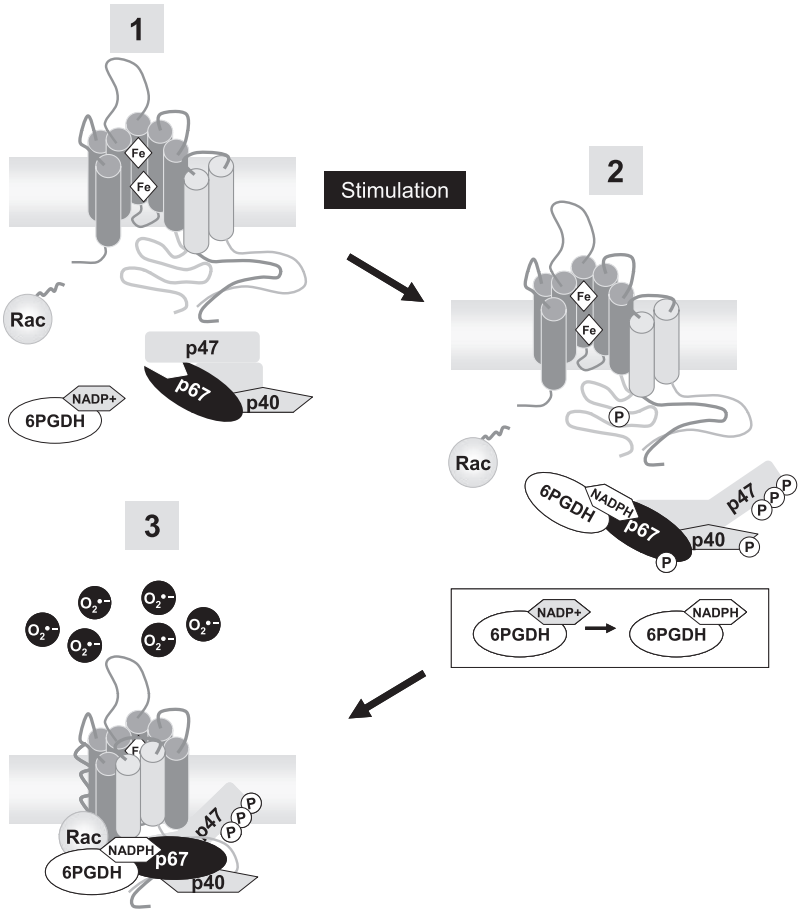

Figure 9. Model of neutrophil NADPH oxidase activity regulation by 6PGDH. *1*) In resting neutrophils, NADPH oxidase regulatory factors are present in the cytosol. *2*) In response to PMN stimulation, phosphorylations occurred, leading to a conformation change of cytosolic regulatory proteins, especially p47-phox and p67-phox. This conformation change may unmask the NADPH binding site on p67-phox. Concomitantly, the PPP is activated: 6PGDH associates with cytosolic *phox* factors and produces NADPH in the proximity of NADPH oxidase components. The local concentration of NADPH increases. *3*) At this stage, cytosolic *phox* proteins and 6PGDH associate with the membrane cytochrome b_{558}, inducing its conformation change and facilitating the binding of NADPH to the NADPH binding site localized on cytochrome b_{558} in order to initiate the enzymatic catalysis.

transfer from NADPH to an artificial acceptor (29–31), whereas only one study was divergent (32). On the basis of both previous published and present data, we propose a model of NADPH oxidase activation involving association between 6PGDH and *phox* cytosolic factors. On cell stimulation, interactions between 6PGDH and *phox* cytosolic factors may favor the binding of NADPH to p67-phox and/or to cytochrome b_{558} after membrane translocation.

Cellular coupling of 6PGDH with NADPH oxidase might represent an additional level of NADPH oxidase activity regulation in order to adapt the production of superoxide anions to specific physiological conditions. In that way, 6PGDH appears to be a new target for therapeutic molecules in order to modulate NADPH oxidase activity in pathological conditions. FJ

This work was supported by grants from the Ministère de l'Enseignement Supérieur de la Recherche et Technologie, Paris; the Région Rhône Alpes, Programme MIRA 2001 and Programme Emergence 2003; the Groupement des Entreprises Françaises dans la Lutte contre le Cancer, Délégation de Grenoble; the Fondation pour la Recherche Médicale, Isère; the Direction Régionale de la Recherche Clinique; the Association Française; la Ligue Nationale contre le Cancer; and the Société Française de Rhumatologie.

REFERENCES

1. Nauseef, W. M. (2008) Nox enzymes in immune cells. *Semin. Immunopathol.* **30,** 195–208
2. Vignais, P. V. (2002) The superoxide-generating NADPH oxidase: structural aspects and activation mechanism. *Cell. Mol. Life Sci.* **59,** 1428–1459
3. Bokoch, G. M. (1995) Regulation of the phagocyte respiratory burst by small GTP-binding proteins. *Trends Cell Biol.* **5,** 109–113
4. Cross, A. R., and Segal, A. W. (2004) The NADPH oxidase of professional phagocytes–prototype of the NOX electron transport chain systems. *Biochim. Biophys. Acta* **1657,** 1–22
5. Heyworth, P. G., Cross, A. R., and Curnutte, J. T. (2003) Chronic granulomatous disease. *Curr. Opin. Immunol.* **15,** 578–584
6. Segal, B. H., Romani, L., and Pucetti, P. (2009) Chronic granulomatous disease. *Cell. Mol. Life. Sci.* **66,** 553–558
7. Weisdorf, D. J., Craddock, P. R., and Jacob, H. S. (1982) Glycogenolysis versus glucose transport in human granulocytes: differential activation in phagocytosis and chemotaxis. *Blood* **60,** 888–893
8. Tan, A. S., Ahmed, N., and Berridge, M. V. (1998) Acute regulation of glucose transport after activation of human peripheral blood neutrophils by phorbol myristate acetate, fMLP, and granulocyte-macrophage colony-stimulation factor. *Blood* **91**, 649–655
9. Paclet, M. H., Berthier, S., Kuhn, L., Garin, J., and Morel, F. (2007) Regulation of phagocyte NADPH oxidase activity: identification of two cytochrome b_{558} activation states. *FASEB J.* **21,** 1244–1255
10. Morel, F., Cohen Tanugi Cholley, L., Brandolin, G., Dianoux, A. C., Martel, C., Champelovier, P., Seigneurin, J. M., François, P., Bost, M., and Vignais, P. V. (1993) The O2- generating oxidase of B lymphocytes: Epstein-Barr virus-immortalized B lymphocytes as a tool for the identification of defective components of the oxidase in chronic granulomatous disease. *Biochim. Biophys. Acta* **1182,** 101–109
11. Kobayashi, S., Imajoh-Ohmi, S., Kuribayashi, F., Nunoi, H., Nakamura, M., and Kanegasaki, S. (1995) Characterization of the superoxide-generating system in human peripheral lymphocytes and lymphoid cell lines. *J. Biochem.* **117,** 758–765
12. Paclet, M. H., Coleman, A. W., Burritt, J. B., and Morel, F. (2001) NADPH oxidase of Epstein-Barr-virus immortalized B lymphocytes. Effect of cytochrome b(558) glycosylation. *Eur. J. Biochem.* **268,** 5197–5208

13. Paclet, M. H., Coleman, A. W., Vergnaud, S., and Morel, F. (2000) P67-phox-mediated NADPH oxidase assembly: imaging of cytochrome b_{558} liposomes by atomic force microscopy. *Biochemistry* **39,** 9302–9310
14. Yu, L., Zhen, L., and Dinauer, M. C. (1997) Biosynthesis of the phagocyte NADPH oxidase cytochrome b_{558}: role of heme incorporation and heterodimer formation in maturation and stability of gp91-phox and p22-phox subunits. *J. Biol. Chem.* **272,** 27288–27294
15. Campion, Y., Paclet, M. H., Jesaitis, A. J., Marques, B., Grichine, A., Berthier, S., Lenormand, J. L., Lardy, B., Stasia, M. J., and Morel, F. (2007) New insights into the membrane topology of the phagocyte NADPH oxidase: characterization of an anti-gp91-phox conformational monoclonal antibody. *Biochimie (Paris)* **89,** 1145–1158
16. Berthier, S., Paclet, M. H., Lerouge, S., Roux, F., Vergnaud, S., Coleman, A. W., and Morel, F. (2003) Changing the conformation state of cytochrome b_{558} initiates NADPH oxidase activation: MRP8/MRP14 regulation. *J. Biol. Chem.* **278,** 25499–25508
17. Batot, G., Paclet, M. H., Doussière, J., Vergnaud, S., Martel, C., Vignais, P. V., and Morel, F. (1998) Biochemical and immunochemical properties of B lymphocyte cytochrome b_{558}. *Biochim. Biophys. Acta* **1406,** 188–202
18. Vergnaud, S., Paclet, M. H., El Benna, J., Pocidalo, M. A., and Morel, F. (2000) Complementation of NADPH oxidase in p67-phox-deficient CGD patients p67-phox/p40-phox interaction. *Eur. J. Biochem.* **267,** 1059–1067
19. Paclet, M. H., Henderson, M. H., Campion, Y., Morel, F., and Dagher, M. C. (2004) Localization of Nox2 N-terminus using polyclonal antipeptide antibodies. *Biochem. J.* **382,** 981–986
20. Laemmli, U. K. (1970) Cleavage of structural proteins during the assembly of the head of bacteriophage T4. *Nature* **227,** 680–685
21. Campion, Y., Jesaitis, A. J., Nguyen, M. V. C., Grichine, A., Herenger, Y., Baillet, A., Berthier, S., Morel, F., and Paclet, M. H. (2009) New p22-phox monoclonal antibodies: identification of a conformational probe for cytochrome b_{558}. *J. Innate Immun.* **1,** 556–569
22. Batot, G., Martel, C., Capdeville, N., Wientjes, F., and Morel, F. (1995) Characterization of neutrophil NADPH oxidase activity reconstituted in a cell-free assay using specific monoclonal antibodies raised against cytochrome b_{558}. *Eur. J. Biochem.* **234,** 208–215
23. Towbin, H., Staehelin, T., and Gordon, J. (1979) Electrophoretic transfer of proteins from polyacrylamide gels to nitrocellulose sheets: procedure and some applications. *Proc. Natl. Acad. Sci. U. S. A.* **76,** 4350–4354
24. He, W., Wang, Y., Liu, W., and Zhou, C. Z. (2007) Crystal structure of *Saccharomyces cerevisiae* 6-phosphogluconate dehydrogenase Gnd 1. *BMC Struct. Biol.* **7,** 38
25. Kindzelskii, A. L., Ueki, T., Michibata, H., Chaiworapongsa, T., Romero, R., and Petty, H. R. (2004) 6-Phosphogluconate dehydrogenase and glucose-6-phosphate dehydrogenase form a supramolecular complex in human neutrophils that undergoes retrograde trafficking during pregnancy. *J. Immunol.* **172,** 6373–6381
26. Minaschek, G., Gröschel-Stewart, U., Blum, S., and Bereiter-Hahn, J. (1992) Microcompartmentation of glycolytic enzymes in cultured cells. *Eur. J. Cell Biol.* **58,** 418–428
27. Cotton, D. J., Seligmann, B., O'Brien, W. F., and Gallin, J. I. (1983) Selective defect in human neutrophil superoxide anion generation elicited by the chemoattractant *N*-formylmethionyl-leucylphenylalanine in pregnancy. *J. Infect. Dis.* **148,** 194–199
28. Smith, R. M., Curnutte, J. T., Mayo, L. A., and Babior, B. M. (1989) Use of an affinity label to probe the function of the NADPH binding component of the respiratory burst of human neutrophils. *J. Biol. Chem.* **264,** 12243–12248
29. Smith, R. M., Connor, J. A., Chen, M., and Babior, B. M. (1996) The cytosolic subunit p67-phox contains an NADPH-binding site that participates in catalysis by the leukocyte NADPH oxidase. *J. Clin. Invest.* **98,** 977–983
30. Dang, P. M. C., Babior, B. M., and Smith, R. M. (1999) NADPH dehydrogenase activity of p67-phox, a cytosolic subunit of the leukocyte NADPH oxidase. *Biochemistry* **38,** 5746–5753
31. Dang, P. M. C., Johnson, J. L., and Babior, B. M. (2000) Binding of nicotinamide adenine dinucleotide phosphate to the tetratricopeptide repeat domains at the N-terminus of p67-phox, a subunit of the leukocyte nicotinamide adenine dinucleotide phosphate oxidase. *Biochemistry* **39,** 3069–3075
32. Baciou, L., Erard, M., Dagher, M. C., Bizouarn, T. (2009) The cytosolic subunit p67-phox of the NADPH-oxidase complex does not bind NADPH. *FEBS Lett.* **583,** 3225–3229

Received for publication October 14, 2010.
Accepted for publication March 17, 2011.

Article 2

6-phosphofructo-2-kinase modulates neutrophil NADPH oxidase activity through Adenosine triphosphate availability.

6-phosphofructo-2-kinase modulates neutrophil NADPH oxidase activity through adenosine triphosphate availability.

Athan Baillet [a, b], Marc-André Hograindleur [a], Jamel El Benna [c], Alexei Grichine [d], Sylvie Berthier [a, e], Françoise Morel [a], Marie-Hélène Paclet [a, e] *

From the [a]GREPI AGIM FRE3405 CNRS / Université Joseph Fourier, –CHU Grenoble / France; [b] Rheumatology Department, CHU Grenoble / France; [c] INSERM, U773, Centre de Recherche Biomédicale Bichat Beaujon CRB3, Université Paris 7 site Bichat, UMRS 773, Paris, France; [d]Platform 'Optical microscopy – cell imaging' – UJF, Inserm U823, Institut Albert Bonniot, La Tronche Cedex / France; [e]Laboratory "Biochimie des Enzymes et des Protéines", Institut de Biologie et Pathologie, C.H.U. Grenoble / France.

Running title: Nox2 activity regulation by PFK-2

*Correspondence: Marie-Hélène PACLET, GREPI AGIM FRE3405 CNRS/UJF, CHU Albert Michallon, 6ème étage Unité E, BP 217, 38043 Grenoble Cedex 9, France.
Tel.: +33 4 76 76 62 20; Fax: +33 4 76 76 56 08; E-mail: MHPaclet@chu-grenoble.fr

ABSTRACT

The phagocyte NADPH oxidase is an enzymatic complex whose activity is mainly regulated by the translocation of cytosolic regulatory factors named p67-phox, p47-phox, p40-phox and Rac to the membrane catalytic component, the membrane cytochrome b_{558}. Few years ago, a constitutively active NADPH oxidase complex was isolated from neutrophil fractions. A proteomic analysis pointed out the presence of the 6-phosphofructo-2-kinase/fructose-2,6-bisphosphatase heart isoenzyme in the purified oxidase complex from neutrophils. In order to investigate the specificity of this interaction, a siRNA approach was used to deplete 6-phosphofructo-2-kinase in differentiated PLB985 cells. Results showed a significant decrease in NADPH oxidase activity after 6-phosphofructo-2-kinase-targeting siRNA transfection. In the isolated neutrophil oxidase complex, 6-phosphofructo-2-kinase/fructose-2,6-bisphosphatase was phosphorylated on Ser^{466}, indicating an activation of the 6-phosphofructo-2-kinase. In its phosphorylated form, this enzyme is responsible for the production of fructose-2,6-bisphosphate, an allosteric activator of phosphofructo-1-kinase, the limiting enzyme in glycolysis. As expected, depletion in 6-phosphofructo-2-kinase led to a decrease in cytosolic ATP concentration but also to a drop in p47-phox phosphorylation which is a key event in the formation of active NADPH oxidase complex. Confocal microscopy experiments showed a cell-stimulation dependent colocalization of 6-phosphofructo-2-kinase with both cytochrome b_{558} and lipid rafts. The present data propose the cellular micro-compartmentation of the NADPH oxidase with enzymes involved in the energetic metabolism as a supplementary level of NADPH oxidase activity regulation.

Key words: phagocyte NADPH oxidase; phox; siRNA transfection; cytochrome b_{558}; PFK-2

Introduction

The phagocyte NADPH oxidase (*phox*) is a key enzyme in the innate immunity. It is a multi-protein complex formed by a transmembrane cytochrome b_{558} and cytosolic regulators (p67-phox, p47-phox, p40-phox and Rac1 or Rac2) [1-4]. Cytochrome b_{558} is the catalytic core of the enzyme. It is formed by two subunits, Nox2 (gp91-phox) and p22-phox. Upon cell stimulation and association with cytosolic regulatory factors, it becomes activated and produces a huge amount of superoxide anions $O_2^{\bullet -}$. In neutrophils, its activity is essential for the pathogen killing. NADPH oxidase activity defect leads to chronic granulomatous disease (CGD) which is characterized by recurrent and severe infections due to the incapacity of phagocytic cells to kill pathogens. CGD is caused by mutations in any one of the four genes encoding the major oxidase subunits: Nox2, p22-phox, p47-phox, and p67-phox [5-6].

In a previous work, we characterized the whole NADPH oxidase complex isolated in a constitutively active form [7]. In the constitutively active oxidase complex isolated from neutrophils, the 6-phosphofructo-2-kinase/fructose-2,6-bisphosphatase (PFK-2/FBase-2) heart isoenzyme was identified. This enzyme was absent in the oxidase complex prepared with B lymphocyte cytosol suggesting that the association of PFK-2/FBase-2 with the neutrophil oxidase complex was specific [7]. As the constitutive activity of the oxidase complex prepared with neutrophil cytosol was higher than that obtained with the complex prepared with EBV-B lymphocyte cytosol, we assumed that the presence of PFK-2/FBase-2 in the neutrophil NADPH oxidase activation process could affect NADPH oxidase activity.

PFK-2/FBase-2 is a bifunctional enzyme. PFK-2/FBase-2 catalyses both the synthesis and the degradation of fructose-2,6-bisphosphate a metabolite that both activates 6-phosphofructo-1-kinase and consequently glycolysis, and inhibits fructose-1,6-bisphosphatase and gluconeogenesis. In mammals, four PFK-2 isoenzymes have been identified, namely the liver, heart, brain/placenta and testis isoenzymes [8]. These isoenzymes differ mainly in the sequence of their catalytic core. The activity of PFK-2 and FBase-2 isoenzymes is controlled by phosphorylation events. In contrast to that observed for the PFK-2/FBase-2 liver isoenzyme, phosphorylation induces the activation of the PFK-2 heart isoenzyme, and consequently glycolysis stimulation, while the phosphatase activity is inhibited.

NADPH oxidase activation is dependent on cytoskeleton modifications [9,10] and phosphorylation events that occur on both cytosolic factors, especially p47-phox, and cytochrome b_{558} (Nox2 and p22-phox) [11, 18]. All the activation process requires energy. In

neutrophils, it has been described that the principal source of energy is glycolysis-derived ATP [19, 20]. The presence of PFK-2/FBase-2 in the constitutively active oxidase complex isolated from neutrophils suggests an association between enzymes of energetic metabolism and the phagocyte NADPH oxidase.

In the present study, we pointed out that phosphorylated PFK-2 was associated with the constitutively active NADPH oxidase complex isolated from neutrophil fractions and co-immunoprecipitated with cytosolic oxidase regulatory factors. The use of pharmacological PFK-2-phosphorylation inhibitors led to a significant decrease in NADPH oxidase activity in response to various stimuli indicating a role of activated PFK-2 in the modulation of NADPH oxidase activity. PFK-2-cell depletion led to significant drop in both cytosolic ATP level and cell-stimulation-dependent superoxide anion production. These results suggested a physical link between PFK-2, a key enzyme in the glycolytic pathway activation, and NADPH oxidase complex. Present data illustrated the modulation of neutrophil NADPH oxidase activity by a cellular microcompartmentation with enzymes involved in the energetic metabolism.

Material and methods

Materials

Chemical reagents used in this study were obtained from the following sources: diisopropyl fluorophosphate (DFP) (Acros Organics, Noisy-Le-Grand, France); ECL Western blotting detection reagents (Amersham Pharmacia Biotech, Uppsala, Sweden); PMA (Sigma Chemicals, St. Louis, MO, USA); PFK-2 car targeting siRNA, AllStars Negative Control siRNA coupled to Alexa Fluor 488 (Qiagen, Courtaboeuf, France). Polyclonal antibodies directed against either PFK-2 car, p-PFK-2 car (Ser466), or HRP-conjugated anti-actin, and a mouse monoclonal antibody directed against CD55 were from Santa Cruz Biotechnology, Inc (Heidelberg, Germany). H-89 was obtained from Euromedex (Souffelweyersheim, France). Akt inhibitor XIII was from Merk Chemicals (Nottingham, UK). ENLITEN® ATP Assay System was from Promega (Charbonnières, France).

Antibodies

Rabbit polyclonal antibodies were raised against polypeptides corresponding to the C-terminal region of p47-phox (residues 371-390), p67-phox (residues 511-526), p40-phox (residues 325-339), Nox2 (residues 562-569), p22-phox (residues 184-195) and to the internal region shared by Rac1 and Rac2 (residues 123-145) [21, 22]. Immunoglobulins were purified from rabbit antisera on 1 ml protein A-Sepharose as previously described [21].

To detect Nox2 and p22-phox by confocal microscopy, monoclonal antibodies raised against Nox2 (clone 13B6) [23] and p22-phox (clone 16G6) [24] were used.

To analyze p47-phox phosphorylation, a mixture of two rabbit polyclonal antibodies directed against either phospho-Ser^{315}-p47-phox or phospho-Ser^{328}-p47-phox were used as previously described [25].

PLB985 cell line

PLB985 cells were grown in RPMI-1640 medium supplemented with 2 mM glutamine, 10% (v/v) fetal bovine serum, 100 U/ml penicillin, 100 µg/ml streptomycin at 37°C and in 5% CO_2 atmosphere. For granulocytic differentiation, PLB985 cells (5×10^5 cells/ml) were treated with 0.5% (v/v) DMF for 4-6 days [26].

Transfection of differentiated PLB985 cells with PFK-2 targeting siRNA

After two days of differentiation, 0.8×10^6 PLB985 cells were collected and suspended in the electroporation buffer (RPMI 1640 containing 7 mM Na_2HPO_4 and 272 mM sucrose). Cells were electroporated in presence of either 400 nM PFK-2 targeting siRNA or 400 nM of

negative-control siRNA during 40 ms at 250V by using the ECM 830 electroporation system (BTX, Holliston, U.S.A.). These transfection conditions lead to more than 50% efficacy [27].

Measurement of NADPH oxidase activity in differentiated-PLB985 cells

Differentiated-PLB985 cells were washed once in PBS, adjusted at the concentration of 5×10^6 cells / ml in PBS. PLB (2.5×10^5 cells in 50 µl) were mixed with 200 µl PBS containing 0.9 mM $CaCl_2$, 0.5 mM $MgCl_2$, 20 mM glucose, 20 µM luminol and 10 U/ml horseradish peroxidase. NADPH oxidase activity was measured by chemiluminescence after adding PMA (130 nM). In some experiments cells were stimulated with fMLP (100 nM) and ionomycine (2.5 µM). Photon emission was recorded at 37°C for 30 min with a Luminoscan (Labsystem, Pontoise, France) [28].

Reconstitution of NADPH oxidase activity in vitro

Crude membrane and cytosolic fractions were prepared from siRNA-transfected and untransfected differentiated-PLB-985 as previously described [28]. Membranes (7.5 µg proteins) were incubated with cytosol (75 µg proteins) in presence of 40 µM GTPγS and 5 mM $MgCl_2$ in a final volume of 100 µl. An optimum amount of arachidonic acid (40 to 100 nmol) was used for activation [21]. After 10 min incubation at 25 °C, the medium was transferred into a photometric cuve containing 150 µM NADPH in order to initiate the reaction. Superoxide anion production was assessed by measuring the superoxide-dismutase-sensitive portion of cytochrome *c* reduction recorded at 550 nm ($\varepsilon_{550} = 21.1\ mM^{-1}.cm^{-1}$) [29].

Pharmacological inhibition of phosphokinase A (PKA) and phosphokinase B (Akt/PKB)

After 6 days of differentiation, PLB985 were incubated for 30 min at 37°C with PKA inhibitor (H-89, 10µM), Akt/PKB inhibitor (Akt inhibitor XIII 5µM) or DMSO 0.01 % (v/v) in culture medium. All inhibitors were used at a sub-lethal concentration and viability was measured by Trypan-blue exclusion after incubation. After incubation, cells were collected by centrifugation (350 × g for 8min at 20°C), washed twice with PBS. Cells were then used to measure NADPH oxidase activity in response at various stimuli by chemiluminescence in order to perform Western-blot on cell lysates.

Preparation of stimulated PLB985 cell lysates

PLB985 cells (2.5×10^6 cells) were resuspended in 1 ml PBS containing 0.9 mM $CaCl_2$ and 0.5 mM $MgCl_2$ and then stimulated with either PMA (130 nM), fMLP (100 nM), ionomycine (2 µM) or DMSO (0.1%, v/v) as control. The stimulation was stopped by the addition of the same volume of ice-cold PBS. Cells were collected after centrifugation

(1000×g for 10min at 4°C) and lysed in 90 µl of PBS containing 1% (w/v) Triton X100 and a mixture of protease inhibitors (10 µM Nα-p-tosyl-L-lysine chloromethyl ketone, 1.8 µM leupeptin, and 1.5 µM pepstatin) for 20 min on ice. The lysate was centrifuged at 14,000×g for 15min at 4°C and the supernatant was used for Western-blot analysis of PFK-2 phosphorylation.

Isolation of oxidase complex

Oxidase complex was prepared with neutrophils membrane isolated from PMA-stimulated neutrophils and cytosol isolated from unstimulated- or PMA-stimulated day 6-differentiated PLB985 cells as described previously [7, 27]. Oxidase complex was purified on heparin agarose followed by Sephacryl S300 gel filtration. In oxidase complex, cytochrome b_{558} was quantified by reduced-minus-oxidized difference spectra and by measuring the difference of absorbance between the Soret band at 426 nm and the valley at about 410-411 nm. The absorption coefficient used was 106 $mM^{-1}.cm^{-1}$ at 426 nm [30].

SDS-PAGE and immunoblotting

Proteins were fractioned by 11% SDS-PAGE [31] and then electrotranfered on nitrocellulose [32]. Proteins on nitrocellulose were detected with specific antibodies: anti-PFK-2 (purified IgG dilution 1/1000) anti- pPFK-2 (purified IgG dilution 1/1000), mAb anti-p22-phox (purified IgG dilution 1/5000) or anti-actin (dilution 1/500). Immune complexes were detected with goat anti rabbit IgG combined with peroxidase. Peroxidase activity was detected using ECL reagent.

Measurement of NADPH concentration in PLB985 cell cytosol

Cytosolic fractions isolated from PFK-2 siRNA- transfected PLB985 cells and untransfected PLB985 were obtained as previously described [27] and adjusted at a protein concentration 0.5 mg/ml. NADPH concentration standards were prepared in duplicate, ranging from 0 to 100 µM. Absorbance of standards and cytosolic fractions was measured at 343 nm on a DU640 spectrophotometer (Beckman Coulter, Roissy CDG, France).

Determination of ATP cytosolic concentration in PLB985 cell cytosol

ATP concentration was evaluated using the ENLITEN® ATP assay system following the manufacturer instructions. Briefly, ATP standards were prepared at a concentration ranging from 10^{-7} to 10^{-11} M. Ten microliters of cytosol (0.5 µg/ml) were drawn in 50µl of

reaction medium. Photon emission was recorded at room temperature after 2s delay with 2s integration time with a Luminoscan (Labsystem, Pontoise, France).

Immunoprecipitation with anti-phosphoPFK-2 antibody

Cytosol from resting and PMA-stimulated neutrophils (645 µg in 150 µl PBS buffer) was incubated with 4 µg of either anti-phosphoPFK-2 mAb or an irrelevant mAb for 1 h at 4 °C. Then 5 mg protein A-Sepharose CL-4B was added for 1h-incubation and subsequently pelleted (14,000 g for 5 min at 4°C). After three successive washes with respectively PBS containing 1% (w/v) Triton X100, PBS with 0.5 M NaCl and finally PBS alone, the protein A-Sepharose beads were drawn in the Laemmli sample buffer [21] for SDS/PAGE and immunoblotting.

Confocal microscopy

PMA-stimulated or unstimulated day 6 - differentiated PLB985 cells (2×10^5 cells in 50 µl PBS) were incubated on 0.01 % (w/v) poly-L-lysine-coated round glass cover-slips for 15 min at 37 °C. Cells were fixed with 4 % (w/v) paraformaldehyde for 10 min at room temperature and permeabilized with 0.1% (w/v) Triton X100 for 1 min at room temperature as previously described [14]. Cells were incubated with specific antibodies (5 µg in 50 µl PBS containing 1 % (w/v) BSA) for 1h at room temperature. Cells were washed three times for 10 min with PBS containing 1 % (w/v) BSA prior to a 1-h incubation with 100 µl of Alexa Fluor secondary antibody (1: 250 in PBS containing 1 % (w/v) BSA). After two washes with PBS, cell nuclei were stained with 40 µl Hoechst 33258 (0.5 µg/ml). Samples were then mounted in 8 µl DABCO solution, sealed, and stored at 4 °C in the dark. Fixed cells were imaged at room temperature using the inverted confocal and two-photon laser-scanning microscope (LSM 510 NLO, Carl Zeiss) equipped with a 40x/1.3 Plan-Neofluar oil immersion objective [27].

Statistical analysis

Data were expressed as the mean ± SD. Statistical analysis was performed using the unpaired *t* test. The results are reported when significantly different ($P<0.05$) from the controls.

RESULTS

Phosphorylated PFK-2 is associated with the NADPH oxidase complex.

PFK-2/FBase-2 enzyme was first identified by MALDI-TOF mass spectrometry in the constitutively active oxidase complex isolated from neutrophil fractions [7]. It is well known that PFK-2 heart isoenzyme is activated by phosphorylation, especially on C-terminal serines. Phosphorylations on both Ser^{466} and Ser^{483} were shown to increase the affinity of PFK-2 heart isoenzyme for the substrate, fructose-6-phosphate, while phosphorylation on Ser^{466} alone was shown to increase the V_{max} of PFK-2 [33]. In order to clarify whether activated PFK-2 or activated FBase-2 was associated with NADPH oxidase complex, the phosphorylation state of PFK-2/FBase-2 was analyzed in resting and PMA-stimulated differentiated PLB985 cells. Phosphorylation of Ser^{466}, a critical phosphorylation site for activation was evaluated by using an antibody directed against the phosphorylated Ser^{466} (anti-PFK-2-phospho-Ser^{466}) of heart PFK-2 isoenzyme. Western-blots, performed on cytosolic fractions isolated from resting and PMA-stimulated differentiated PLB985, and their densitometry analysis exhibited a strong increase in PFK-2 phosphorylation on Ser^{466} after cell-stimulation (Fig. 1A**)** indicating that PMA-stimulation induced PFK-2 activation. To confirm the association of activated PFK-2 with the NADPH oxidase, we analyzed. In a previous work, we showed that cell stimulation was required to purify a constitutively active oxidase complex [7, 27]. Western-blots performed on oxidase complexes prepared with cytosol isolated either from resting PLB985 cells or from stimulated PLB985 cells [27] showed the presence of phosphorylated PFK-2 in crude fractions isolated from heparin column in complexes prepared with resting and stimulated cells (Fig. 1B). Interestingly, after the gel filtration purification step, necessary to get the purified oxidase complex, a five-fold increase in PFK-2 phosphorylation was observed in the constitutively active oxidase complex prepared with cytosol from PMA-stimulated cells *versus* those prepared with cytosol from resting cells (Fig. 1A). These results indicated that phosphorylated PFK-2 copurified with the constitutively active NADPH oxidase complex, suggesting a link between NADPH oxidase activation and activated PFK-2.

Phosphorylated PFK-2 co-immunoprecipitated with cytosolic factors of phagocyte NADPH oxidase in cytosol from stimulated PMN

As PFK-2 is a cytosolic enzyme, we postulated that, upon cell stimulation, PFK-2 translocated from cytosol to plasma membrane. Therefore, we examined potential protein-protein interactions between PFK-2 and cytosolic NADPH oxidase in cytosol isolated from resting and activated PMN. Co-immunoprecipitation analysis was performed by using anti-

PFK-2-phospho-Ser^{466} antibodies in cytosol from resting and PMA-stimulated PMN. Interestingly, phosphorylated PFK-2 co-immunoprecipated with p67^{phox}, p47^{phox}, p40^{phox} in cytosol from PMA-stimulated PMN but not with Rac. Co-immunoprecipitation did not occur in resting cells (Fig. 2). These data strongly argue in favor of a co-translocation of PFK-2 with cytosolic oxidase factors to membrane upon cell stimulation.

Colocalization of PFK-2 and phagocyte NADPH oxidase in an activated state upon PMA stimulation.

In order to evaluate *ex vivo* the colocalization of PFK2 with active NADPH oxidase, we performed confocal microscopy of PLB985 cells before and after PMA-stimulation by using both the anti-PFK-2 antibody and the mAb 13B6, an anti-Nox2 conformational monoclonal antibody that was previously shown to recognize preferentially cytochrome b_{558} in its active state [23]. Results displayed a significant increase in colocalisation of PFK-2 with Nox2 after cell-stimulation (Fig. 3B *versus* 3A**).** Colocalization of PFK-2 in Nox2 was quantified by using a specific software and reached 95% upon cell stimulation while only roughly 47% of colocalization was observed in resting cells (Fig. 3C**).** It has been previously reported that neutrophil cytochrome b_{558} was located in lipid rafts, metabolically active membrane microdomains. Upon cell stimulation, cytosolic factors were recruited to lipid rafts [35, 36]. Colocalization of PFK-2 with lipid rafts was investigated by confocal microscopy in resting and PMA-stimulated PLB985 cells by using the anti-PFK-2 antibody and an antibody directed against CD55, a raft label. Results showed an increased colocalization of PFK-2 with CD55 in PMA-stimulated cells as compared to resting cells (84% versus 39% respectively) (Fig 4, right panel *versus* left panel).

Pharmacological inhibition of PFK-2 phosphorylation decreases NADPH oxidase activity in differentiated PLB985 cells.

As phosphorylated PFK-2 copurified with the NADPH oxidase complex, we evaluated the impact of PFK-2 phosphorylation inhibition by using a pharmacological approach on NADPH oxidase activity. Several studies reported that PFK-2 heart isoenzyme is a substrate for protein kinase A (PKA). It has also been reported that PFK-2 might be phosphorylated by protein kinase B (PKB) and protein kinase C (PKC) [8]. Phosphorylation mediated by PKA or PKB was shown to increase PFK-2 activity [37] while PKC-mediated phosphorylation has no effect [34]. In order to study the role of PFK-2 phosphorylation on NADPH oxidase activity, PKA and PKB inhibitors were used to inhibit PFK-2 phosphorylation in cells stimulated with either PMA, fMLP or ionomycine. These stimuli are known to activate the phagocyte

NADPH oxidase. Pre-treatment of cells with the PKB inhibitor led to a significant decrease in PFK-2 phosphorylation after stimulation whatever the stimulus used (Fig.5). A similar result was obtained with the PKA inhibitor except for PMA-stimulated cells where the decrease was not statistically significant. In parallel, NADPH oxidase activity was measured in cells pre-incubated with the PKA or the PKB inhibitor and then stimulated with PMA, fMLP or ionomycine. A slight decrease in NADPH oxidase activity was obtained in response to PMA in cells treated with PKA or PKB inhibitor (Fig. 5A). In contrast, a clear reduction of NADPH oxidase activity was observed in response to fMLP and ionomycine when PKA or PKB was inhibited (Fig. 5B, 5C) and correlated with the decrease in PFK-2 phosphorylation.

PFK-2 depletion decreases NADPH oxidase activity of PLB985 cells

In order to determine the mechanism by which PFK-2 influenced NADPH oxidase activity, cells were depleted in PFK-2 by using a siRNA approach. Differentiated PLB985 cells (8×10^6 cells in 400µl transfection buffer) were transfected by electroporation with 80 and 160 pmol siRNA targeting the heart isoform PFK-2. The transfection conditions were standardized in order to achieve a transfection rate higher than 50% [27]. A moderate but significant 25%-decrease in PFK-2 protein expression was observed in cell lysates 48h after transfection with 80 pmol PFK-2-targeting siRNA as compared to lysates of cells transfected with a control siRNA (Fig. 6A), and quantified after normalization with p22-phox expression in each sample (Fig. 6B). The NADPH oxidase activity was measured in PMA-stimulated cells by chemiluminescence. The activity was 20% decreased in cells transfected with PFK-2 targeting siRNA, confirming a link between PFK-2 and superoxide anion production reduction (Fig. 6C). Similar results were obtained after reconstitution of NADPH oxidase activity with membrane and cytosol from PFK-2-siRNA transfected differentiated PLB985 cells. The histogram presented in Fig. 6D showed a 40% decrease in NADPH oxidase activity reconstituted with cytosol from cells transfected with PFK-2 targeting siRNA *versus* control siRNA-transfected cells. Data strongly argue in favor of a specific role of PFK-2 in the phagocyte oxidase activation**.**

PFK-2 depletion decreased cytosolic ATP concentration but not NADPH concentration in differentiated PLB985 cells.

Activated PFK-2 is responsible for the production of fructose-2,6- bisphosphate, the allosteric activator of 6-phosphofructo-1-kinase, the key enzyme of glycolysis. In neutrophils, the glycolytic pathway is the main source of ATP. It is well known that NADPH oxidase activation requires ATP, especially for the activation of kinases, and a large and continuous

supply of NADPH, the substrate of the enzyme, released from the pentose phosphate pathway. Glycolysis and pentose phosphate pathway used glucose 6-phosphate as substrate. The relative choice between glycolysis and pentose phosphate pathway depends on cellular requirements. In order to identify the impact of PFK-2 depletion on both pathways, the concentration of NADPH and ATP was measured in cytosol isolated from cells transfected with either PFK-2-targeting siRNA or control siRNA. Cytosol from differentiated PLB985 cells transfected with PFK-2 targeting siRNA displayed a trend towards a higher concentration of cytosolic NADPH, albeit this difference was not statistically significant. Anyway, the decrease in NADPH oxidase activity of PFK-2-siRNA-transfected PLB985 cells could not be explained by a change in the substrate concentration (Fig. 7A**)**, i.e. the NADPH. In contrast, a significant decrease in ATP concentration was observed after transfection with PFK-2 targeting siRNA (Fig. 7B**)** suggesting a link between PFK-2 depletion and a decrease in the glycolysis rate.

PFK-2 depletion decreased p47-phox phosphorylation in differentiated PLB985 cells.

As ATP is required for various biochemical reactions, several hypothesis may explain the impact of the decrease in ATP level on the reduction of NADPH oxidase activity especially a decrease in activity of kinases involved in NADPH oxidase activation. We then investigated the impact of PFK-2 depletion in p47-phox phosphorylation which is required for the translocation of cytosolic factors to membrane cytochrome b_{558}. Western-blot performed with specific antibodies directed against p47-phox phospho-site (phospho-Ser^{315} and phospho-Ser^{328}) (Fig. 8A) and analyzed by densitometry after normalization to the amount of total p47-phox (Fig. 8B) showed a significant decrease in p47-phox phosphorylation (~50 %) in cells transfected with PFK-2 targeting siRNA.

DISCUSSION

We report in this paper that PFK-2 activity modulates phagocyte NADPH oxidase activity in PLB985 cells differentiated in pseudo-neutrophils. Upon cell stimulation, neutrophil PFK-2/FBase-2 was phosphorylated on Ser^{466} which has been shown, for the PFK-2/FBase-2 heart isoenzyme, to promote the PFK-2 activity. Additionally, the present work shows that cell stimulation induces interaction between phosphorylated PFK-2 and cytosolic factors ($p67^{phox}$, $p47^{phox}$, $p40^{phox}$), translocation of PFK-2 to the plasma membrane in lipid rafts and a colocalization of PFK-2 with membrane cytochrome b_{558}. PFK-2 phosphorylation seems to be a key event in its association with the NADPH oxidase complex. PFK-2 heart isoform activation is mainly due to phosphorylation by PKA or PKB. PKB has been shown to be activated in stimulated neutrophils with a maximum of activation that correlates with the respiratory burst kinetics [38]. Moreover, it was reported that prompt and brief elevations of cAMP occur in PMN upon stimulation suggesting protein kinase A activation [39]. Inhibition of PKA and PKB, two kinases involved in phosphorylation-mediated PFK-2 activation [34, 37] leads to a significant decrease in NADPH oxidase activity in response to various stimuli confirming the implication of phosphorylated PFK-2 in the NADPH oxidase activation pathway.

In a second step, we tried to identify by which mechanism PFK-2 activity was linked to NADPH oxidase activation. In cells, PFK-2 produces fructose-2,6-bisphosphate the physiological allosteric activator of PFK-1. PFK-1 is the limiting enzyme of glycolysis. We hypothesized that PFK-2 depletion could result in a decrease in the glycolysis rate and consequently in a reduced cellular energetic status. In most aerobic cell types, energy required for cell maintenance and function is produced by the mitochondrial respiration. However, neutrophils are exceptional cells for this aspect. First of all neutrophil mitochondria are limited [40-42]. Secondly, the use of mitochondrial respiration inhibitors did not affect neutrophil functions indicating that neutrophil mitochondria hardly participate in the production of ATP required for cellular metabolism [19, 20]. However, neutrophil mitochondria were shown to participate in neutrophils apoptosis [20]. Acellular measurements of phagocyte NADPH oxidase activity suggests that the enzymatic activity was rather GTP-dependent than ATP-dependent [43]. However in intact cells ATP-dependent steps including cytoskeleton modifications, kinases activation, must precede the GTP-requiring event [44]. In the present study, we did not observe a proportional correlation between the ATP decrease, mediated by PFK-2 depletion, and the reduction of NADPH oxidase activity, most likely because ATP impacts on several biological functions in activated cells. Additionally, a

difference may exist between the ATP concentration measured in cytosol and the local ATP concentration in cellular micro-compartments.

It was previously reported that ATP enhances NADPH oxidase activity. First, ATP-dependent actin polymerization is a critical step for oxidase assembly and oxidative burst [45]. Thus, changes in actin network may modulate NADPH oxidase activity [9, 10].

Second, ATP may also enhance the assembly process by affecting the activity of kinases involved in phosphorylation of NADPH oxidase components [11]. It has been described that all NADPH oxidase components, p47-phox, p40-phox, p67-phox, p22-phox and Nox2, are phosphorylated upon cell stimulation [11-18]. These phosphorylations regulate the complex assembly and the activation process. Phosphorylation events are well characterized for p47-phox which is the first NADPH oxidase factor phosphorylated upon cell stimulation [46]. *In vivo*, depending on the nature of the stimulus, p47-phox phosphorylation may be due to a combination of kinases: PKC, p21-activated kinase, AKT/PKB, PI3 kinase [47] and ERK 1/2 [48] have been shown to promote NADPH oxidase assembly while phosphorylations by p38-MAP kinase were responsible for a priming effect [48]. In the present work, western-blot performed on cytosol isolated from PMA-stimulated PFK-2 targeting-siRNA transfected cells, by using a combination of antibodies directed against p47-phox phospho-sites (phospho-Ser^{315} and phospho-Ser^{328}), shows a significant decrease in p47-phox phosphorylation as compared to that of mock-siRNA transfected cells. This result confirms a link between PFK-2 activity and NADPH oxidase activation.

Third, ATP may be converted to GTP by the nucleoside diphosphate kinase (NDPK) in presence of GMP and GDP [49, 50]. This newly formed GTP may increase oxidase activity by activating the exchange GDP to GTP on Rac [51]. In previous studies, it has been shown that there was a NDP kinase activity in both cytosolic and membrane fractions isolated from human neutrophils [52] and NDP kinase was proposed to modulate NADPH oxidase activation. NDP kinase was not detected by western-blot in purified NADPH oxidase complexes isolated from neutrophils fractions (data not shown) however, confocal microscopy analysis performed on resting and stimulated PLB985 cells showed a colocalization of NDPK with cytochrome b_{558} that was strongly increased in stimulated cells arguing in favor of a link between NDPK activity and NADPH oxidase activation (Fig.9).

The microdomain compartimentation is an emerging level of oxidase activity regulation in which cytochrome b_{558}, cytosolic factors and others regulatory effectors may concentrate [35, 36, 48, 53]. Since membrane rafts provide a spatially preferable environment for a variety of enzyme systems, the colocalization of PFK-2 and cytochrome b_{558} in an active

conformation in lipid rafts is probably not casual but is likely a way to locally supply a sufficient amount of ATP required for all the process leading to the neutrophil respiratory burst, from cytoskeleton modifications until cytosolic factor phosphorylations and Rac activation.

Our results suggest a role for PFK-2 in neutrophil NADPH oxidase activation through ATP cytosolic concentration modulation. Cellular coupling of PFK-2 and NADPH oxidase complex appears to tightly regulate ATP content in lipid rafts in order to gather the optimal conditions for the cytochrome b_{558} change into the most active conformation [7, 27]. All these data suggest that enzyme subcellular microcompartmentation is a supplementary level of regulation allowing adapting NADPH oxidase activity to a specific cell type.

REFERENCES

[1] Vignais, P. V. The superoxide-generating NADPH oxidase: structural aspects and activation mechanism. Cell. Mol. Life Sci. 59: 1428-1459; 2002.

[2] Nauseef, W. M. Nox enzymes in immune cells. Semin. Immunopathol. 30: 195-208; 2008.

[3] Cross, A. R.; Segal, A. W. The NADPH oxidase of professional phagocytes--prototype of the NOX electron transport chain systems. Biochim. Biophys. Acta 1657: 1-22; 2004.

[4] Bokoch, G. M. Regulation of the phagocyte respiratory burst by small GTP-binding proteins. Trends Cell Biol. 5: 109-113; 1995.

[5] Heyworth, P. G.; Cross, A. R.; Curnutte J. T. Chronic granulomatous disease. Curr. Opin. Immunol. 15: 578-584; 2003.

[6] Stasia, M.J.; Li, X.L. Genetics and immunopathology of chronic granulomatous disease. Semin Immunopathol. 30:209-35; 2008.

[7] Paclet, M.H.; Berthier, S.; Kuhn, L.; Garin, J.; Morel, F. Regulation of phagocyte NADPH oxidase activity: identification of two cytochrome b_{558} activation states. FASEB J. 21: 1244-1255; 2007.

[8] Rider, M.H.; Bertrand, L.; Vertommen, D, Michels, PA, Rousseau, G.G., Hue, L. 6-phosphofructo-2-kinase/fructose-2,6-bisphosphatase: head-to-head with a bifunctional enzyme that controls glycolysis. Biochem J. 381: 561-79; 2004.

[9] Bengtsson, T.; Dahlgren, C.; Stendahl, O.; Andersson, T. Actin assembly and regulation of neutrophil function: effects of cytochalasin B and tetracaine on chemotactic peptide-induced $O_2^{\cdot}$ production and degranulation. J. Leukoc. Biol. 49: 236-244; 1991.

[10] Tamura, M.; Kanno, M.; Endo, Y. Deactivation of neutrophil NADPH oxidase by actin-depolymerizing agents in a cell-free system. Biochem. J. 349: 369-375; 2000.

[11] Park, J.W.; Hoyal, C.R.; Benna, J.E.; Babior, B.M. Kinase-dependent activation of the leukocyte NADPH oxidase in a cell-free system. Phosphorylation of membranes and p47(PHOX) during oxidase activation. J. Biol. Chem. 272: 11035-11043; 1997.

[12] Dang, P.M.; Fontayne, A.; Hakim, J.; El Benna, J.; Perianin, A. Protein kinase C zeta phosphorylates a subset of selective sites of the NADPH oxidase component p47phox and participates in formyl peptide-mediated neutrophil respiratory burst. J. Immunol. 166: 1206-1213; 2001.

[13] El Benna, J.; Dang, P.M.; Gaudry, M.; Fay, M.; Morel, F.; Hakim, J.; Gougerot-Pocidalo, M.A. Phosphorylation of the respiratory burst oxidase subunit p67(phox) during human neutrophil activation. Regulation by protein kinase C-dependent and independent pathways. J. Biol. Chem. 272: 17204-17208; 1997.

[14] Dang, P.M.; Raad, H.; Derkawi, R.A.; Boussetta, T.; Paclet, M.H.; Belambri, S.A.; Makni-Maalej, K.; Kroviarski, Y.; Morel, F.; Gougerot-Pocidalo, M.A.; El-Benna, J. The NADPH oxidase cytosolic component p67phox is constitutively phosphorylated in human neutrophils: Regulation by a protein tyrosine kinase, MEK1/2 and phosphatases 1/2A. Biochem Pharmacol. 82: 1145-1152; 2011.

[15] Bouin, A.P.; Grandvaux, N.; Vignais, P.V.; Fuchs, A. p40(phox) is phosphorylated on threonine 154 and serine 315 during activation of the phagocyte NADPH oxidase. Implication of a protein kinase c-type kinase in the phosphorylation process. J. Biol. Chem. 273: 30097-30103; 1998.

[16] Lopes, L.R.; Dagher, M.C.; Gutierrez, A.; Young, B.; Bouin, A.P.; Fuchs, A.; Babior, B.M. Phosphorylated p40PHOX as a negative regulator of NADPH oxidase. Biochemistry 43: 3723-3730; 2004.

[17] Regier, D.S.; Waite, K.A.; Wallin, R.; McPhail, L.C. A phosphatidic acid-activated protein kinase and conventional protein kinase C isoforms phosphorylate p22(phox), an NADPH oxidase component. J. Biol. Chem. 274: 36601-36608; 1999.

[18] Raad, H.; Paclet, M.H.; Boussetta, T.; Kroviarski, Y.; Morel, F.; Quinn, M.T.; Gougerot-Pocidalo, M.A. ; Dang, P.M.; El-Benna, J. Regulation of the phagocyte NADPH oxidase activity: phosphorylation of gp91phox/NOX2 by protein kinase C enhances its diaphorase activity and binding to Rac2, p67phox, and p47phox. FASEB J. 23: 1011-1022; 2009.

[19] Borregaard, N.; Herlin, T. Energy metabolism of human neutrophils during phagocytosis. J. Clin. Invest. 70: 550-557; 1982.

[20] Maianski, N.A.; Geissler, J.; Srinivasula, S.M.; Alnemri, E.S.; Roos, D.; Kuijpers, T.W. Functional characterization of mitochondria in neutrophils: a role restricted to apoptosis. Cell death and differentiation 11:143-153; 2004.

[21] Vergnaud, S.; Paclet, M.H. ; El Benna, J.; Pocidalo, M.A.; Morel F. Complementation of NADPH oxidase in p67-phox-deficient CGD patients p67-phox/p40-phox interaction. Eur. J. Biochem. 267: 1059-1067; 2000.

[22] Batot, G.; Martel, C.; Capdeville, N.; Wientjes, F.; Morel, F. Characterization of neutrophil NADPH oxidase activity reconstituted in a cell-free assay using specific monoclonal antibodies raised against cytochrome b_{558}. Eur. J. Biochem. 234: 208-215; 1995.

[23] Campion, Y. ; Paclet, M.H. ; Jesaitis, A.J. ; Marques, B. ; Grichine, A. ; Berthier, S. ; Lenormand, J.L. ; Lardy, B. ; Stasia, M.J.; Morel, F. New insights into the membrane topology of the phagocyte NADPH oxidase: characterization of an anti-gp91-phox conformational monoclonal antibody. Biochimie 89:1145-58; 2007.

[24] Campion, Y.; Jesaitis, A. J.; Nguyen, M. V. C.; Grichine, A.; Herenger, Y.; Baillet, A.; Berthier, S.; Morel, F.; Paclet, M.H. New p22-phox monoclonal antibodies: identification of a conformational probe for cytochrome b_{558}. J. Innate Immun. 1: 556-569; 2009.

[25] Boussetta, T.; Gougerot-Pocidalo, M. A.; Hayem, G.; Ciappelloni, S.; Raad, H.; Arabi Derkawi, R.; Bournier, O.; Kroviarski, Y.; Zhou, X.Z.; Malter, J.S.; Lu, P.K.; Bartegi, A.; Dang, P.M.; El-Benna, J. The prolyl isomerase Pin1 acts as a novel molecular switch for TNF-alpha-induced priming of the NADPH oxidase in human neutrophils. Blood. 116: 5795-5802; 2010.

[26] Yu, L.; Zhen, L.; Dinauer, M.C.; Biosynthesis of the phagocyte NADPH oxidase cytochrome b_{558}. Role of heme incorporation and heterodimer formation in maturation and stability of gp91phox and p22phox subunits. J. Biol. Chem. 272: 27288-27294; 1997.

[27] Baillet, A.; Xu, R.; Grichine, A.; Berthier, S. ; Morel F. ; Paclet, M.H. Coupling of 6-phosphogluconate dehydrogenase with NADPH oxidase in neutrophils: Nox2 activity regulation by NADPH availability. FASEB J. 25: 2333-2343; 2011.

[28] Berthier, S.; Paclet, M.H.; Lerouge, S.; Roux, F. ; Vergnaud, S. ; Coleman, A.W. ; Morel, F. Changing the conformation state of cytochrome b_{558} initiates NADPH oxidase activation: MRP8/MRP14 regulation. J. Biol. Chem. 278: 25499-508; 2003.

[29] Paclet, M. H.; Coleman, A. W.; Vergnaud, S.; Morel, F. P67-phox-mediated NADPH oxidase assembly: imaging of cytochrome b_{558} liposomes by atomic force microscopy. Biochemistry 39: 9302-9310; 2000.

[30] Batot, G.; Paclet, M. H.; Doussière, J.; Vergnaud, S.; Martel, C.; Vignais, P. V.; Morel, F. Biochemical and immunochemical properties of B lymphocyte cytochrome b_{558}. Biochim. Biophys. Acta (Molecular Basis of Disease) 1406**:** 188-202; 1998.

[31] Laemmli, U. K. Cleavage of structural proteins during the assembly of the head of bacteriophage T4. Nature 227: 680-685; 1970.

[32] Towbin, H.; Staehelin, T.; Gordon, J. Electrophoretic transfer of proteins from polyacrylamide gels to nitrocellulose sheets: procedure and some applications. Proc. Natl. Acad. Sci. USA 76: 4350-4354; 1979.

[33] Bertrand, L.; Alessi, D.R.; Deprez, J. ; Deak, M. ; Viaene, E. ; Rider, M.H. ; Hue, L. Heart 6-phosphofructo-2-kinase activation by insulin results from Ser-466 and Ser-483 phosphorylation and requires 3-phosphoinositide-dependent kinase-1, but not protein kinase B. J. Biol. Chem. 274: 30927-30933; 1999.

[34] Rider, M.H.; Hue, L. Phosphorylation of purified bovine heart and rat liver 6-phosphofructo-2-kinase by protein kinase C and comparison of the fructose-2,6-bisphosphatase activity of the two enzymes. Biochem. J. 240: 57-61; 1986.

[35] Shao, D.; Segal, A.W.; Dekker, L.V. Lipid rafts determine efficiency of NADPH oxidase activation in neutrophils. FEBS Lett. 550: 101-106; 2003.

[36] David, A.; Fridlich, R.; Aviram I. The presence of membrane Proteinase 3 in neutrophil lipid rafts and its colocalization with FcgammaRIIIb and cytochrome b_{558}. Exp Cell Res. 308: 156-65; 2005.

[37] Deprez, J.; Vertommen, D.; Alessi, D.R. ; Hue, L. ; Rider, M.H. Phosphorylation and activation of heart 6-phosphofructo-2-kinase by protein kinase B and other protein kinases of the insulin signaling cascades. J. Biol. Chem. 272 : 17269-17275;1997.

[38] Tilton, B.; Andjelkovic, M.; Didichenko, S.A.; Hemmings, B.A.; Thelen, M. G-Protein-coupled receptors and Fcgamma-receptors mediate activation of Akt/protein kinase B in human phagocytes. J. Biol. Chem. 272 : 28096-28101; 1997.

[39] Smolen, J.E.; Korchak, H.M.; Weissmann, G. Increased levels of cyclic adenosine-3',5'-monophosphate in human polymorphonuclear leukocytes after surface stimulation. J. Clin. Invest. 65: 1077-1085; 1980.

[40] Zucker-Franklin, D. Electron microscopic studies of human granulocytes: structural variations related to function. Semin. Hematol. 5: 109-133; 1968.

[41] Bainton, D.F.; Ullyot, J.L.; Farquhar, M.G. The development of neutrophilic polymorphonuclear leukocytes in human bone marrow. J. Exp. Med. 134: 907-934; 1971.

[42] Wilson, P.D.; Rustin, G.J.; Peters, T.J. The ultrastructural localization of human neutrophil alkaline phosphatase in normal individuals during pregnancy and in patients with chronic granulocytic leukaemia. Histochem. J. 13: 31-43; 1981.

[43] Klinger, E.; Aviram, I. Involvement of GTP in cell-free activation of neutrophil NADPH oxidase. Studies with GTP analogues. Biochem. J. 285: 635-639; 1992.

[44] Lu, D.J.; Grinstein, S. ATP and guanine nucleotide dependence of neutrophil activation. Evidence for the involvement of two distinct GTP-binding proteins. J. Biol. Chem. 265: 13721-13729; 1990.

[45] El Benna, J.; Ruedi, J.M.; Babior, B.M. Cytosolic guanine nucleotide-binding protein Rac2 operates in vivo as a component of the neutrophil respiratory burst oxidase. Transfer of Rac2 and the cytosolic oxidase components p47phox and p67phox to the submembranous actin cytoskeleton during oxidase activation. J. Biol. Chem. 269: 6729-6734; 1994.

[46] El-Benna, J. ; Dang, P.M. ; Gougerot-Pocidalo, M.A. ; Marie, J.C. ; Braut-Boucher, F. p47phox, the phagocyte NADPH oxidase/NOX2 organizer: structure, phosphorylation and implication in diseases. Exp. Mol. Med. 41: 217-225; 2009.

[47] Dang, P.M.; Fontayne, A.; Hakim, J.; El Benna, J.; Perianin, A. Protein kinase C zeta phosphorylates a subset of selective sites of the NADPH oxidase component p47phox

and participates in formyl peptide-mediated neutrophil respiratory burst. J. Immunol. 166: 1206-1213; 2001.

[48] Guichard, C.; Pedruzzi, E.; Dewas, C.; Fay, M.; Pouzet, C.; Bens, M.; Vandewalle, A. ; Ogier-Denis, E. ; Gougerot-Pocidalo, M.A. ; Elbim, C. Interleukin-8-induced priming of neutrophil oxidative burst requires sequential recruitment of NADPH oxidase components into lipid rafts. J. Biol. Chem. 280: 37021-37032; 2005.

[49] Peveri, P.; Heyworth, P.G.; Curnutte, J.T. Absolute requirement for GTP in activation of human neutrophil NADPH oxidase in a cell-free system: role of ATP in regenerating GTP. Proc. Natl. Acad. Sci. U. S. A. 89: 2494-2498; 1992.

[50] Leino, L.; Forbes, L.; Segal, A.; Cockcroft, S. Reconstitution of GTPgammaS-induced NADPH oxidase activity in streptolysin-O-permeabilized neutrophils by specific cytosol fractions. Biochem. Biophys. Res. Commun. 265: 29-37; 1999.

[51] Mizrahi, A.; Molshanski-Mor, S.; Weinbaum, C.; Zheng, Y.; Hirshberg, M.; Pick, E. Activation of the phagocyte NADPH oxidase by Rac Guanine nucleotide exchange factors in conjunction with ATP and nucleoside diphosphate kinase. J. Biol. Chem. 280: 3802-3811; 2005.

[52] Guignard, F.. Markert, M. The nucleoside diphosphate kinase of human neutrophils. Biochem. J. 316: 233-238; 1996.

[53] Remijsen, Q.; Vanden Berghe, T.; Parthoens, E.; Asselbergh, B.; Vandenabeele, P.; Willems, J. Inhibition of spontaneous neutrophil apoptosis by parabutoporin acts independently of NADPH oxidase inhibition but by lipid raft-dependent stimulation of Akt. J. Leukoc. Biol. 85: 497-507; 2009.

FOOTNOTES

This work was supported by grants from the Ministère de l'Enseignement supérieur de la Recherche et Technologie, Paris, the Région Rhône Alpes, programme MIRA 2001 and programme Emergence 2003, the « Groupement des Entreprises Françaises dans la lutte contre le Cancer », délégation de Grenoble, the « Fondation pour la Recherche Médicale », Isère, the « Direction de la Recherche Clinique et de l'Innovation », the french association « La ligue nationale contre le cancer » and the « Société Française de Rhumatologie ». The authors thank Pr. Edgar Pick (Tel Aviv University, Israel) for helpful discussions on NDPK.

[1]The abbreviations used are: CGD, chronic granulomatous disesase; DFP, diisopropyl fluorophosphate; ECL, enhanced chemiluminescence; EBV, Epstein-Barr virus; FAD, flavin adenine dinucleotide; GMCSF, Granulocyte macrophage colony-stimulating factor ; NDPK (EC 2.7.4.6.), nucleoside diphosphate kinase ; PBS, 137 mM NaCl, 2.7 mM KCl, 1.5 mM KH_2PO_4, 8 mM Na_2HPO_4 pH7.3; PFK-2 (EC 2.7.1.105), phosphofructokinase, pPFK-2 = phosphofructo-2-kinase posphorylated on Ser^{466}; Phox, phagocyte oxidase; PMA, phorbol myristate acetate; PMN, polymorphonuclear neutrophil; SD, standard deviation; SOD (EC 1.15.1.1.), superoxide dismutase; NADPH oxidase (EC 1.6.99.6), nicotinamide adenine dinucleotide phosphate oxidase.

FIGURE LEGENDS

Fig. 1. Analysis of PFK-2 phosphorylation in PMA-stimulated cells and in constitutively active NADPH oxidase complexes isolated from neutrophils fractions. A. Phosphorylation of PFK-2 upon PLB985 stimulation with PMA. After 4 days of differentiation by DMF, cells were stimulated with 130 nM PMA at 37°C for 15 min. Cells were lysed by sonication. Cytosol fractions were obtained after ultracentrifugation. Left panel, Immunodetection of PFK-2 phosphorylation was assessed by using a specific polyclonal antibody directed against phosphorylated Ser^{466} and actine was used as a control. The experiment is representative of three independent experiments. Right panel, Densitometry analysis of PFK-2 phosphorylation on Ser 466 normalized to the actin band. B, Immunodetection of phospho-PFK-2 and p22-phox in NADPH oxidase complexes prepared either with resting (NS) or PMA-stimulated (S) PLB985 cell cytosol [27]. Left panel, Western blot analysis of heparin fractions (Hep) (45ul/lane) and Sephacryl elution fractions (Cx) (45ul/lane) by using specific polyclonal antibodies (left panel). Right panel, densitometry analysis of PFK-2 phosphorylation normalized to p22-phox amount in purified oxidase complexes (Sephacryl fractions). The Western-blot is representative of two independent experiments. * Indicates a result statistically different ($p < 0.05$) from that obtained with resting cytosol.

Fig. 2. Co-immunoprecipitation of NADPH oxidase cytosolic factors with phosphorylated PFK-2 in cytosol from PMA-stimulated PMN. pPFK-2 was immunoprecipitated from cytosol isolated from PMA-stimulated or resting PMN (860 µg) with 5 µg of specific antibody. A control experiment was performed by using 5 µg of an irrelevant antibody (IR) Immunoprecipitates obtained with pPFK-2 antibody on stimulated cytosol (pPFK2 S), with pPFK-2 antibody on resting cytosol (pPFK2 NS) and with irrelevant antibody were analyzed by Western-blot for the presence of PFK-2 phosphorylated on Ser^{466} and cytosolic factors p67-phox, p47-phox, p40-phox and Rac. Cytosol from stimulated PMN (50 µg) was loaded as a positive control. The results are representative of 3 independent experiments.

Fig. 3. Colocalisation of PFK-2 with cytochrome b_{558} in PMA-stimulated cells. A, Detection of both PFK-2 and Nox2 in resting and PMA-stimulated PLB985 cells was performed by confocal microscopy. Differentiated PLB985 cells were incubated with PMA (130 nM) or DMSO for 10 min at 37°C. Resting and stimulated cells (2×10^5 cells) were then fixed, permeabilized and labeled with both anti-13B6 monoclonal antibody directed against Nox2 and anti-PFK-2 polyclonal antibody (5 µg) for 1h at room temperature as described in the Methods. An Alexa Fluor 546 secondary antibody was used to detect PFK-2 and an Alexa

Fluor 488 secondary antibody was used to detect Nox2. Fluorescence images were recorded. The yellow color on merge images indicated a colocalization of both proteins. B, Determination of the percentage of colocalization of PFK-2 in Nox2 before and after PMA-stimulation using Zen 2010® software. The correlation coefficient for colocalization analysis was significantly increased (at least doubled) in stimulated cells. * Indicates a result statistically different ($p < 0.05$) from that obtained with resting cells.

Fig. 4. Translocation of PFK-2 to plasma membrane lipid rafts upon PMA stimulation. A, Immunodetection of PFK-2 and CD55, a lipid raft labelling, in resting and PMA-stimulated PLB985 cells by confocal microscopy. Differentiated PLB985 cells were incubated with PMA (130 nM) or DMSO for 10 min at 37°C. Resting and stimulated cells (2×10^5 cells) were then fixed, permeabilized and labeled with both anti-CD55 monoclonal antibody and anti-PFK-2 polyclonal antibody (5 µg) for 1h at room temperature as described in the Methods. An Alexa Fluor 488 secondary antibody was used to detect PFK-2 and an Alexa Fluor 546 to detect lipid rafts (CD55). Fluorescence images were recorded by confocal microscopy. The yellow color on merge images indicated a colocalization of both proteins. B, Determination of the percentage of colocalization of PFK-2 in CD55 before and after PMA-stimulation using Zen 2010® software. The correlation coefficient for colocalization analysis was significantly increased (at least doubled) in stimulated cells. * Indicates a result statistically different ($p < 0.05$) from that obtained with resting cells.

Fig. 5. Impact of PKA and PKB inhibitors on PFK-2 phosphorylation and oxydase activity upon PMA stimulation. Differentiated PLB985 cells were treated with either PKA inhibitor (H89, 10 µM), PKB inhibitor (Akt inhibitor XIII, 5µM) or DMSO 0.01 % (v/v) (-) at 37°C during 30 min. PLB lysate. The impact on ROS production of intact PLB985 cells was assessed. 105 cells were stimulated with PMA 130nM (A), fMLP 100 nM (B) and ionomycine 2.5 µM and the NADPH oxidase activity was measured by chemiluminescence. PFK-2 phosphorylation on Ser^{466} was immunodetected in PLB lysates (10^5 cell equivalent) with a specific polyclonal antibody and normalized to the amount of p22-phox as a positive control upon PMA stimulation in PLB985 cells upon PMA 130nM (A), fMLP 100 nM (B) and ionomycine (2.5 µM). * Indicates a statistical difference ($p < 0.05$) with the control condition obtained with 0.01 % (v/v) DMSO incubation.

Fig. 6. PFK-2 depletion decreases NADPH oxidase activity of PLB985 cells. PLB985 cells were differentiated into pseudo-neutrophils by DMF treatment. PFK-2 mRNA expression in PLB985 cells transfected with 6PGDH-targeting siRNA. Differentiated PLB985 were

transfected with PFK-2 targeting siRNA. A. Immunodetection of transfected and untransfected PLB lysates (10^5 cells equivalent) with a specific polyclonal antibody. $P22^{phox}$ and actine were used as a positive control. B. Densitometry of the PFK-2 band normalized to the actine band in control and transfected PLB985 immunoblotting. PFK-2 depletion impacts on ROS production of intact PLB985. 10^5 cells were stimulated with PMA (130 nM) and the NADPH oxidase activity was measured by chemiluminescence. (100 % corresponded to 490 ± 61 RLU). D. PFK-2 depletion decreases NADPH oxidase activity reconstituted in a cell-free assay. NADPH oxidase activity was reconstituted after incubation of a membrane fraction (7.5 µg) with a cytosol fraction (75 µg) in presence of 40 µM GTPγS, 5 mM $MgCl_2$ and an optimal amount of arachidonic acid. The superoxide anion production was measured after addition of NADPH by the SOD-sensitive portion of the cytochrome c reduction recorded at 550 nm. Results are expressed as the average ± SD of at least 3 different experiments. * Indicates a result statistically different ($p < 0.05$) from that obtained for mock siRNA.

Fig. 7. PFK-2 depletion induced a decrease in cytosolic ATP concentration in differentiated PLB985 cell cytosol. Cytosolic fractions isolated from differentiated PLB985 cells transfected either with PFK-2-targeting siRNA or mock siRNA were adjusted to 0.5mg protein /ml. A, The cytosol absorbance at 340 nm was measured and compared to a NADPH standard curve ranging from 0 to 100mM in order to estimate the intracellular NADPH concentration. B, The concentration of ATP was assessed by luminescence using a commercial kit and ATP-concentration standards. Results are representative of 2 independent experiments. Results are expressed as the average ± SD of at least 2 independent experiments. * Indicates a result statistically different ($p < 0.05$) from that obtained with control cytosol.

Fig. 8. Decrease in p47-phox phosphorylation upon PMA stimulation in PFK-2-targeting siRNA PLB985 cells. P47-phox phosphorylation was detected in 1% (w/v) Triton X100 cellular extract from differentiated PLB985 cells transfected with either PFK-2-targeting siRNA (PFK2) or mock siRNA (Mock), or untransfected (-). A, Western blot performed on cellular extract (5×10^6 cell equivalent). P47-phox was detected by using a polyclonal specific antibody and phosphoPFK-2 was detected by using a mixture of antibodies directed against p47-phox phospho-Ser^{318} and p47-phox phospho-Ser^{328}. B, Densitometry analysis of the Western-blot to analyze the amount of p47-phosphorylation normalized the total amount of p47-phox. Results are expressed as a percentage of p47-phox phosphorylation measured in fractions obtained from mock-siRNA transfected cells. * Indicates a result statistically different ($p < 0.05$) from that obtained for mock siRNA.

Fig. 9. Colocalization of NDP-kinase with cytochrome b_{558} in PMA-stimulated cells. A, Detection of both NDPK and Nox2 in resting and PMA-stimulated PLB985 cells was performed by confocal microscopy. Differentiated PLB985 cells were incubated with PMA (130 nM) or DMSO for 10 min at 37°C. Resting and stimulated cells (2×10^5 cells) were then fixed, permeabilized and labeled with both anti-13B6 monoclonal antibody directed against Nox2 and anti-NDPK polyclonal antibody (5 µg) for 1h at room temperature as described in the Methods. An Alexa Fluor 546 secondary antibody was used to detect Nox2 and an Alexa Fluor 488 secondary antibody was used to detect NDPK. Fluorescence images were recorded. The yellow color on merge images indicated a colocalization of both proteins. B, Determination of the percentage of colocalization before and after PMA-stimulation using Zen 2010® software. The correlation coefficient for colocalization analysis was significantly increased (at least doubled) in stimulated cells. * Indicates a result statistically different ($p < 0.05$) from that obtained with resting cells.

Figure 1 Baillet *et al*

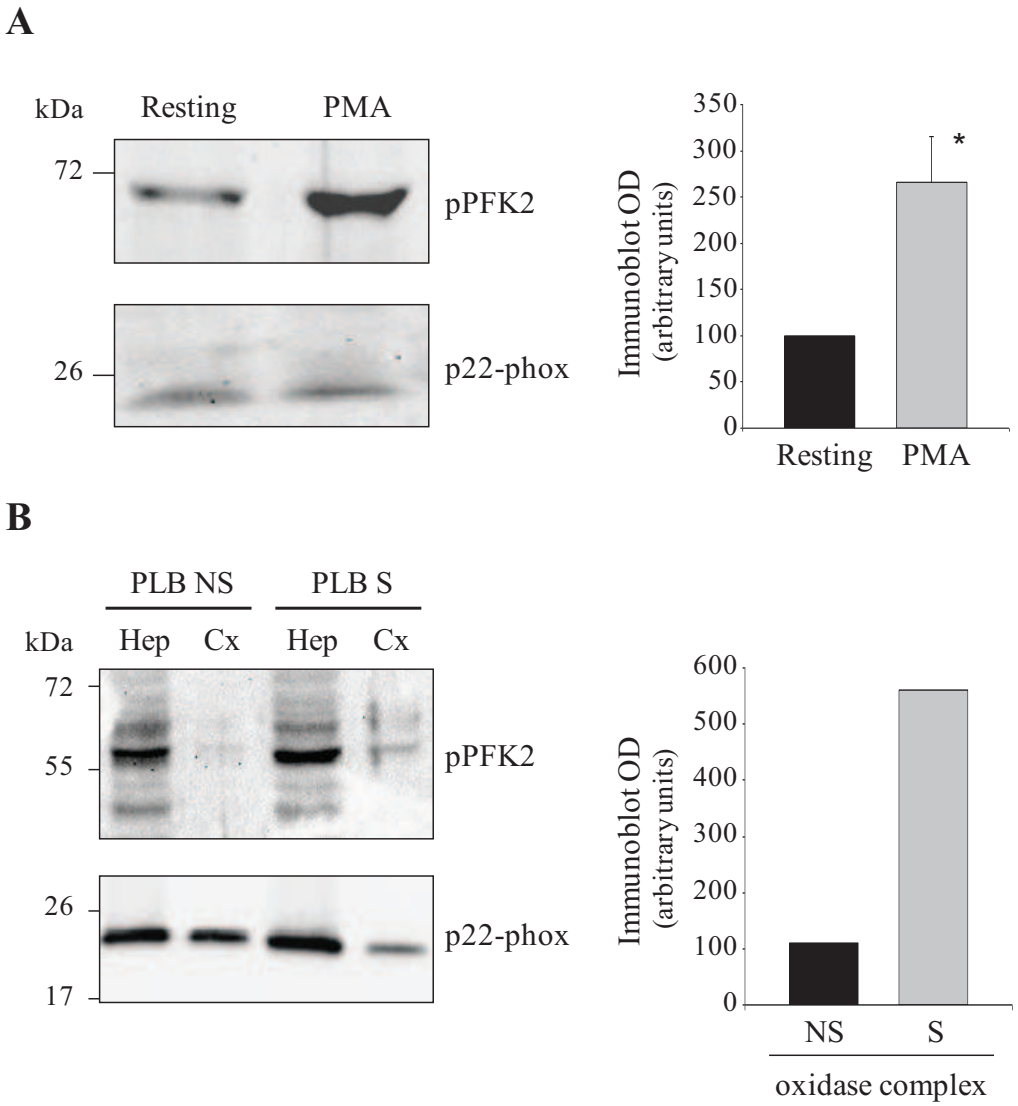

Fig. 1. *Analysis of PFK-2 phosphorylation in PMA-stimulated cells and in constitutively active NADPH oxidase complexes isolated from neutrophils fractions. A. Phosphorylation of PFK-2 upon PLB985 stimulation with PMA. After 4 days of differentiation by DMF, cells were stimulated with 130 nM PMA at 37°C for 15 min. Cells were lysed by sonication. Cytosol fractions were obtained after ultracentrifugation. Left panel, Immunodetection of PFK-2 phosphorylation was assessed by using a specific polyclonal antibody directed against phosphorylated* Ser^{466} *and actine was used as a control. The experiment is representative of three independent experiments. Right panel, Densitometry analysis of PFK-2 phosphorylation on Ser 466 normalized to the actin band. B, Immunodetection of phospho-PFK-2 and p22-phox in NADPH oxidase complexes prepared either with resting (NS) or PMA-stimulated (S) PLB985 cell cytosol [27]. Left panel, Western blot analysis of heparin fractions (Hep) (45ul/lane) and Sephacryl elution fractions (Cx) (45ul/lane) by using specific polyclonal antibodies (left panel). Right panel, densitometry analysis of PFK-2 phosphorylation normalized to p22-phox amount in purified oxidase complexes (Sephacryl fractions). The Western-blot is representative of two independent experiments. * Indicates a result statistically different (*$p < 0.05$*) from that obtained with resting cytosol.*

Figure 2 Baillet *et al*

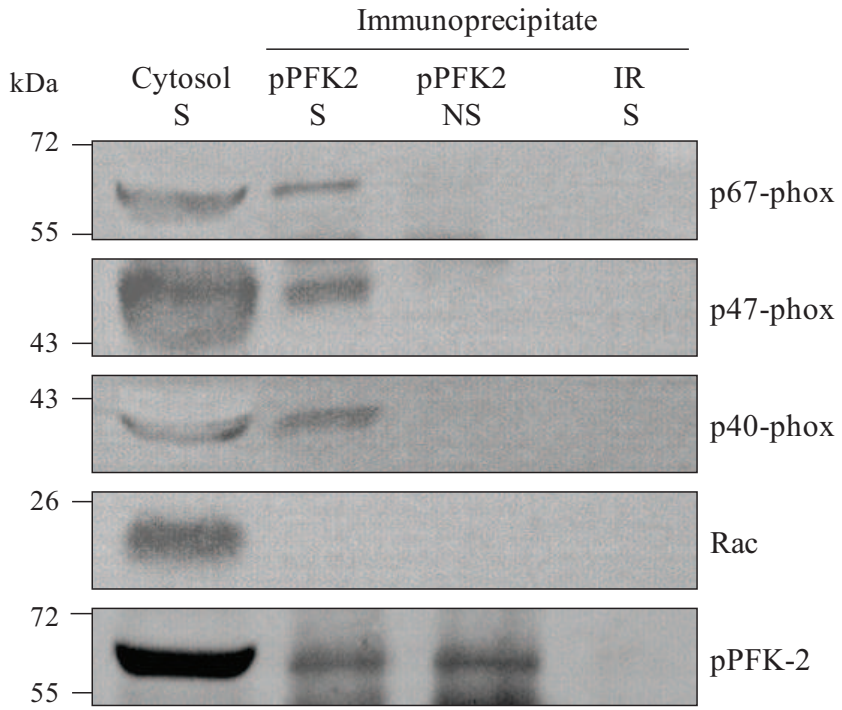

Fig. 2. *Co-immunoprecipitation of NADPH oxidase cytosolic factors with phosphorylated PFK-2 in cytosol from PMA-stimulated PMN. pPFK-2 was immunoprecipitated from cytosol isolated from PMA-stimulated or resting PMN (860 µg) with 5 µg of specific antibody. A control experiment was performed by using 5 µg of an irrelevant antibody (IR) Immunoprecipitates obtained with pPFK-2 antibody on stimulated cytosol (pPFK2 S), with pPFK-2 antibody on resting cytosol (pPFK2 NS) and with irrelevant antibody were analyzed by Western-blot for the presence of PFK-2 phosphorylated on Ser^{466} and cytosolic factors p67-phox, p47-phox, p40-phox and Rac. Cytosol from stimulated PMN (50 µg) was loaded as a positive control. The results are representative of 3 independent experiments.*

Figure 3 Baillet *et al*

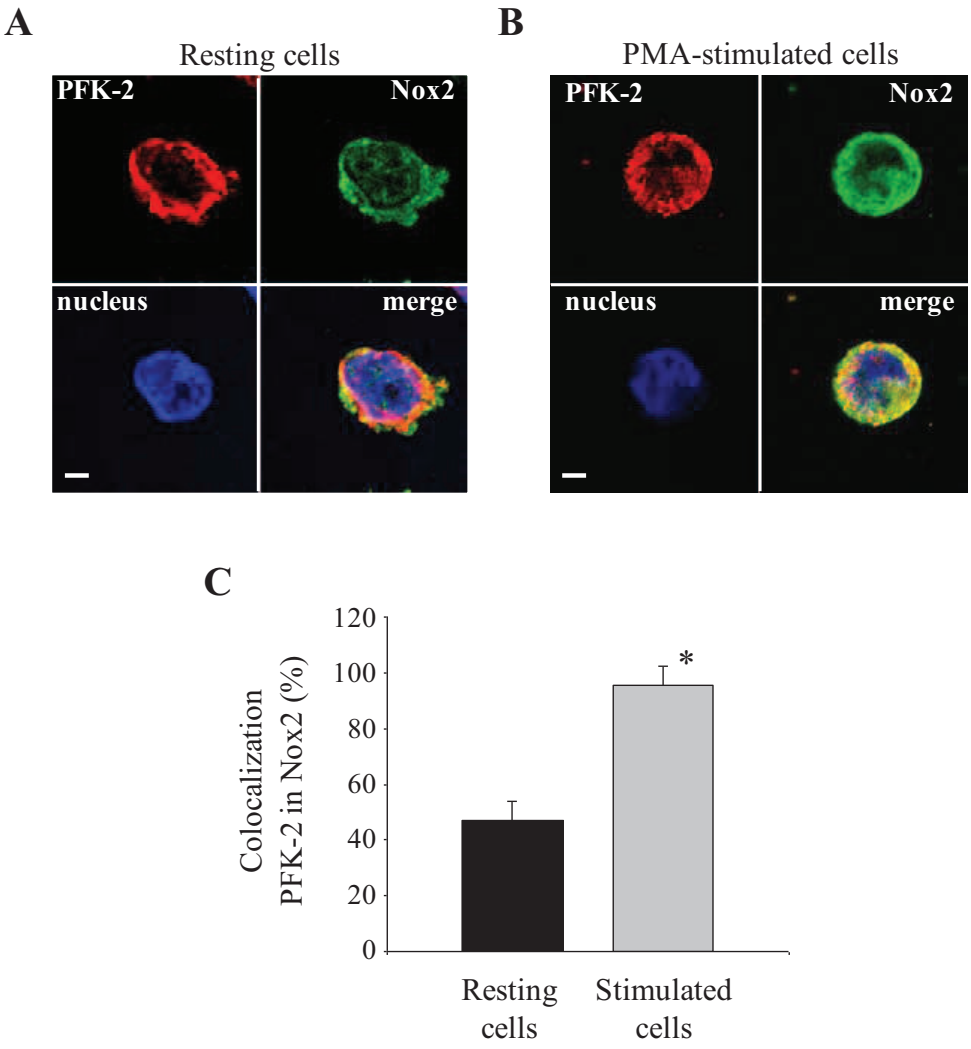

Fig. 3. *Colocalisation of PFK-2 with cytochrome b_{558} in PMA-stimulated cells. A, Detection of both PFK-2 and Nox2 in resting and PMA-stimulated PLB985 cells was performed by confocal microscopy. Differentiated PLB985 cells were incubated with PMA (130 nM) or DMSO for 10 min at 37°C. Resting and stimulated cells (2×10^5 cells) were then fixed, permeabilized and labeled with both anti-13B6 monoclonal antibody directed against Nox2 and anti-PFK-2 polyclonal antibody (5 µg) for 1h at room temperature as described in the Methods. An Alexa Fluor 546 secondary antibody was used to detect PFK-2 and an Alexa Fluor 488 secondary antibody was used to detect Nox2. Fluorescence images were recorded. The yellow color on merge images indicated a colocalization of both proteins. B, Determination of the percentage of colocalization of PFK-2 in Nox2 before and after PMA-stimulation using Zen 2010® software. The correlation coefficient for colocalization analysis was significantly increased (at least doubled) in stimulated cells. * Indicates a result statistically different ($p < 0.05$) from that obtained with resting cells.*

Figure 4 Baillet *et al*

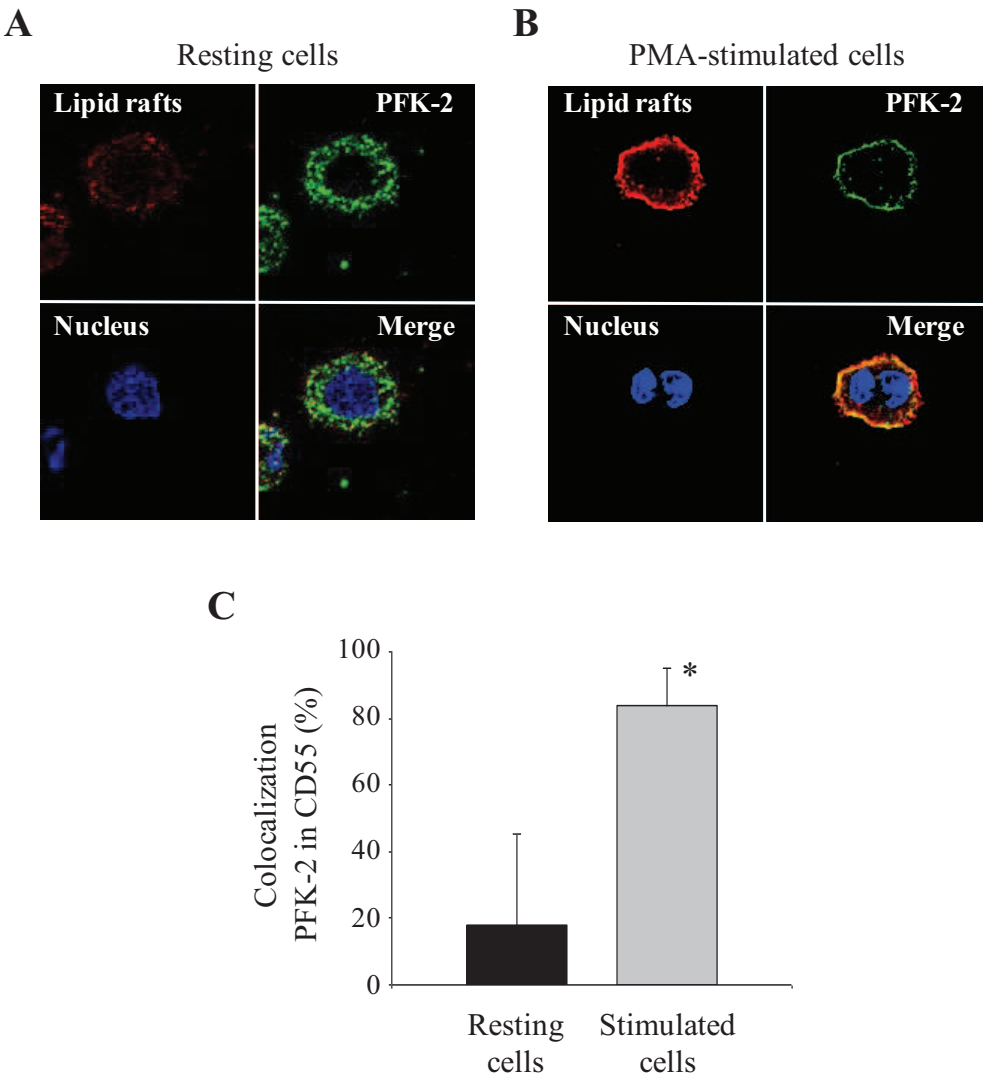

Fig. 4. *Translocation of PFK-2 to plasma membrane lipid rafts upon PMA stimulation. A, Immunodetection of PFK-2 and CD55, a lipid raft labelling, in resting and PMA-stimulated PLB985 cells by confocal microscopy. Differentiated PLB985 cells were incubated with PMA (130 nM) or DMSO for 10 min at 37°C. Resting and stimulated cells (2 × 10^5 cells) were then fixed, permeabilized and labeled with both anti-CD55 monoclonal antibody and anti-PFK-2 polyclonal antibody (5 µg) for 1h at room temperature as described in the Methods. An Alexa Fluor 488 secondary antibody was used to detect PFK-2 and an Alexa Fluor 546 to detect lipid rafts (CD55). Fluorescence images were recorded by confocal microscopy. The yellow color on merge images indicated a colocalization of both proteins. B, Determination of the percentage of colocalization of PFK-2 in CD55 before and after PMA-stimulation using Zen 2010® software. The correlation coefficient for colocalization analysis was significantly increased (at least doubled) in stimulated cells. * Indicates a result statistically different ($p < 0.05$) from that obtained with resting cells.*

Figure 5 Baillet *et al*

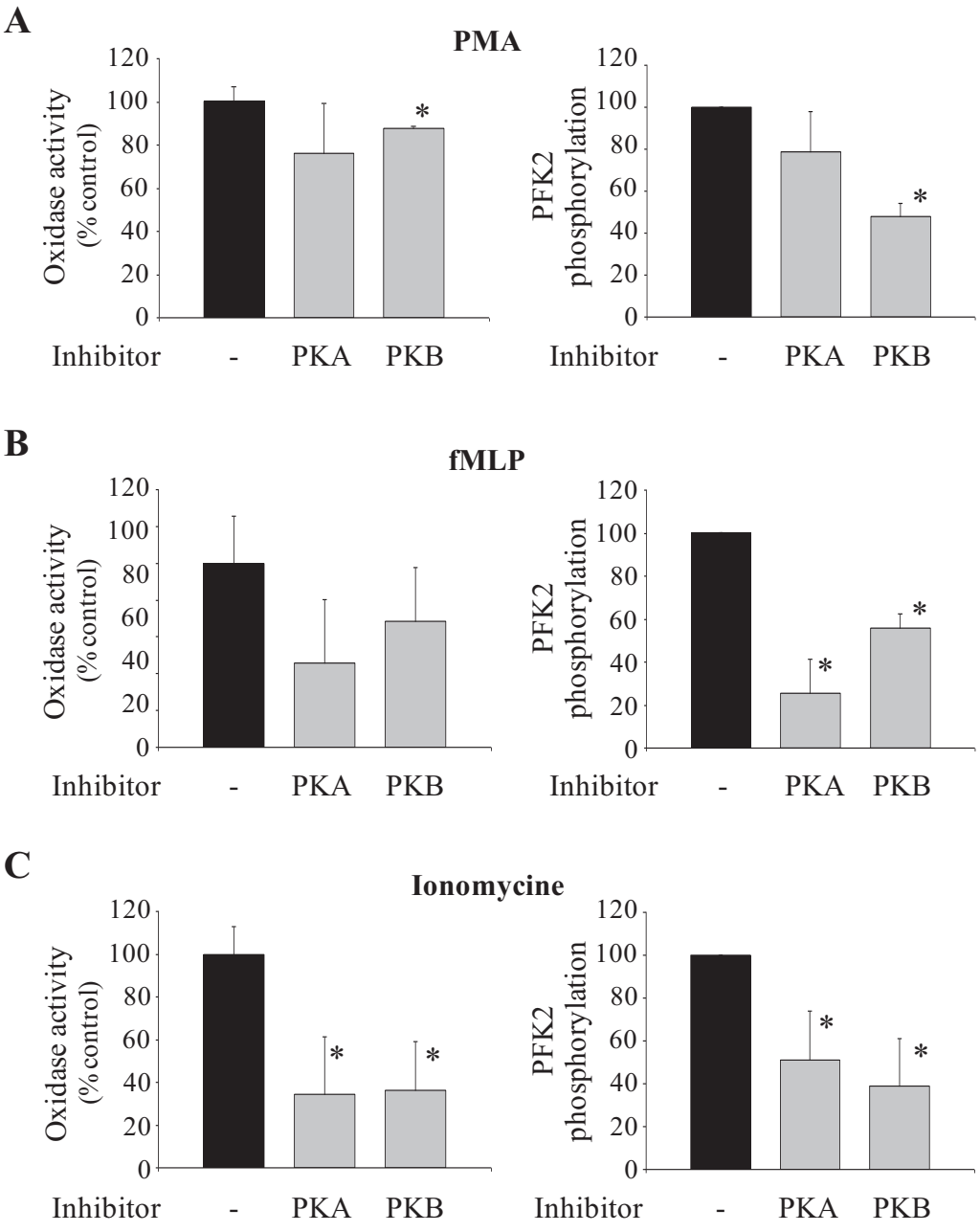

Fig. 5. *Impact of PKA and PKB inhibitors on PFK-2 phosphorylation and oxydase activity upon PMA stimulation. Differentiated PLB985 cells were treated with either PKA inhibitor (H89, 10 µM), PKB inhibitor (Akt inhibitor XIII, 5µM) or DMSO 0.01 % (v/v) (-) at 37°C during 30 min. PLB lysate. The impact on ROS production of intact PLB985 cells was assessed. 105 cells were stimulated with PMA 130nM (A), fMLP 100 nM (B) and ionomycine 2.5 µM and the NADPH oxidase activity was measured by chemiluminescence.*
*PFK-2 phosphorylation on Ser^{466} was immunodetected in PLB lysates (10^5 cell equivalent) with a specific polyclonal antibody and normalized to the amount of p22-phox as a positive control upon PMA stimulation in PLB985 cells upon PMA 130nM (A), fMLP 100 nM (B) and ionomycine (2.5 µM). * Indicates a statistical difference ($p < 0.05$) with the control condition obtained with 0.01 % (v/v) DMSO incubation.*

Figure 6 Baillet *et al*

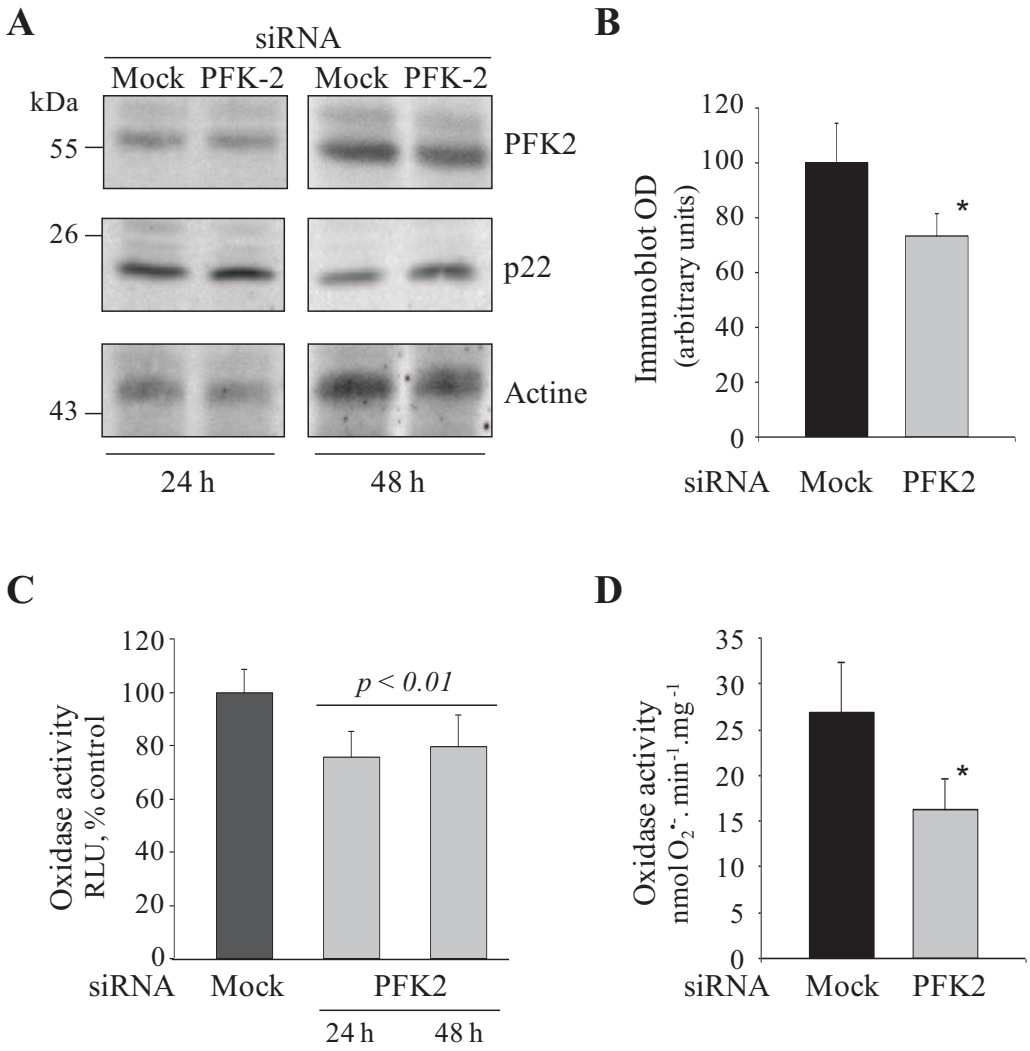

Fig. 6. *PFK-2 depletion decreases NADPH oxidase activity of PLB985 cells. PLB985 cells were differentiated into pseudo-neutrophils by DMF treatment. PFK-2 mRNA expression in PLB985 cells transfected with 6PGDH-targeting siRNA. Differentiated PLB985 were transfected with PFK-2 targeting siRNA. A. Immunodetection of transfected and untransfected PLB lysates (10^5 cells equivalent) with a specific polyclonal antibody. $P22^{phox}$ and actine were used as a positive control. B. Densitometry of the PFK-2 band normalized to the actine band in control and transfected PLB985 immunoblotting. PFK-2 depletion impacts on ROS production of intact PLB985. 10^5 cells were stimulated with PMA (130 nM) and the NADPH oxidase activity was measured by chemiluminescence. (100 % corresponded to 490 ± 61 RLU). D. PFK-2 depletion decreases NADPH oxidase activity reconstituted in a cell-free assay. NADPH oxidase activity was reconstituted after incubation of a membrane fraction (7.5 µg) with a cytosol fraction (75 µg) in presence of 40 µM GTPγS, 5 mM $MgCl_2$ and an optimal amount of arachidonic acid. The superoxide anion production was measured after addition of NADPH by the SOD-sensitive portion of the cytochrome c reduction recorded at 550 nm. Results are expressed as the average ± SD of at least 3 different experiments. * Indicates a result statistically different ($p < 0.05$) from that obtained for mock siRNA.*

Figure 7 Baillet *et al*

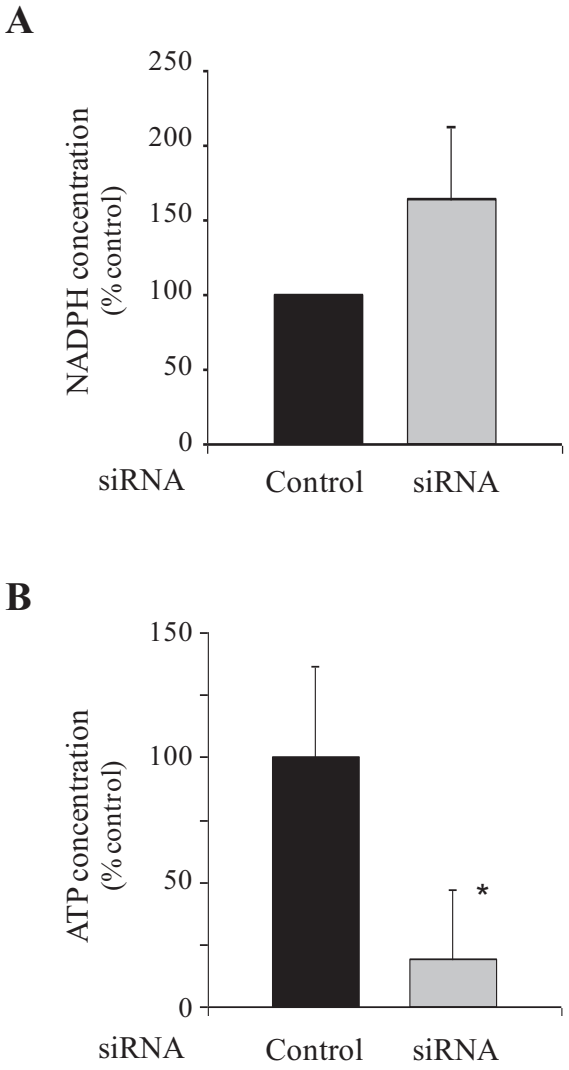

Fig. 7. *PFK-2 depletion induced a decrease in cytosolic ATP concentration in differentiated PLB985 cell cytosol. Cytosolic fractions isolated from differentiated PLB985 cells transfected either with PFK-2-targeting siRNA or mock siRNA were adjusted to 0.5mg protein /ml. A, The cytosol absorbance at 340 nm was measured and compared to a NADPH standard curve ranging from 0 to 100mM in order to estimate the intracellular NADPH concentration. B, The concentration of ATP was assessed by luminescence using a commercial kit and ATP-concentration standards. Results are representative of 2 independent experiments. Results are expressed as the average ± SD of at least 2 independent experiments. * Indicates a result statistically different ($p < 0.05$) from that obtained with control cytosol.*

Figure 8 Baillet *et al*

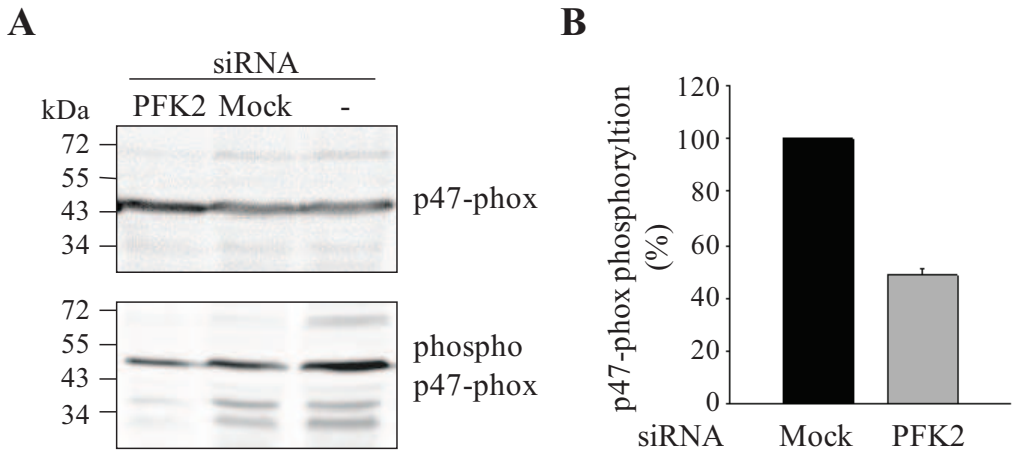

Fig. 8. *Decrease in p47-phox phosphorylation upon PMA stimulation in PFK-2-targeting siRNA PLB985 cells. P47-phox phosphorylation was detected in 1% (w/v) Triton X100 cellular extract from differentiated PLB985 cells transfected with either PFK-2-targeting siRNA (PFK2) or mock siRNA (Mock), or untransfected (-). A, Western blot performed on cellular extract (5 ×10^6 cell equivalent). P47-phox was detected by using a polyclonal specific antibody and phosphoPFK-2 was detected by using a mixture of antibodies directed against p47-phox phospho-Ser^{318} and p47-phox phospho-Ser^{328}. B, Densitometry analysis of the Western-blot to analyze the amount of p47-phosphorylation normalized the total amount of p47-phox. Results are expressed as a percentage of p47-phox phosphorylation measured in fractions obtained from mock-siRNA transfected cells.*
** Indicates a result statistically different ($p < 0.05$) from that obtained for mock siRNA.*

Figure 9 Baillet *et al*

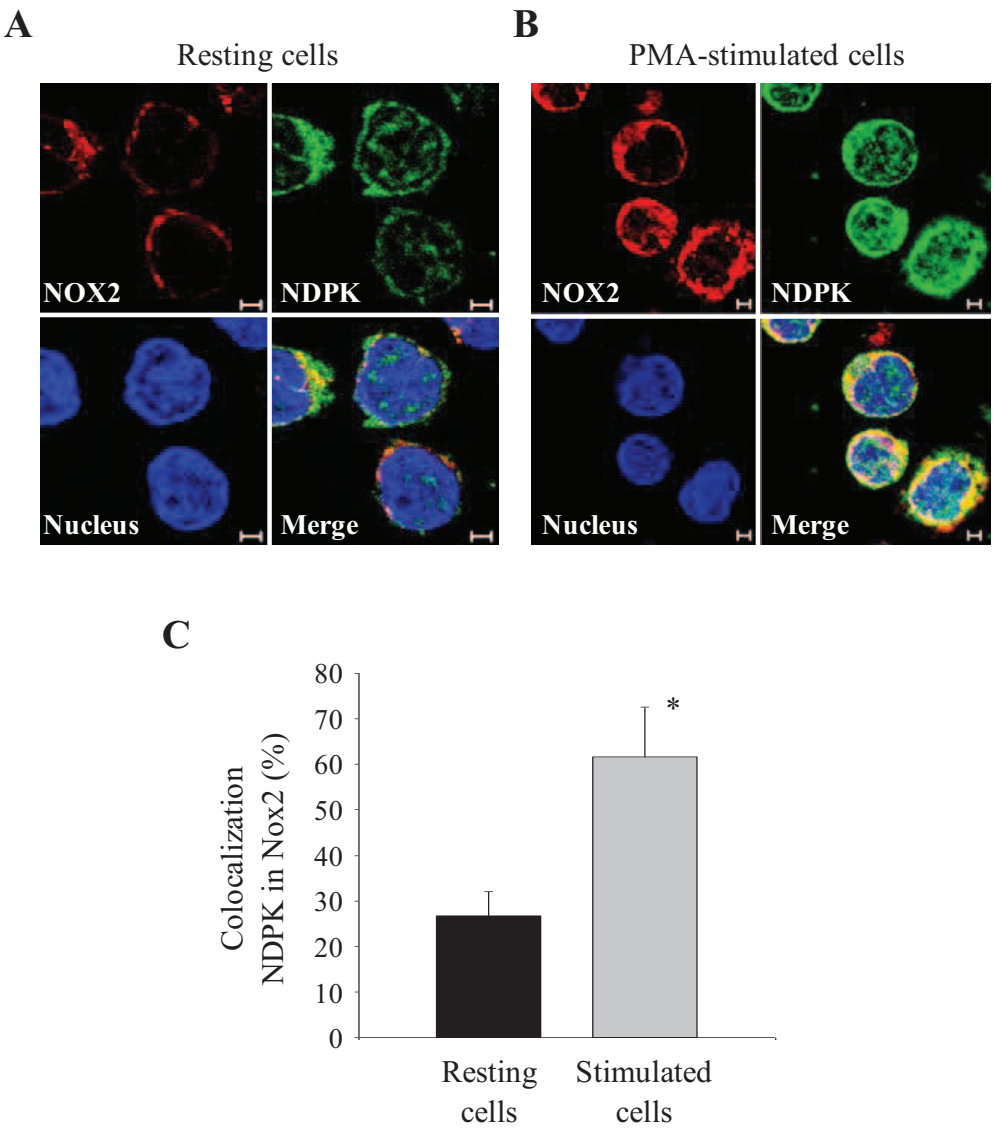

Fig. 9. *Colocalization of NDP-kinase with cytochrome b_{558} in PMA-stimulated cells. A, Detection of both NDPK and Nox2 in resting and PMA-stimulated PLB985 cells was performed by confocal microscopy. Differentiated PLB985 cells were incubated with PMA (130 nM) or DMSO for 10 min at 37°C. Resting and stimulated cells (2 × 10^5 cells) were then fixed, permeabilized and labeled with both anti-13B6 monoclonal antibody directed against Nox2 and anti-NDPK polyclonal antibody (5 µg) for 1h at room temperature as described in the Methods. An Alexa Fluor 546 secondary antibody was used to detect Nox2 and an Alexa Fluor 488 secondary antibody was used to detect NDPK. Fluorescence images were recorded. The yellow color on merge images indicated a colocalization of both proteins. B, Determination of the percentage of colocalization before and after PMA-stimulation using Zen 2010® software. The correlation coefficient for colocalization analysis was significantly increased (at least doubled) in stimulated cells. * Indicates a result statistically different ($p < 0.05$) from that obtained with resting cells.*

CHAPITRE II

La protéine S100A8, élément déterminant de l'activation de la NADPH oxydase des phagocytes

Article 3

Partie 2 : La protéine S100A8, élément déterminant dans l'activation de la NADPH oxydase

S100A8 et S100A9 représentent 40% des protéines cytosoliques du PMN et sont impliquées dans le transport de l'acide arachidonique, le réarrangement du cytosquelette et l'activation de la NADPH oxydase. Elles ont une masse moléculaire de 10 et 14 kDa et possèdent deux motifs EF-Hand permettant la fixation de calcium. Lors de l'association de S100A8/A9 en dimère ou tétramère, un site potentiel de fixation du zinc émerge à l'interface des deux partenaires, au niveau de la partie C-terminale.

Les résultats rapportés dans la littérature, et plus particulièrement dans notre laboratoire, suggèrent que les protéines S100A8/A9 sont impliquées dans l'activation de la NADPH oxydase phagocytaire :

1. Il a été démontré, *in vitro* ou *ex vivo*, que les protéines S100A8/A9 potentialisent à la fois l'activité constitutive [Paclet *et al.* 2007] et inductible [Berthier *et al.* 2003] de la NADPH oxydase phagocytaire. La transfection des deux gènes codant pour ces protéines dans les lymphocytes B-EBV, dépourvus de S100A8/A9, demeure indispensable pour acquérir une conformation active et pour générer une activité oxydase, suggérant l'interdépendance, *in vivo,* de S100A8 et S100A9.
2. Lors de la stimulation du PMN, il est probable que S100A8/A9 s'associent aux facteurs cytosoliques d'activation pour leur translocation à la membrane plasmique. Des liens privilégiés de S100A8 avec $p67^{phox}$ ont été rapportés [Kerkhoff *et al.* 2005].
3. Les protéines S100A8/A9 interviennent par leurs propriétés d'effecteurs allostériques de régulation de la NADPH oxydase des phagocytes : elles augmentent l'affinité de $p67^{phox}$ pour le cytochrome b_{558} et induisent le changement de conformation de NOX2 [Berthier *et al.* 2003; Paclet *et al.* 2007] qui initie le transfert d'électrons.

Dans ce travail, notre objectif a été d'examiner l'impact de l'hétérocomplexe S100A8/A9 sur l'activation de la NADPH oxydase des phagocytes. De plus, nous avons cherché à caractériser les domaines impliqués dans l'interaction entre les protéines S100A8/A9 et le cytochrome b_{558}.

Des protéines recombinantes exprimées et produites dans *Escherichia coli* ou *Pseudomonas aeruginosa* ont été utilisées pour tenter d'analyser le rôle respectif de S100A8 et S100A9. Des protéines chimères, obtenues en fusionnant S100A9 et S100A8, ont été générées afin de préciser quels domaines étaient impliqués dans l'activation de l'oxydase. Des expériences de microscopie confocale et de réticulation avec des protéines chimères natives ou tronquées ont exploré les domaines d'interaction entre S100A8/A9 et le cytochrome b_{558} ainsi que leur localisation subcellulaire au cours de l'activation de l'oxydase.

Les résultats montrent que :
- S100A8 est déterminante dans l'activation de la NADPH oxydase phagocytaire. La partie C-terminale de S100A8 est directement impliquée. In vivo, S100A8 et S100A9, chargées en calcium, s'associent pour acquérir une conformation active nécessaire à leur fonction.

- Lors de l'activation de la NADPH oxydase par le PMA, l'hétérocomplexe S100A8/A9 est transféré à la membrane plasmique. A ce niveau, son interaction, transitoire, avec le cytochrome b_{558} conduit à son activation.

Dans ce projet, mon travail a permis de confirmer *ex vivo* le rôle critique de S100A8 lors de l'activation de NOX2 en révélant que le cytochrome b_{558} est constitutivement actif lorsque sa purification comporte une étape d'incubation avec les protéines chimères dans lesquelles la partie C-terminale de S100A8 est disponible. De plus, j'ai analysé la localisation subcellulaire de S100A8/A9 lors de l'activation de l'oxydase.

Article 3 : Berthier S., **Baillet A.**, Paclet M.H., Nguyen M.V., Polack B., and Morel F. S100A8 (Myeloid Related Protein MRP8) is a positive effector of phagocyte NADPH oxidase activation. Prochainement soumis à *Plos one.*

S100A8 (Myeloid Related Protein MRP8) is a positive effector of phagocyte NADPH oxidase activation.

Berthier Sylvie, Baillet Athan* †, Paclet Marie-Hélène* ‡ §, NGuyen Minh Vu Chuong*, Polack Benoît ‖ §, and Morel Françoise*[1].*

*Groupe de Recherche et d'Etude du Processus Inflammatoire (GREPI), Laboratoire « Aging Imaging Modeling » (AGIM), Formation de Recherche en évolution (FRE) Centre National de la Recherche Scientifique CNRS 3405, UJF-EPHE,
†Clinic of Rheumatology, and ‡ « Laboratoire des Enzymes et des Protéines » § « Institut de Biologie et Pathologie », Centre Hospitalier Universitaire (CHU), Grenoble, France;
‖Techniques de l'Ingénierie Médicale et de la Complexité–Informatique, Mathématiques et Applications de Grenoble (TIMC-IMAG)Unite´ Mixte de Recherche (UMR) 5525 Centre National de la Recherche Scientifique
(CNRS), Universite´ Joseph Fourier (UJF),Grenoble,France.

Abbreviations: S100A8 or MRP8, Myeloid Related Protein; S100A9 or MRP14; ExoS, Exotoxin S of *Pseudomonas aeruginosa*; TTSS, Type Three Secretion System; EBV, Epstein-Barr-Virus; RLU, Relative Luminescence Unit; NOX, NADPH oxidase; DSS, Disuccinimidyl Suberate; PMA, Phorbol Myristate Acetate

Foot-notes: S100A9/A8 is the *in vivo* complex; S100A9-A8 or S100A8-A9 are the constructed chimera.

Keywords: S100 calcium-binding-protein; oxidase complex assembly ; cytochrome b_{558}/NOX2 regulation; protein-delivery via TTSS.

Short title: S100A8/A9 protein/cytochrome b_{558} interaction

1. To whom correspondence should be addressed (email: FrMorel.enzymo@chu-grenoble.fr)

Synopsis

S100A8 and S100A9 are two calcium binding Myeloid Related Proteins, and important mediators of inflammatory diseases. They were recently introduced as partners for phagocyte NADPH oxidase regulation. We had for aim to (i) evaluate the impact of S100 proteins on NADPH oxidase activity, (ii) to characterize molecular interaction of either S100A8, S100A9 or S100A8/A9 heterocomplex with cytochrome b_{558} (iii), and to determine the S100A8 sequence involved in the cytochrome b_{558} /S100 interface. Recombinant full length or S100A9- truncated A8 chimeras and ExoS/S100 fusion proteins were expressed in *E. coli* and in *P. aeruginosa* respectively. S100A8 proved to be the strategic partner for NADPH oxidase activation, contrary to S100A9 but the calcium and combination with phosphorylated S100A9 are essential *in vivo*. Recombinant S100A8, loaded with calcium and fused with the first 129 or 54 N-terminal amino acid residues of the *P. Aeruginosa* ExoS toxin, induces *in vitro,* a similar oxidase activation to the one observed in the presence of S100A9 *in vivo*, suggesting that S100A8 is the limiting factor. Endogenous S100A8/A9 colocalize in differentiated and PMA stimulated PLB985 cells, with NOX2/gp91^{phox} and p22^{phox}. The C-terminal region of S100A8 is directly involved in the molecular interface with cytochrome b_{558}: rS100A9-truncated 90S100A8 chimera, as opposed to rS100A9-truncated 86 S100 A8, activates the NADPH oxidase function of cytochrome b_{558}. The data points to 4 amino acid residues HEES of the zinc-binding-site on the S100A8 C-terminal sequence; these amino acid residues are critical for cytochrome b_{558} interaction and then oxidase activation.

Introduction

Myeloid-Related Proteins, S100A8 (MRP8) and S100A9 (MRP14), are two calcium-binding proteins of the multigenic S100 family and are specifically linked to innate immunity [Roth *et al.* 2003]. They are mainly expressed in cells of myeloid origin such as neutrophils or monocytes, but not at all in Epstein-Barr-Virus immortalized B lymphocytes [Berthier *et al.* 2003]. They were also identified in epithelial cells and keratinocytes [Benedyk *et al.* 2007; Voss *et al.* 2011]. In phagocytes, S100A8 and S100A9 associate in the presence of calcium to calprotectin, the physiologically heteromeric complex that binds polyunsaturated fatty acids such as arachidonic acid [Kerkhoff *et al.* 1999]. S100A8/A9 protein complex accounts for the entire arachidonic acid-binding capacity of neutrophil cytosol. Binding proceeds in a calcium dependent manner, via the carboxyl group at the C terminal tail of S100A9. The crystal structure of calprotectin was recently characterized [Korndorfer *et al.* 2007].

S100A8/A9 have a wide range of intra and extra-cellular functions: inside neutrophils, they are involved in the regulation of NADPH oxidase [Berthier *et al.* 2009]. They participate in its activation through the assembly of oxidase complex and the transfer of arachidonic acid to membrane bound cytochrome b_{558}/NOX2. During this transfer, S100A8/A9 associate with $p67^{phox}$ and Rac [Doussière *et al.* 2002; Kerkhoff *et al.* 2005]; moreover, they are known to interact with subunits of NOX2 [Berthier *et al.* 2003]. Their relevant role in oxidative response is probably mediated via their Ca^{++} and phosphorylation-dependent translocation to plasma membrane where the oxidase complex assembles and NOX2 is activated [Roth *et al.* 1993; Schenten *et al.* 2010; Schenten *et al.* 2011]. S100A8/A9 are also secreted outside of the cells via a Golgi-independent pathway. They bind heparin sulphate and accumulate at the endothelial surface. In this context, both proteins were reported at local sites of inflammation, [Baillet *et al.* 2010; Gebhardt *et al.* 2006] in neoplastic tumours [Nicolas *et al.* 2011], and in skin diseases [Benedyk *et al.* 2007], where they trigger a crucial danger signal. The term of "Alarmin" was introduced recently for these molecules [Foell *et al.* 2007]. However S100A8, and to some extent S100A9, may also have a protective role since they are particularly susceptible to oxidative modifications [Lim *et al.* 2009]. Moreover, the calprotectin heterotetramer displays a high affinity for Zn^{++}, due to two HXXXH motifs responsible for Zn^{++} binding, located at the interface between S100A8 and S100A9 subunits.

NOX2 is the prototype of NADPH oxidase family, from which 7 NOX-DUOX were characterized in humans [Bedard *et al.* 2007a]. $Gp91^{phox}$ or NOX2, the β subunit of

cytochrome b_{558} in neutrophils, is the redox core of NADPH oxidase [Morel 2007; Vignais 2002] and the membrane anchorage site for assembly with cytosolic factors, $p67^{phox}$, $p47^{phox}$, $p40^{phox}$, and Rac1/2. NADPH oxidase complex is unassembled and inactive in resting cells, but upon stimulation by inflammatory mediators or during phagocytosis, phosphorylation of phox proteins induces intra and intermolecular rearrangements that stabilize the complex at the membrane level to give an optimal cytochrome b_{558} conformation and NADPH oxidase activity.

An allosteric regulation of NADPH oxidase activity was reported recently in which cytochrome b_{558} is the catalytic sub-unit and cytosolic factors are regulatory effectors as $p47^{phox}$ an adaptor and $p67^{phox}$, the limiting factor [Paclet *et al.* 2000]. The binding of $p67^{phox}$ to cytochrome b_{558}, mediates the transition from an inactive to an active conformation of the hemoprotein [Paclet *et al.* 2000]. Recent data suggests that S100 A8 /A9 are new allosteric effectors of NADPH oxidase regulation in neutrophils [Berthier *et al.* 2003]. In fact, S100 A8 /A9 were introduced as novel partners for two NADPH oxidases: NOX2 [Berthier *et al.* 2009] and NOX5 [Benedyk *et al.* 2007]. They potentiate activation of NADPH oxidase and ROS production in neutrophils. However the mechanisms by which S100A8/A9 proteins increase NADPH oxidase activity remain unknown.

This article emphasizes the respective functions of S100A8 and S100A9 in phagocytes and their role in NADPH oxidase activation. Our data confirm that S100A8 is the privileged interactive partner of cytochrome $b_{558.}$ The interaction of S100A8 with cytochrome b_{558} proceeds through a strategic calcium mediated conformation change *in vivo*, involving both S100A8 and S100A9.

Materials and Methods

Materials – Chemical reagents used in this study were obtained from the following sources: Heparin agarose, arachidonic acid, PMA, carbenicillin, luminol (5-amino2, 3-dihydro-1, 4-phtalazinedione) (Sigma Chemicals Co., St Louis, MO, USA); S100A8 (Calgranulin A C19), S100A9 (Calgranulin B C19), goat polyclonal antibody, donkey anti-goat IgG antibody (Santa Cruz Biotechnology, Inc., Santa Cruz, CA, USA); anti-goat and anti rabbit IgG Alexa Fluor 488, or anti mouse IgG Alexa Fluor 546 (Molecular Probes Europe BV Leiden, The Netherlands); PIA (DIFCO Laboratories, Detroit, MI, USA); ECL Western blot detection reagent, sephacryl S300 HR, diethylaminoethyl (DEAE) sepharose CL-6B, CM sepharose CL-6B, octyl sepharose CL-4B (Amersham Pharmacia Biotech, Uppsala, Sweden); n-octyl glucoside (Roche diagnostic, Meylan, France); DSS (Disuccinimidyl suberate) (Pierce Chemical Co, USA).

Methods –

Neutrophils, lymphoid cell line, and PLB985 cells.

Human neutrophils and B-lymphocytes are usually isolated according to previously described methods [Paclet *et al.* 2001]. B lymphocytes were immortalized with the B95-8 strain of Epstein-Barr Virus (EBV); the EBV-B lymphocytes were cultured in RPMI 1640 supplemented with 10% (v/v) foetal calf serum, 2mM L-glutamine at 37°C in 5% CO_2 atmosphere. Cytosolic fraction from EBV-B lymphocytes and membrane fraction from purified neutrophils previously treated with 3mM DFP were prepared as described [Batot *et al.* 1995]. PLB985 cells were grown in RPMI 1640 medium supplemented with 2mM glutamic acid, 10% (v/v) foetal bovine serum, 100 U/ml penicillin, 100µg streptomycin at 37°C and 5% CO_2 atmosphere. For granulocyte differentiation, PLB 985 cells ($5x10^5$ cells/ml) were treated with 0.5% (v/v) DMF for 1-6 days [Baillet *et al.* 2011b].

Bacterial strains and growth conditions

The *Pseudomonas aeruginosa* wild type strain (CHA) was grown from a mucoid bronchopulmonary isolated in a cystic fibrosis patient (Grenoble teaching hospital) in

overnight cultures in Luria-Bertani broth, at 37°C in air atmosphere and agitated at 300 rpm. Bacterial growth was monitored spectrophotometrically using a 600 nm absorbance (A_{600}). Liquid cultures of *P. aeruginosa* were supplemented with 300 µg/ml of carbenicillin. *P. aeruginosa* type III secretion properties were induced *in vivo* upon cell contact and *in vitro* upon calcium depletion by 5 mM EGTA in the presence of 20 mM $MgCl_2$ [Polack *et al.* 2000].

Plasmid constructions

Plasmids, containing respectively the ExoS-S100A8 and ExoS-S100A9 in frame fusion, were obtained by ligating the ExoS XbaI-SalI fragment and the S100A8 SalI-SphI or S100A9 SalI-SphI fragments in the XbaI-SphI-opened *E. coli-Pseudomonas* shuttle vector pUCP20, as previously described [Polack *et al.* 2000]. The ExoS clone that contained the coding sequence of N-terminal amino acids of ExoS and orf 1, its specific chaperone, was amplified by PCR, from the genomic DNA of the *P. aeruginosa* CHA strain [Polack *et al.*]. S100A8- and S100A9-SalI-SphI were obtained by reverse transcription PCR, using total RNA from fresh PMN; they were then verified by sequencing.

For the chimera fusion protein ExoS S100A8-A9 plasmid construction, a SalI-S100A8GGG-BamHI and a BamHI-GGGS100A9-SphI fragment were developed by PCR and ligated in a SalI-SphI pUCP20 ExoS opened plasmid. At the same time the ExoS S100A9-A8 plasmid was generated by ligation of SalI-S100A9GGG-BamHI and BamHI-GGGS100A8-SphI amplified fragments in the SalI-SpHI pUCP20 ExoS plasmid.

A S100A9-S100A8 SalI-NotI fragment was developed by PCR, using the previous ExoS-S100A9-A8 plasmid. It was attached in the SalI-NotI opened pGEX 5x2 *E. coli* protein production plasmid. Then, various forms of S100A9-A8, truncated at amino acid 90, 86, and 57 of S100A8, were also generated and cloned in frame with GST in the pGEX 5x2 plasmid, instead of the full length S100A9-A8 chimera protein.

The ExoS 17–S100A8 and ExoS 30-S100A8 fusion proteins were also produced in *E. coli,* using the pGEX 5x2 plasmid. We extracted in Xba-SalI the ExoS 54 DNA from the pUCP20 ExoS 54-S100A8 plasmid, and replaced it by ExoS 17 Xba-SalI or ExoS 30 Xba-SalI fragment developed by PCR. Then ExoS 17-S100A8 or ExoS 30-S100A8 BamHI-XhoI fragments, obtained by PCR, were ligated in the BamHI-XhoI pGEX 5x2 opened plasmid (*Table I)*.

Expression of recombinant ExoS-S100A8 and ExoS-S100A9 fusion proteins by *P. aeruginosa*

Plasmids pUCP20 (empty vector), pUCP20-ExoS (expressing the 54 N-terminal or the 129 N-terminal residues of ExoS), pUCP20-ExoS-S100A8 and pUCP20-ExoS-S100A9, and the chimera pUCP20-ExoS-S100A9-S100A8 or pUCP20-ExoS-S100A8-S100A9 were electroporated into CHA *P. aeruginosa* strains [Polack *et al.* 2000]. After overnight culture, bacteria suspended in Luria-Bertani medium were diluted to $OD_{600\ nm}$ = 0.2 in LB medium containing 300 µg/ml carbenicillin, and then cultured for 1 to 5 h. Secretion of recombinant proteins was induced by adding 5 mM EGTA when bacterial growth, evaluated by $OD_{600\ nm,}$ reached 0. 6. Culture medium was supplemented with 20

mM $MgCl_2$. After incubation at 37°C for 3 h, the induced culture suspensions were centrifuged at 12,000 x *g* for 15 min at 4°C. The secreted proteins were pelleted down overnight from the later

supernatant with 55% (w/v) diammonium sulphate. After 12,000g centrifugation (20min, 4°C) the pellet was resuspended in 6ml PBS and dialyzed overnight at 4°C. Proteins of the suspended pellet were fractionated by SDS-PAGE. S100A8 and S100A9 proteins were immunodetected using specific polyclonal antibodies after Western blotting.

Delivery of S100A8 or S100A9 in EBV-B lymphocytes by *P. aeruginosa* Type Three Secretion System (TTSS)

The induced bacteria and EBV-B lymphocytes were suspended in RPMI 1640 medium containing 10% (v/v) human AB serum. The B cells (8×10^7 cells/ml) were loaded onto the bacteria with a MOI of 10. Incubation at 37°C under mixing for 90 min allowed mutual adhesion. At the end of incubation, the mixture of bacteria and EBV-B lymphocytes was submitted to 300g centrifugation. After PBS washing, the recovered pellet containing EBV-B lymphocytes, 2×10^6 cells, was used to measure NADPH oxidase activity upon stimulation [Polack *et al.* 2000].

Expression of recombinant ExoS 17-S100A8, ExoS 30-S100A8, and S100A9-A8 truncated proteins in *E. coli.*

BL21(DE3) competent *E. coli* were transformed with pGEX 5x2 containing DNA encoding for ExoS 17-S100A8, ExoS 30-S100A8, and S100A9-truncated A8 chimera proteins [Paclet *et al.* 2007]. Bacteria growth, in LB medium supplemented by 100 µg/ml ampicillin at 37°C, was carried out from DO_{600nm} 0.2 to 1.5. The production of recombinant proteins was induced by IPTG 0. 2 mM overnight, at 16°C. GST fusion proteins were affinity purified on

glutathione-Sepharose. After washing in PBS, recombinant proteins were cleaved directly on the matrix, using XA factor in PBS, overnight at 4°C The matrix and soluble recombinant proteins were separated by filtration; recombinant proteins were stored at -20°C until further use.

Measurement of NADPH oxidase activity in EBV-B lymphocytes, using chemiluminescence

EBV-B-Lymphocytes (2 x 10^6) suspended in 50 µl PBS were added to 200 µl PBS containing 0. 9 mM $CaCl_2$, 0. 5 mM $MgCl_2$, 20 mM glucose, 20 µM luminol, and 10 U/ml horseradish peroxidase. Superoxide production was measured by chemiluminescence after adding 10 µl of a 2µg/ml PMA solution [Berthier *et al.* 2003]. Photon emission was recorded at 37°C for 1 h with a Luminoscan (Labsystem, Pontoise, France). Oxidase activity was expressed as RLU per 2 x 10^6 cells.

NADPH oxidase activity measurement in a cell-free assay with purified cytochrome b_{558}

Cytochrome b_{558} was purified from the plasma membranes of 10^{10} PMA stimulated neutrophils as previously reported [Paclet *et al.* 2000]. It was then quantified by reduced-minus-oxidized difference spectra using an absorption coefficient of 106 mM^{-1} cm^{-1}. Oxidase activity was reconstituted by incubating purified cytochrome b_{558} (0.2 pmoles) with cytosol isolated from EBV-B lymphocytes (300 µg) in the presence of 10 µM FAD, 40 µM GTPγS, 5 mM $MgCl_2$, and an optimal amount of arachidonic acid (80 – 100 nmol) in a final volume of 100 µl of PBS. In some experiments, the effect of a mixture of rS100A8 and rS100A9 and of recombinant ExoS-S100 fusion proteins was investigated after loading with 500nM $CaCl_2$ for 20min [Berthier *et al.* 2003]. The reaction was initiated by introducing 150 µM NADPH in the medium. Oxidase activity was estimated by measuring the reduction of cytochrome c in the absence or the presence of superoxide dismutase at 550 nm (ε_{550} = 21. 1 mM^{-1} cm^{-1}), and was expressed as turnover, mol of $O_2^{\cdot -}$. s^{-1}. mol of heme b^{-1} [Paclet *et al.* 2001].

Isolation of activated cytochrome b_{558}

Purified membranes from PMA stimulated neutrophils were used for extraction of cytochrome b_{558} in the presence of 2% (w/v) n-octyl glucoside followed by purification [Paclet *et al.* 2007]. Protein fractionation from soluble extract was performed onto anion exchange columns and then heparin agarose matrix; cytochrome b_{558} bound to the later matrix. At this stage Triton X100 was replaced by 40mM n-octyl glucoside added to the purification buffer. A mixture (1/1) of recombinant rS100A8 and rS100A9 preloaded with 500nM $CaCl_2$ or of the intact or truncated chimera S100A9-A8 (3mg), was applied to the

matrix after an extensive washing of the heparin matrix [Berthier *et al.* 2009]. Cytochrome b_{558} bound to the heparin agarose, was eluted using a NaCl gradient ranging from 0 to 0.5M. The presence of cytochrome b_{558} was detected by measuring the "reduced minus oxidized" differential spectrum and quantified at 426nm using a ε_{426} value of $106 mM^{-1}.cm^{-1}$. Fractions containing cytochrome b_{558} were pooled and filtrated on a Sephacryl S-300 column. A control experiment was carried out by using purified cytochrome b_{558} prepared from stimulated cells without S100 incubation. NADPH oxidase activity was measured in the presence of NADPH, but without any stimulation by arachidonic acid, and was expressed as turnover (s^{-1}) [Paclet *et al.* 2007].

Covalent cross-linking

A 25 mM Disuccinimidyl Suberate (DSS) solution was prepared shortly before use in DMSO. 10 pmol of purified relipidated cytochrome b_{558} or of 100 pmol of recombinant S100 proteins were cross-linked with DSS (0 to 2 mM) for 1h, at room temperature, in a preliminary experiment. The reaction was quenched by adding 10mM Tris, HCl pH 7.5, and mixed for 15 min. Protein samples cross-linked with DSS were incubated in a denaturating sample buffer containing SDS and 2.5% β-mercaptoethanol. They were separated by 12.5% SDS-PAGE and immunodetected by Western Blotting. S100A8/A9 were detected with rabbit polyclonal antibodies (material and methods). Cytochrome b_{558} was immunodetected by using rabbit polyclonal antibodies raised against

C-terminal peptides of $gp91^{phox}$ and (or) $p22^{phox}$ sequences, respectively [Batot *et al.* 1995]**.** Cytochrome b_{558} was cross-linked with 1.5 nmol of each S100 protein: S100 A9/A8 proteins were preincubated in a 500 nM $CaCl_2$ medium for 20 min before adding: first 10 pmol of cytochrome b_{558}, 10µM FAD, 40µM GTPγS, 5mM MgCl2, and then 0.8 mM arachidonic acid. After 10 min of incubation at room temperature, cross-linking started by adding 2mM DSS. After 1h of incubation at room temperature, the reaction was stopped by 10mM Tris, HCl pH 7.5. Fractionation of complexed proteins was performed by SDS-PAGE (7%) followed by Western Blotting using anti gp91 antibodies.

Confocal microscopy

Confocal microscopy was carried out as previously described [Baillet *et al.* 2011b; Campion *et al.* 2007].

Briefly, control EBV-B lymphocytes, *P. aeruginosa* incubated-EBV-B lymphocytes, and PMA-stimulated or unstimulated day 6-differentiated PLB 985 cells (2×10^5 cells in 50µl PBS) were coated onto a poly-L-lysine-coated round glass cover-slip, before fixing with 4%

(w/v) paraformaldehyde (10min/EBV- B lymphocytes; 20min/PLB985 cells). The cells were permeabilised with 0.1% (v/v) Triton X100 (1 min at room temperature) after extensive washing with PBS and quenching fluorescence of paraformaldehyde by 50mM NH_4Cl, and subsequently incubated (1h/EBV-B lymphocytes or 45min/PLB cells) with primary antibodies as follows: polyclonal or monoclonal antibodies were diluted in PBS containing 1% (w/v) BSA. Samples were incubated with:

-50µl (0. 2µg) of polyclonal goat anti-S100A8 antibodies or 50µl (1µg) of rabbit polyclonal purified anti-S100A8/A9 home made antibodies, followed by 1h incubation with 100µl (1: 250) of Alexa Fluor 488 donkey antigoat IgG or antirabbit IgG respectively.

-50µl (4µg) mouse monoclonal anti-$p22^{phox}$ Ig, (16G6: [Campion *et al.* 2009]), or anti $gp91^{phox}$ Ig (13B6: [Campion *et al.* 2007]), followed by 1h incubation with 100µl (1: 250) Alexa Fluor 546 anti mouse IgG.

Cell nuclei were stained with 40µl Hoechst 33258 (0.5µg). Colocalisation of S100A8/A9 with either $gp91^{phox}$ or $p22^{phox}$ was demonstrated by adding monoclonal antibodies (13B6 or 16G6) and rabbit S100A8/A9 antibodies (50µl) to the permeabilised cells of both mouse types, followed by incubation with a mixture of secondary antibodies (100µl: 1: 250). Fixed cells were imaged at room temperature using the inverted confocal and two-photon laser-scanning microscope (LSM 510 NLO, Carl Zeiss) equipped with a 40x/1. 3 Plan-Neofluar oil immersion lens [Baillet *et al.* 2011b].

SDS-PAGE and Western Blot

Proteins were fractionated by 7%, 11%, or 12.5% SDS-PAGE [Laemmli 1970] and electrotransferred to nitrocellulose [Towbin *et al.* 1979].Immunodetection was performed using rabbit polyclonal antibodies raised against either S100A8/A9 (IgG dilution, 1: 1000), or $gp91^{phox}$, or $p22^{phox}$ (serum dilution, 1/500). Immune complexes were detected with goat anti rabbit secondary antibody combined with peroxidase. Peroxidase activity was detected using ECL reagents.

Toxicity of the CHA strain assessment

Toxicity of the CHA strain was assessed by measuring lactate dehydrogenase activity in the medium: it started after 2.5h of contact with normal EBV-B lymphocytes [Dacheux *et al.* 2000]**.**

Statistical analysis

Data represents means ± SD. Student test was used to determine the statistical significance of results ($p<0.05$).

Results

Ex vivo S100 protein delivery by bacterial Type Three Secretion System.

The effect of S100A8 and S100A9 on NADPH oxidase activity previously observed *in vivo* as *in vitr*o [Berthier *et al.* 2003] was corroborated *ex vivo* by direct protein transfer to native EBV-B lymphocytes using TTSS of *P. aeruginosa* [Polack *et al.* 2000]. ExoS-S100A8 and ExoS-S100A9 chimera proteins were prepared by the fusion of the first 54 or the first 129 N-terminal amino acid residues of ExoS toxin sequence from *P. aeruginosa* with the N-terminal region of S100A8 or S100A9, or with the N-terminal region of S100A8 in the chimera S100A8-A9, or that of S100A9 of chimera S100A9-A8 **(table 1).** *P. aeruginosa* CHA strains encoding for ExoS fusion proteins, were grown in a calcium-depleted medium to induce secretion. After induction, the fusion proteins were identified in the extracellular medium of bacteria cultures by specific polyclonal antibodies raised against S100A8/A9 proteins: they have an apparent molecular mass of ~30-35kDa as shown by SDS-PAGE **(Fig 1 A).** No protein was visible in the bacteria pellet (not shown). There were no S100 fusion proteins in the extracellular medium of non-induced CHA. In the next experiment illustrated by **Fig 1 B**, CHA-S100A8 and CHA-S100A9 were used to deliver the hybrid fusion proteins into the cytosol of normal EBV-B lymphocytes. Superoxide production of PMA-stimulated EBV-B lymphocytes was measured by chemiluminescence, after contact with bacteria. When the CHA strain was transformed with the empty vector pUCP20 or CHA-ExsA- which does not have secretion capacity, EBV-B lymphocytes did not generate superoxide over the control value (not shown); but NADPH oxidase activity was increased upon delivery of ExoS129-S100A8 into normal EBV-B lymphocytes **(Fig 1B).** On the contrary, the release of ExoS-S100A9 had no effect on EBV-B cells oxidase activation, whereas injection of both ExoS-S100A8 and ExoS-S100A9 reversed the positive activation of oxidase mediated by ExoS-S100A8. To validate the results and to explain discordant observations obtained *in vivo* or *in vitro*, chimera fusion proteins, ExoS129-S100A8 and ExoS129-S100A9 on one side, and ExoS129-S100A8-A9 or ExoS129-S100A9-A8 on the other, were expressed from various plasmid constructions (**Table I**). A significant activation of NADPH oxidase was obtained with chimera ExoS129-S100A9-A8 delivery **(Fig 1B)** contrary to what was observed with ExoS129-S100A8-A9 (not shown). Similar results were obtained with ExoS54-S100 proteins. The efficiency of TTSS injection of chimera S100 A9-A8 proteins by *P. aeruginosa* to EBV-B lymphocytes was highlighted by confocal microscopy (**Fig 1C**). The data focused mainly

on a plasma membrane subcellular localization in EBV-B cells of the injected S100 fusion proteins.

Concentration dependence of ExoS-S100 fusion proteins on NADPH oxidase turnover

ExoS-S100A8 and ExoS-S100A9 were collected from the cultured medium of EGTA induced bacteria and were tested *in vitro* on NADPH oxidase activity in a cell-free assay. Purified cytochrome b_{558} was incubated with the cytosol of EBV-B lymphocytes containing $p67^{phox}$, $p47^{phox}$ $p40^{phox}$, and Rac 1/2 as activating factors but no S100 proteins **(Fig 2).** Adding calcium loaded ExoS129-S100A8 to the medium of cell-free assay, led to a specific enhancement of NADPH oxidase activity **(Fig 2A).** There were no effect of ExoS129-S100A9, or of the mixture 1/1 of ExoS129-S100A8 and ExoS129-S100A9.

A similar experiment with recombinant fusion proteins and purified cytochrome b_{558} was performed in the absence of lymphocyte cytosol but in the presence of GTPγS, $MgCl_2$, FAD, and NADPH. Oxidase activity was measured after adding an optimal amount of arachidonic acid and was expressed as oxidase turnover (s^{-1}). The addition of calcium loaded ExoS-S100A8 to the reconstitution medium led to a specific enhancement of NADPH oxidase activity as opposed to what was observed with rS100A8 prepared in *E. coli* (not shown), or with ExoS-S100A9 **(Fig S1A).** The enhancement of oxidase turnover is correlated to concentration of ExoS 54-S100A8 (with an optimum at 2µg) and of ExoS54-S100A9-A8 **(Fig 2C);** while both ExoS54-S100A9 **(FigS1B)** and ExoS54-S100A8-A9 had no effect.

These results suggested firstly a concentration dependence of ExoS-S100A8 fusion proteins on NADPH oxidase activity, secondly a specific interaction between the C-terminal region of S100A8 and cytochrome b_{558}, and thirdly a mandatory association of S100A8 with either S100A9 *in vivo* (stoichiometry 1/1) or with ExoS *in vitro*.

Minimal domain of ExoS required for secretion

ExoS is the main type III toxin of CHA strain and orf1 is necessary for its optimal secretion [Polack *et al.*]**.** Cytotoxicity was determined by the release of intra cellular lactate dehydrogenase (LDH) [Dacheux *et al.* 2000]**.** Type III secreted toxins are composed of various domains: we previously showed that the first 129 N-terminal amino-acid of ExoS allowed the secretion and intracellular injection of ExoS129-$p67^{phox}$ fusion protein [Polack *et al.* 2000].

ExoS fusion proteins were generated with the first 129, 54, 30, and 17 N-terminal amino-acids. Orf1, the putative chaperone, was included in all constructions in its original orientation, to increase secretion efficiency **(Table1).** The *P. aeruginosa* CHA strain harbouring plasmids encoding for ExoS-S100 fusion proteins was tested for its ability to secrete fusion proteins in the extracellular medium. The first 54 N-terminal amino-acids of ExoS correspond to the minimal domain required for an optimal secretion [Derouazi *et al.* 2008; Quenee *et al.* 2005]. There were no detectable ExoS-30 or Exo17-S100 fusion proteins in the supernatant fraction. On the contrary, fusion proteins with the 129 and 54 first N-terminal amino-acids of ExoS were highly secreted (not shown).

Furthermore, recombinant ExoS30-S100A8 and rExoS17-S100A8, rS100A8, and rS100A9 were generated in *E. coli,* as described in Material and Methods, and they were used for *in vitro* reconstitution experiments.

Cell-free assay was performed by incubating cytochrome $b_{558,}$ as previously reported, with the various recombinant proteins expressed from *P. Aeruginosa* and *E. coli*, respectively. The medium was complemented with GTPγS, MgCl2, FAD, and NADPH. NADPH oxidase activity was measured after arachidonic acid stimulation. An optimum oxidase turnover of ~$60s^{-1}$ was obtained with ExoS129-S100A8 as shown in **Fig2B**; it decreased according to secretion domain size. A similar effect was also observed with chimera ExoS54-S100A9-A8. But there was no activation when the fusion protein was prepared with S100A9, or with ExoS30, or ExoS17. It is interestingly to note an absence of activation observed with rS100A8 alone (not shown), while the association of rS100A8 plus rS100A9 gave a similar oxidase activation to the one obtained with ExoS129-S100A8.

The results confirmed that S100A9 was not involved directly in the intracellular activation of NADPH oxidase. But they also suggested that activation of NADPH oxidase, required an active conformation of S100A8 *in vivo,* either by association with S100A9 in the presence of calcium, or *in vitro* by using a fusion protein with the first 54 or 129 N-terminal amino-acid residues of *P. aeruginosa* ExoS toxin.

Size dependence of NADPH oxidase activation with chimera rS100A9-truncated (Δ) S100A8 proteins

We demonstrated **(1)** *in vivo*, after transfection of the genes encoding *S100A8/A9* [Berthier *et al.* 2003], **(2)** *ex vivo* after injection of ExoS129/54-S100A8 by *P. Aeruginosa* to EBV B-lymphocytes, and **(3)** *in vitro* (cell-free assay) by using recombinant ExoS129/54-S100A8 or

rS100A8/rS100A9, that S100A8 was a positive effector of NADPH oxidase (NOX2) activation. The S100A8 size dependence of NADPH oxidase was investigated. Since S100A9 is necessary *in vivo*, we expressed recombinant chimera S100A9- S100A8 (S100A9-A8) truncated at 57, 86, or 90 amino-acid residues of S100A8 sequence. They were generated as GST fusion proteins in *E. coli* (Material and Methods) (**Fig 3A).** They were analysed by 11% SDS-PAGE and Western Blot (not shown). Intact full length S100A8 includes 93 amino acid residues. Full length recombinant chimera, and rS100A9-Δ90, Δ86, and Δ57 S100A8 chimera were incubated (1μg each) after calcium loading, with purified cytochrome b_{558}, in the presence of GTPγS, $MgCl_2$, and FAD. NADPH oxidase activity was measured after adding NADPH upon arachidonic acid stimulation, and was expressed as turnover (s^{-1}). The results illustrate a S100A8 size dependence of NADPH oxidase activation (**Fig3B).** There were no effects of rS100A9-Δ86A8. This data supports the importance of a short sequence between S100A9-Δ90A8 and S100A9-Δ86A8 for oxidase activation; this sequence was previously shown to be specific for Zinc binding [Korndorfer *et al.* 2007]**.**

Preloading of S100 proteins was carried out with calcium or zinc to evaluate a putative role of zinc in mediating NADPH oxidase activation. The chimera rS100A9-A8, preloaded with 20 μM $CaCl_2$, enhanced oxidase activity (**Fig3C).** But there was no activation when 20μM $ZnCl_2$ was added instead of calcium, and when both Zn^{++} or Ca^{++} were used independently as controls, without S100 proteins. The results confirmed that without calcium, rS100A9-A8 was inactive in the oxidase activation process as reported *in vivo* for the complex S100A8/A9. A dose-effect relationship of preloading with calcium or zinc was performed: a concentration of 500 nM calcium was shown to be sufficient as opposed to zinc that had no effect on activation, whatever the concentration used. Moreover, adding both calcium and zinc (1/1) or vice/versa, inhibited the effect of calcium, suggesting a specific effect of calcium on S100A8 mediated NADPH oxidase activation.

Cross-linking of cytochrome b_{558} with chimera S100A9-A8.

The possible interaction of chimera S100A9-A8 with cytochrome b_{558} was shown after DSS cross-linking **(Fig4).** A mixture of rS100A8 and rS100A9 (prepared in *E. coli*), preloaded with calcium, was used to determine the optimum concentration of DSS for cross-linking **(Fig4A left panel).** A similar experiment was performed with relipidated cytochrome b_{558} (**Fig4A right panel**). Cytochrome b_{558} (10 pmol) was shown to cross-link with a mixture of calcium preloaded S100A8 and S100A9, in the presence of 2mM DSS (**Fig4 B, lane 3**). A

similar experiment was performed with chimera S100A9-full length A8 (**Fig4 B, lane 4**), and chimera S100A9-Δ90 (lane 5), Δ86 (lane 6), or Δ57 (lane 7) A8. As shown on (**Fig4 B, lane 5**) cross-linking proceeds only with chimera rS100A9-Δ90 A8 compared to chimera rS100A9-full length A8 **(Fig4B lane 4),** and to control **(Fig4B lane 3).**

The results suggested a specific interaction of the C-terminal S100A8 sequence in chimera rS100A9-A8 with cytochrome b_{558}, as previously reported in the cell-free assay (**Fig1C and 2C**).

Size dependence of cytochrome b_{558} activation, and of constitutive NADPH oxidase activity with chimera rS100A9- truncated Δ A8.

We previously isolated a functional phagocyte oxidase complex on an affinity matrix, [Paclet *et al.* 2007]. Surprisingly, NADPH oxidase was constitutively active, suggesting that cytochrome b_{558} assembled with cytosolic activating factors on the matrix. A mixture of rS100A8 and rS100A9, preincubated with calcium, was also shown, to directly activate cytochrome b_{558} instead of cytosolic factors. The results suggested that cytochrome b_{558}, bound to the matrix, changed the conformation after adding either cytosolic factors or rS100A9/A8, and became active [Paclet *et al.* 2007; Paclet *et al.* 2000]. A similar experiment was carried out with chimera rS100A9-ΔA8 to confirm that the C-terminal sequence of S100A8 was directly involved in the interaction with cytochrome b_{558}. The results (**Fig 5)** were that rS100A9-FLA8 activated cytochrome b_{558} with a turnover of ~20s^{-1}, in the same range as previously reported. Moreover, NADPH oxidase activity was constitutive suggesting an active conformation of cytochrome b_{558}. The experiment performed with chimera rS100A9-Δ A8, revealed a size dependence of S100A8 on the constitutive oxidase activity and that only chimera rS100A9-Δ90A8 activated cytochrome b_{558}, whereas rS100A9-Δ86 A8 and rS100A9-Δ57 A8 did not (**Figure 5B, C, and D)**. All this data suggested that the C-terminal sequence of S100A8, in between 86 and 90 amino-acid residues, was necessary for the activation and specific interaction with the hemoprotein.

Colocalisation of S100A8/A9 and cytochrome b_{558} in PLB985

PLB985 cells were used to investigate by confocal microscopy, the subcellular localization of endogenous S100A8/A9 proteins. Fixed unstimulated and PMA stimulated PLB985 cells (6 days of differentiation) were permeabilised with 0.1% Triton X100 and incubated, first with mouse monoclonal anti gp91phox antibodies or anti p22phox antibodies, and then with rabbit

S100A8/A9 polyclonal antibodies. S100A8/A9 partitioned at rest (left) between cytosol and plasma membrane, while after stimulation of PLB985 cells with PMA (right), S100A8/A9 translocated to the plasma membrane, colocalized with cytochrome b_{558} (gp91^{phox}/NOX2 and p22^{phox}) (**Fig 6)**. NADPH oxidase was active in stimulated PLB985 cells: the oxidase complex assembled at the plasma membrane level where S100A8/A9 colocalized, suggesting a putative interaction of S100 proteins with active cytochrome b_{558} as opposed to what observed in resting cells.

Discussion

We previously demonstrated, through *in vitro* and *ex vivo* approaches, that two proteins of S100 family, S100A8 and S100A9 highly expressed in myeloid cells and mainly in neutrophils, promote NADPH oxidase activation [Berthier *et al.* 2009; Berthier *et al.* 2003; Paclet *et al.* 2007]**.** Our results strongly suggest a specific interaction of S100A8 with cytochrome $b_{558,}$ the redox component of NADPH oxidase. In the process, S100A8 is introduced first as a positive effector of NADPH oxidase regulation and second as one of the main limiting components of activity.

S100A8 and S100A9 are EF-hand molecules that need calcium to be active. It is well established that calcium binding leads to conformation changes of S100 proteins that become capable of binding other proteins [Streicher *et al.* 2010]. Cell calcium concentration is an important determinant for the biologic relevance of S100 proteins oligomerisation. In the presence of calcium, S100A8/A9 proteins associate to calprotectin, the structure of which was recently described [Korndorfer *et al.* 2007]. Two different putative zinc binding sites emerge at the S100A8/A9 subunit interface that may explain the well-known Zn^{++} binding activity of calprotectin, the over expression of which can cause a strong deregulation of zinc homeostasis and an apparent inhibition of matrix metalloproteinases (MMPs).
We observed that, contrary to S100A8/A9 loaded with calcium, S100A8/A9 do not activate NADPH oxidase after loading with zinc. Zinc is directly involved in the proteolysis activity mediated by matrix metalloproteinases [Jagnandan *et al.* 2007]. Deletion of the S100A8 zinc-binding-site should decrease metalloproteinase activity and impair interaction of S100A8 with cytochrome b_{558} and S100A8/A9 mediated oxidase activation.

After inflammatory stimuli, the transitory elevation of calcium in neutrophils initiates reaction cascades beginning in cytosol with phosphorylation of cytosolic activating factors, mainly $p47^{phox}$ and $p67^{phox}$, and also phosphorylation of S100A9 [Berthier *et al.* 2003]**.** It was suggested that phosphorylation could enhance S100A9 affinity for calcium; therefore it could improve the Ca^{++} loading of S100A8/A9 and its translocation to plasma membrane [Schenten *et al.* 2010]**.** But the calcium source leading to its mobilization has not been formally identified. Recently, the activity of NOX5 was reported to be regulated in a Ca^{++} dependent manner. Phosphorylation of NOX5 by PKC and calmodulin, another S100 protein, increase

the sensitivity of NOX5 to intracellular calcium [Tirone *et al.* 2010]**.** This data suggests that, in the NOX family, calcium combined to phosphorylation of the NOX or of partners, are protagonists of NADPH oxidase activation.

S100A8/A9 are an intracellular reservoir for arachidonic acid in neutrophils [Sopalla *et al.* 2002]. A conformation change in the tertiary structure of S100A8/A9, caused by an interaction with arachidonic acid, may facilitate its binding to membrane or extracellular surfaces [Berthier *et al.* 2003]. At the membrane level, S100 proteins, bound to arachidonic acid, raise its local concentration and facilitate interaction with cytochrome b_{558}. Thus, in the oxidase complex assembly, partners are stabilized not only by negative charges, but also via arachidonic acid and S100A8/A9 proteins. NADPH oxidase is activated both *in vitro* (cell free assay) or *in vivo* [Doussière *et al.* 1996; Foubert *et al.* 2002] by arachidonic acid; but the whole oxidase complex can also be isolated in a S100A8/A9 mediated active state that is constitutive, suggesting that S100A8/A9 were able to activate the hemoprotein on the matrix, in the absence of arachidonic acid. A siRNA strategy supported the hypothesis that inducible phospholipase A2 controlled S100A8/A9 complex translocation and NOX2 activity [Schenten *et al.* 2010]**.**

Interaction of S100A8/A9 with cytochrome b_{558} was illustrated by Atomic Force Microscopy [Berthier *et al.* 2003] and by the indirect activation of oxidase complex [Paclet *et al.* 2007]**.** We demonstrated a visible interface by DSS cross-linking of partners and colocalisation of endogenous S100A8/A9 with cytochrome b_{558} subunits, in PMA stimulated PLB 985 cells. But it was not possible to recover S100A8/A9 in the isolated active oxidase complex or after immune-precipitation suggesting a transient interaction mechanism of both partners.

Pseudomonas aeruginosa is an opportunistic bacterium; one of its major toxins, ExoS, is translocated into EBV-B lymphocytes through a type III secretion pathway [Polack *et al.* 2000]**.** This original procedure of a strategic protein injection into a target cell, allowed discriminating between S100A8 or S100A9, the main effector of NADPH oxidase activation. As *in vivo* with S100A8/A9, the *ex vivo* delivery of ExoS129- S100A8 fusion protein activated NADPH oxidase of EBV-B lymphocytes.

The results were confirmed *in vitro*; we used TTSS with *P. aeruginosa* grown in calcium-depleted conditions, to secrete recombinant fusion proteins constructed with both the N

terminal ExoS toxin combined with the orf chaperone and S100A8 or S100A9, in the bacterial growth medium [Derouazi *et al.* 2008]**.** We demonstrated that the first 129 and 54 N-terminal amino acid residues of ExoS were the optimized N-terminal domain required for the secretion of fusion protein. Rucks and Olson [Rucks *et al.* 2005], reported that the N-terminal region of ExoS included a GTPase activating GAP domain. The smallest GAP exoS domain described is composed of the N-terminal 130 amino acid residues [Wurtele *et al.* 2001]**.** We confirmed that, *in vitro,* ExoS129-S100A8 and ExoS54-S100A8 had a similar activating effect on NADPH oxidase activity, while the helix involved in GAP activity was only present in the ExoS129 domain, and not at all in the ExoS54 domain. The data excludes any involvement of GAP activity in ExoS-S100A8 oxidase activation.

In conclusion, we showed that:

1. S100A8 was critical and specifically involved in NADPH oxidase activation as an allosteric effector of regulation; its native conformation, in the absence of S100A9, was inactive contrary to that of calcium mediated oligomeric, (dimer or tetramer) structure of S100A8/A9 protein complex.

2. The high affinity of S100A8/A9 interaction could stabilize *in vivo*, the active conformation of S100A8 and facilitate the translocation of S100A8/A9 to plasma membrane; at this level, stabilization of the assembled oxidase complex is favoured by phosphorylation of both cytosolic factors and S100A9. The flexible ExoS of ExoS-S100A8 fusion protein could have a similar stabilizing conformation effect. Moreover, GST-S100A8 had a similar effect without adding S100A9, suggesting a mandatory 3D structure conformation for S100A8 (not shown). Furthermore, the tertiary structure of the critical S100A8 domain involved in oxidase activation is probably the same in the calcium-loaded ExoS-S100A8 and in the S100A8/A9 complex. In the activation process, ExoS acted as a molecular "messenger" for protein delivery; it permitted not only a functional targeting of a delivery protein to its site of action, but also a specific interaction of the injected protein with its partner.

3. S100A8 is the privileged partner of cytochrome b_{558}: it can promote inducible and constitutive NADPH oxidase function, either *in vivo* in combination with S100A9, or *ex vivo* as a fusion protein with the first 129 or 54 N-terminal ExoS toxin residues. The zinc-binding site of S100A8 is directly involved in this interaction. 4 amino acid residues HEES are required; they are believed to be critical for both interaction with cytochrome b_{558} and oxidase

activation. Further studies are needed to determine the corresponding consensus site on the hemoprotein and to address allosteric mechanisms of NADPH oxidase activation.

ACKNOWLEDGEMENTS

This study was supported by grants from the "Ministère de l'Enseignement Supérieur de la Recherche et Technologie, Paris", the "UFR de Médecine, Université Joseph Fourier, Grenoble", the "Région Rhône-Alpes, programme Emergence 2003 and ARCUS France/Chine 2007-2008", the CGD research Trust 2006-2007, UK, the "Groupement des Entreprises Françaises dans la lutte contre le Cancer, délégation de Grenoble", the "Société Française de Rhumatologie" and the "Délégation à la Recherche Clinique et à l'Innovation, Centre Hospitalier Universitaire, Grenoble"

The authors thank Dr Alexeï Grichine for his support in confocal microscopy experiments and Dr Frank Fieschi for his critical comments regarding the participation of ExoS toxin and S100 proteins in oxidase activation as well as his collaboration for other experimental approaches. The authors also thank Dr Pierre-Emmanuel Colle for copy-editing the article.

.

References

1 Roth, J., Vogl, T., Sorg, C. and Sunderkotter, C. (2003) Phagocyte-specific S100 proteins: a novel group of proinflammatory molecules. Trends Immunol. **24**, 155-158

2 Berthier, S., Paclet, M. H., Lerouge, S., Roux, F., Vergnaud, S., Coleman, A. W. and Morel, F. (2003) Changing the conformation state of cytochrome b_{558} initiates NADPH oxidase activation: MRP8/MRP14 regulation. J. Biol. Chem. **278**, 25499-25508

3 Benedyk, M., Sopalla, C., Nacken, W., Bode, G., Melkonyan, H., Banfi, B. and Kerkhoff, C. (2007) HaCaT keratinocytes overexpressing the S100 proteins S100A8 and S100A9 show increased NADPH oxidase and NF-kappaB activities. J. Invest. Dermatol. **127**, 2001-2011

4 Voss, A., Bode, G., Sopalla, C., Benedyk, M., Varga, G., Bohm, M., Nacken, W. and Kerkhoff, C. (2011) Expression of S100A8/A9 in HaCaT keratinocytes alters the rate of cell proliferation and differentiation. FEBS Lett. **585**, 440-446

5 Kerkhoff, C., Klempt, M., Kaever, V. and Sorg, C. (1999) The two calcium-binding proteins, S100A8 and S100A9, are involved in the metabolism of arachidonic acid in human neutrophils. J. Biol. Chem. **274**, 32672-32679

6 Korndorfer, I. P., Brueckner, F. and Skerra, A. (2007) The crystal structure of the human (S100A8/S100A9)2 heterotetramer, calprotectin, illustrates how conformational changes of interacting alpha-helices can determine specific association of two EF-hand proteins. J. Mol. Biol. **370**, 887-898

7 Berthier, S., Baillet, A., Paclet, M. H., Gaudin, P. and Morel, F. (2009) How important are S100A8/S100A9 calcium binding proteins for the activation of phagocyte NADPH oxidase, Nox2. AIAAMC. **8**, 282-284

8 Kerkhoff, C., Nacken, W., Benedyk, M., Dagher, M. C., Sopalla, C. and Doussiere, J. (2005) The arachidonic acid-binding protein S100A8/A9 promotes NADPH oxidase activation by interaction with p67phox and Rac-2. FASEB J. **19**, 467-469

9 Doussiere, J., Bouzidi, F. and Vignais, P. V. (2002) The S100A8/A9 protein as a partner for the cytosolic factors of NADPH oxidase activation in neutrophils. Eur. J. Biochem. **269**, 3246-3255

10 Roth, J., Burwinkel, F., van den Bos, C., Goebeler, M., Vollmer, E. and Sorg, C. (1993) MRP8 and MRP14, S-100-like proteins associated with myeloid differentiation, are translocated to plasma membrane and intermediate filaments in a calcium-dependent manner. Blood. **82**, 1875-1883

11 Schenten, V., Brechard, S., Plancon, S., Melchior, C., Frippiat, J. P. and Tschirhart, E. J. (2010) iPLA2, a novel determinant in Ca2+- and phosphorylation-dependent S100A8/A9 regulated NOX2 activity. Biochim. Biophys. Acta. **1803**, 840-847

12 Schenten, V., Melchior, C., Steinckwich, N., Tschirhart, E. J. and Brechard, S. (2011) Sphingosine kinases regulate NOX2 activity via p38 MAPK-dependent translocation of S100A8/A9. J. Leukoc. Biol. **89**, 587-596

13 Gebhardt, C., Nemeth, J., Angel, P. and Hess, J. (2006) S100A8 and S100A9 in inflammation and cancer. Biochem. Pharmacol. **72**, 1622-1631
14 Baillet, A., Trocme, C., Berthier, S., Arlotto, M., Grange, L., Chenau, J., Quetant, S., Seve, M., Berger, F., Juvin, R., Morel, F. and Gaudin, P. (2010) Synovial fluid proteomic fingerprint: S100A8, S100A9 and S100A12 proteins discriminate rheumatoid arthritis from other inflammatory joint diseases. Rheumatology (Oxford). **49**, 671-682
15 Nicolas, E., Ramus, C., Berthier, S., Arlotto, M., Bouamrani, A., Lefebvre, C., Morel, F., Garin, J., Ifrah, N., Berger, F., Cahn, J. Y. and Mossuz, P. (2011) Expression of S100A8 in leukemic cells predicts poor survival in de novo AML patients. Leukemia. **25**, 57-65
16 Foell, D., Wittkowski, H., Vogl, T. and Roth, J. (2007) S100 proteins expressed in phagocytes: a novel group of damage-associated molecular pattern molecules. J. Leukoc. Biol. **81**, 28-37
17 Lim, S. Y., Raftery, M. J., Goyette, J., Hsu, K. and Geczy, C. L. (2009) Oxidative modifications of S100 proteins: functional regulation by redox. J. Leukoc. Biol. **86**, 577-587
18 Bedard, K. and Krause, K. H. (2007) The NOX family of ROS-generating NADPH oxidases: physiology and pathophysiology. Physiol. Rev. **87**, 245-313
19 Morel, F. (2007) Molecular aspects of chronic granulomatous disease. "the NADPH oxidase complex". Bull. Acad. Natl. Med. **191**, 377-392
20 Vignais, P. V. (2002) The superoxide-generating NADPH oxidase: structural aspects and activation mechanism. Cell Mol. Life Sci. **59**, 1428-1459
21 Paclet, M. H., Coleman, A. W., Vergnaud, S. and Morel, F. (2000) P67-phox-mediated NADPH oxidase assembly: imaging of cytochrome b_{558} liposomes by atomic force microscopy. Biochemistry. **39**, 9302-9310
22 Paclet, M. H., Coleman, A. W., Burritt, J. and Morel, F. (2001) NADPH oxidase of Epstein-Barr-virus immortalized B lymphocytes. Effect of cytochrome b_{558} glycosylation. Eur. J. Biochem. **268**, 5197-5208
23 Batot, G., Martel, C., Capdeville, N., Wientjes, F. and Morel, F. (1995) Characterization of neutrophil NADPH oxidase activity reconstituted in a cell-free assay using specific monoclonal antibodies raised against cytochrome b558. Eur. J. Biochem. **234**, 208-215
24 Baillet, A., Xu, R., Grichine, A., Berthier, S., Morel, F. and Paclet, M. H. (2011) Coupling of 6-phosphogluconate dehydrogenase with NADPH oxidase in neutrophils: Nox2 activity regulation by NADPH availability. FASEB J. **25**, 2333-2343
25 Polack, B., Vergnaud, S., Paclet, M. H., Lamotte, D., Toussaint, B. and Morel, F. (2000) Protein delivery by Pseudomonas type III secretion system: Ex vivo complementation of p67(phox)-deficient chronic granulomatous disease. Biochem. Biophys. Res. Commun. **275**, 854-858
26 Polack, B., Toussaint, B., Quénée, L. and inventors. Outil de transfert et de production de protéines mettant en oeuvre le système de sécrétion de type III de Pseudomonas. Patent WO2005049644.
27 Paclet, M. H., Berthier, S., Kuhn, L., Garin, J. and Morel, F. (2007) Regulation of phagocyte NADPH oxidase activity: identification of two cytochrome b558 activation states. FASEB J. **21**, 1244-1255
28 Campion, Y., Paclet, M. H., Jesaitis, A. J., Marques, B., Grichine, A., Berthier, S., Lenormand, J. L., Lardy, B., Stasia, M. J. and Morel, F. (2007) New insights into the membrane topology of the phagocyte NADPH oxidase: characterization of an anti-gp91-phox conformational monoclonal antibody. Biochimie. **89**, 1145-1158
29 Campion, Y., Jesaitis, A. J., Nguyen, M. V., Grichine, A., Herenger, Y., Baillet, A., Berthier, S., Morel, F. and Paclet, M. H. (2009) New p22-phox monoclonal antibodies: identification of a conformational probe for cytochrome b 558. J. Innate Immun. **1**, 556-569

30 Laemmli, U. K. (1970) Cleavage of structural proteins during the assembly of the head of bacteriophage T4. Nature. **227**, 680-685
31 Towbin, H., Staehelin, T. and Gordon, J. (1979) Electrophoretic transfer of proteins from polyacrylamide gels to nitrocellulose sheets: procedure and some applications. Proc. Natl. Acad. Sci. U.S.A. **76**, 4350-4354
32 Dacheux, D., Toussaint, B., Richard, M., Brochier, G., Croize, J. and Attree, I. (2000) Pseudomonas aeruginosa cystic fibrosis isolates induce rapid, type III secretion-dependent, but ExoU-independent, oncosis of macrophages and polymorphonuclear neutrophils. Infect. Immun. **68**, 2916-2924
33 Quenee, L., Lamotte, D. and Polack, B. (2005) Combined sacB-based negative selection and cre-lox antibiotic marker recycling for efficient gene deletion in pseudomonas aeruginosa. Biotechniques. **38**, 63-67
34 Derouazi, M., Toussaint, B., Quenee, L., Epaulard, O., Guillaume, M., Marlu, R. and Polack, B. (2008) High-yield production of secreted active proteins by the Pseudomonas aeruginosa type III secretion system. Appl. Environ. Microbiol. **74**, 3601-3604
35 Streicher, W. W., Lopez, M. M. and Makhatadze, G. I. (2010) Modulation of quaternary structure of S100 proteins by calcium ions. Biophys. Chem. **151**, 181-186
36 Jagnandan, D., Church, J. E., Banfi, B., Stuehr, D. J., Marrero, M. B. and Fulton, D. J. (2007) Novel mechanism of activation of NADPH oxidase 5. Calcium sensitization via phosphorylation. J. Biol. Chem. **282**, 6494-6507
37 Tirone, F., Radu, L., Craescu, C. T. and Cox, J. A. (2010) Identification of the binding site for the regulatory calcium-binding domain in the catalytic domain of NOX5. Biochemistry. **49**, 761-771
38 Sopalla, C., Leukert, N., Sorg, C. and Kerkhoff, C. (2002) Evidence for the involvement of the unique C-tail of S100A9 in the binding of arachidonic acid to the heterocomplex S100A8/A9. Biol. Chem. **383**, 1895-1905
39 Foubert, T. R., Burritt, J. B., Taylor, R. M. and Jesaitis, A. J. (2002) Structural changes are induced in human neutrophil cytochrome b by NADPH oxidase activators, LDS, SDS, and arachidonate: intermolecular resonance energy transfer between trisulfopyrenyl-wheat germ agglutinin and cytochrome b_{558}. Biochim. Biophys. Acta. **1567**, 221-231
40 Doussiere, J., Gaillard, J. and Vignais, P. V. (1996) Electron transfer across the O2-generating flavocytochrome b of neutrophils. Evidence for a transition from a low-spin state to a high-spin state of the heme iron component. Biochemistry. **35**, 13400-13410
41 Rucks, E. A. and Olson, J. C. (2005) Characterization of an ExoS Type III translocation-resistant cell line. Infect. Immun. **73**, 638-643
42 Wurtele, M., Wolf, E., Pederson, K. J., Buchwald, G., Ahmadian, M. R., Barbieri, J. T. and Wittinghofer, A. (2001) How the Pseudomonas aeruginosa ExoS toxin downregulates Rac. Nat. Struct. Biol. **8**, 23-26

Legends of figures

Figure 1. *Injection by Pseudomonas aeruginosa Type Three Secretion System (TTSS) of ExoS-S100 proteins in EBV-B Lymphocytes. Measurements of NADPH oxidase activity in injected intact cells and detection of injected ExoS-S100 proteins in EBV-B Lymphocytes by confocal microscopy.*

A- Production of ExoS129-S100A8 and ExoS129-S100A9 by *Pseudomonas aeruginosa*. Secretion medium of induced *Pseudomonas aeruginosa* was analysed by Western blot after SDS-PAGE. ExoS129 S100A8 and ExoS129 S100A9 were detected with rabbit polyclonal antibodies raised against S100A8 and S100A9 as described in Material and Methods.

B- CHA strains were transfected with pUCP20 (empty vector), or pUCP20-ExoS129-S100A8, pUCP20-ExoS129-S100A9, or the chimera pUCP20-ExoS129-S100A9-A8. TTSS properties were induced by contact between CHA strains and EBV-B lymphocytes in the presence of 10% v/v human AB serum (RPMI 1640 medium, MOI 10). In some experiments, the two fusion proteins, ExoS 129-S100A8 from CHA S100A8 MOI 5, and ExoS 129-S100A9 from CHA S100A9 MOI 5, were concomitantly injected in EBV-LB. NADPH oxidase activity of $2x10^6$ EBV-B lymphocytes, collected after injection of fusion proteins by TTSS, was measured by chemiluminescence after 30 min of incubation at 37°C, after stimulation by 80ng/ml PMA. Activity was expressed as RLU.
Number of experiments n = 3 to 5.

C- EBV-B lymphocytes control or **D-** EBV-B lymphocytes after ExoS 54-S100A9-A8 injection by *P. aeruginosa* were fixed, permeabilised, and labelled with goat anti human S100A8 antibodies for analysis by confocal microscopy, as described in Materials and Methods. An Alexa Fluor 488 anti goat antibody was used to detect the fusion protein, stained in green, in cells where ExoS 54-S100A9-A8 was present. EBV-BL nuclei were stained in blue with Hoechst 33258.

Figure 2. *Effect of recombinant S100 proteins secreted by induced P. aeruginosa on NADPH oxidase activity measured in a cell-free assay.*

A- Recombinant S100 proteins secreted by induced (EGTA, 5mM) *P. aeruginosa* were precipitated from the extracellular medium by 55% (w/v) ammonium sulphate, overnight at 4°C. Recombinant ExoS fusion proteins were used in a cell free assay as follows: 0.2 pmol of

cytochrome b_{558} purified from neutrophils was incubated with 300 µg EBV-B lymphocytes cytosol in the presence of 10 µM FAD, 40 µM GTPγS, 5mM $MgCl_2$, and an optimal amount of arachidonic acid (~1 mM) in 100µl PBS. ExoS-S100 fusion proteins (2.4 µg ExoS129-S100A8 and 3.75 µg ExoS129-S100A9 or ExoS alone) were preincubated first in 500nM $CaCl_2$ 20 min; then, purified and relipidated cytochrome b_{558} was added followed by cytosol and other reagents. Superoxide production was estimated by measuring the reduction of cytochrome *c* in the presence or absence of superoxide dismutase at 550 nm. The activity was expressed as oxidase turnover (s^{-1})

Number of experiments n=6

B- Size dependence of ExoS on S100A8 mediated NADPH oxidase activity.

ExoS129-S100A8, ExoS129-S100A9, ExoS54-S100A8, ExoS54-S100A9 fusion proteins were purified from induced *P. aeruginosa* (culture medium) as previously described. ExoS30-S100A8 and ExoS17- S100A8 were expressed in *E. coli* after IPTG induction as GST-fusion proteins by using a pGEX 5x2 vector. Recombinant S100A8 and rS100A9 were obtained in *E. coli,* in the same way. Calcium loaded recombinant S100 fusion proteins were used at the following concentrations: ExoS129-S100A8 (2.4µg), ExoS129-S100A9 (3.75 µg), ExoS54-S100A8 (5µg), ExoS54-S100 A9 (5µg), ExoS30-S100A8 (0.7µg), ExoS17-S100A8 (0.8µg), rS100A8 plus rS100A9 (0.78µg 1/1). NADPH oxidase was reconstituted in a cell-free assay as reported in Material and Methods. Oxidase activity was expressed as oxidase turnover (s^{-1}).

Number of experiments n=6

C- Effect of chimera ExoS54-S100A8-A9 and ExoS54-S100A9-A8.

Various concentrations of ExoS54-S100A8-A9 and ExoS54-S100A9-A8 were incubated with purified cytochrome b_{558} after 500nM $CaCl_2$ pre-incubation, as described previously in Material and Methods.

NADPH oxidase activity was expressed as turnover (s^{-1}).

Number of experiments n=6.

Figure 3. *Effect of S100A9-A8 chimera on NADPH oxidase activity in the presence (or not) of* Ca^{++} *and (or)* Zn^{++}.

A- C Terminal sequence of full length and truncated S100A8. The four chimera S100A9-full length S100A8 named S100A9-A8, S100A9-truncated S100A8 named S100A9-Δ90A8, S100A9-Δ86A8, S100A9-Δ57A8 were expressed in *E. coli* as described in Material and Methods.

B-The effect of chimera S100A9-full length or truncated A8 (1μg), preloaded with 500 nM $CaCl_2$ for 20 min, were tested on NADPH oxidase activity in a cell free assay as described in Material and Methods. After adding 0.2 pmoles cytochrome b_{558}, 10μM FAD, 40μM GTPγS, and 5mM $MgCl_2$, the medium was incubated in the presence of an optimal amount (80-100nmol) of arachidonic acid. Superoxide production was measured after adding 150μM NADPH. NADPH oxidase activity was expressed as turnover (s^{-1}).

Number of experiments N= 6.

C- Effect of zinc on calcium loaded S100A9-A8 mediated NADPH oxidase activation. NADPH oxidase activity was measured as previously described (Fig3B) in a cell-free assay with purified cytochrome b_{558}, in the presence (or not) of recombinant chimera S100A9-A8 pre-incubated with either 20 μM Zinc, or 20 μM $CaCl_2$, or both (calcium plus zinc or zinc plus calcium).

NADPH oxidase activity was expressed as turnover (s^{-1}).

Number of experiments n=6.

Figure 4- *Disuccinimidyl suberate (DSS) complex formation between cytochrome b_{558} and recombinant S100A8 and S100A9 proteins*.

A-**left panel**. Determination of the DSS concentration necessary to cross-link cytochrome b_{558} and S100 proteins. 100 pmol of rS100A8 and 100 pmol of rS100A9 were pre-incubated with 500nM $CaCl_2$ for 20min, before adding 0 to 2mM DSS freshly prepared in DMSO. After 1h incubation at room temperature, proteins were separated by 12.5% SDS-PAGE and electro-transferred on a nitrocellulose matrix. Immune complexes were detected by using rabbit polyclonal antibodies raised against S100A8/S100A9. **Right panel**. A similar experiment was performed with 10pmol purified cytochrome b_{558}. Specific staining was obtained with rabbit specific polyclonal antibodies raised against C terminal peptides of $gp91^{phox}$ and $p22^{phox}$ sequences [Batot *et al.* 1995]**.**

B-Cross-linking of rS100A8(1. 5nmol) and rS100A9(1. 5nmol) with cytochrome b_{558} (10 pmol) in the presence of 2mM DSS.

1. Cytochrome b_{558} alone; **2.** Cytochrome b_{558} plus DSS; **3**. Cytochrome b_{558} plus rS100A8 and rS100A9, plus DSS; **4.** Cytochrome b_{558} plus chimera S100A9-93(FL)A8 and DSS; cytochrome b_{558} plus DSS and **5.** Chimera S100A9-Δ90A8 **6.** Chimera S100A9-Δ86A8; **7.**

Chimera S100A9-Δ57A8. Complexed proteins were fractionated by 7% SDS-PAGE and Western blotted.

Figure 5-*Specific interaction of intact and truncated S100A8 in S100A9-A8 chimera with cytochrome b_{558} bound to heparin agarose matrix after purification; constitutive NADPH oxidase activity of eluted cytochrome b_{558}. .*

NADPH oxidase activity was reconstituted through the purification of cytochrome b_{558} isolated from PMA stimulated neutrophils, on a heparin affinity matrix in the presence of rS100A9-full length or truncated A8 chimera, as described in Material and Methods [Paclet *et al.* 2007].

Constitutive cytochrome b_{558} NADPH oxidase activity was measured without adding arachidonic acid as a stimulating agent, in a cell free assay with 0.2 pmol cytochrome b_{558}/assay, in the presence of 10µM FAD, 40µMGTPγS, and 5mM MgCl2 in a final 100 µl PBS volume and after adding 150µM NADPH (final concentration). NADPH oxidase activity was expressed as turnover (s^{-1}) (black square). The concentration of cytochrome b_{558} was determined by measuring the "reduced minus oxidized" differential spectrum and quantified at 426 nm (open circle).

A- S100A9-93(FL)A8; B-S100A9-Δ90A8; C-S100A9-Δ86A8; D-S100A9-Δ57A8.

E - Optimum oxidase turnover measured after interaction of 0.2 pmol cytochrome b_{558} with chimera S100A9-Full length or truncated ΔA8, versus control (cytochrome b_{558} alone).

Number of experiments n=6

Figure 6-*Colocalisation of NOX2/gp91^{phox} and S100A8/ A9 in PLB985 cells, as shown by confocal microscopy.*

Resting or PMA-stimulated differentiated PLB985 cells were incubated on poly-L-lysine-coated cover-slips. They were fixed with 4% (w/v) paraformaldehyde and then permeabilised with 0.1 % (w/v) TritonX100 as described in material and methods. To localise S100A8/A9 with NOX2/gp91^{phox} or p22^{phox}, permeabilised cells were incubated first with both mouse monoclonal anti gp91^{phox} Ig (13B6) or anti p22^{phox} Ig (16G6) (4µg each in 50 µl PBS

containing 1% (w/v) BSA), then with 50µl (1µg) rabbit-S100A8/A9 polyclonal home-made antibodies, followed by addition of 100µl (1: 250) of Alexa Fluor546 antimouse IgG (gp91^{phox} and p22^{phox}) or Alexa Fluor488 (S100A8/A9) donkey antirabbit IgG. Cell nuclei were stained with 40µl Hoechst 33258 (0. 5µg/ml). Fixed cells were imaged by confocal microscopy, at room temperature, using an inverted confocal and two-photon laser-scanning microscope (LSM 510 NLO, Carl Zeiss) equipped with a 40x/1. 3 Plan-Neofluar oil immersion lens.

Fig S1

Concentration dependence of ExoS S100 protein on activation of purified cytochrome b_{558} in a cell-free assay.

A-NADPH oxidase activity, expressed as turnover (s^{-1}), was measured in a cell-free assay, as described in Fig3B, after incubation of 0.2 pmol cytochrome b_{558} with various concentrations (3.75µg, 7.5µg, 11.25µg) of calcium loaded ExoS 129-S100A9 versus control: negative control=cytochrome b_{558} alone; positive control=, cytochrome b_{558} plus ExoS129-S100A8.

B-Similar experiment with ExoS54-S100A8 and ExoS54-S100A9.

Figure 1

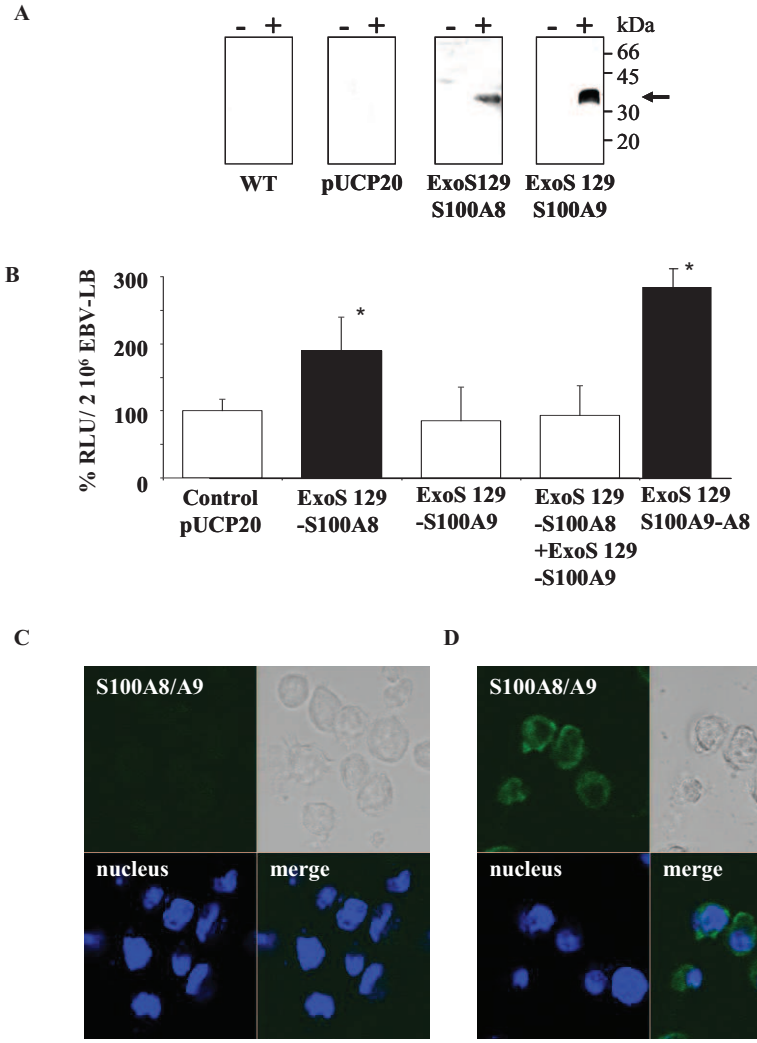

Figure 1. *Injection by Pseudomonas aeruginosa Type Three Secretion System (TTSS) of ExoS-S100 proteins in EBV-B Lymphocytes. Measurements of NADPH oxidase activity in injected intact cells and detection of injected ExoS-S100 proteins in EBV-B Lymphocytes by confocal microscopy.*

A- *Production of ExoS129-S100A8 and ExoS129-S100A9 by Pseudomonas aeruginosa. Secretion medium of induced Pseudomonas aeruginosa was analysed by Western blot after SDS-PAGE. ExoS129 S100A8 and ExoS129 S100A9 were detected with rabbit polyclonal antibodies raised against S100A8 and S100A9 as described in Material and Methods.*
B- *CHA strains were transfected with pUCP20 (empty vector), or pUCP20-ExoS129-S100A8, pUCP20-ExoS129-S100A9, or the chimera pUCP20-ExoS129-S100A9-A8. TTSS properties were induced by contact between CHA strains and EBV-B lymphocytes in the presence of 10% v/v human AB serum (RPMI 1640 medium, MOI 10). In some experiments, the two fusion proteins, ExoS 129-S100A8 from CHA S100A8 MOI 5, and ExoS 129-S100A9 from CHA S100A9 MOI 5, were concomitantly injected in EBV-LB. NADPH oxidase activity of 2x106 EBV-B lymphocytes, collected after injection of fusion proteins by TTSS, was measured by chemiluminescence after 30 min of incubation at 37°C, after stimulation by 80ng/ml PMA. Activity was expressed as RLU.*
Number of experiments n = 3 to 5.
C- *EBV-B lymphocytes control or D- EBV-B lymphocytes after ExoS 54-S100A9-A8 injection by P. aeruginosa were fixed, permeabilised, and labelled with goat anti human S100A8 antibodies for analysis by confocal microscopy, as described in Materials and Methods. An Alexa Fluor 488 anti goat antibody was used to detect the fusion protein, stained in green, in cells where ExoS 54-S100A9-A8 was present. EBV-BL nuclei were stained in blue with Hoechst 33258.*

Figure 2

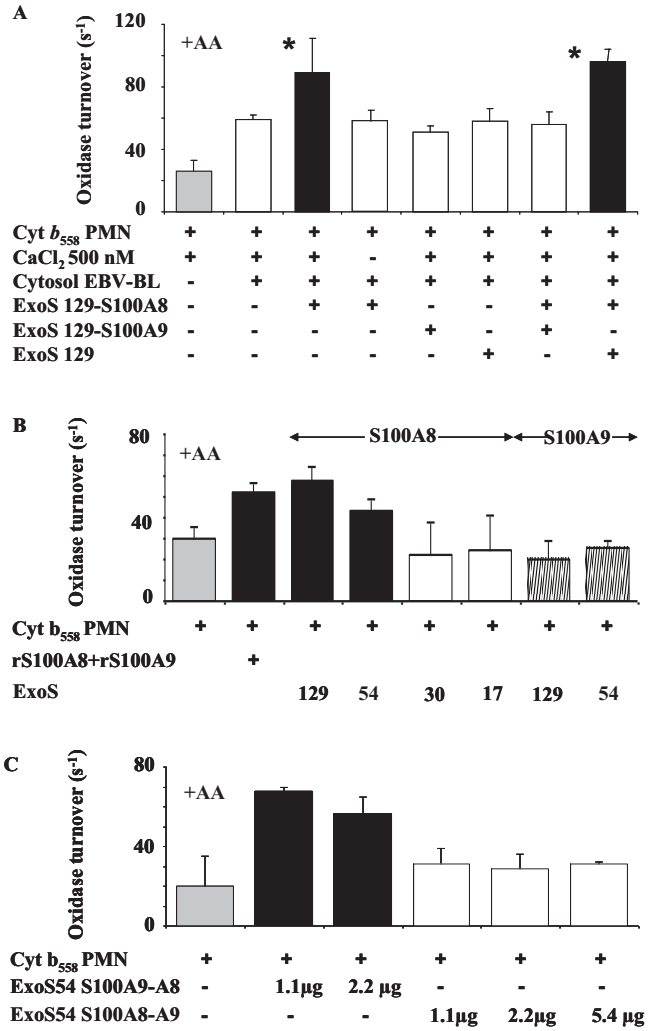

Figure 2. *Effect of recombinant S100 proteins secreted by induced P. aeruginosa on NADPH oxidase activity measured in a cell-free assay.*

A- *Recombinant S100 proteins secreted by induced (EGTA, 5mM) P. aeruginosa were precipitated from the extracellular medium by 55% (w/v) ammonium sulphate, overnight at 4°C. Recombinant ExoS fusion proteins were used in a cell free assay as follows: 0.2 pmol of cytochrome b_{558} purified from neutrophils was incubated with 300 µg EBV-B lymphocytes cytosol in the presence of 10 µM FAD, 40 µM GTPγS, 5mM $MgCl_2$, and an optimal amount of arachidonic acid (~1 mM) in 100µl PBS. ExoS-S100 fusion proteins (2.4 µg ExoS129-S100A8 and 3.75 µg ExoS129-S100A9 or ExoS alone) were preincubated first in 500nM $CaCl_2$ 20 min; then, purified and relipidated cytochrome b_{558} was added followed by cytosol and other reagents. Superoxide production was estimated by measuring the reduction of cytochrome c in the presence or absence of superoxide dismutase at 550 nm. The activity was expressed as oxidase turnover (s^{-1}). Number of experiments n=6.*

B- *Size dependence of ExoS on S100A8 mediated NADPH oxidase activity.*
ExoS129-S100A8, ExoS129-S100A9, ExoS54-S100A8, ExoS54-S100A9 fusion proteins were purified from induced P. aeruginosa (culture medium) as previously described. ExoS30-S100A8 and ExoS17- S100A8 were expressed in E. coli after IPTG induction as GST-fusion proteins by using a pGEX 5x2 vector. Recombinant S100A8 and rS100A9 were obtained in E. coli, in the same way. Calcium loaded recombinant S100 fusion proteins were used at the following concentrations: ExoS129-S100A8 (2.4µg), ExoS129-S100A9 (3.75 µg), ExoS54-S100A8 (5µg), ExoS54-S100 A9 (5µg), ExoS30-S100A8 (0.7µg), ExoS17-S100A8 (0.8µg), rS100A8 plus rS100A9 (0.78µg 1/1). NADPH oxidase was reconstituted in a cell-free assay as reported in Material and Methods. Oxidase activity was expressed as oxidase turnover (s^{-1}). Number of experiments n=6.

C- *Effect of chimera ExoS54-S100A8-A9 and ExoS54-S100A9-A8.*
Various concentrations of ExoS54-S100A8-A9 and ExoS54-S100A9-A8 were incubated with purified cytochrome b_{558} after 500nM $CaCl_2$ pre-incubation, as described previously in Material and Methods.
NADPH oxidase activity was expressed as turnover (s^{-1}). Number of experiments n=6.

Figure 3

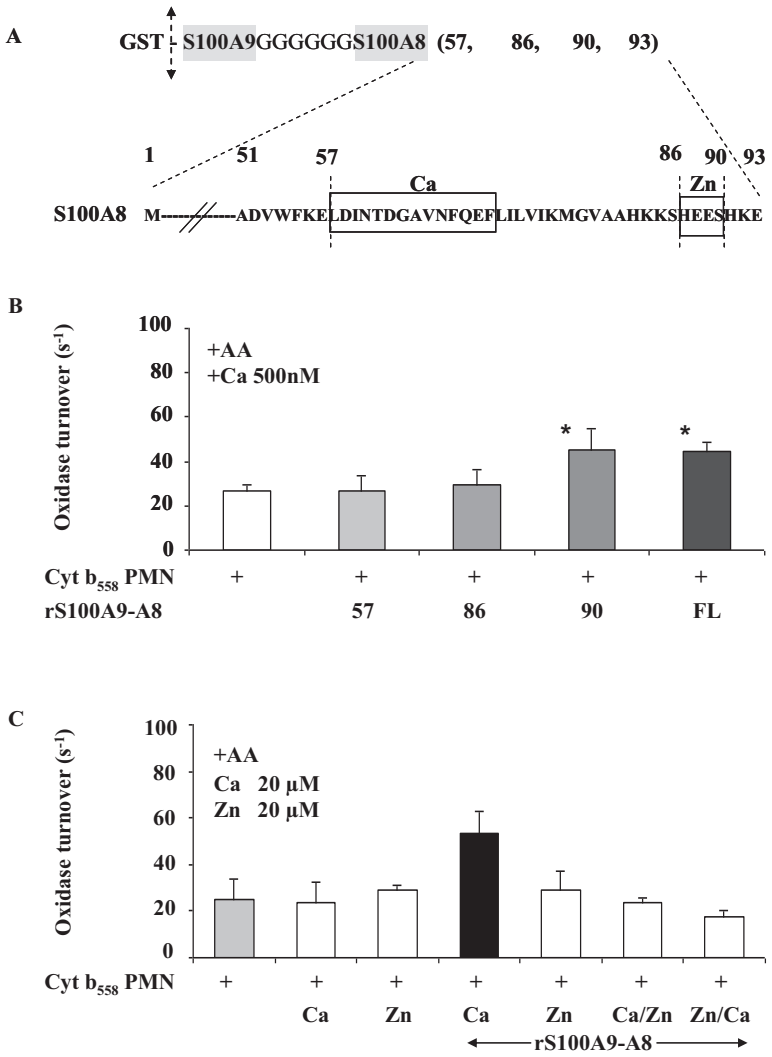

Figure 3. *Effect of S100A9-A8 chimera on NADPH oxidase activity in the presence (or not) of Ca^{++} and (or) Zn^{++}.*

A- *C-Terminal sequence of full length and truncated S100A8. The four chimera S100A9-full length S100A8 named S100A9-A8, S100A9-truncated S100A8 named S100A9-Δ90A8, S100A9-Δ86A8, S100A9-Δ57A8 were expressed in E. coli as described in Material and Methods.*

B- *The effect of chimera S100A9-full length or truncated A8 (1µg), preloaded with 500 nM $CaCl_2$ for 20 min, were tested on NADPH oxidase activity in a cell free assay as described in Material and Methods. After adding 0.2 pmoles cytochrome b_{558}, 10µM FAD, 40µM GTPγS, and 5mM $MgCl_2$, the medium was incubated in the presence of an optimal amount (80-100nmol) of arachidonic acid. Superoxide production was measured after adding 150µM NADPH. NADPH oxidase activity was expressed as turnover (s^{-1}). Number of experiments N= 6.*

C- *Effect of zinc on calcium loaded S100A9-A8 mediated NADPH oxidase activation. NADPH oxidase activity was measured as previously described (Fig3B) in a cell-free assay with purified cytochrome b_{558}, in the presence (or not) of recombinant chimera S100A9-A8 pre-incubated with either 20 µM Zinc, or 20 µM $CaCl_2$, or both (calcium plus zinc or zinc plus calcium).*

NADPH oxidase activity was expressed as turnover (s^{-1}).

Number of experiments n=6.

Figure 4

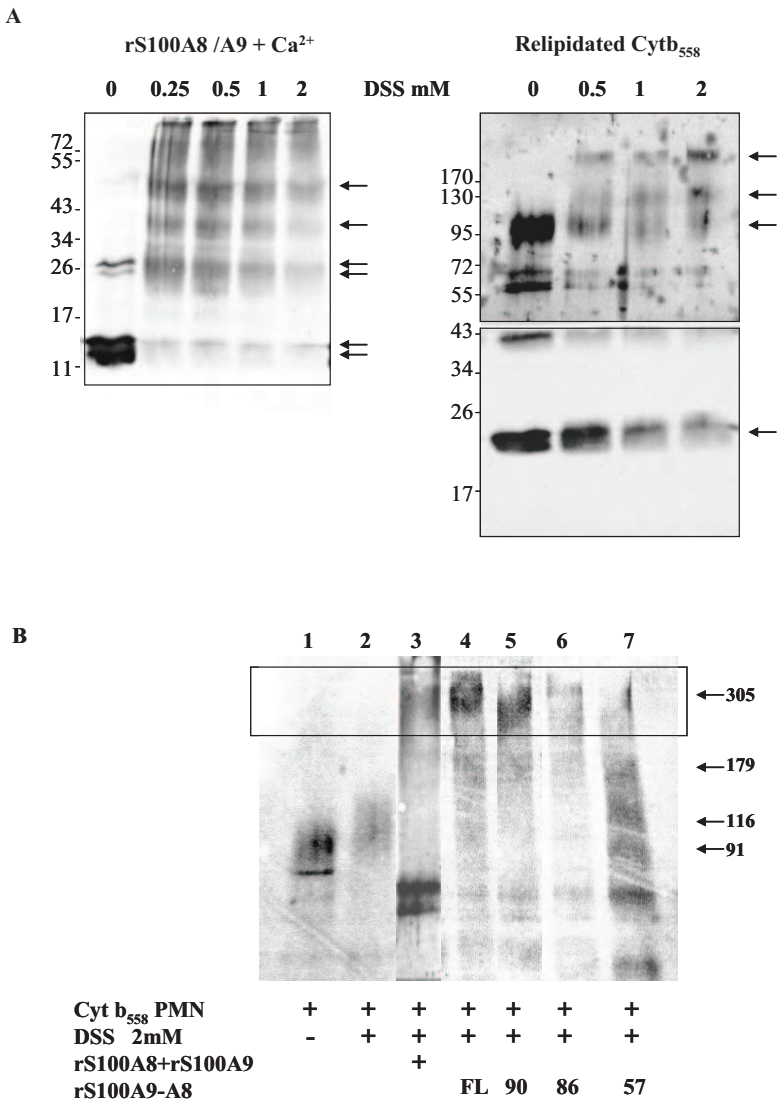

Figure 4*- Disuccinimidyl suberate (DSS) complex formation between cytochrome b_{558} and recombinant S100A8 and S100A9 proteins.*

*A-**left panel**. Determination of the DSS concentration necessary to cross-link cytochrome b_{558} and S100 proteins. 100 pmol of rS100A8 and 100 pmol of rS100A9 were pre-incubated with 500nM $CaCl_2$ for 20min, before adding 0 to 2mM DSS freshly prepared in DMSO. After 1h incubation at room temperature, proteins were separated by 12.5% SDS-PAGE and electro-transferred on a nitrocellulose matrix. Immune complexes were detected by using rabbit polyclonal antibodies raised against S100A8/S100A9. **Right panel**. A similar experiment was performed with 10pmol purified cytochrome b_{558}. Specific staining was obtained with rabbit specific polyclonal antibodies raised against C terminal peptides of $gp91^{phox}$ and $p22^{phox}$ sequences [Batot et al. 1995].*

B-Cross-linking of rS100A8(1. 5nmol) and rS100A9(1. 5nmol) with cytochrome b_{558} (10 pmol) in the presence of 2mM DSS.
***1.** Cytochrome b_{558} alone; **2.** Cytochrome b_{558} plus DSS; **3**. Cytochrome b_{558} plus rS100A8 and rS100A9, plus DSS; **4.** Cytochrome b_{558} plus chimera S100A9-93(FL)A8 and DSS; cytochrome b_{558} plus DSS and **5.** Chimera S100A9-Δ90A8 **6.** Chimera S100A9-Δ86A8; **7.** Chimera S100A9-Δ57A8. Complexed proteins were fractionated by 7% SDS-PAGE and Western blotted.*

Figure 5

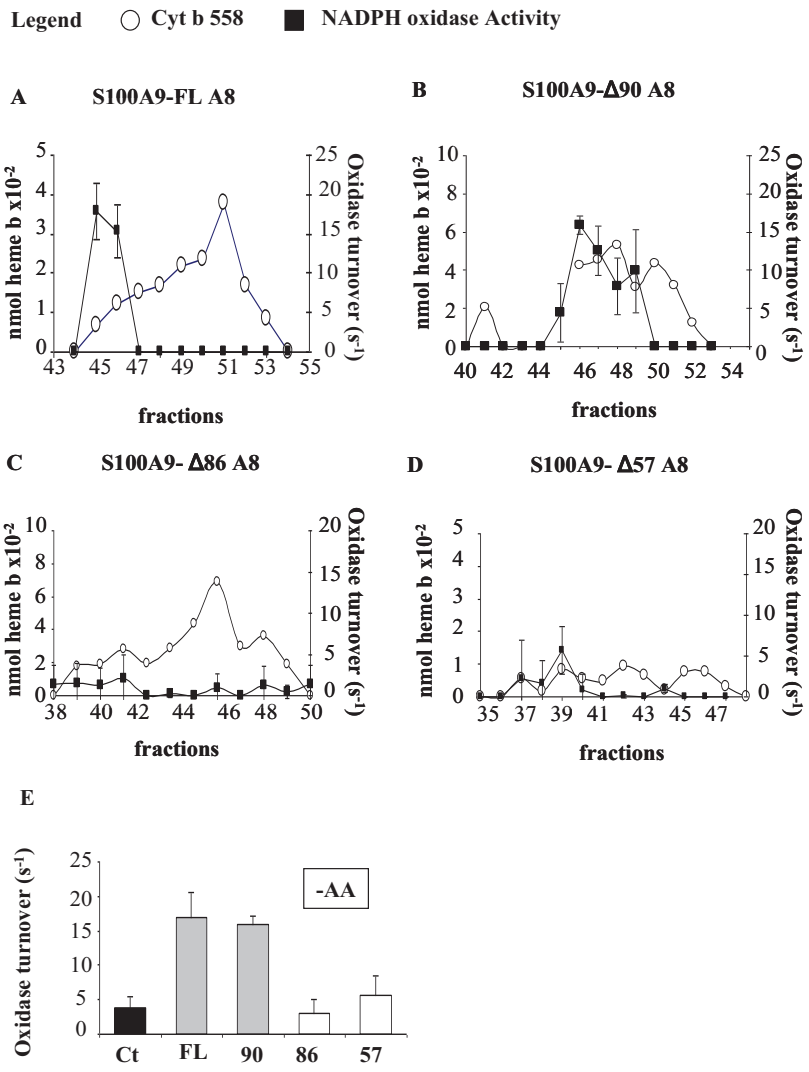

Figure 5*-Specific interaction of intact and truncated S100A8 in S100A9-A8 chimera with cytochrome b_{558} bound to heparin agarose matrix after purification; constitutive NADPH oxidase activity of eluted cytochrome b_{558}. .*

NADPH oxidase activity was reconstituted through the purification of cytochrome b_{558} isolated from PMA stimulated neutrophils, on a heparin affinity matrix in the presence of rS100A9-full length or truncated A8 chimera, as described in Material and Methods [Paclet et al. 2007].
Constitutive cytochrome b_{558} NADPH oxidase activity was measured without adding arachidonic acid as a stimulating agent, in a cell free assay with 0.2 pmol cytochrome b_{558}/assay, in the presence of 10µM FAD, 40µMGTPγS, and 5mM MgCl2 in a final 100 µl PBS volume and after adding 150µM NADPH (final concentration). NADPH oxidase activity was expressed as turnover (s^{-1}) (black square). The concentration of cytochrome b_{558} was determined by measuring the "reduced minus oxidized" differential spectrum and quantified at 426 nm (open circle).
A- *S100A9-93(FL)A8;* ***B-*** *S100A9-Δ90A8;* ***C-*** *S100A9-Δ86A8;* ***D-*** *S100A9-Δ57A8.*
E- *Optimum oxidase turnover measured after interaction of 0.2 pmol cytochrome b_{558} with chimera S100A9-Full length or truncated ΔA8, versus control (cytochrome b_{558} alone).*
Number of experiments n=6.

Figure 6

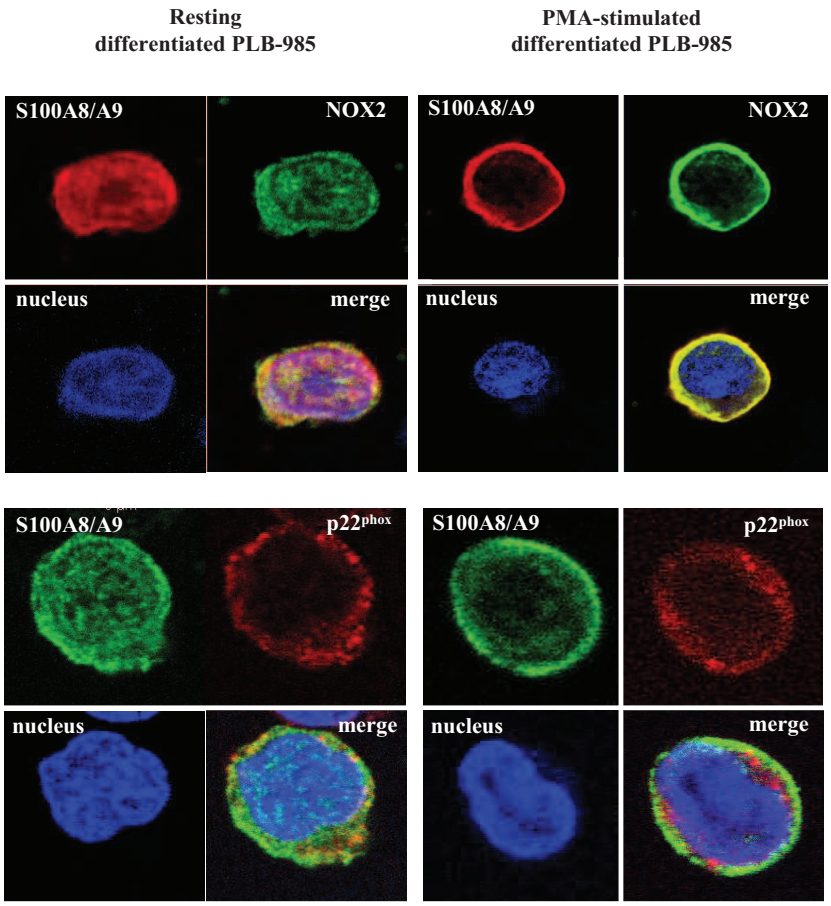

Figure 6*-Colocalisation of Nox2/gp91^{phox} and S100A8/ A9 in PLB985 cells, as shown by confocal microscopy.*

Resting or PMA-stimulated differentiated PLB985 cells were incubated on poly-L-lysine-coated cover-slips. They were fixed with 4% (w/v) paraformaldehyde and then permeabilised with 0.1 % (w/v) TritonX100 as described in material and methods. To localise S100A8/A9 with Nox2/gp91^{phox} or p22^{phox}, permeabilised cells were incubated first with both mouse monoclonal anti gp91^{phox} Ig (13B6) or anti p22^{phox} Ig (16G6) (4µg each in 50 µl PBS containing 1% (w/v) BSA), then with 50µl (1µg) rabbit-S100A8/A9 polyclonal home-made antibodies, followed by addition of 100µl (1: 250) of Alexa Fluor546 antimouse IgG (gp91^{phox} and p22^{phox}) or Alexa Fluor488 (S100A8/A9) donkey antirabbit IgG. Cell nuclei were stained with 40µl Hoechst 33258 (0. 5µg/ml). Fixed cells were imaged by confocal microscopy, at room temperature, using an inverted confocal and two-photon laser-scanning microscope (LSM 510 NLO, Carl Zeiss) equipped with a 40x/1. 3 Plan-Neofluar oil immersion lens.

Supplementary data S1

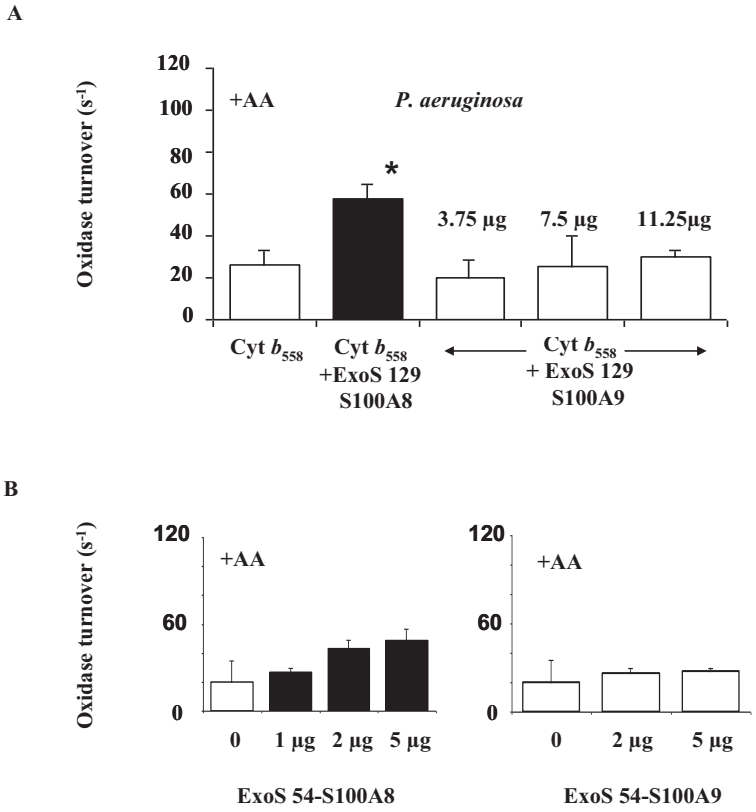

Fig S1

Concentration dependence of ExoS S100 protein on activation of purified cytochrome b_{558} in a cell-free assay.
A- *NADPH oxidase activity, expressed as turnover (s^{-1}), was measured in a cell-free assay, as described in Fig3B, after incubation of 0.2 pmol cytochrome b_{558} with various concentrations (3.75µg, 7.5µg, 11.25µg) of calcium loaded ExoS 129-S100A9 versus control: negative control=cytochrome b_{558} alone; positive control=, cytochrome b_{558} plus ExoS129-S100A8.*

B- *Similar experiment with ExoS54-S100A8 and ExoS54-S100A9.*

Table I: plasmid constructions for protein expression

cDNA coding for S100A8. S100A9 or fusion chimera proteins were introduced in pUCP20 or pGEX 5x2 plasmids using the indicated restriction enzyme. Protein expression was carried out in *P. aeruginosa* or *E. coli*.

Plasmid	**sequence for protein and restriction enzymes**	**Insertion of fragments and restriction sites**
1- In ***P. aeruginosa***		
pUCP20	*XbaI* orf I – exoS 129 *SalI*	*SalI* S100A8 *SphI* *SalI* S100A9 *SphI* *SalI* S100A9GGG *BamHI GGG*S100A8 *SphI* *SalI* S100A8GGG *BamHI GGG*S100A9 *SphI*
	XbaI orf I – exoS 54 *SalI*	*SalI* S100A8 *SphI* *SalI* S100A9 *SphI* *SalI* S100A9GGG *BamHI GGG*S100A8 *SphI* *SalI* S100A8GGG *BamHI GGG*S100A9 *SphI*
2- In ***E. coli***		
pGEX 5x2	GST	*XbaI* exoS 30 *SalI* S100A8 *XhoI* *XbaI* exoS 17 *SalI* S100A8 *XhoI*
pGEX 5x2	GST	*SalI* S100A9GGG *BamHI GGG*FL S100A8 *NotI* *SalI* S100A9GGG *BamHI GGG*Δ90 S100A8 *NotI* *SalI* S100A9GGG *BamHI GGG*Δ86 S100A8 *NotI* *SalI* S100A9GGG *BamHI GGG*Δ86 S100A8 *NotI*
pGEX 5x2	GST	*SalI* S100A8 *NotI* *SalI* S100A9 *NotI*

CHAPITRE III

S100A8/A9 extra-cellulaires biomarqueurs de la PR

Articles 4 et 5

Chapitre 3 : S100A8/A9 sécrétées dans le milieu extra-cellulaire sont des biomarqueurs de la PR

La mise sur le marché de nouvelles thérapeutiques dans le traitement des rhumatismes inflammatoires chroniques, dont il est difficile à priori de prédire l'efficacité à l'échelon individuel, illustre parfaitement le besoin de développer une médecine personnalisée pour offrir une prise en charge adaptée à chaque patient.

La comparaison de l'empreinte protéomique de liquides biologiques offre une formidable opportunité de caractériser de nouveaux biomarqueurs utiles au diagnostic des rhumatismes inflammatoires, à la détermination du pronostic et à l'évaluation de la réponse au traitement (**Annexe 3**).

La technique SELDI-TOF ("Surface Enhanced Laser Desorption/Ionization- Time of Flight") permet, en un temps extrêmement court et avec un faible volume d'échantillon, d'établir la signature spécifique d'une maladie. Cette méthode est donc particulièrement adaptée à l'identification de la signature protéique d'une condition pathologique sur un grand nombre de patients. Elle consiste en une première phase de fractionnement protéique sur une surface chromatographique. Par la suite, la masse des protéines d'intérêt est déterminée par un spectromètre de masse selon le temps de vol. Après l'analyse statistique des variations entre les profils protéomiques des différentes conditions pathologiques, l'identification des biomarqueurs d'intérêt passe par des techniques plus classiques de biochimie, notamment de purification et de séquençage de protéines.

Ainsi, nous avons récemment montré que les protéines Apolipoprotéine A1 (Apo-A1) et Platelet Factor 4 (PF4) étaient respectivement associées à une bonne ou mauvaise réponse au traitement de patients atteints de PR par l'infliximab [Trocmé *et al.* 2008].

Notre objectif était de caractériser des protéines spécifiques de la PR dans le liquide synovial et la membrane synoviale de patients souffrant de PR.

1. Les protéines S100A8, S100A9 et S100A12, biomarqueurs de la PR

Les ACPA ("anti-citrullinated protein or peptide auto anti-bodies"), anciennement dénommés anticorps anti-peptides citrullinés, offrent une excellente spécificité pour le diagnostic de PR. Cependant au stade inaugural de la maladie leur sensibilité demeure insuffisante [Nishimura *et al.* 2007] pour poser un diagnostic avec certitude. Nous nous sommes donc proposés

d'identifier des protéines spécifiques de la PR en nous focalisant sur un tissu situé au coeur du processus inflammatoire de la PR, le liquide synovial.
Le profil protéique du liquide synovial de 30 patients souffrant de PR a été comparé par technique SELDI-TOF à celui de 17 patients atteints d'arthrose et 18 malades souffrant d'un rhumatisme inflammatoire ou microcristallin en poussée.

Les résultats montrent que :
- 74 pics protéiques permettent de discriminer le liquide synovial de PR et d'arthrose alors que 27 biomarqueurs ont une intensité statistiquement différente dans liquide synovial de patients souffrant de PR et de synovite non rhumatoïde.

- Les protéines S100A8, S100A12 et S100A9 sont les biomarqueurs les plus significativement surexprimés dans le liquide articulaire rhumatoïde. Leur expression est corrélée au compte des PMNs dans les arthrites non rhumatoïdes. Chez les patients atteints de PR, cette association n'existe plus.

2. S100A8 est exprimée par les synoviocytes fibroblastiques

Notre précédent travail suggère une production ectopique de certaines protéines S100 dans la membrane synoviale rhumatoïde. Or, ces protéines sont exprimées quasi-exclusivement dans la lignée myéloïde et secrétées sur le site inflammatoire principalement lors de la stimulation du PMN. Dans un premier temps, nous avons cherché à confirmer la synthèse des protéines S100A8/A9 dans le tissu articulaire. Dans un deuxième temps, nous avons examiné si les synoviocytes fibroblastiques, cellules résidantes de l'articulation subissant une transformation phénotypique dans la PR, pouvaient contribuer, avec les PMNs infiltrant le pannus rhumatoïde, à la surexpression de S100A8/A9.
Le protéome de membranes synoviales de patients souffrant de PR a été comparé à celui de la membrane synoviale saine ou d'une synovite autre que la PR. Des coupes tissulaires de 10µm ont été analysées par technique SELDI-TOF chez 28 patients. La reproductibilité de cette technique a été évaluée. Des cultures de synoviocytes fibroblastiques rhumatoïdes ont permis une analyse de la production de protéines S100A8/A9 dans ce type cellulaire.

Les résultats montrent que :

- L'analyse de la signature de la PR dans le tissu articulaire par technique SELDI-TOF est reproductible. La protéine S100A8 est significativement surexprimée dans la membrane synoviale rhumatoïde.

- Les synoviocytes fibroblastiques produisent l'hétérocomplexe S100A8/A9. L'incubation d'IL-1β et TNFα tend à augmenter la synthèse de S100A8/A9 par le synoviocyte fibroblastique rhumatoïde alors que la production demeure inchangée dans l'arthrose.

En conclusion, l'expression de S100A8, S100A9 et S100A12 est augmentée dans le liquide articulaire de patients souffrant de PR. Les synoviocytes fibroblastiques rhumatoïdes sont responsables d'une production de S100A8/A9, stimulable par l'IL-1β et le TNFα.

Dans cette étude, mon travail a porté sur la mise au point et la réalisation de l'analyse du liquide articulaire et de la membrane synoviale par technique SELDI-TOF. J'ai également mené l'analyse statistique des variations entre les différents protéomes étudiés. Enfin, j'ai analysé l'expression de S100A8/A9 dans des cultures de synoviocytes de type fibroblastique.

Article 4 : **Baillet A.,** Trocme C., Berthier S., Arlotto M., Grange L., Chenau J., Quetant S., Seve M., Berger F., Juvin R., Morel F., and Gaudin P. (2010), Synovial fluid proteomic fingerprint: S100A8, S100A9 and S100A12 proteins discriminate rheumatoid arthritis from other inflammatory joint diseases. *Rheumatology (Oxford)* 49 671-82.

Article 5: Trocme C., **Baillet A.**, Berthier S., Arlotto M., Hograindleur M., Mercier N., Corcella D., Grange L., Berger F., Juvin R., Morel F., and Gaudin P. S100A8 production by fibroblast-like synoviocytes detected by a proteomic profiling of Rheumatoid Arthritis synovium with a new Surface Enhanced Laser Desorption and Ionization Time-Of-Flight Mass Spectrometry-based approach. Soumis à *Arthritis Rheumatism.*

Article 4

Synovial fluid proteomic fingerprint: S100A8, S100A9 and S100A12 proteins discriminate rheumatoid arthritis from other inflammatory joint diseases.

RHEUMATOLOGY

Rheumatology 2010;49:671–682
doi:10.1093/rheumatology/kep452
Advance Access publication 25 January 2010

Original article

Synovial fluid proteomic fingerprint: S100A8, S100A9 and S100A12 proteins discriminate rheumatoid arthritis from other inflammatory joint diseases

Athan Baillet[1,2,*], Candice Trocmé[1,3,*], Sylvie Berthier[1], Marie Arlotto[4], Laurent Grange[1,2], Jérôme Chenau[5], Sébastien Quétant[1], Michel Sève[5], François Berger[4], Robert Juvin[2], Françoise Morel[1] and Philippe Gaudin[1,2]

Abstract

Objective. We investigated SF and serum proteomic fingerprints of patients suffering from RA, OA and other miscellaneous inflammatory arthritides (MIAs) in order to identify RA-specific biomarkers.

Methods. SF profiles of 65 patients and serum profiles of 31 patients were studied by surface-enhanced laser desorption and ionization–time-of-flight-mass spectrometry technology. The most discriminating RA biomarkers were identified by matrix-assisted laser desorption ionization–time of flight and their over-expression was confirmed by western blotting and ELISA.

Results. Three biomarkers of 10 839, 10 445 and 13 338 Da, characterized as S100A8, S100A12 and S100A9 proteins, were the most up-regulated proteins in RA SF. Their expression was about 10-fold higher in RA SF *vs* OA SF. S100A8 exhibited a sensitivity of 82% and a specificity of 69% in discriminating RA from other MIAs, whereas S100A12 displayed a sensitivity of 79% and a specificity of 64%. Three peptides of 3351, 3423 and 3465 Da, corresponding to the α-defensins-1, -2 and -3, were also shown to differentiate RA from other MIAs with weaker sensitivity and specificity. Levels of S100A12, S100A8 and S100A9 were statistically correlated with the neutrophil count in MIA SF but not in the SF of RA patients. S100A8, S100A9, S100A12 and α-defensin expression in serum was not different in the three populations.

Conclusion. The most enhanced proteins in RA SF, the S100A8, S100A9 and S00A12 proteins, distinguished RA from MIA with high accuracy. Possible implication of resident cells in this increase may play a role in RA physiopathology.

Key words: Rheumatoid arthritis, Proteomics, S100 Proteins, Synovial fluid, Biomarker.

Introduction

RA is the most common inflammatory arthritis, with a prevalence range in European countries of between 0.3 and 0.8% [1]. Mechanisms of synovium inflammation are still unclear and often lead to progressive joint destruction and deformation. Cells of the adaptative immunity pathway were thought to be the principal actors of RA pathogenesis. However, an increasing body of evidence suggests that cells of the innate immunity and resident articular cells are involved in RA pathogenesis [2, 3]. Indeed, the activation of synovial macrophages or fibroblast-like synoviocytes may trigger lymphocytes and subsequently synovium inflammation since inactivating these cells reduces arthritis in experimental models [4]. It has been hypothesized that several cytosolic peptides, when released in the extracellular matrix during cell necrosis, could be recognized by cells

[1]GREPI CNRS UMR 5525, Grenoble University, [2]Clinic of Rheumatology, CHU Hôpital Sud, [3]Laboratory of Enzymology, BEP, CHU Hôpital Michallon, [4]Grenoble Institut Neurosciences, INSERM U836 and [5]Biology Innovation Center, CHU Hôpital Michallon, Grenoble, France.

Submitted 24 July 2009; revised version accepted 3 December 2009.

Correspondence to: Athan Baillet, GREPI TIMC-Imag UMR CNRS 5525, C.H.U. de Grenoble, B 217, 38043 Grenoble Cedex, France. E-mail: abaillet@chu-grenoble.fr

*Athan Baillet and Candice Trocmé contributed equally to this work.

of the innate immunity pathway as danger signals [3]. Among them, S100 proteins could be implicated in RA pathogenesis. The S100A8, S100A9 and S100A12 proteins are predominantly expressed by myelomonocytic cells and constitute ~40% of the polymorphonuclear neutrophil (PMN) cytosolic proteins. They have a critical role in inflammation as they can activate the innate immunity pathway sensed by receptors for advanced glycation end products (RAGEs) or Toll-like receptors [5–7]. S100A8 and S100A9 are also expressed by keratinocytes and epithelial cells under inflammatory conditions [8].

Several reasons prompted us to perform SF proteome profiling using surface-enhanced laser desorption and ionization–time-of-flight mass spectrometry (SELDI–TOF-MS) [9, 10]. First, the currently available biological tests are not precocious and accurate enough, leading to delayed diagnosis of the disease [11]. The discovery of new biomarkers is of particular interest for earlier diagnosis. Secondly, SELDI–TOF-MS technology, whose relevance has been emphasized not only in cancer [12–14] but also in the rheumatology field [15–18], is likely to detect numerous RA-specific biomarkers. Thirdly, since the synovium–cartilage junction is a critical zone of the disease development [19], disease-specific proteins may localize into SF rather than in other biological materials. Thus, we decided to investigate the SF and the serum proteomic fingerprint of patients suffering from RA, OA and miscellaneous inflammatory arthritides (MIAs) in order to identify RA-specific biomarkers.

Patients and methods

Patient populations

Seventy-four patients were recruited in the rheumatology clinic between March 2001 and 2007. The study was approved by the local ethics committee (Comité de Protection des Personnes). Sixty-five SFs and 31 sera were obtained during therapeutic or diagnostic procedures, after patients gave their informed consent to the study. The RA group comprised 30 patients for the SF analysis and 14 patients for the serum analysis, fulfilling the 1987 modified ACR criteria for RA [20]. The 1986 clinical and radiographic criteria were fulfilled by 24 patients of the OA group (17 SF and 7 sera) [21]. The inflammation control group was composed of 18 patients (nine AS, six pseudogout, one SLE and two juvenile idiopathic arthritis) for the SF analysis and 10 patients (eight AS, one pseudogout and one SLE) for the serum study. All patients suffering from AS, juvenile idiopathic arthritis and SLE fulfilled, respectively, the modified New York criteria [22], ILAR criteria [23] and the 1982 ACR criteria [24]. The SF of patients suffering from pseudogout displayed a leucocyte count over 2000/mm^3 and CP crystals. Demographic parameters are summarized in Table 1.

Sample processing

Sera were treated by a protease inhibitor cocktail (Roche Diagnostics, Meylan, France), and were subsequently aliquoted and stored at −80°C. SFs were centrifuged [500 *g*, 10 min, room temperature (RT)], supernatants were incubated with hyaluronidase (40 IU/ml of SF) for 30 min at RT, centrifuged again (1800 *g*, 10 min, RT), treated with the same protease inhibitor cocktail and aliquoted at −80°C.

SELDI–TOF-MS analysis

Serum and SF protein profiles were obtained by the SELDI–TOF-MS method (Ciphergen Biosystems, Fremont, CA, USA), using a cation exchange array (CM10), an anion exchange array (Q10), a nickel affinity array [immobilized metal affinity capture (IMAC-Ni)] and a copper affinity array (IMAC-Cu).

Table 1 Demographic and biological characteristics of the population

	RA ($n = 44$)	OA ($n = 24$)	MIA ($n = 28$)	*P*-value
Age, years	55.0 (44.0–62.0)	71.0 (62.0–78.0)	52.0 (41.0–67.0)	0.001
Disease duration, year	8.5 (2.8–12.5)	0.5 (0.1–5.0)	4.0 (0.9–7.0)	0.885
RF, IU/ml	19.5 (10.5–81.0)	NA	6.0 (3.5–31.3)	0.035
ESR, mm/h	39.0 (26.0–67.0)	20.0 (8.5–46.5)	33.5 (8.3–73.0)	0.018
CRP, mg/l	30.5 (12.0–49.5)	5.0 (5.0–18.0)	60.0 (24.0–146.0)	0.049
SF count, cells/mm^3				
Leucocytes	10 000 (8125–18 000)	200 (120–290)	7000 (5000–10 000)	<0.001
PMN	6885 (4620–13320)	67 (17–80)	5355 (2100–9685)	<0.001
Lymphocytes	1260 (480–1822)	48 (35–80)	560 (2–845)	<0.001
Treatment, *n* (%)		NA		
Biologicals	19 (43.2)		3 (10.7)	0.024
DMARDs	21 (47.7)		8 (28.6)	0.243
Steroids	8 (18.1)		2 (7.1)	0.012

Values are presented as median (interquartile range) except for treatment where values are numerical (%). Statistical significance was calculated using ANOVA or χ^2-test where appropriate. RF assessed by Waaler–Rose technique ($n < 15$ IU/ml); ESR ($n < 20$ mm); CRP ($n < 10$ mg/l); NA: not applicable.

As SF volume varied considerably among patients, a constant amount of protein in each sample was analysed in order to rule out the influence of protein concentration on the results. Protein concentration of SF was measured using the Bradford method: 5 μg were used for the proteome profiling on CM10, IMAC-Cu and IMAC-Ni, whereas 2 μg were loaded on Q10 arrays. Ten microlitres of serum were mixed with 15 μl of a denaturation buffer [phosphate-buffered saline (PBS), 9 M urea, 1% 3[(3-Cholamidopropyl)dimethylammonio]-propanesulfonic acid (CHAPS) pH 7.3] under constant motion for 20 min and 2 μl of this solution were loaded on each array.

Samples were processed robotically on a Biomek 2000 Automation Workstation (Beckman Coulter, Villepinte, France). IMAC-Cu and IMAC-Ni arrays were activated with, respectively, 100 μl of 100 mM $CuSO_4$ or 100 mM $NiSO_4$. Then spots were washed twice with 200 μl H_2O, once with 200 μl sodium acetate pH 4 and finally with 200 μl H_2O. Then the following procedure was applied to each chip. Arrays were equilibrated with 200 μl of the corresponding loading/washing buffer [20 mM Tris, 0.1% Triton X-100 (v/v) pH 8 for Q10; 20 mM sodium acetate, 0.1% Triton X-100 pH 4 for CM10; PBS, 0.5 M NaCl, 0.1% Triton X-100 pH 7.3 for IMAC-Cu and IMAC-Ni]. Respective amounts of SF or serum were incubated in 50 μl of loading/washing buffer for 60 min. Spots were washed twice with 200 μl of washing buffer, twice with 200 μl of the same buffer without Triton X-100 and finally with 200 μl of 5 mM Tris pH 8 (Q10), 5 mM sodium acetate pH 4 (CM10) or 5 mM HEPES pH 7 (IMAC-Cu and IMAC-Ni). After drying, spots were loaded twice with 0.8 μl of saturated sinapinic acid in 0.5% trifluoroacetic acid, 50% acetonitrile and chips were analysed on the PCS-4000 ProteinChip reader. Two laser intensities (3200 and 4500 nJ) were used to analyse protein profiles and mass data processing was performed with the Ciphergen Express software, following the classical steps of spectra calibration, normalization, peak detection and aligning.

Protein purification and identification

S100A8, S100A9 and S100A12 proteins were purified from 500 μl of RA SF by protein precipitation with 70% ammonium sulphate. After centrifugation (10 000 *g*, 30 min, 4°C), the supernatant was dialysed in 5 mM Tris pH 7.5 in Spectra/Por dialysis membranes (molecular weight cut off: 5000 Da) and proteins were lyophilized in a freeze–dry system. The powder was suspended in 1 ml H_2O; 900 μg of protein evaluated by the Bradford method were loaded on a 16% acrylamide tricine–SDS–PAGE gel, and the gel was further stained with Coomassie blue R-250 [25]. Bands revealed at about 10 800, 10 400 and 13 300 Da were digested by trypsin and identified by MS using a 4800 MALDI–TOF/TOF analyser. Database searches were performed in the UniProtKB database (release 12.0) using the Mascot (Matrix Science) search algorithm. Validity of the identification results was evaluated by the molecular weighted search (MOWSE) score.

Immunoblotting

SF (300 μg) of patients suffering from RA, OA and AS were loaded on a 12.5% acrylamide SDS–PAGE gel. Recombinant S100A8 and S100A9 (1 μg) were used as positive controls [26, 27]. After electrophoresis, proteins were transferred onto a 0.45 mm nitrocellulose membrane. The membrane was further incubated with home-made rabbit anti-calprotectin (S100A8/S100A9 hetero-complex) antibody (1:1000 dilution). Anti-rabbit antibodies conjugated to horseradish peroxidase (1:5000 dilution) were added the next day and revelation was performed with ECL Reagent (GE Healthcare, Little Chalfont, UK).

α-Defensin concentration

Alpha-defensin concentration was evaluated in SF by an ELISA kit according to the manufacturer's instructions (HyCult Biotechnology, Uden, The Netherlands) [28].

Statistical analysis

Differences in demographic and biological parameters between groups were explored using ANOVA or χ^2-test, where appropriate. Mann–Whitney U-test or Kruskall–Wallis test was used to compare SELDI–TOF-MS peak intensities and α-defensin concentration assessed by ELISA (Statview 5.0; SAS Institute, Marlow, UK). Receiver operating characteristic curve analyses were performed to measure the diagnostic accuracy of each protein and correlation between biomarker intensity and synovial PMN count was determined using Spearman's test. Multivariate comparison between two populations was performed by supervised hierarchical clustering analyses of the characterized biomarkers and results were visualized by heat maps which are a graphical representation of overexpressed (red), decreased (green) or unchanged (black) proteins previously identified as differentially expressed in the two studied populations.

Results

SF proteome profiling

RA vs OA. Distinct protein profiles of SF were observed on the four arrays. Among 194 proteins detected in OA and RA SF, 74 were differentially expressed in both populations ($P < 0.05$). The most differentially expressed biomarkers were three proteins isolated on the four arrays at 10 445 (3.8), 10 839 (4.5) and 13 338 (17.3) Da, which were all overexpressed in RA SF (Fig. 1A). Their mean intensities were four to twelve times higher in RA than in OA, with significant statistical differences between the two populations ($P < 0.0001$, Table 2). Another cluster of three peptides of ~3000 Da was differentially expressed in OA and RA SF (Fig. 1B). These biomarkers of 3351 (2.9), 3423 (3.1) and 3465 (2.5) Da, characterized on the IMAC-Cu, IMAC-Ni and CM10 arrays, were statistically enhanced in RA SF (Table 2). They were slightly less accurate than the previous biomarkers for the discrimination of the RA population from the OA group.

FIG. 1 Characterization by SF proteome profiling of biomarkers discriminating a RA population from OA patients.

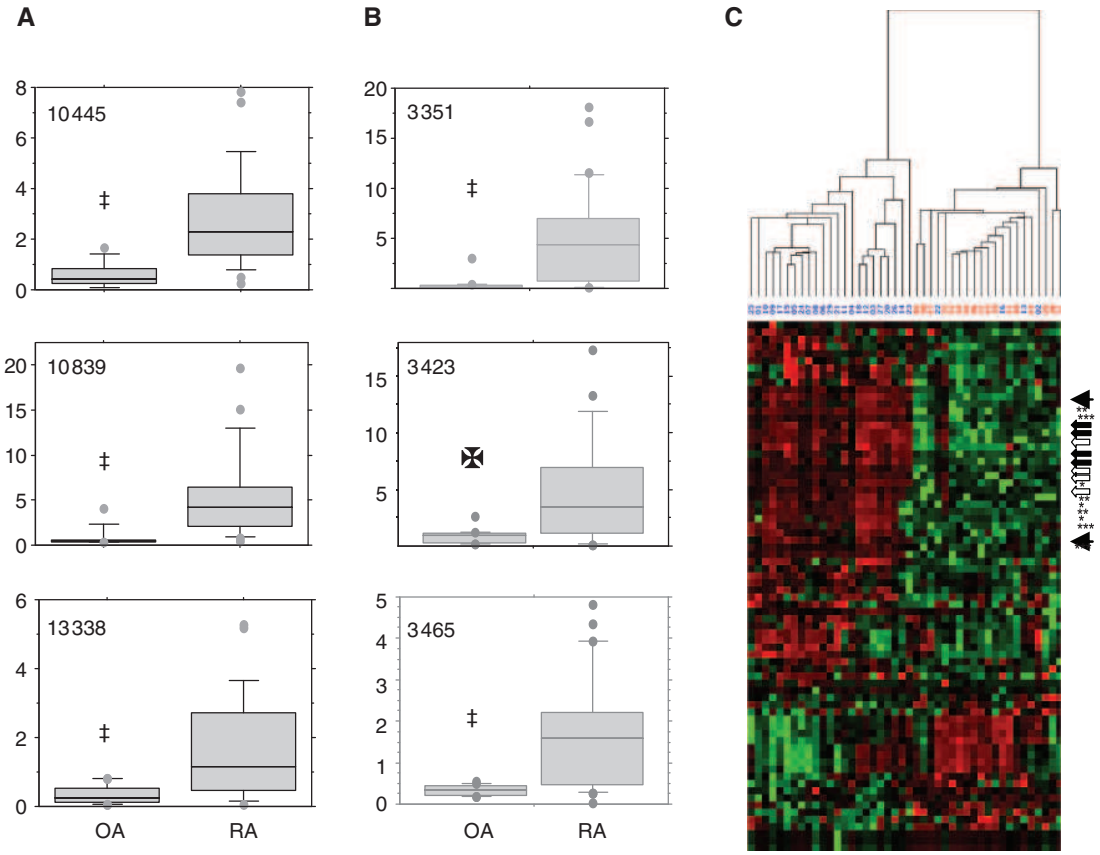

Relative SELDI–TOF-MS peak intensity of the 10 445, 10 839 and 13 338 Da proteins on a Q10 array (**A**) and of 3351, 3423 and 3465 Da peptides on a CM10 array (**B**). Boxes represent the interquartile range, the line across the box is the median and the whiskers represent the 5th and 95th percentiles. ‡$P < 0.0001$, ✠$P < 0.005$. Heat map visualization of the 74 biomarkers significantly differentially expressed in RA *vs* OA SF (**C**). Enhancement of the 10 445 (←), 10 839 (⇐), 13 338 (➡), 3351 (*), 3423 (**) and 3465 Da (***) biomarkers in patients suffering from RA (blue numbers) compared with OA patients (red numbers).

The 74 biomarkers whose expression was significantly different in OA and RA groups were visualized in a heat map (Fig. 1C). Most of them were increased in RA and decreased in OA SF. Hierarchical clustering classification, according to these proteins, created a first group exclusively constituted of RA samples. The sensitivity of this analysis in classifying RA patients in this group was 87%, with only four misclassified samples. No OA sample was classified in the RA-pattern group, corresponding to a specificity of 100%.

RA vs MIA. Although almost 200 peaks were detected in RA and MIA spectra, only 27 proteins were statistically differentially expressed between the two populations. Among them, the previously characterized 10 445 and 10 839 Da proteins were the most relevant to differentiation of the two populations, whereas the 13 338 Da biomarker was a little less discriminating (Table 2). The average intensity of the 10 839 Da peak was 5.05 (4.40) in the RA set *vs* 1.88 (1.25) in the MIA group **(**Fig. 2A), providing the best sensitivity and specificity for the diagnosis of RA in these two populations (Table 2). Concerning the three peptides of ~3000 Da, mean intensities of each peak were significantly higher in RA SF than in MIA SF (Fig. 2B). However, their specificity and sensitivity in discriminating RA from MIA patients were lower than those of the aforementioned biomarkers (Table 2). Classification of samples according to the 27 proteins whose expression was significantly different in MIA and RA groups, did not improve the breakdown of the population in each group compared with the discriminating potential of individual markers: this hierarchical clustering map displayed a sensibility of 75% and a specificity of 56% in differentiating RA from MIA samples (Fig. 2C).

Characterization of the detected biomarkers

The group of the 3000 Da peptides was previously identified as α-defensin-1, -2 and -3 in several SELDI–TOF-MS studies [14, 29]. Evaluation of the whole concentration of

Table 2 Characteristics and identification of biomarkers

	Biomarker characteristics					Biomarker MALDI–TOF-MS/MS identification				
Biomarker, Da	*P*-value	Sensitivity, %	Specificity, %	AUC	Cut-off	Accession number	MOWSE score	*P*-value	Peptide number	Peptide sequence
RA *vs* OA										
10 445	<0.0001	88	76	0.89	0.94	P80511	365	<0.01	6	ELANTIK, GHFDTLSK, KGHFDTLSK, AAHYHTHKE, GHFDTLSKGELK, TKLEEHLEGIVNIFHQYSVR
10 839	<0.0001	93	83	0.88	0.86	P05109	334	<0.01	10	GADVWFK, MGVAAHKK, MLTELEK, KGADVWFK, GNFHAVYR, SHEESHKE, ALNSIIDVYHK, LLETECPQYIR, LLETECPQYIRK, YSLIKGNFHAVYR
13 338	<0.0001	91	75	0.80	0.38	P06702	643	<0.01	10	MSQLER, DLQNFLK, LTWASHEK, DLQNFLKK, MTCKMSQLER, LGHPDTLNQGEFK, VIEHIMEDLDTNAD, NIETIINTFHQYSVK, LGHPDTLNQGEFKELVR, MHEGDEGPGHHHKPGLGEGTP
3351	<0.0001	81	65	0.84	2.32	Not applicable				
3423	0.0002	78	59	0.78	10.11					
3465	<0.0001	81	65	0.87	4.11					
RA *vs* MIA										
10 445	0.0023	79	64	0.77	1.35	P80511	365	<0.01	6	ELANTIK, GHFDTLSK, KGHFDTLSK, AAHYHTHKE, GHFDTLSKGELK, TKLEEHLEGIVNIFHQYSVR
10 839	0.0015	82	69	0.80	2.07	P05109	334	<0.01	10	GADVWFK, MGVAAHKK, MLTELEK, KGADVWFK, GNFHAVYR, SHEESHKE, ALNSIIDVYHK, LLETECPQYIR, LLETECPQYIRK, YSLIKGNFHAVYR
13 338	0.0429	61	80	0.71	0.92	P06702	643	<0.01	10	MSQLER, DLQNFLK, LTWASHEK, DLQNFLKK, MTCKMSQLER, LGHPDTLNQGEFK, VIEHIMEDLDTNAD, NIETIINTFHQYSVK, LGHPDTLNQGEFKELVR, MHEGDEGPGHHHKPGLGEGTP
3351	0.0429	71	56	0.67	3.40	Not applicable				
3423	0.0710	75	56	0.66	6.12					
3465	0.0454	75	56	0.70	5.94					

Statistical significance, cut-off value, AUC, specificity and sensitivity were obtained from Q10 (10 445, 10 839 and 13 338 Da biomarkers) or CM10 (3351, 3423 and 3465 Da biomarkers) SF profiling. Biomarker identification was performed by MALDI–TOF. AUC: area under the curve.

FIG. 2 Characterization by SF proteome profiling of biomarkers discriminating a RA population from MIA patients.

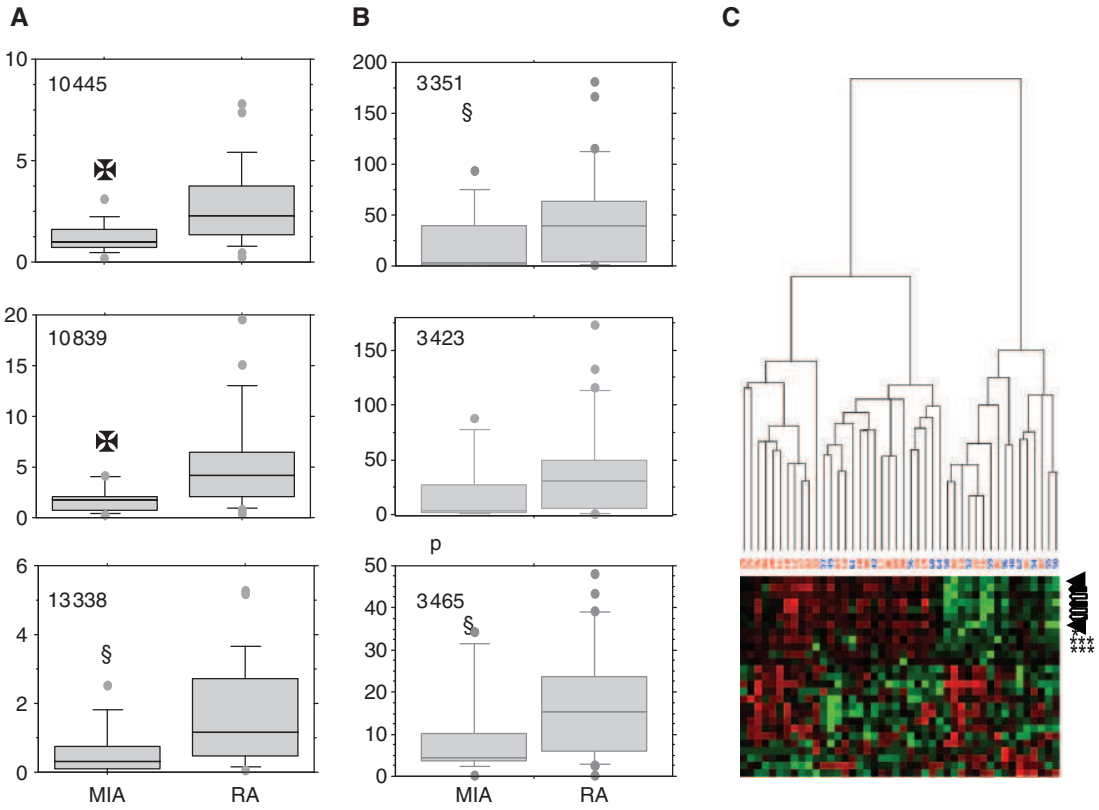

Relative SELDI–TOF-MS peak intensity of the 10 445, 10 839 and 13 338 Da proteins on Q10 array (**A**) and of 3351, 3423 and 3465 Da peptides on CM10 array (**B**). Boxes represent the interquartile range, the line across the box is the median and the whiskers represent the 5th and 95th percentile. $^{\star}P < 0.005$, $^{\S}P < 0.05$. Heat map visualization of the 27 biomarkers significantly differentially expressed in MIA *vs* RA SF (**C**). Enhancement of the 10 445 (←), 10 839 (⇐), 13 338 (**←**), 3351 (*) and 3465 Da (***) biomarkers in patients suffering from RA (red numbers) compared with MIA patients (blue numbers).

the three α-defensins by ELISA confirmed significant overexpression of these peptides in RA SF *vs* MIA SF [8.81 (6.83) *vs* 4.46 (7.48) ng/ml, $P = 0.006$]. Moreover, these values were greatly correlated with SELDI–TOF-MS peak intensity ($\rho = 0.722$, $P < 0.0001$).

Then we focused on the 10 445, 10 839 and 13 338 Da biomarkers, which are the most relevant biomarkers for the RA diagnosis. Three proteins at about 10 400, 10 800 and 13 300 Da were purified from a RA SF and were subjected to MS/MS analysis (Fig. 3). They were, respectively, identified as S100A12 (calgranulin C), S100A8 (also called MRP-8 or calgranulin A) and S100A9 (MRP-14 or calgranulin B) proteins (Table 2). The molecular masses of S100A12 (10 445 Da) and S100A8 (10 839 Da) were in agreement with their published masses of 10 444 and 10 835 Da [30]. The difference between the 13 338 Da peak and the S100A9 expected mass (13 243 Da) may be explained by phosphorylation at Thr113 as previously described [31]. Indeed, we confirmed by immunoblotting that S100A8 and S100A9 were increased in RA SF in comparison with OA or MIA SF (Fig. 3A). The relative intensities of bands correlated with SELDI–TOF-MS peak intensities (Fig. 3B and C). We also checked that several parameters did not influence the biomarker expression as evaluated by SELDI–TOF-MS (Table 3).

Origin of the S100A12, S100A8 and S100A9 proteins according to the disease

S100A12, S100A8 and S100A9 are mainly produced by PMN in inflammatory diseases. Although synovial levels of these proteins were significantly different between RA and MIA populations, no statistical difference in the synovial neutrophil count was observed (Table 1). Moreover, we found a significant correlation between peak intensity of S100A12, S100A8 and S100A9 and neutrophil count in the SF of MIA patients ($\rho = 0.965$, $P = 0.0005$; $\rho = 0.833$, $P = 0.0027$; and $\rho = 0.832$, $P = 0.0058$, respectively) but

Fig. 3 Identification of S100A12, S100A8 and S100A9 as biomarkers.

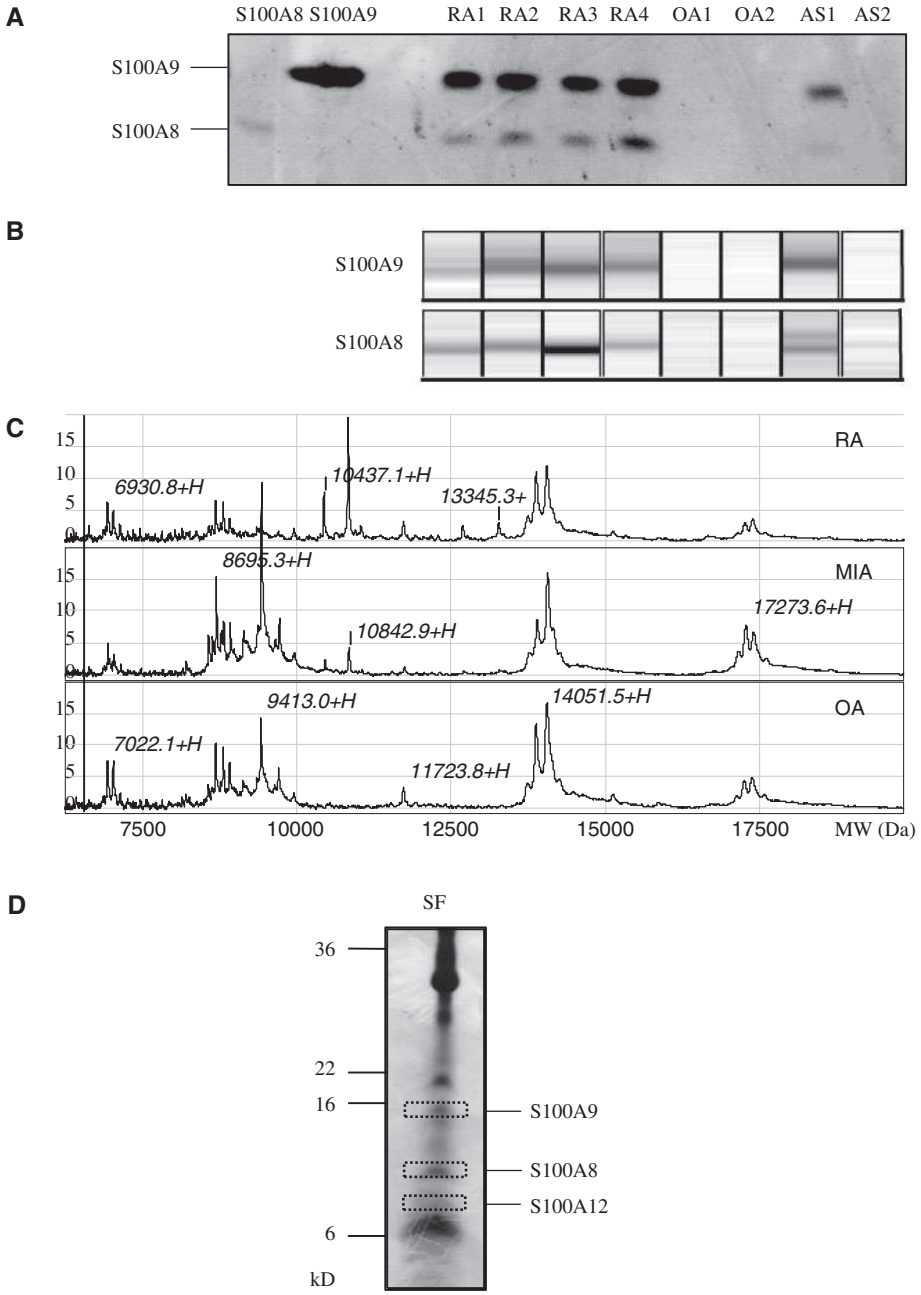

S100A8 and S100A9 immunoblotting (**A**), matching SELDI–TOF-MS peak intensity (**B**) and SELDI–TOF-MS fingerprint in RA, OA and AS SF (**C**). Three Coomassie blue stained gel bands migrating at about 10 400, 10 800 and 13 300 Da were cut off (broken lines) and subjected to MS/MS analysis (**D**).

not in the RA population ($\rho = 0.234$, $P = 0.25$; $\rho = 0.321$, $P = 0.12$; $\rho = 0.187$, $P = 0.39$, respectively) (Fig. 4A–C). Similarly, we demonstrated a statistical correlation between α-defensin concentration and neutrophil count in MIA SF ($\rho = 0.857$, $P = 0.003$) but not in RA SF ($\rho = 0.316$, $P = 0.18$) (Fig. 4D). Additionally, the α-defensin concentration was correlated with S100A12 ($\rho = 0.820$, $P = 0.003$), S100A8 ($\rho = 0.903$, $P = 0.001$) and S100A9 levels ($\rho = 0.934$, $P < 0.001$) in the MIA group, whereas in the RA population, no correlation could be found between

Table 3 Biomarker expression according to population characteristics and sample preparation

Biomarkers	Age			Gender			RF			Treatment			Frozen duration		
	< 55 years	⩾ 55 years	*P*-value	Male	Female	*P*-value	< 15 IU/ml	⩾ 15 IU/ml	*P*-value	No biological	Biologicals	*P*-value	< 2 years	> 2 years	*P*-value
S100A12															
Median (IQR)	2.3 (1.9–3.7)	2.3 (1.7–3.1)	0.950	2.4 (1.5–3.8)	2.3 (1.7–3.3)	0.924	2.3 (1.4–5.5)	2.3 (1.9–3.9)	0.535	2.6 (1.93.7)	2.1 (1.3–2.3)	0.198	5.6 (1.6–11.3)	2.3 (1.6–3.1)	0.794
S100A8															
Median (IQR)	3.9 (2.6–6.8)	3.9 (2.5–5.6)	0.901	3.6 (1.6–6.0)	4.3 (3.0–5.8)	0.680	3.6 (2.1–5.5)	5.7 (3.2–7.0)	0.214	5.3 (3.1–6.3)	3.3 (1.5–5.4)	0.292	2.5 (2.3–3.9)	4.3 (2.3–5.8)	0.884
S100A9															
Median (IQR)	1.3 (0.3–1.9)	1.2 (0.6–2.7)	0.950	1.2 (0.2–1.8)	1.3 (0.6–2.7)	0.504	1.2 (0.5–1.9)	1.5 (0.6–2.8)	0.457	1.3 (0.5–2.5)	1.1 (0.3–1.9)	0.412	4.5 (3.0–6.5)	1.2 (0.5–2.4)	0.999
α-Defensin-2															
Median (IQR)	43.3 (4.9–60.8)	39.2 (2.6–69.1)	0.158	14.0 (2.1–52.1)	49.4 (23.4–73.5)	0.273	16.8 (2.1–53.4)	54.1 (40.0–74.0)	0.051	45.5 (9.4–86.9)	43.3 (2.7–54.1)	0.594	28.6 (3.2–52.0)	49.4 (4.0–54.1)	0.999
α-Defensin-1															
Median (IQR)	33.2 (7.1–40.7)	35.1 (3.6–67.7)	0.205	13.9 (1.2–48.2)	35.8 (20.1–54.7)	0.247	15.3 (2.3–50.0)	37.3 (30.6–74.2)	0.072	36.9 (11.0–69.6)	15.9 (2.3–35.6)	0.332	16.0 (5.1–26.6)	37.1 (6.1–48.2)	0.528
α-Defensin-3															
Median (IQR)	16.0 (6.5–22.1)	12.4 (5.1–27.4)	0.371	6.8 (4.3–17.6)	18.1 (8.4–28.7)	0.319	6.6 (4.1–18.7)	20.8 (15.5–28.1)	0.111	15.8 (7.3–29.8)	17.5 (4.3–21.2)	0.734	84.2 (6.5–140.5)	54.1 (6.5–120.8)	0.698

Statistical significance was calculated from Q10 (S100 proteins) or CM10 (α-defensins) SELDI–TOF-MS protein biomarker intensities (i.e. peak height from baseline) using Mann–Whitney U-test. RF assessed by Waaler–Rose technique ($n < 15$ IU/ml).

Fig. 4 Origin of the S100A12, S100A8 and S100A9 proteins according to the disease.

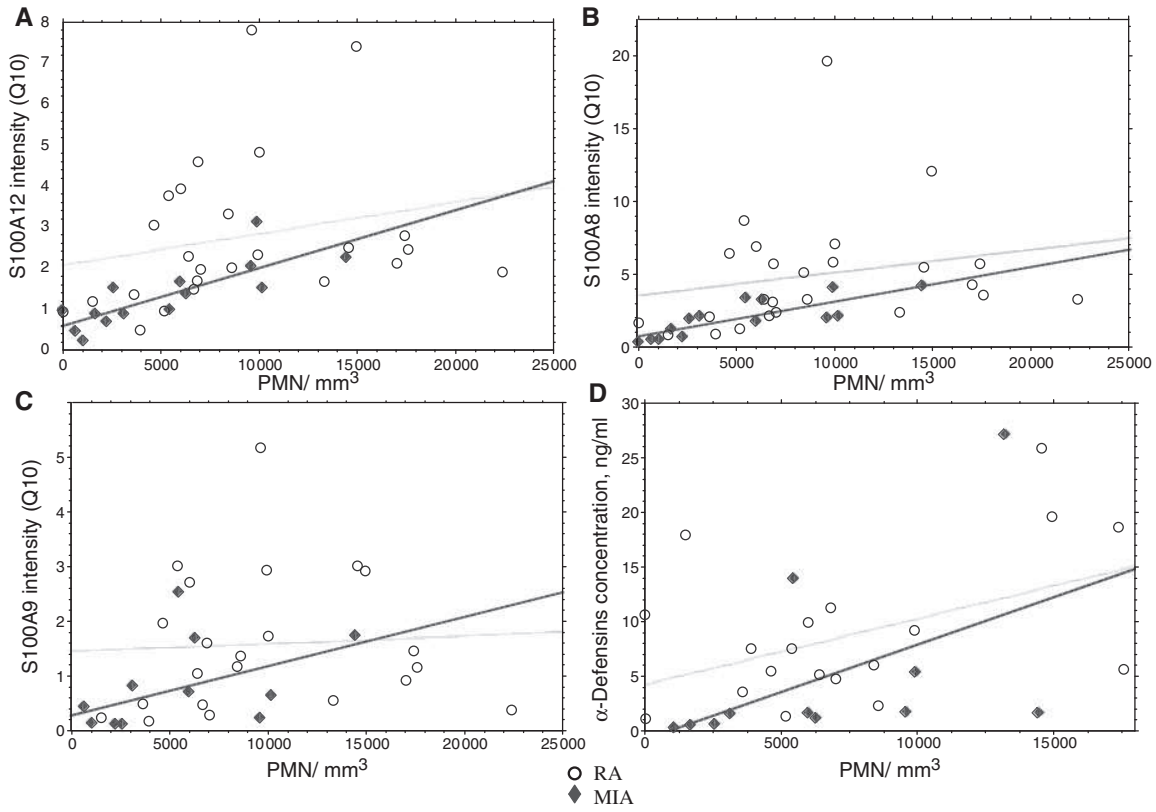

Correlation between PMN count in SF and SELDI–TOF-MS intensity of S100A8, S100A9 and S100A12 proteins on Q10 array or concentration of α-defensins assessed by ELISA. S100A12 (**A**), S100A8 (**B**), S100A9 (**C**) and α-defensin (**D**) concentration correlates with neutrophil count in MIAs, (bold line), but not in RA (broken line).

α-defensin concentration and S100A12 ($\rho = 0.277$, $P = 0.16$), S100A8 ($\rho = 0.292$, $P = 0.14$) or S100A9 intensity ($\rho = 0.289$, $P = 0.19$).

Serum proteome profiling

We also investigated the serum protein profiles of the three populations in order to determine whether serum could contain biomarkers as discriminating as those characterized in SF. Among 361 peaks detected in spectra of RA and OA samples, 21 were differentially expressed between both groups whereas comparison of RA and MIA populations showed only seven statistically differentially expressed proteins among 393 identified peaks. Contrary to the SF analysis, we did not detect any 10 444 and 3465 Da peaks in the serum of any population. Moreover, no statistical difference in the intensity of the other SF biomarkers, such as the 10 845 ($P = 0.76$), 13 338 ($P = 0.35$), 3351 ($P = 0.96$) and 3423 Da ($P = 0.83$) proteins was characterized when comparing RA spectra with the profile of other groups.

Discussion

The diagnosis of RA is often delayed because of the poor sensitivity of biological and radiological tests. The discovery of new biomarkers could lead to earlier diagnosis and treatment, a better understanding of the disease and to the development of new therapies. As arthritis is the hallmark of RA, we chose to evaluate in this study the proteome of the SF by high-throughput SELDI–TOF-MS technology. The proteomic profile of the RA group was compared with both an OA population, displaying little joint inflammation, and a MIA group, which exhibited a similar joint inflammation pattern. Among several proteins characteristic of RA, three peptides, the α-defensins-1, -2 and -3 were significantly increased in RA fluids compared with OA samples and to a lesser extent compared with MIA SFs. Though the best RA biomarkers were three proteins of 10 445, 10 839 and 13 338 Da (identified, respectively, as S100A12, S100A8 and S100A9 proteins), which discriminated not only RA from OA but also RA from other inflammatory arthritides with high sensitivity and specificity. Moreover, a statistical correlation was demonstrated

between synovial PMN concentration and levels of S100A8, S100A9, S100A12 and α-defensins in inflammatory joint diseases but not in RA, suggesting that these biomarkers were produced not only by neutrophil effusion but rather by RA synovial membrane.

Proteomic tests have been developed in the rheumatology field for several years. First 2D gel electrophoresis [32–35] and more recently, SELDI–TOF-MS technology [16–18] have been used to analyse the proteome of SF [32–34], blood [16, 17, 32, 33] or synovium [35] and to detect RA biomarkers compared with OA. All these surveys reported, among several markers, the enhancement of S100A8 in RA and/or S100A9 in SF [18, 32, 33], serum [16, 17] or tissue [35], sometimes associated with S100A12 [17, 32]. Levels of these inflammation markers correlated with the disease activity [34, 36, 37], radiological damage [37] and response to treatment [33, 38, 39]. In this study, we demonstrated that the synovial concentration of S100A8, S100A9 and S100A12 can also discriminate RA patients from other inflammatory arthritic patients. However, our results of serum proteome profiling showed few biomarkers compared with the SF proteome profiling.

S100A8, S100A9, S100A12 and α-defensins are mainly expressed by PMNs. Although it was not surprising that levels of these proteins were associated with neutrophil count in non-RA inflammatory arthritides, the absence of such a correlation in RA was noteworthy. Indeed α-defensins, which were detected in both synovial membrane [40] and SF [28], are also produced by other cells infiltrating the synovial tissue during RA such as B cells and NK lymphocytes. Moreover, an increase in S100A8 and S100A9 mRNA expression by fibroblast-like synoviocytes in a murine model of RA [41], has been reported and both S100A8 and S100A9 proteins were detected in synovial resident cells in the cartilage–pannus junction of RA synovial membranes [42]. Similarly, S100A12 cannot be found in healthy synovial tissue [38], but is strongly produced by RA synovial membrane. These data suggest that another cell type of the synovium may produce S100A8, S100A9 and S100A12 proteins in RA, potentially taking part in the disease pathogenesis.

Indeed, an increased body of evidence suggests that S100A8, S100A9 and S100A12 may be implicated in joint inflammation. First, S100A8 and S100A9 interfere with control mechanisms of inflammatory pain [43, 44]. Secondly, these proteins are involved in the activation of NADPH oxidase [26], leading to the production of reactive oxygen species and to cartilage destruction. Thirdly, S100A12 binds to RAGE [5, 7] of RA fibroblast-like synoviocytes, which induces *in vitro* a pseudo-tumoral phenotype characterized by a higher proliferation rate, invasiveness [45] and production of MMPs [46]. Moreover, S100A8, S100A9 and S100A12 are essential neutrophil chemokines [47] and stimulate the secretion of pro-inflammatory cytokines [6]. Finally, the enhanced cardiovascular morbidity in RA may be related to their ability to promote endothelial stress, atherosclerosis [48] and possibly acute coronary syndrome [49].

Our study underlines the potential use of the synovial expression of S100A8, S100A9 and S100A12 for RA diagnosis. As these proteins were detected in the synovium early during disease onset [42], their evaluation may be very helpful in undetermined early arthritides. Further studies are required to explore the possible link between increased S100A8 and S100A9 level and atherosclerosis in RA. Moreover, the control of their expression may represent a therapeutic target in RA, considering their proinflammatory properties.

Rheumatology key messages

- S100A8, S100A9 and S100A12 proteins are up-regulated in RA SF.
- S100A8, S100A9 and S100A12 proteins discriminate RA from other inflammatory arthritides.

Acknowledgements

We would like to thank Pr François Moutet and Pr Dominique Saragaglia for management and technical help.

Funding: This work was supported by unrestricted grants from Abbott France, Wyeth Pharmaceuticals France, the Région Rhône-Alpes (MIRA 2007–2008, ARCUS 2007–2008 and Emergence 2003–2006), the UFR Médecine from Joseph Fourier University (Vivier de la Recherche), the Groupement des Entreprises Françaises et Monégasques dans la Lutte contre le Cancer (Department of Grenoble), the Direction Régionale de la Recherche Clinique (CHU Grenoble), the Ligue Nationale contre le Cancer, the Association Nationale de Défense contre L'Arthrite Rhumatoïde, the CGD Research Trust 2006–2007, the Association Nationale de Défense contre L'Arthrite Rhumatoïde, the CNRS Institute and the Société Française de Rhumatologie.

Disclosure statement: The authors have declared no conflicts of interest.

References

1 Roux CH, Saraux A, Le Bihan E *et al*. Rheumatoid arthritis and spondyloarthropathies: geographical variations in prevalence in France. J Rheumatol 2007;34:117–22.

2 Leadbetter EA, Rifkin IR, Hohlbaum AM, Beaudette BC, Shlomchik MJ, Marshak-Rothstein A. Chromatin–IgG complexes activate B cells by dual engagement of IgM and Toll-like receptors. Nature 2002;416:603–7.

3 Matzinger P. The danger model: a renewed sense of self. Science 2002;296:301–5.

4 McInnes IB, Schett G. Cytokines in the pathogenesis of rheumatoid arthritis. Nat Rev Immunol 2007;7:429–42.

5 Leclerc E, Fritz G, Vetter SW, Heizmann CW. Binding of S100 proteins to RAGE: an update. Biochim Biophys Acta 2008;1793:993–1007.

6 Vogl T, Tenbrock K, Ludwig S *et al*. Mrp8 and Mrp14 are endogenous activators of Toll-like receptor 4, promoting

lethal, endotoxin-induced shock. Nat Med 2007;13:1042–9.

7 Ghavami S, Rashedi I, Dattilo BM *et al*. S100A8/A9 at low concentration promotes tumor cell growth via RAGE ligation and MAP kinase-dependent pathway. J Leukoc Biol 2008;83:1484–92.

8 Broome AM, Ryan D, Eckert RL. S100 protein subcellular localization during epidermal differentiation and psoriasis. J Histochem Cytochem 2003;51:675–85.

9 Seibert V, Wiesner A, Buschmann T, Meuer J. Surface-enhanced laser desorption ionization time-of-flight mass spectrometry (SELDI TOF-MS) and ProteinChip technology in proteomics research. Pathol Res Pract 2004;200:83–94.

10 Vorderwulbecke S, Kramer G, Merz F *et al*. Low temperature of GroEL/ES overproduction permits growth of *Escherichia coli* cells lacking trigger factor DnaK. FEBS Lett 2005;579:181–7.

11 Schellekens GA, Visser H, de Jong BA *et al*. The diagnostic properties of rheumatoid arthritis antibodies recognizing a cyclic citrullinated peptide. Arthritis Rheum 2000;43:155–63.

12 Clarke CH, Buckley JA, Fung ET. SELDI–TOF-MS proteomics of breast cancer. Clin Chem Lab Med 2005;43:1314–20.

13 Zhang Z, Bast RC Jr, Yu Y *et al*. Three biomarkers identified from serum proteomic analysis for the detection of early stage ovarian cancer. Cancer Res 2004;64:5882–90.

14 Albrethsen J, Bogebo R, Gammeltoft S, Olsen J, Winther B, Raskov H. Upregulated expression of human neutrophil peptides 1, 2 and 3 (HNP 1–3) in colon cancer serum and tumours: a biomarker study. BMC Cancer 2005;5:8.

15 Trocme C, Marotte H, Baillet A *et al*. Apolipoprotein A-I and platelet factor 4 are biomarkers for infliximab response in rheumatoid arthritis. Ann Rheum Dis 2008;68:1328–33.

16 de Seny D, Fillet M, Meuwis MA *et al*. Discovery of new rheumatoid arthritis biomarkers using the surface-enhanced laser desorption/ionization time-of-flight mass spectrometry ProteinChip approach. Arthritis Rheum 2005;52:3801–12.

17 de Seny D, Fillet M, Ribbens C *et al*. Monomeric calgranulins measured by SELDI–TOF mass spectrometry and calprotectin measured by ELISA as biomarkers in arthritis. Clin Chem 2008;54:1066–75.

18 Uchida T, Fukawa A, Uchida M, Fujita K, Saito K. Application of a novel protein biochip technology for detection and identification of rheumatoid arthritis biomarkers in synovial fluid. J Proteome Res 2002;1:495–9.

19 Pap T, Muller-Ladner U, Gay RE, Gay S. Fibroblast biology. Role of synovial fibroblasts in the pathogenesis of rheumatoid arthritis. Arthritis Res 2000;2:361–7.

20 Arnett FC, Edworthy SM, Bloch DA *et al*. The American Rheumatism Association 1987 revised criteria for the classification of rheumatoid arthritis. Arthritis Rheum 1988;31:315–24.

21 Altman R, Asch E, Bloch D *et al*. Development of criteria for the classification and reporting of osteoarthritis. Classification of osteoarthritis of the knee. Diagnostic and Therapeutic Criteria Committee of the American Rheumatism Association. Arthritis Rheum 1986;29:1039–49.

22 van der Linden S, Valkenburg HA, Cats A. Evaluation of diagnostic criteria for ankylosing spondylitis. A proposal for modification of the New York criteria. Arthritis Rheum 1984;27:361–8.

23 Petty RE, Southwood TR, Manners P *et al*. International League of Associations for Rheumatology classification of juvenile idiopathic arthritis: second revision, Edmonton, 2001. J Rheumatol 2004;31:390–2.

24 Tan EM, Cohen AS, Fries JF *et al*. The 1982 revised criteria for the classification of systemic lupus erythematosus. Arthritis Rheum 1982;25:1271–7.

25 Schagger H. Tricine-SDS-PAGE. Nat Protoc 2006;1:16–22.

26 Berthier S, Paclet MH, Lerouge S *et al*. Changing the conformation state of cytochrome b558 initiates NADPH oxidase activation: MRP8/MRP14 regulation. J Biol Chem 2003;278:25499–508.

27 Paclet MH, Berthier S, Kuhn L, Garin J, Morel F. Regulation of phagocyte NADPH oxidase activity: identification of two cytochrome b558 activation states. FASEB J 2007;21:1244–55.

28 Bokarewa MI, Jin T, Tarkowski A. Intraarticular release and accumulation of defensins and bactericidal/permeability-increasing protein in patients with rheumatoid arthritis. J Rheumatol 2003;30:1719–24.

29 Buhimschi IA, Buhimschi CS, Weiner CP *et al*. Proteomic but not enzyme-linked immunosorbent assay technology detects amniotic fluid monomeric calgranulins from their complexed calprotectin form. Clin Diagn Lab Immunol 2005;12:837–44.

30 McMorran BJ, Patat SA, Carlin JB *et al*. Novel neutrophil-derived proteins in bronchoalveolar lavage fluid indicate an exaggerated inflammatory response in pediatric cystic fibrosis patients. Clin Chem 2007;53:1782–91.

31 Lominadze G, Rane MJ, Merchant M, Cai J, Ward RA, McLeish KR. Myeloid-related protein-14 is a p38 MAPK substrate in human neutrophils. J Immunol 2005;174:7257–67.

32 Sinz A, Bantscheff M, Mikkat S *et al*. Mass spectrometric proteome analyses of synovial fluids and plasmas from patients suffering from rheumatoid arthritis and comparison to reactive arthritis or osteoarthritis. Electrophoresis 2002;23:3445–56.

33 Drynda S, Ringel B, Kekow M *et al*. Proteome analysis reveals disease-associated marker proteins to differentiate RA patients from other inflammatory joint diseases with the potential to monitor anti-TNFalpha therapy. Pathol Res Pract 2004;200:165–71.

34 Liao H, Wu J, Kuhn E *et al*. Use of mass spectrometry to identify protein biomarkers of disease severity in the synovial fluid and serum of patients with rheumatoid arthritis. Arthritis Rheum 2004;50:3792–803.

35 Tilleman K, Van Beneden K, Dhondt A *et al*. Chronically inflamed synovium from spondyloarthropathy and rheumatoid arthritis investigated by protein expression profiling followed by tandem mass spectrometry. Proteomics 2005;5:2247–57.

36 Wulffraat NM, Haas PJ, Frosch M *et al*. Myeloid related protein 8 and 14 secretion reflects phagocyte activation and correlates with disease activity in juvenile idiopathic arthritis treated with autologous stem cell transplantation. Ann Rheum Dis 2003;62:236–41.

37 Hammer HB, Odegard S, Fagerhol MK *et al*. Calprotectin (a major leucocyte protein) is strongly and independently correlated with joint inflammation and damage in rheumatoid arthritis. Ann Rheum Dis 2007;66:1093–7.

38 Foell D, Kane D, Bresnihan B *et al*. Expression of the pro-inflammatory protein S100A12 (EN-RAGE) in rheumatoid and psoriatic arthritis. Rheumatology 2003;42: 1383–9.

39 Foell D, Wittkowski H, Hammerschmidt I *et al*. Monitoring neutrophil activation in juvenile rheumatoid arthritis by S100A12 serum concentrations. Arthritis Rheum 2004;50: 1286–95.

40 Paulsen F, Pufe T, Conradi L *et al*. Antimicrobial peptides are expressed and produced in healthy and inflamed human synovial membranes. J Pathol 2002;198:369–77.

41 van Lent PL, Grevers L, Blom AB *et al*. Myeloid-related proteins S100A8/S100A9 regulate joint inflammation and cartilage destruction during antigen-induced arthritis. Ann Rheum Dis 2008;67:1750–8.

42 Youssef P, Roth J, Frosch M *et al*. Expression of myeloid related proteins (MRP) 8 and 14 and the MRP8/14 heterodimer in rheumatoid arthritis synovial membrane. J Rheumatol 1999;26:2523–8.

43 Dale CS, Pagano Rde L, Paccola CC *et al*. Effect of the C-terminus of murine S100A9 protein on experimental nociception. Peptides 2006;27:2794–802.

44 Mitchell K, Yang HY, Tessier PA *et al*. Localization of S100A8 and S100A9 expressing neutrophils to spinal cord during peripheral tissue inflammation. Pain 2008;134: 216–31.

45 Steenvoorden MM, Toes RE, Ronday HK, Huizinga TW, Degroot J. RAGE activation induces invasiveness of RA fibroblast-like synoviocytes in vitro. Clin Exp Rheumatol 2007;25:740–2.

46 Tolboom TC, Pieterman E, van der Laan WH *et al*. Invasive properties of fibroblast-like synoviocytes: correlation with growth characteristics and expression of MMP-1, MMP-3, and MMP-10. Ann Rheum Dis 2002;61:975–80.

47 Ryckman C, McColl SR, Vandal K *et al*. Role of S100A8 and S100A9 in neutrophil recruitment in response to monosodium urate monohydrate crystals in the air-pouch model of acute gouty arthritis. Arthritis Rheum 2003;48: 2310–20.

48 McCormick MM, Rahimi F, Bobryshev YV *et al*. S100A8 and S100A9 in human arterial wall. Implications for atherogenesis. J Biol Chem 2005;280:41521–9.

49 Altwegg LA, Neidhart M, Hersberger M *et al*. Myeloid-related protein 8/14 complex is released by monocytes and granulocytes at the site of coronary occlusion: a novel, early, and sensitive marker of acute coronary syndromes. Eur Heart J 2007;28: 941–8.

Article 5

S100A8 Production by Fibroblast-Like Synoviocytes Detected by Profiling of Rheumatoid Arthritis Synovium with a New Proteomic-Based Approach

S100A8 Production by Fibroblast-Like Synoviocytes Detected by Profiling of Rheumatoid Arthritis Synovium with a New Proteomic-Based Approach

Candice Trocmé[*,1,2] (PhD), Athan Baillet[*,1,3] (MD, M. Sc.), Sylvie Berthier[1], Marie Arlotto[4], Marc-André Hograindleur[1], Numa Mercier[5] (MD), Denis Corcella[6] (MD), Laurent Grange[1,3] (MD, PhD), François Berger[4] (MD, PhD), Robert Juvin[3] (MD, PhD), Françoise Morel[1] (PhD), Philippe Gaudin[1,3] (MD, PhD)

* Both authors contributed equally to this work

1: GREPI FRE3405 – AGIM – CNRS / Université Joseph Fourier / EPHE, Grenoble, France
2. Laboratory of Enzymology / BEP, CHU Hôpital Michallon, Grenoble / France
3: Rheumatology Department, CHU Hôpital Sud, Grenoble / France
4. Grenoble Institut Neurosciences, INSERM U836, Grenoble / France
5. Orthopedic Surgery Department, CHU Hôpital Sud, Grenoble / France
6. Hand Surgery Department, CHU Hôpital Michallon, Grenoble / France

Correspondence: Candice Trocmé
Laboratory of Enzymology / BEP
CHU Hôpital Michallon
BP 217
38043 Grenoble Cedex 9 / France
Tel :+33 (0)4 76 76 54 83
Fax : +33 (0)4 76 76 56 08
Email: ctrocme@chu-grenoble.fr

Running head: FLS produce S100A8 protein in RA synovium

The authors thank the "Société Française de Rhumatologie" and the "Délégation à la Recherche Clinique et à l'Innovation" of the CHU of Grenoble for their financial support.
The authors declare no conflict of interest

ABSTRACT

Objective: We investigated the proteome of the synovial tissue of patients suffering from rheumatoid arthritis (RA), non-inflammatory diseases (NI) and other control inflammatory pathologies (CI) in order to identify RA-specific biomarkers.

Methods: Protein profiling of 7 RA, 9 CI and 12 NI synovium was realized by a modified protocol of the SELDI-TOF-MS (Surface Enhanced Laser Desorption and Ionization Time-Of-Flight Mass Spectrometry) technique. Expression of one biomarker, the S100A8 protein, was evaluated in *in-vitro* cultured fibroblast-like synoviocytes (FLS) by confocal immunochemistry and ELISA measurement of S100A8 concentration in cell lysates.

Results: SELDI-TOF-MS was a reliable technique for direct biomarker detection in synovial tissue (correlation of duplicate values, Rho =0.648, $p<0.0001$). Comparison of RA synovium with either NI or CI synovial tissue retrieved respectively 53 and 69 proteins which were statistically differentially expressed. Among them, the human neutrophil peptide HNP-3 and the S100A8 protein were overexpressed in RA tissue in comparison with other synovium. Although S100A8 production is usually attributed to inflammatory cells, immunochemistry experiment and ELISA dosage demonstrated in FLS a cytosolic expression of S100A8 which was enhanced upon TNF-α and IL-1β stimulation only in RA.

Conclusion: Among the several RA biomarkers characterized in synovium by this original approach, S100A8 was found to be specifically overexpressed by RA-stimulated FLS.

INTRODUCTION

Discovery of rheumatoid arthritis (RA) related biomarkers is a challenge for early diagnosis and improvement of patient treatment. Indeed the currently available biologic tests are not precocious and accurate enough, leading to delayed diagnosis of the disease. We identified, in a previous study, specific RA biomarkers in synovial fluids using a SELDI-TOF-MS (Surface Enhanced Laser Desorption and Ionization Time-Of-Flight Mass Spectrometry) approach [Baillet *et al.* 2010]. We demonstrated that rise of S100A8/A9 proteins was not correlated to the inflammatory cell count in RA synovial fluid, contrary to other inflammatory diseases, suggesting they may be produced by another cell type. Considering the involvement of S100A8/A9 in RA etiopathogenesis, we aimed at discovering which cells produced these danger signals in order to improve the knowledge of the disease mechanisms.

In this study, we focused on the trigger zone of the RA clinical picture, the synovial tissue, that gets inflamed and proliferates during progression of the disease, using an original proteomic approach which was developed to allow the proteome analysis of tissue samples [Bouamrani *et al.* 2006]. We identified several RA biomarkers in the synovium, two among them being highly specific to RA compared to other rheumatic inflammatory diseases. Finally one of these biomarkers, the S100A8 protein, was shown to be expressed, in addition to phagocytes, by fibroblast-like synoviocytes (FLS).

PATIENTS AND METHODS

Patients

Twenty-eight patients were recruited in the Rheumatology department, according to local ethic committee recommendations. Synovial tissues were obtained during synovectomy of 7 RA patients fulfilling the 1987 modified ACR criteria, and 9 patients undergoing an idiopathic carpal tunnel surgery (control inflammatory group (CI)). The non-inflammatory group (NI) was composed of 6 patients with osteoarthritis (OA) and 6 patients undergoing arthroplasty after hip fracture. Synovial tissues were sent to the laboratory in dry ice and immediately stored at -80°C. The mean age in RA, CI and NI population (respectively 56.6±18.9, 48.8±14.5 and 59.4±21.1 years) and the sex ratio (85.7, 66.7 and 41.7% of the female patients) were not significantly different.

Sample processing and SELDI-TOF analysis

Ten µm slices of synovial tissues were obtained with a Leica Cryocut 1800 cryostat. Duplicate sections of each synovium were deposited on a cation exchange array (CM10), an anion exchange array (Q10) and a reversed phase array (H50). CM10 and Q10 analysis was performed as previously described [Bouamrani *et al.* 2006]. H50 arrays were incubated with 200 µl of binding buffer (10% acetonitrile, 0.1% trifluoroacetic acid) for 35 min. Then arrays were washed three times with the same buffer and after drying, loaded twice with 0.8 µl of saturated sinapinic acid in 50% acetonitrile, 0.5% trifluoroacetic acid. Arrays were analyzed on the SELDI-TOF PCS-4000 mass spectrometer with two laser intensities (3200 nJ and 4500 nJ). Spectra of one RA, one CI and 4 NI samples were removed from the statistical analysis of the experiment because of blood contamination.

Isolation and culture of fibroblast-like synoviocytes (FLS)

Synoviocytes were isolated by centrifugation (1800g – 15 min – RT) from the synovial fluids of 3 RA and 2 NI patients. Collected cells were washed in Dulbecco's modified Eagle's medium (DMEM) and cultured in 6-well plates in the same medium containing 10% foetal calf serum (FBS), 100 U/ml penicillin and 100 µg/ml streptomycin. Medium was changed daily the next two days to remove non-adherent cells. Adherent cells which were round (macrophages) or spindle-shaped (FLS) were grown until the latter cells reached confluence (macrophages do not proliferate). Cells were treated with trypsin 0.25% for 15 min at 37°C:

only FLS came off and were passaged to new culture flasks. The phenotype of synovial fluid-derived synoviocytes was previously shown to be similar to synovium-derived synoviocytes [Neidhart *et al.* 2003].

Confocal microscopy

Confocal microscopy experiments were performed as previously described [Baillet *et al.* 2011b]. Briefly, RA synoviocytes, grown on cover-slips were fixed with 4% (w/v) paraformaldehyde for 10 min. Auto-fluorescence was quenched with 50mM NH_4Cl. FLS were permeabilised with 0.1% (w/v) Triton X-100, washed twice with PBS and subsequently incubated with either home-made monoclonal antibody specific to the complex S100A8/A9 (5A10 - 0.1 µg/ml) or control isotype mouse IgG1 antibody for 1 hour. Then cells were incubated with 100 µl (1:250) of Alexa Fluor 488 goat anti-mouse IgG and nuclei were stained with 0.5 µg/ml Hoechst 33258. FLS were imaged using the inverted confocal and two-photon laser-scanning microscope (LSM 510 NLO, Carl Zeiss) equipped with a x63/1.3 Plan-Neofluar oil immersion objective.

S100A8 expression by synoviocytes

Cells were washed twice in DMEM and cultured for 18h in 0.5% FBS and some synoviocytes were stimulated by TNF-α (5 ng/ml) and IL-1β (2 ng/ml). Cells were trypsinised, washed, suspended in PBS and lysed by 5 freeze-thaw cycles and protein concentration was measured by the Bradford method. S100A8/A9 level in lysates was evaluated by ELISA (BMA Biomedicals, Augst, Switzerland) and concentration was expressed as ng S100A8/A9 / mg protein.

Statistics

Mann–Whitney U-test was used to compare SELDI–TOF-MS peak intensities. Reproducibility of spectra was assessed by evaluation of the duplicate variability of the 10 most differentially expressed biomarkers by the Pearson's correlation coefficient.

RESULTS

Reproducibility of the proteome profiling of synovium by SELDI-TOF-MS

Two pieces of synovial tissue sliced withdrawn 40 to 60 µm apart were analyzed for each sample. We first checked that reproductive data were recovered on each type of arrays. As shown on Figure 1, spectra obtained from two pieces of one synovial tissue were identical, showing the validity of SELDI-TOF for the analysis of synovium proteome. Only the protein profile changed according to the type of array and the group of tissue sample (Figure 1). The reliability of this approach was shown by a significant correlation between duplicates ($Rho=0.648$, $p<0.0001$).

Discovery of RA-specific biomarkers in synovium

In a previous study [Baillet *et al.* 2010], levels of several myeloid-restricted proteins did not correlate to the count of polymorphonuclear neutrophils (PMN) in RA synovial fluid suggesting that these proteins may be produced in RA synovium. To test this hypothesis, protein profiles were compared to characterize RA biomarkers in synovial tissues. Among 216 proteins detected in NI and RA synovial tissues, 53 were differentially expressed in both populations ($p<0.05$). Comparison of the proteome of CI and RA synovium identified 199 proteins, among which 69 were differentially expressed between both groups. Some of these biomarkers, only characterized by their molecular weight and the type of array they bound to, were previously identified in another SELDI-TOF study (1). We showed here that human neutrophil peptide (HNP)-1 (3.42 kDa), HNP-3 (3.47 kDa), S100A12 (10.44 kDa) and S100A8 (10.84 kDa) were overexpressed in RA synovium in comparison to NI synovial tissue. Moreover S100A8 and HNP-3 were also upregulated in RA synovium compared to CI synovial tissue (Figure 2), confirming our hypothesis of an ectopic production of these proteins apart from synovial fluid leukocytes.

S100A8 production by RA FLS

Since synovium contains several resident cell types and is sometimes infiltrated by myeloid cells, we aimed at precising which cell type produce S100A8 in RA synovium. Therefore, the expression of S100A8 by FLS isolated from synovial fluid was examined. First S100A8 was investigated in FLS by confocal microscopy with an antibody reacting with the complex S100A8/A9, as both proteins associated to form a heterodimer [Teigelkamp *et al.* 1991] : S100A8 was found in the cytosol of RA FLS, as well as in NI synoviocytes (Figure 3).

Similarly S100A8 was detected at a low level by ELISA in lysates of non-stimulated FLS, whether cells were isolated from RA (79.5 ng/mg prot) or NI (84.3 ng/mg prot) synovial fluids. The S100A8 concentration increased greatly in the lysates of RA synoviocytes (195.6 % of non-stimulated cells) compared to NI cells (103.9 %).

DISCUSSION

Most of the studies looking for diagnosis biomarkers of RA investigated fluids distant from the disease specific site, i.e. synovium, such as blood or synovial fluid. We analyzed the proteome of the synovial tissue in order to characterize RA biomarkers in the tissue directly affected by the disease pathological events. Although such proteomic studies were previously done by others [Tilleman *et al.* 2005], it is the first time that the SELDI-TOF technology was used to analyze the protein content of the synovium.

The SELDI-TOF technology, albeit sometimes criticized about its low resolution, is nowadays approved by regulatory agencies for the investigation of biological fluids with high sensitivity. We reported here a new reproducible technique of tissue proteome analysis without protein extraction, which decreased the step number of the analysis and therefore reduced experimental bias and mistakes. We identified, using this method, several RA biomarkers in synovial tissue. Comparison of these proteins to results of a previous study characterizing RA biomarkers in synovial fluids [Baillet *et al.* 2010] revealed that most of them were specific to synovium, as they were only retrieved in synovial tissue. Indeed only 5 common biomarkers were recovered in both types of samples. Among them, the S100A8 protein and the human neutrophil peptide HNP-3, which were up-regulated in RA synovial fluids (1), were also significantly increased in RA synovium compared to non-inflammatory diseases, as well as to other inflammatory conditions.

S100A8 and S100A9 levels are increased in rheumatic diseases, mainly because of an overexpression by inflammatory cells such as infiltrating macrophages [Sunahori *et al.* 2006] and PMN [Van Lent *et al.* 2008a]. However expression of S100A8 was characterized in CD68-/CD3- mononuclear cells of a juvenile rheumatoid arthritis biopsy [Frosch *et al.* 2000] and a differential localization of S100A8 and CD68 was also shown in an immunohistochemistry experiment of a psoriatic arthritis synovial tissue [Kane *et al.* 2003]. Both studies suggested, like our research, that S100A8 expression was not restricted to inflammatory cells. Indeed S100A8/A9 was also identified in chondrocytes [Van Lent *et al.* 2008b] and osteoblasts [Zreiqat *et al.* 2007], but the expression of this protein by the main cell type of the synovial tissue, the FLS, was never investigated. Immunochemistry and measurement of S100A8 concentration in FLS lysates by ELISA showed that S100A8 was expressed in the cytosol of FLS. Both RA and NI synoviocytes produced S100A8, but cell stimulation by TNF-α and IL-1β induced a rise of S100A8 content only in RA FLS, suggesting that the inflammatory environment of FLS was not sufficient to increase the

biomarker concentration, and that a RA-specific pattern of FLS was required. S100A8 expression by FLS was minor compared to its production by phagocytes (about 10 ng for 10^6 FLS in this study vs. 3.6 µg for 10^6 RA macrophages) [Sunahori *et al.* 2006]. However the high proliferation rate of FLS stimulated by proinflammatory cytokines in RA synovium may produce locally a significant amount of S100A8. This release of S100A8 protein by stimulated RA FLS may contribute to the discrepancy between the PMN count and the S100 levels in synovial fluid from RA patients, contrasting with other inflammatory conditions where S100 rate correlates with PMN count. However these results need to be confirmed on more FLS cultures.

Another striking result of our study was that the upregulation, in RA synovium, of S100A8 was not linked with an increase of S100A9, despite S100A8 most frequently forming a heterodimer with S100A9 [Teigelkamp *et al.* 1991]. This may be explained by the higher hydrophobicity of S100A9 compared to S100A8 [Itou *et al.* 2002], which then binds lightly on SELDI-TOF arrays, as it was shown previously by the differential intensity of both proteins in SELDI-TOF spectra (about 5 for S100A8 and 1 for S100A9 in RA) (1).

The critical role of S100A8/A9 proteins in joint inflammation and cartilage destruction has been thoroughly examined [Van Lent *et al.* 2008a]. Their expression is dramatically enhanced in inflamed joints [Van Lent *et al.* 2008b]. S100A8/A9 release from both infiltrating and residents cells is implicated in the breakdown of cartilage through up-regulation of metalloproteinases [Van Lent *et al.* 2008b]. Indeed, S100A8/A9 that were first identified as cytosolic proteins implicated in ROS production via NADPH oxidase activation [Berthier *et al.* 2003], are nowadays considered as DamageAssociated Molecular Pattern molecules (DAMPs) initiating and maintaining the inflammatory response through the stimulation of the innate immunity receptor TLR-4 [Vogl *et al.* 2007].

This study identified several RA biomarkers in synovium, some of them being also recovered in synovial fluids. The S100A8 protein was confirmed to be highly specific to RA, probably because its expression was induced in stimulated proliferating RA FLS. The production of S100A8 in RA FLS may drive the initiation and/or development of the arthritis. Thus pharmaceutical targeting of S100A8/A9 proteins may be particularly relevant and may offer some new therapeutic strategies for RA patients.

REFERENCES

1. Baillet A, Trocme C, Berthier S, Arlotto M, Grange L, Chenau J, et al. Synovial fluid proteomic fingerprint: S100A8, S100A9 and S100A12 proteins discriminate rheumatoid arthritis from other inflammatory joint diseases. Rheumatology (Oxford) 2010;49:671-82.
2. Bouamrani A, Ternier J, Ratel D, Benabid AL, Issartel JP, Brambilla E, et al. Direct-tissue SELDI-TOF mass spectrometry analysis: a new application for clinical proteomics. Clin Chem 2006;52:2103-6.
3. Neidhart M, Seemayer CA, Hummel KM, Michel BA, Gay RE, Gay S. Functional characterization of adherent synovial fluid cells in rheumatoid arthritis: destructive potential in vitro and in vivo. Arthritis Rheum 2003;48:1873-80.
4. Baillet A, Xu R, Grichine A, Berthier S, Morel F, Paclet MH. Coupling of 6-phosphogluconate dehydrogenase with NADPH oxidase in neutrophils: Nox2 activity regulation by NADPH availability. Faseb J 2011;25:2333-43.
5. Teigelkamp S, Bhardwaj RS, Roth J, Meinardus-Hager G, Karas M, Sorg C. Calcium-dependent complex assembly of the myeloic differentiation proteins MRP-8 and MRP-14. J Biol Chem 1991;266:13462-7.
6. Tilleman K, Van Beneden K, Dhondt A, Hoffman I, De Keyser F, Veys E, et al. Chronically inflamed synovium from spondyloarthropathy and rheumatoid arthritis investigated by protein expression profiling followed by tandem mass spectrometry. Proteomics 2005;5:2247-57.
7. Sunahori K, Yamamura M, Yamana J, Takasugi K, Kawashima M, Yamamoto H, et al. The S100A8/A9 heterodimer amplifies proinflammatory cytokine production by macrophages via activation of nuclear factor kappa B and p38 mitogen-activated protein kinase in rheumatoid arthritis. Arthritis Res Ther 2006;8:R69.
8. van Lent PL, Grevers L, Blom AB, Sloetjes A, Mort JS, Vogl T, et al. Myeloid-related proteins S100A8/S100A9 regulate joint inflammation and cartilage destruction during antigen-induced arthritis. Ann Rheum Dis 2008;67:1750-8.
9. Frosch M, Strey A, Vogl T, Wulffraat NM, Kuis W, Sunderkotter C, et al. Myeloid-related proteins 8 and 14 are specifically secreted during interaction of phagocytes and activated endothelium and are useful markers for monitoring disease activity in pauciarticular-onset juvenile rheumatoid arthritis. Arthritis Rheum 2000;43:628-37.
10. Kane D, Roth J, Frosch M, Vogl T, Bresnihan B, FitzGerald O. Increased perivascular synovial membrane expression of myeloid-related proteins in psoriatic arthritis. Arthritis Rheum 2003;48:1676-85.
11. van Lent PL, Grevers LC, Blom AB, Arntz OJ, van de Loo FA, van der Kraan P, et al. Stimulation of chondrocyte-mediated cartilage destruction by S100A8 in experimental murine arthritis. Arthritis Rheum 2008;58:3776-87.
12. Zreiqat H, Howlett CR, Gronthos S, Hume D, Geczy CL. S100A8/S100A9 and their association with cartilage and bone. J Mol Histol 2007;38:381-91.
13. Itou H, Yao M, Fujita I, Watanabe N, Suzuki M, Nishihira J, et al. The crystal structure of human MRP14 (S100A9), a Ca(2+)-dependent regulator protein in inflammatory process. J Mol Biol 2002;316:265-76.
14. Berthier S, Paclet MH, Lerouge S, Roux F, Vergnaud S, Coleman AW, et al. Changing the conformation state of cytochrome b_{558} initiates NADPH oxidase activation: MRP8/MRP14 regulation. J Biol Chem 2003;278:25499-508.
15. Vogl T, Tenbrock K, Ludwig S, Leukert N, Ehrhardt C, van Zoelen MA, et al. Mrp8 and Mrp14 are endogenous activators of Toll-like receptor 4, promoting lethal, endotoxin-induced shock. Nat Med 2007;13:1042-9.

ACKNOWLEDGMENTS

The authors also thank Dr Alexeï Grichine for his support in confocal microscopy experiments.

LEGENDS

Figure 1. Duplicate spectra of three synovial tissues obtained by SELDI-TOF analysis on Q10 arrays

Figure 2. Relative SELDI-TOF peak intensity of S100A8 and HNP-3 on CM10 array. Boxes represent the interquartile range, the line across the box is the median and the whiskers represent the 5^{th} and 95^{th} percentile. ✠$p<0.005$, ‡$p<0.01$, §$p<0.05$.

Figure 3. Expression of S100A8 expressed in RA fibroblast-like synoviocytes. Confocal analysis of cultured synoviocytes isolated from RA and NI synovial fluids. S100A8 is depicted in green and nucleus is colored in blue. Mouse monoclonal IgG1 was used as control antibody.

Figure 1

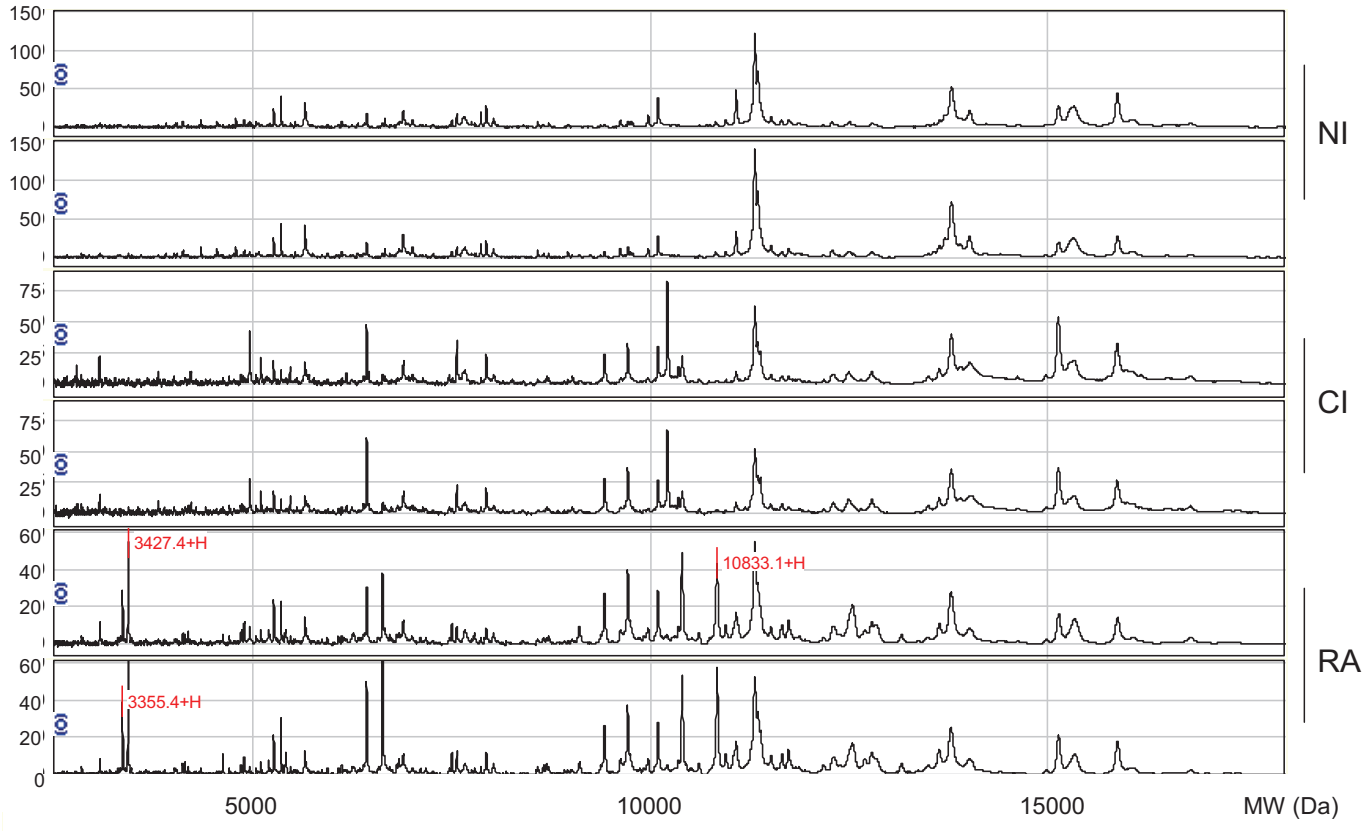

Figure 1. Duplicate spectra of three synovial tissues obtained by SELDI-TOF analysis on Q10 arrays.

Figure 2

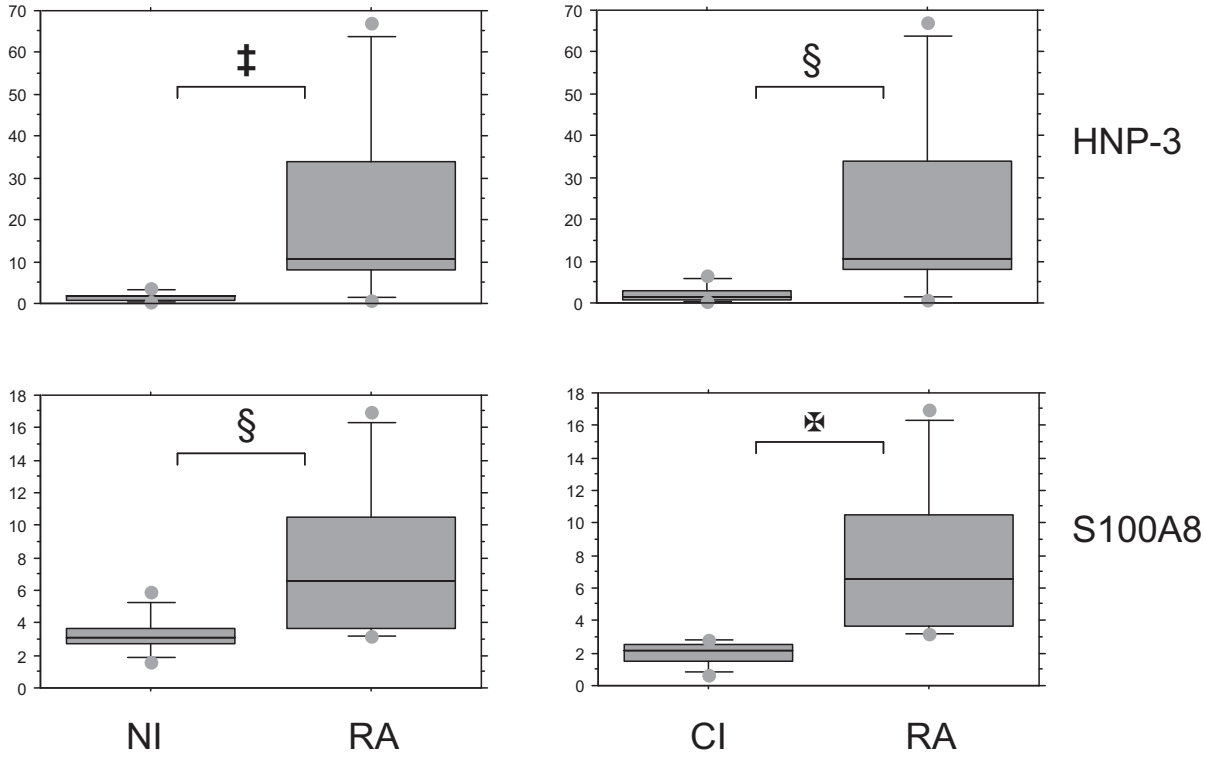

Figure 2. Relative SELDI-TOF peak intensity of S100A8 and HNP-3 on CM10 array.

Boxes represent the interquartile range, the line across the box is the median and the whiskers represent the 5th and 95th percentile. ✠p<0.005, ‡p<0.01, §p<0.05.

Figure 3

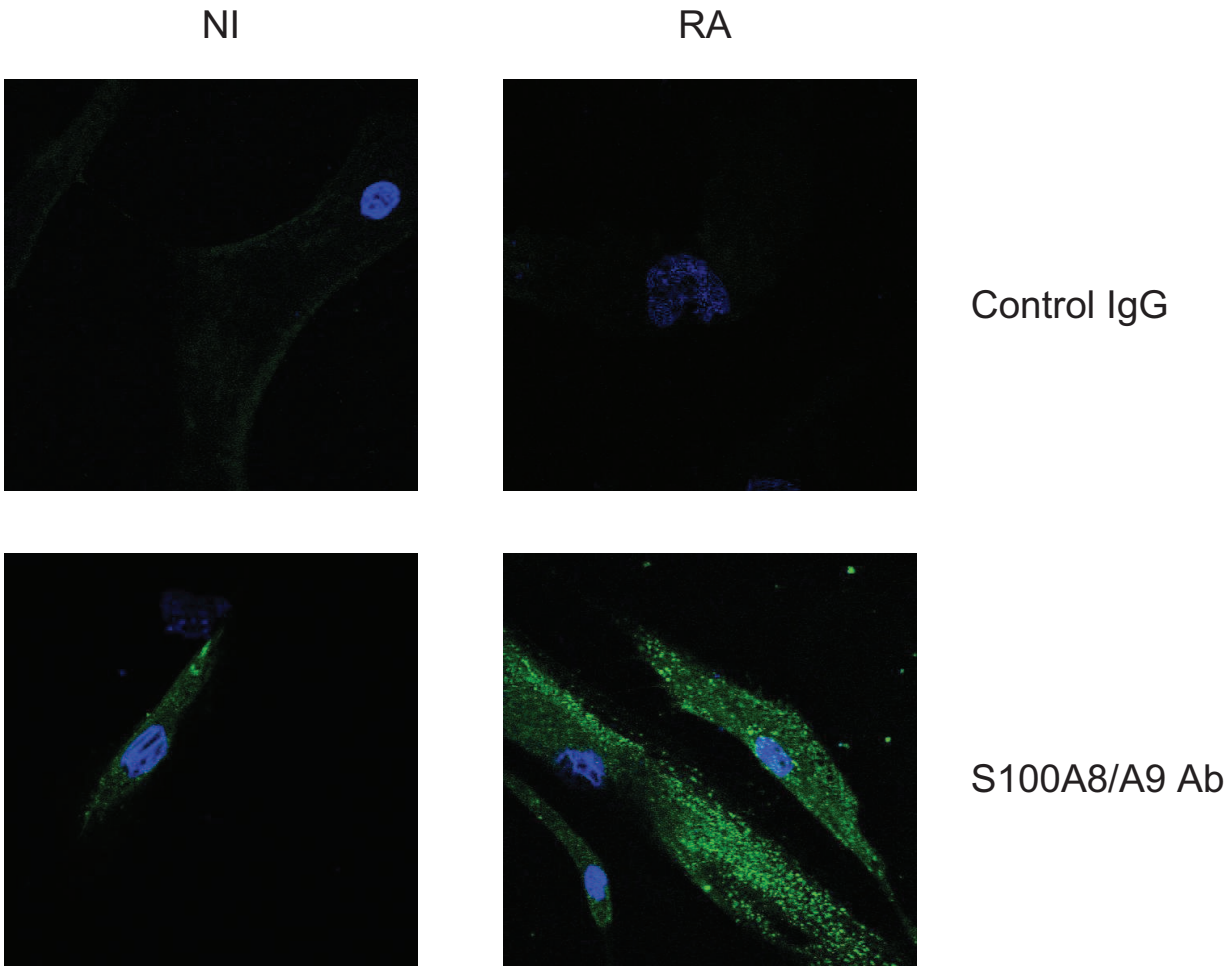

Figure 3. Expression of S100A8 expressed in RA fibroblast-like synoviocytes.

Confocal analysis of cultured synoviocytes isolated from RA and NI synovial fluids. S100A8 is depicted in green and nucleus is colored in blue. Mouse monoclonal IgG1 was used as control antibody.

DISCUSSION GENERALE

La production de ROS par le phagocyte est un mécanisme essentiel de défense de l'immunité innée vis-à-vis des pathogènes. L'activité de la NADPH oxydase phagocytaire résulte de l'assemblage des facteurs cytosoliques $p67^{phox}$, $p47^{phox}$, $p40^{phox}$ et Rac1/2 au niveau du cytochrome b_{558} et en particulier de son cœur catalytique, NOX2. L'existence de partenaires spécifiques de la NADPH oxydase est suggérée par l'explosion oxydative des PMNs qui est notoirement différente de la production de ROS de cellules non-phagocytaires telles que le lymphocyte B sur le plan qualitatif et quantitatif. Le potentiel délétère de la production de ROS sur les tissus est tel que l'activité catalytique de la NADPH oxydase nécessite d'être étroitement régulée afin d'atteindre rapidement son acmé, pour une bactéricidie optimale, sans occasionner de lésions tissulaires de type peroxydation lipidique excessive et oxydation incontrôlée des protéines ou de l'ADN. L'activité NADPH oxydase doit donc être finement adaptée à l'environnement cellulaire ainsi qu'au statut énergétique cellulaire. Nous nous sommes focalisés, d'une part, sur les partenaires potentiels de NOX2, 6PGDH et PFK2, co-purifiés avec le complexe cytosolique de la NADPH oxydase des PMNs et d'autre part notre intérêt s'est porté sur le rôle des protéines S100A8/A9, spécifiques du PMN, dans l'activation de la NADPH des phagocytes.

Notre objectif a été tout d'abord d'asseoir l'implication de la PFK2 et de la 6PGDH dans l'activation de l'oxydase. En d'autres termes, il nous a fallu déterminer si la co-purification des enzymes du métabolisme du glucose, 6PGDH et PFK2, et du complexe NADPH oxydase des PMNs procédait d'une co-localisation fortuite ou d'une interaction spécifique régulant l'activité catalytique.
Dans un deuxième temps, nous avons tenté de mieux caractériser l'interaction entre le cytochrome b_{558} et l'hétérocomplexe S100A8/A9 tout en tâchant de clarifier les mécanismes par lesquels ces protéines activent la NADPH oxydase phagocytaire.

I. Spécificité de l'implication de la 6PGDH et de la PFK2 dans l'activité NADPH oxydase des phagocytes

Ce travail suggère que la 6PGDH et la PFK2 sont deux nouveaux régulateurs de la NADPH oxydase phagocytaire. Lors de la stimulation des neutrophiles, ces enzymes du métabolisme du glucose migrent à la membrane et s'associent aux autres facteurs cytosoliques de la NADPH oxydase phagocytaire. La 6PGDH augmente l'affinité de NOX2 pour son substrat ainsi que la concentration de substrat, le NADPH. La PFK2 stimule la production d'ATP

disponible, d'une part pour la phosphorylation de $p47^{phox}$ et d'autre part pour la Nucleoside diphosphate Kinase (NDPK). Cette dernière enzyme pourrait secondairement activer Rac en catalysant la synthèse de GTP à partir d'ATP (**Figure 27**).

Notre étude confirme de précédents travaux qui avaient souligné une chute de l'activité NADPH oxydase lors de l'inhibition de la glycolyse par inactivation de la PFK1 [Anderson *et al.* 1991] ou de la glycéraldéhyde-3-phosphate déshydrogénase (G3PDH), $6^{ème}$ enzyme de la glycolyse [Anderson *et al.* 1990]. De même, lors de la grossesse, la diminution de translocation de la 6PGDH à la membrane plasmique des PMNs en réponse à un stimulus inflammatoire s'accompagne d'une baisse de production de ROS par la NADPH oxydase des phagocytes [Cotton *et al.* 1983].

Le couplage de l'activité NADPH oxydase avec les produits des voies métaboliques de la glycolyse ou des pentoses phosphates semble cohérent au regard des besoins en ATP et en NADPH lors de l'explosion oxydative. Dans la glycolyse et la voie des pentoses phosphates, enzymes et substrats sont rassemblés près de la membrane plasmique, ce qui va favoriser une vitesse réactionnelle optimale. Cette compartimentation, sans membrane, pourrait être l'occasion de positionner aussi certaines de ces enzymes au voisinage direct de la NADPH oxydase. Le rôle de partenaires de régulation pour la 6PGDH et la PFK2 est suggéré à plusieurs stades de notre travail :

Premièrement, au stade initial du recrutement des facteurs cytosoliques de la NADPH oxydase, les expériences de co-immunoprécipitation et de microscopie confocale indiquent une association entre les facteurs cytosoliques $p67^{phox}$, $p47^{phox}$ et $p40^{phox}$ d'une part et la PFK2 ainsi que la 6PGDH d'autre part. Cette interaction, est constatée lors de l'activation de la NADPH oxydase mais n'est pas observée dans les cellules au repos suggérant que l'association entre ces enzymes du métabolisme du glucose et les facteurs cytosoliques intervient spécifiquement lors de l'assemblage du trimère $p67^{phox}$/$p47^{phox}$/$p40^{phox}$.

De plus, nous n'avons pu mettre en évidence, dans le cytosol de PMNs activés, une co-immunoprécipitation entre la 6PGDH ou la PFK2 et Rac qui est transféré à la membrane plasmique indépendamment des autres facteurs cytosoliques [Heyworth *et al.* 1994]. Il semble donc qu'à ce stade précoce de l'activation de l'oxydase, le recrutement de $p67^{phox}$ soit associé à la mobilisation de la PFK2 et de la 6PGDH. La proximité entre la 6PGDH et $p67^{phox}$ pourrait faciliter la fixation du NADPH sur $p67^{phox}$ [Smith *et al.* 1996]. Le transfert de

l'élément activateur, $p67^{phox}$, sur le cytochrome b_{558} est donc contemporain et contigu du transfert à la membrane plasmique de la PFK2 et de la 6PGDH. Ces deux enzymes délivrent localement d'importantes concentrations de NADPH ou d'ATP impliqués dans la stimulation de l'activité catalytique de l'oxydase par phosphorylation de NOX2 [Raad *et al.* 2009] ou l'activation de Rac de manière indirecte par la NDPK [Guignard *et al.* 1996; Mizrahi *et al.* 2005]. Le couplage de la NDPK avec une GEF ("Guanine nucleotide Exchange Factor") permet d'activer Rac en convertissant l'ATP produit par la glycolyse en GTP [Otsuki *et al.* 2001; Palacios *et al.* 2002]. En outre, l'ATP cytosolique régule l'homéostasie du cytosquelette qui est un élément clé de l'activation de l'oxydase dans le PMN [El Benna *et al.* 1994b; Quinn *et al.* 1989]. D'une part, l'ATP est indispensable à la polymérisation du cytosquelette, mais d'autre part, il est probablement engagé dans l'inactivation de la NADPH oxydase par la chélation du magnésium (Mg^{++}) en stabilisant les filaments d'actine (actine-F) [Tamura *et al.* 2001]. Plusieurs études indiquent que le traitement du PMN par la toxine botulique C2 ou la cytochalasine B, inhibiteurs de la polymérisation de l'actine globulaire (actine G) en actine F, augmente l'activité NADPH oxydase [Al-Mohanna *et al.* 1987a; Al-Mohanna *et al.* 1987b; Hawkins 1973; Norgauer *et al.* 1988]. Cependant, le lien de causalité entre la diminution de la polymérisation de l'actine et l'augmentation de l'activité NADPH oxydase est contestable. En effet, ces inhibiteurs modifient également la production de messagers secondaires. Par exemple, la cytochalasine B augmente la production de phosphoinositides dans les thymocytes stimulés par la concavaline A [Treves *et al.* 1987]. L'utilisation de la tétracaïne, un agent favorisant la polymérisation de l'actine, conduit également à une augmentation de l'activité NADPH oxydase de PMNs stimulés par le fMLP [Bengtsson *et al.* 1991], si bien qu'il est difficile de conclure sur le rôle direct de la polymérisation de l'actine sur l'activité catalytique de NOX2.

Deuxièmement, au niveau de la membrane plasmique les expériences de microcopie confocale plaident en faveur d'une proximité entre la NADPH oxydase et la PFK2 et la 6PGDH. La co-localisation de la PFK2 et de la 6PGDH avec respectivement NOX2 et $p67^{phox}$ n'est pas un argument suffisant pour affirmer l'interaction spécifique de ces 2 enzymes avec la NADPH oxydase des phagocytes. Cependant, nos résultats révèlent un rationnel fonctionnel pour une telle association. En effet, la proximité entre, d'une part la NADPH oxydase et d'autre part la PFK2 ou la 6PGDH, a été décelée dans une zone métaboliquement active, les radeaux lipidiques, où il est habituel de constater des interactions entre protéines participant à un même processus physiologique. Ces micro-domaines membranaires sont des

plateformes qui permettent une interaction privilégiée par contiguïté. Outre l'amélioration des interactions protéines-protéines, cette micro-compartimentation permet une augmentation circonscrite de la quantité de NADPH au-delà de la concentration cytosolique à laquelle la vitesse catalytique de la NADPH oxydase n'est pas maximale. Par ailleurs, le couplage d'enzymes de la voie des pentoses phosphates et de la glycolyse potentialise la production du substrat de la NADPH oxydase [Kindzelskii *et al.* 2004].

Troisièmement, la participation de la 6PGDH et de la PFK2 dans l'activation de la NADPH oxydase n'a été suggérée que pour le PMN [Paclet *et al.* 2007]. Les fractions contenant le complexe NADPH oxydase purifié à partir de cytosol et de membrane de lymphocyte B ne contiennent pas ces deux enzymes. La présence de mitochondries fonctionnelles dans la lignée lymphoïde permet une synthèse d'ATP par la chaîne respiratoire. Contrairement aux lymphocytes B, les PMNs sont entièrement dépendants de la glycolyse pour la synthèse d'ATP et nécessitent, lors de leur explosion oxydative, une grande quantité de NADPH. Dans ce contexte, la localisation de la PFK2 et de la 6PGDH, à proximité immédiate de site catalytique, semble parfaitement adaptée au fonctionnement de la NADPH oxydase des phagocytes.

Enfin, l'impact spécifique de la 6PGDH sur l'activité de la NADPH oxydase des phagocytes est également indiqué par la mesure de la constante de Michaelis (Km) de la NADPH oxydase pour le NADPH. Lors de la purification à partir de pseudo-neutrophiles PLB985 dont l'expression de la 6PGDH a été diminuée par transfection d'ARN interférants, le Km de l'enzyme pour son substrat passe de 50µM à 200µM, indiquant une baisse significative d'affinité. En d'autres termes, la 6PGDH n'intervient pas seulement par la modulation de la concentration du substrat, mais elle augmente également l'affinité de la NADPH oxydase pour le NADPH.

Figure 27. Implication de la PFK2 et de la 6PGDH dans l'activation de la NADPH oxydase des phagocytes

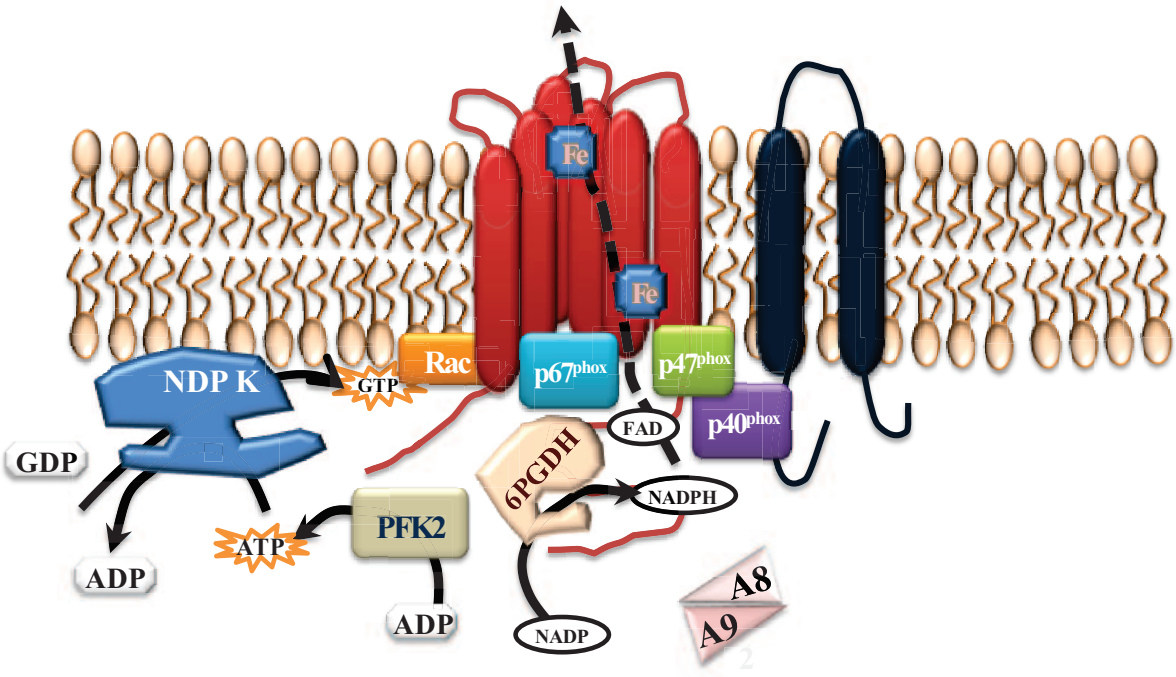

II. Dualité fonctionnelle des protéines S100A8/A9 intra et extra-cellulaires dans le processus inflammatoire

Notre travail confirme l'implication de S100A8/A9 dans l'activation de la NADPH oxydase des phagocytes. La partie C-terminale de S100A8 est la région de l'hétérocomplexe qui participe à cette activation dépendante du calcium. Les derniers acides aminés de cette région sont engagés dans l'interaction avec le cytochrome b_{558}.

Il est vraisemblable que les protéines S100A8/A9 régulent de manière allostérique l'activité catalytique de NOX2 [Berthier *et al.* 2003; Paclet *et al.* 2000]. En effet la NADPH oxydase est une enzyme multimérique [Kawahara *et al.* 2011] ce qui est une condition requise pour évoquer une régulation de ce type. De plus, elle présente deux conformations différentes en fonction de son état d'activation pouvant correspondre à des stades de faible et de forte affinité pour le substrat [Paclet *et al.* 2007]. Bien que notre travail précise les sites d'interaction de S100A8 avec le cytochrome b_{558}, il reste à déterminer sur NOX2 le site au niveau duquel S100A8 se fixe, site distant du site catalytique.

Des travaux récents suggèrent que les protéines S100A8/A9 constituent un commutateur de l'activation de la NADPH oxydase, dépendant de la signalisation calcique, lors de la stimulation des récepteurs au fMLP [Schenten *et al.* 2010] ainsi que des récepteurs au domaine Fc des immunoglobulines [Steinckwich *et al.* 2011]. Lors d'une stimulation par le fMLP, la formation d'inositol triphosphate par les phospholipases C permet la vidange du stock calcique du réticulum endothélial. STIM1 détecte alors la chute de concentration du calcium dans le réticulum endoplasmique et va interagir avec les canaux SOC qui déclenchent l'entrée massive de calcium depuis le milieu extra-cellulaire vers le cytosol. L'influx calcique permet l'activation de Sphingosine-kinase, SphK1/2, qui stimule la p38 MAP-Kinase. Cette kinase permet la phosphorylation de S100A9 sur la Thr^{113}, déclenchant ainsi le transfert de l'hétérocomplexe S100A8/S100A9 à la membrane plasmique, vers le cytochrome b_{558} qu'il active [Schenten *et al.* 2011] à la faveur d'un changement de conformation [Paclet *et al.* 2007].

Bien que la physiopathologie de la PR soit encore mal connue, les ROS produites par la NADPH oxydase des phagocytes semblent des protagonistes de premier plan dans cette pathologie. Les PMNs, cellules infiltrantes majoritaires du liquide articulaire, sont donc au cœur de l'étiopathogénèse de la PR [Davies *et al.* 1990]. Tout indique que, dans cette pathologie, l'activation du PMN au sein du site inflammatoire est exacerbée [El Benna *et al.* 2002]. Il n'est donc pas étonnant que les biomarqueurs les plus discriminants du liquide articulaire de PR que nous avons pu caractériser soient des protéines que le PMN déverse dans le milieu extra-cellulaire lors de son activation : les défensines HNP1-3 ("Human neutrophil peptide") et les protéines S100A8, S100A9 et S100A12. L'étude du profil protéique, par technique SELDI-TOF, indique que ces protéines de l'immunité innée permettent de discriminer le liquide synovial de PR, de l'arthrose et d'arthrite non rhumatoïde avec une bonne sensibilité et spécificité (**article 4**). Ainsi, la signature protéomique spécifique du liquide synovial de PR que nous avons mis en évidence porte principalement l'empreinte de l'activation des PMNs, ce qui témoigne du rôle prépondérant des PMNs dans la PR.

Lors de l'activation du PMN, l'exocytose des granules azurophiles permet le transfert des défensines vers le milieu extra-cellulaire [Ganz 1987] alors que la mobilisation des protéines S100A8 et S100A9 s'effectue par une voie dépendante des tubulines [Ryckman *et al.* 2004]. Ces protéines sécrétées localement par les neutrophiles activés, sont des marqueurs inflammatoires nettement plus sensibles que les protéines de la phase aiguë de l'inflammation

à synthèse hépatique [Foell *et al.* 2004]. Les protéines S100A8/A9 sont donc des outils prometteurs pour la prise en charge de patients souffrant de PR, chez qui le diagnostic est souvent retardé par manque de biomarqueurs sensibles et spécifiques [Schellekens *et al.* 2000]. Nos résultats sont confirmés par d'autres études qui ont rapporté, par des méthodes aussi variées que la chromatographie 2D, l'immunohistochimie ou encore les techniques ELISA, une élévation de la concentration des protéines S100A8, S100A9, et S100A12, dans le liquide synovial, le sérum et le tissu synovial de patients atteints de PR par rapport à un groupe témoin constitué de patients arthrosiques (**Tableau 2**). Chez l'homme, une concentration plasmatique élevée de protéines S100A8 et S100A9 est corrélée à la sévérité clinique de la PR, aux lésions radiologiques [Hammer *et al.* 2007; Hammer *et al.* 2008] et donc au pronostic global du patient polyarthritique. Dans le cadre de l'arthrite juvénile idiopathique, les concentrations des protéines S100A8 et S100A9 sont proportionnelles au handicap [Wulffraat *et al.* 2003]. Après instauration du traitement de fond, l'expression des protéines S100A8, S100A9 et S100A12 chute rapidement chez les patients répondeurs pouvant permettre un suivi de la réponse aux traitements.

Après avoir suggéré une production ectopique par le pannus rhumatoïde des protéines S100A8, S100A9 et S100A12 (**article 4**) nous avons pu révéler la production par les synoviocytes rhumatoïdes de type fibroblastique des protéines S100A8 et S100A9 (**article 5**). L'originalité de ce dernier résultat se base sur la mise au point d'une technique inédite d'analyse protéomique de la membrane synoviale par SELDI-TOF, sensible et reproductible.

Les protéines S100A8/A9 sont donc exprimées dans la jonction pannus-cartilage, une zone clé [Pap *et al.* 2000] de la PR. Leur rôle est probablement plus important qu'un simple stigmate de l'activation du PMN et des biomarqueurs de la PR. D'autres résultats plaident pour une implication directe de l'expression de S100A8/A9 du milieu extra-cellulaire dans la physiopathologie de la PR. La plupart des études indiquent que les protéines S100A8, S100A9 et S100A12 initient et amplifient la réaction inflammatoire. Ces protéines occupent donc une place centrale dans la progression des lésions articulaires [Van Lent *et al.* 2008a]. En effet, dans le milieu extra-cellulaire, l'hétérocomplexe S100A8/A9, déversé sur le site inflammatoire à l'occasion de la stimulation ou de la nécrose des PMNs, constitue un signal de danger permettant l'activation des cellules de l'immunité via leur fixation sur le récepteur TLR4. D'une part, les protéines S100A8/A9 participent au recrutement et à la stimulation des cellules infiltrantes du pannus, par leurs propriétés chimiotactiques [Ryckman *et al.* 2003a], et

l'induction de cytokines pro-inflammatoires [Vogl *et al.* 2004]. D'autre part, S100A8, S100A9 et S100A12 produites par les cellules résidantes ou infiltrantes de l'articulation rhumatoïde contribuent probablement au phénotype pseudotumoral des synoviocytes fibroblastiques [Hiratsuka *et al.* 2006; Steenvoorden *et al.* 2007b].

Les propriétés inflammatoires de S100A8/A9 extra-cellulaires, s'exercent principalement à travers l'activation du PMN. En effet, S100A8/A9 lorsqu'elles sont sécrétées, stimulent plusieurs fonctions effectrices du PMN. Tout d'abord, elles favorisent la mobilisation du PMN vers le site inflammatoire. De plus, la protéine S100A9, permet la dégranulation [Simard *et al.* 2010] et augmente la bactéricidie du PMN [Simard *et al.* 2011]. L'équipe de Tessier *et al*. a montré l'induction de l'activité de la NO synthase des cellules de la lignée myéloïde incubées en présence S100A8/A9 [Pouliot *et al.* 2008]. Il serait donc particulièrement intéressant d'étudier l'impact des protéines S100A8/A9 sur une manifestation de l'activation du PMN : la production de ROS par la NADPH oxydase. A une faible concentration de S100A8/A9, de l'ordre de 10µg/ml, l'hétérocomplexe peut exercer une inhibition de l'activité NADPH oxydase [Sroussi *et al.* 2010]. Mais cette valeur ne correspond pas à la concentration du liquide articulaire qui est d'environ 500µg/ml dans le cadre de la PR ([Drynda *et al.* 2004] et données non publiées).

Les travaux du groupe de Carolyn Geczy montrent qu'après sa sécrétion dans le milieu extra-cellulaire, l'hétérocomplexe S100A8/A9 subit des modifications post traductionnelles [Harrison *et al.* 1999] principalement attribuables à la production de ROS par la NADPH oxydase phagocytaire [Raftery *et al.* 2001]. L'oxydation du résidu Met^{78} de S100A8 (ou Met^{74} pour S100A8 murin) diminue la formation de l'hétérodimère S100A8/A9 au profit de la formation d'homodimère de S100A8 [McCormick *et al.* 2005]. L'importante sensibilité aux oxydations de ces protéines [McCormick *et al.* 2005] limite la toxicité des ROS pour les autres protéines du site inflammatoire. Ainsi, les protéines S100A8/A9 sont considérées comme des molécules piégeant les ROS engendrés sur le site inflammatoire. En d'autres termes, lors de l'activation du PMN, l'hétérocomplexe S100A8/A9 qui en position intra-cellulaire active la production de ROS par la NADPH oxydase, est sécrété dans le milieu extra-cellulaire où il en limite la toxicité (**Figure 28**).

Figure 28. S100A8/A9 sécrétées dans le milieu extra-cellulaire sont susceptibles de subir des modifications post-traductionnelles induites par les ROS produits par la NADPH oxydase

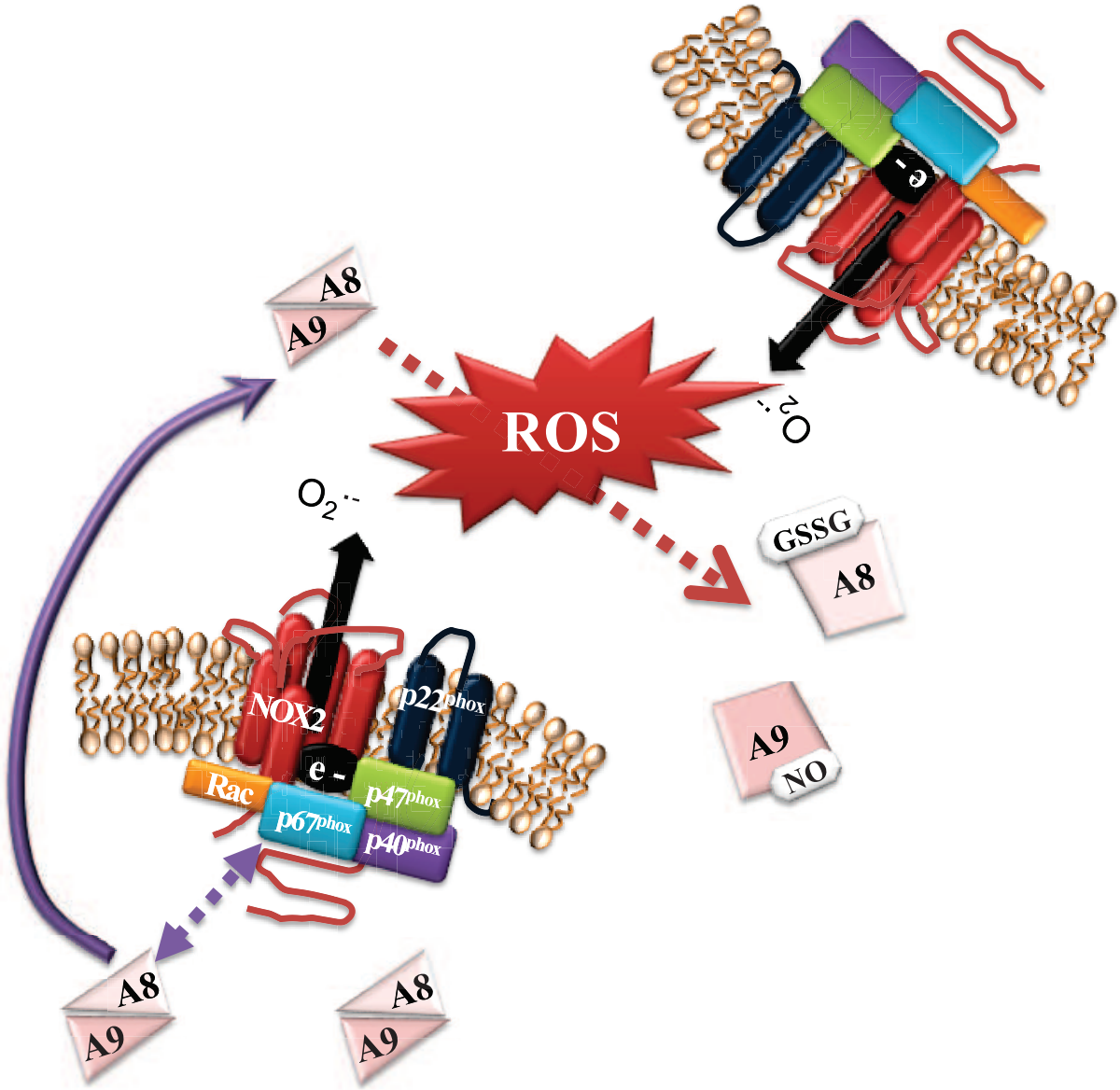

La production de ROS par la NADPH oxydase est donc à l'origine de modifications post-traductionnelles permettant l'acquisition de propriétés anti-inflammatoires par les protéines S100A8/A9. L'infiltration et l'activation [El Benna *et al.* 2002] d'un nombre considérable de PMNs dans le liquide articulaire de patients atteints de PR (2-100 x 10^6 /ml) engendrent une production substantielle de ROS et de protéases dégradant la matrice extra-cellulaire. Il est possible que la sécrétion de S100A8/A9, contemporaine de l'activation de la NADPH oxydase, permette non seulement de limiter la toxicité des ROS mais puisse également

concourir à la résolution de l'arthrite. Comme la plupart des signaux de danger, les modifications post-traductionnelles de S100A8/A9 modifient les propriétés effectrices [Lim *et al.* 2011]. Par exemple, la fixation d'une molécule de glutathion sur une cystéine de S100A8 ou de S100A9 réduit significativement les propriétés chimiotactiques de l'hétérocomplexe [Lim *et al.* 2010]. S100A8 est une des rares protéines à pouvoir bénéficier *in vivo* d'une nitrosylation [Raftery *et al.* 2001]. Lorsque le résidu Cys^{41} de S100A8 subit cette modification post-traductionnelle, il exerce une répulsion pour les leucocytes de la microcirculation. Il semble donc capital d'étudier l'impact des protéines S100A8/A9 extra-cellulaires et leurs modifications post-traductionnelles afin de savoir si elles constituent des éléments sensibles au statut redox et sont capables de participer à la désactivation de la NADPH oxydase.

CONCLUSIONS ET PERSPECTIVES

Dans ce travail, nous présentons de nouveaux mécanismes de régulation de la NADPH oxydase phagocytaire permettant d'adapter l'activité catalytique au métabolisme cellulaire. Notre étude suggère que la 6PGDH module la disponibilité en substrat ainsi que l'affinité de la NADPH oxydase pour le NADPH. La PFK2, qui contrôle la quantité d'ATP produit par la glycolyse, intervient donc indirectement sur les phosphorylations du cytochrome b_{558} et des facteurs cytosoliques. De plus, il semble exister une régulation par compartimentation en microdomaines membranaires. Enfin, nous suggérons une régulation allostérique de l'activité catalytique de NOX2 par S100A8.

Nos résultats constituent un rationnel scientifique solide pour proposer une étude plus approfondie des mécanismes de régulation évoqués.

Il serait intéressant de purifier les radeaux lipidiques afin de confirmer, *in vitro*, la co-localisation de la NADPH oxydase et de la PFK2 ou de la 6PGDH dans ces microdomaines. Nous pourrions également analyser l'impact d'une désorganisation de cette micro-compartimentation sur l'interaction entre ces nouveaux partenaires et NOX2, notamment au moyen de la cyclodextrine qui extrait le cholestérol de la bicouche de phospholipides. Il serait aussi pertinent d'analyser systématiquement les enzymes contenues dans ces radeaux lipidiques afin de savoir si d'autres enzymes impliquées dans le métabolisme du glucose sont susceptibles d'interagir avec la NADPH oxydase ou s'il existe une régulation restreinte à la PFK2 et la 6PGDH.

La spécificité de l'interaction entre $p67^{phox}$ et la 6PGDH mériterait également d'être explorée plus finement afin de confirmer que l'interaction entre ces deux protéines au cours de l'activation du PMN se fait sur un site proche du site de fixation du NADPH sur $p67^{phox}$. Nous pourrions, dans un premier temps, rechercher si la translocation à la membrane plasmique de la 6PGDH est compromise dans des cellules myéloïdes dépourvues de $p67^{phox}$.

Inversement, il serait intéressant d'analyser si l'activité NADPH oxydase influence le métabolisme du glucose. La glycéraldéhyde 3-phosphate déshydrogénase (G3PDH), $6^{ème}$ enzyme de la glycolyse, contient un groupement thiol sur le résidu Cys^{149} qui le rend très sensible aux oxydations [Hu *et al.* 1993]. Ainsi les ROS, produites par la NADPH oxydase, pourrait conduire à l'inactivation la glycolyse au niveau de la G3PDH et donc à une baisse de la production de l'ATP [Anderson *et al.* 1990; Schraufstatter *et al.* 1990]. Certains auteurs ont même suggéré que la chute de la synthèse d'ATP, secondaire à l'oxydation de G3PDH, était un mécanisme d'inactivation de la NADPH oxydase des phagocytes [Theron *et al.* 1994].

L'optimisation des conditions expérimentales de l'analyse protéomique dans les différents tissus étudiés nous a permis de révéler l'intérêt des protéines S100A8 et S100A9 tant au plan de la compréhension de la physiopathologie de la PR que du diagnostic. L'utilisation comme biomarqueurs de ces protéines doit être validée chez un plus grand nombre de patients, à un stade précoce de la maladie où la détermination de marqueurs prédictifs de l'évolution de la maladie est capitale. La pertinence de l'association du dosage des protéines S100A8, S100A9 et S100A12 avec les marqueurs classiques du diagnostic de PR devrait être examinée, dans le cadre d'une analyse multiparamétrique, dans des cohortes de rhumatismes inflammatoires débutants. Nous chercherons à savoir si la prescription de ces nouveaux biomarqueurs de la PR dans la stratégie diagnostique, apporte une plus-value pour le diagnostic, le pronostic et l'évaluation de la réponse au traitement d'un rhumatisme débutant.

Sur un plan plus fondamental, l'activation des nombreuses fonctions du PMN par les protéines S100A8/A9 extra-cellulaires et l'impact des modifications post-traductionnelles doivent être investigués plus précisément.
Des résultats préliminaires indiquent que la stimulation par des protéines recombinantes S100A8/A9, à une concentration égale à celle du liquide synovial de PR (environ 500µg/ml), augmente l'activité NADPH oxydase des PLB985 différenciés en pseudo-neutrophiles (**Figure 29**). Ces premiers résultats devront être confirmés pour les PMNs humains. De plus, il nous faudra caractériser les récepteurs impliqués dans la transduction du signal et vérifier que la stimulation de l'activité NADPH oxydase constatée après stimulation par les protéines S100A8/A9 recombinantes n'est pas attribuable à une contamination par le LPS des bactéries Escherichia Coli dans lesquelles elles sont générées. Enfin, il serait pertinent d'analyser l'impact des modifications post-traductionnelles de S100A8/A9 extra-cellulaires, induites par les ROS (oxydations et nitrosylations), sur l'activation de la NADPH oxydase des phagocytes.

Figure 29. Analyse de la production de ROS par des PLB985, différenciés en pseudo-neutrophiles (J+3), incubés avec 500µg/ml de S100A8/A9.

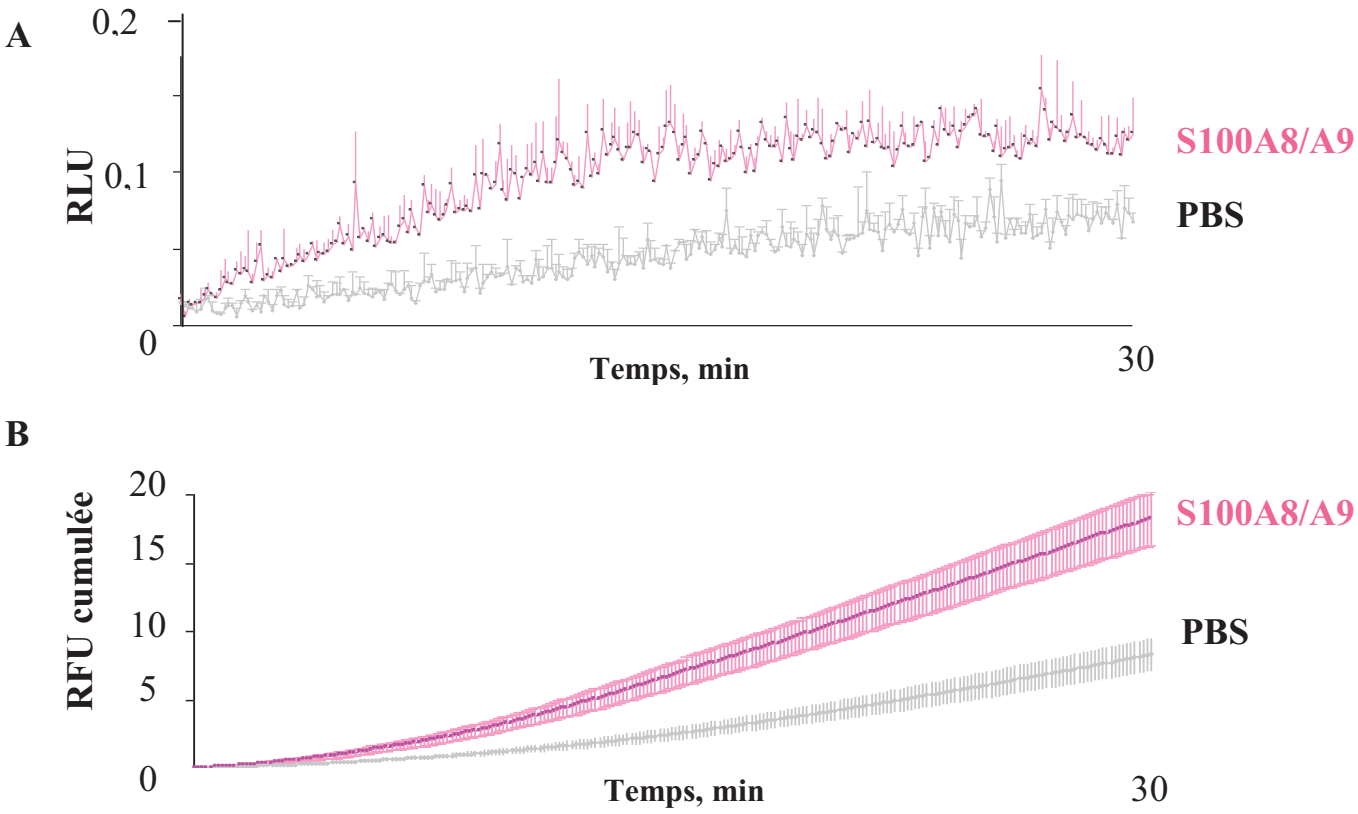

*Les PLB985 sont différenciés en pseudo neutrophiles pendant 72 heures en milieu RPMI contenant 10% (v:v) de sérum de veau fœtal et 0,5% (v:v) de diméthylformamide. Après centrifugation (350g, 8 min à 20°C) les cellules sont lavées en PBS, puis incubées 60 min à 37°C avec 500µg/ml de protéines S100A8/A9 produites dans Escherichia coli [Paclet et al. 2007]. Après un lavage en PBS, la production de ROS est détectée pendant 30 min par chimiluminescence du luminol (**A**) ou fluorométrie en utilisant la technique de l'Amplex Red (**B**).Les résultats sont représentatifs d'au moins trois expériences indépendantes.*

REFERENCES

Adams M.J., Archibald I.G., Bugg C.E., Carne A., Gover S., Helliwell J.R., Pickersgill R.W., and White S.W. **(1983)**, The three dimensional structure of sheep liver 6-phosphogluconate dehydrogenase at 2.6 A resolution. *Embo J* 2:1009-14.

Afonso V., Santos G., Collin P., Khatib A.M., Mitrovic D.R., Lomri N., Leitman D.C., and Lomri A. **(2006)**, Tumor necrosis factor-alpha down-regulates human Cu/Zn superoxide dismutase 1 promoter via JNK/AP-1 signaling pathway. *Free Radic Biol Med* 41:709-21.

Ahmed S., Prigmore E., Govind S., Veryard C., Kozma R., Wientjes F.B., Segal A.W., and Lim L. **(1998)**, Cryptic Rac-binding and p21(Cdc42Hs/Rac)-activated kinase phosphorylation sites of NADPH oxidase component p67(phox). *J Biol Chem* 273:15693-701.

Al-Mohanna F.A., and Hallett M.B. **(1987a)**, Actin polymerization modifies stimulus-oxidase coupling in rat neutrophils. *Biochim Biophys Acta* 927:366-71.

Al-Mohanna F.A., Ohishi I., and Hallett M.B. **(1987b)**, Botulinum C2 toxin potentiates activation of the neutrophil oxidase. Further evidence of a role for actin polymerization. *FEBS Lett* 219:40-4.

Aletaha D., Neogi T., Silman A.J., Funovits J., Felson D.T., Bingham C.O., 3rd, Birnbaum N.S., Burmester G.R., Bykerk V.P., Cohen M.D., Combe B., Costenbader K.H., Dougados M., Emery P., Ferraccioli G., Hazes J.M., Hobbs K., Huizinga T.W., Kavanaugh A., Kay J., Kvien T.K., Laing T., Mease P., Menard H.A., Moreland L.W., Naden R.L., Pincus T., Smolen J.S., Stanislawska-Biernat E., Symmons D., Tak P.P., Upchurch K.S., Vencovsky J., Wolfe F., and Hawker G. **(2011)**, 2010 Rheumatoid arthritis classification criteria: an American College of Rheumatology/European League Against Rheumatism collaborative initiative. *Arthritis Rheum* 62:2569-81.

Aletaha D., Strand V., Smolen J.S., and Ward M.M. **(2008)**, Treatment-related improvement in physical function varies with duration of rheumatoid arthritis: a pooled analysis of clinical trial results. *Ann Rheum Dis* 67:238-43.

Allen R.E., Blake D.R., Nazhat N.B., and Jones P. **(1989)**, Superoxide radical generation by inflamed human synovium after hypoxia. *Lancet* 2:282-3.

Altwegg L.A., Neidhart M., Hersberger M., Muller S., Eberli F.R., Corti R., Roffi M., Sutsch G., Gay S., von Eckardstein A., Wischnewsky M.B., Luscher T.F., and Maier W. **(2007)**, Myeloid-related protein 8/14 complex is released by monocytes and granulocytes at the site of coronary occlusion: a novel, early, and sensitive marker of acute coronary syndromes. *Eur Heart J* 28:941-8.

Alving A.S., Carson P.E., Flanagan C.L., and Ickes C.E. **(1956)**, Enzymatic deficiency in primaquine-sensitive erythrocytes. *Science* 124:484-5.

Ambruso D.R., Knall C., Abell A.N., Panepinto J., Kurkchubasche A., Thurman G., Gonzalez-Aller C., Hiester A., deBoer M., Harbeck R.J., Oyer R., Johnson G.L., and Roos D. **(2000)**, Human neutrophil immunodeficiency syndrome is associated with an inhibitory Rac2 mutation. *Proc Natl Acad Sci U S A* 97:4654-9.

Anderson R., Smit M.J., Joone G.K., and Van Staden A.M. **(1990)**, Vitamin C and cellular immune functions. Protection against hypochlorous acid-mediated inactivation of glyceraldehyde-3-phosphate dehydrogenase and ATP generation in human leukocytes as a possible mechanism of ascorbate-mediated immunostimulation. *Ann N Y Acad Sci* 587:34-48.

Anderson R., Van Rensburg C.E., Joone G.K., and Lessing A. **(1991)**, Auranofin inactivates phosphofructokinase in human neutrophils, leading to depletion of intracellular ATP and inhibition of superoxide generation and locomotion. *Mol Pharmacol* 40:427-34.

Arden C., Hampson L.J., Huang G.C., Shaw J.A., Aldibbiat A., Holliman G., Manas D., Khan S., Lange A.J., and Agius L. **(2008)**, A role for PFK-2/FBPase-2, as distinct from fructose 2,6-bisphosphate, in regulation of insulin secretion in pancreatic beta-cells. *Biochem J* 411:41-51.

Asghar A.H., Ardati K.O., Tabbara K.S., and Bajakian K.M. **(1998)**, Bactericidal activity of polymorphonuclear neutrophils in individuals severely deficient in glucose-6-phosphate dehydrogenase. *Ann Saudi Med* 18:363-5.

Auger I., Sebbag M., Vincent C., Balandraud N., Guis S., Nogueira L., Svensson B., Cantagrel A., Serre G., and Roudier J. **(2005)**, Influence of HLA-DR genes on the production of rheumatoid arthritis-specific autoantibodies to citrullinated fibrinogen. *Arthritis Rheum* 52:3424-32.

Avina-Zubieta J.A., Choi H.K., Sadatsafavi M., Etminan M., Esdaile J.M., and Lacaille D. **(2008)**, Risk of cardiovascular mortality in patients with rheumatoid arthritis: a meta-analysis of observational studies. *Arthritis Rheum* 59:1690-7.

Baehner R.L., Johnston R.B., Jr., and Nathan D.G. **(1972)**, Comparative study of the metabolic and bactericidal characteristics of severely glucose-6-phosphate dehydrogenase-deficient polymorphonuclear leukocytes and leukocytes from children with chronic granulomatous disease. *J Reticuloendothel Soc* 12:150-69.

Baillet A. **(2010)**, S100A8, S100A9 and S100A12 proteins in rheumatoid arthritis. *Rev Med Interne* 31:458-61.

Baillet A., Gaujoux-Viala C., Mouterde G., Pham T., Tebib J., Saraux A., Fautrel B., Cantagrel A., Le Loet X., and Gaudin P. **(2011a)**, Comparison of the efficacy of sonography, magnetic resonance imaging and

conventional radiography for the detection of bone erosions in rheumatoid arthritis patients: a systematic review and meta-analysis. *Rheumatology (Oxford)* 50:1137-47.

Baillet A., Trocme C., Berthier S., Arlotto M., Grange L., Chenau J., Quetant S., Seve M., Berger F., Juvin R., Morel F., and Gaudin P. **(2010)**, Synovial fluid proteomic fingerprint: S100A8, S100A9 and S100A12 proteins discriminate rheumatoid arthritis from other inflammatory joint diseases. *Rheumatology (Oxford)* 49:671-82.

Baillet A., Xu R., Grichine A., Berthier S., Morel F., and Paclet M.H. **(2011b)**, Coupling of 6-phosphogluconate dehydrogenase with NADPH oxidase in neutrophils: Nox2 activity regulation by NADPH availability. *Faseb J* 25:2333-43.

Bainton D.F., Ullyot J.L., and Farquhar M.G. **(1971)**, The development of neutrophilic polymorphonuclear leukocytes in human bone marrow. *J Exp Med* 134:907-34.

Baker M.S., Feigan J., and Lowther D.A. **(1989)**, The mechanism of chondrocyte hydrogen peroxide damage. Depletion of intracellular ATP due to suppression of glycolysis caused by oxidation of glyceraldehyde-3-phosphate dehydrogenase. *J Rheumatol* 16:7-14.

Banfi B., Molnar G., Maturana A., Steger K., Hegedus B., Demaurex N., and Krause K.H. **(2001)**, A Ca(2+)-activated NADPH oxidase in testis, spleen, and lymph nodes. *J Biol Chem* 276:37594-601.

Barland P., Novikoff A.B., and Hamerman D. **(1962)**, Electron microscopy of the human synovial membrane. *J Cell Biol* 14:207-20.

Batot G., Martel C., Capdeville N., Wientjes F., and Morel F. **(1995)**, Characterization of neutrophil NADPH oxidase activity reconstituted in a cell-free assay using specific monoclonal antibodies raised against cytochrome b_{558}. *Eur J Biochem* 234:208-15.

Bedard K., and Krause K.H. **(2007a)**, The NOX family of ROS-generating NADPH oxidases: physiology and pathophysiology. *Physiol Rev* 87:245-313.

Bedard K., Lardy B., and Krause K.H. **(2007b)**, NOX family NADPH oxidases: not just in mammals. *Biochimie* 89:1107-12.

Benedyk M., Sopalla C., Nacken W., Bode G., Melkonyan H., Banfi B., and Kerkhoff C. **(2007)**, HaCaT keratinocytes overexpressing the S100 proteins S100A8 and S100A9 show increased NADPH oxidase and NF-kappaB activities. *J Invest Dermatol* 127:2001-11.

Bengis-Garber C., and Gruener N. **(1993)**, Calcium-binding myeloid protein (P8,14) is phosphorylated in fMet-Leu-Phe-stimulated neutrophils. *J Leukoc Biol* 54:114-8.

Bengis-Garber C., and Gruener N. **(1996)**, Protein kinase A downregulates the phosphorylation of p47 phox in human neutrophils: a possible pathway for inhibition of the respiratory burst. *Cell Signal* 8:291-6.

Bengtsson T., Dahlgren C., Stendahl O., and Andersson T. **(1991)**, Actin assembly and regulation of neutrophil function: effects of cytochalasin B and tetracaine on chemotactic peptide-induced O2- production and degranulation. *J Leukoc Biol* 49:236-44.

Bengtsson T., Orselius K., and Wettero J. **(2006)**, Role of the actin cytoskeleton during respiratory burst in chemoattractant-stimulated neutrophils. *Cell Biol Int* 30:154-63.

Benito-Miguel M., Garcia-Carmona Y., Balsa A., Perez de Ayala C., Cobo-Ibanez T., Martin-Mola E., and Miranda-Carus M.E. **(2009)**, A dual action of rheumatoid arthritis synovial fibroblast IL-15 expression on the equilibrium between CD4+CD25+ regulatory T cells and CD4+CD25- responder T cells. *J Immunol* 183:8268-79.

Berthier S., Baillet A., Paclet M.H., Gaudin P., and Morel F. **(2009)**, How important are S100A8/S100A9 Calcium Binding Proteins for the Activation of Phagocyte NADPH Oxidase, Nox2. *Anti-Inflammatory & Anti-Allergy Agents in Medicinal Chemistry* 8:282-284.

Berthier S., Paclet M.H., Lerouge S., Roux F., Vergnaud S., Coleman A.W., and Morel F. **(2003)**, Changing the conformation state of cytochrome b_{558} initiates NADPH oxidase activation: MRP8/MRP14 regulation. *J Biol Chem* 278:25499-508.

Bertrand L., Alessi D.R., Deprez J., Deak M., Viaene E., Rider M.H., and Hue L. **(1999)**, Heart 6-phosphofructo-2-kinase activation by insulin results from Ser-466 and Ser-483 phosphorylation and requires 3-phosphoinositide-dependent kinase-1, but not protein kinase B. *J Biol Chem* 274:30927-33.

Blake D.R., Merry P., Unsworth J., Kidd B.L., Outhwaite J.M., Ballard R., Morris C.J., Gray L., and Lunec J. **(1989)**, Hypoxic-reperfusion injury in the inflamed human joint. *Lancet* 1:289-93.

Blue M.L., Conrad P., Webb D.L., Sarr T., and Macaro M. **(1993)**, Interacting monocytes and synoviocytes induce adhesion molecules by a cytokine-regulated process. *Lymphokine Cytokine Res* 12:213-8.

Blumenauer B., Judd M., Cranney A., Burls A., Coyle D., Hochberg M., Tugwell P., and Wells G. **(2003)**, Etanercept for the treatment of rheumatoid arthritis. *Cochrane Database Syst Rev*CD004525.

Bokoch G.M., Quilliam L.A., Bohl B.P., Jesaitis A.J., and Quinn M.T. **(1991)**, Inhibition of Rap1A binding to cytochrome b_{558} of NADPH oxidase by phosphorylation of Rap1A. *Science* 254:1794-6.

Borregaard N., and Cowland J.B. **(1997)**, Granules of the human neutrophilic polymorphonuclear leukocyte. *Blood* 89:3503-21.

Borregaard N., Heiple J.M., Simons E.R., and Clark R.A. **(1983)**, Subcellular localization of the b-cytochrome component of the human neutrophil microbicidal oxidase: translocation during activation. *J Cell Biol* 97:52-61.

Bouamrani A., Ternier J., Ratel D., Benabid A.L., Issartel J.P., Brambilla E., and Berger F. **(2006)**, Direct-tissue SELDI-TOF mass spectrometry analysis: a new application for clinical proteomics. *Clin Chem* 52:2103-6.

Bouin A.P., Grandvaux N., Vignais P.V., and Fuchs A. **(1998)**, p40(phox) is phosphorylated on threonine 154 and serine 315 during activation of the phagocyte NADPH oxidase. Implication of a protein kinase c-type kinase in the phosphorylation process. *J Biol Chem* 273:30097-103.

Boussetta T., Gougerot-Pocidalo M.A., Hayem G., Ciappelloni S., Raad H., Arabi Derkawi R., Bournier O., Kroviarski Y., Zhou X.Z., Malter J.S., Lu P.K., Bartegi A., Dang P.M., and El-Benna J. **(2010)**, The prolyl isomerase Pin1 acts as a novel molecular switch for TNF-alpha-induced priming of the NADPH oxidase in human neutrophils. *Blood* 116:5795-802.

Bouzidi F., and Doussiere J. **(2004)**, Binding of arachidonic acid to myeloid-related proteins (S100A8/A9) enhances phagocytic NADPH oxidase activation. *Biochem Biophys Res Commun* 325:1060-5.

Brechard S., Brunello A., Bueb J.L., and Tschirhart E.J. **(2006)**, Modulation by cADPr of Ca2+ mobilization and oxidative response in dimethylsulfoxide- or retinoic acid-differentiated HL-60 cells. *Biochim Biophys Acta* 1763:129-36.

Brechard S., Bueb J.L., and Tschirhart E.J. **(2005)**, Interleukin-8 primes oxidative burst in neutrophil-like HL-60 through changes in cytosolic calcium. *Cell Calcium* 37:531-40.

Brechard S., and Tschirhart E.J. **(2008)**, Regulation of superoxide production in neutrophils: role of calcium influx. *J Leukoc Biol* 84:1223-37.

Brown G.E., Stewart M.Q., Bissonnette S.A., Elia A.E., Wilker E., and Yaffe M.B. **(2004)**, Distinct ligand-dependent roles for p38 MAPK in priming and activation of the neutrophil NADPH oxidase. *J Biol Chem* 279:27059-68.

Brown G.E., Stewart M.Q., Liu H., Ha V.L., and Yaffe M.B. **(2003)**, A novel assay system implicates PtdIns(3,4)P(2), PtdIns(3)P, and PKC delta in intracellular production of reactive oxygen species by the NADPH oxidase. *Mol Cell* 11:35-47.

Burritt J.B., Foubert T.R., Baniulis D., Lord C.I., Taylor R.M., Mills J.S., Baughan T.D., Roos D., Parkos C.A., and Jesaitis A.J. **(2003)**, Functional epitope on human neutrophil flavocytochrome b_{558}. *J Immunol* 170:6082-9.

Cale C.M., Morton L., and Goldblatt D. **(2007)**, Cutaneous and other lupus-like symptoms in carriers of X-linked chronic granulomatous disease: incidence and autoimmune serology. *Clin Exp Immunol* 148:79-84.

Campion Y., Jesaitis A.J., Nguyen M.V., Grichine A., Herenger Y., Baillet A., Berthier S., Morel F., and Paclet M.H. **(2009)**, New p22-phox monoclonal antibodies: identification of a conformational probe for cytochrome b_{558}. *J Innate Immun* 1:556-69.

Campion Y., Paclet M.H., Jesaitis A.J., Marques B., Grichine A., Berthier S., Lenormand J.L., Lardy B., Stasia M.J., and Morel F. **(2007)**, New insights into the membrane topology of the phagocyte NADPH oxidase: characterization of an anti-gp91-phox conformational monoclonal antibody. *Biochimie* 89:1145-58.

Carmona L., Gonzalez-Alvaro I., Balsa A., Angel Belmonte M., Tena X., and Sanmarti R. **(2003)**, Rheumatoid arthritis in Spain: occurrence of extra-articular manifestations and estimates of disease severity. *Ann Rheum Dis* 62:897-900.

Carsons S., Lavietes B.B., Diamond H.S., and Kinney S.G. **(1985)**, The immunoreactivity, ligand, and cell binding characteristics of rheumatoid synovial fluid fibronectin. *Arthritis Rheum* 28:601-12.

Cassatella M.A., Bazzoni F., Ceska M., Ferro I., Baggiolini M., and Berton G. **(1992)**, IL-8 production by human polymorphonuclear leukocytes. The chemoattractant formyl-methionyl-leucyl-phenylalanine induces the gene expression and release of IL-8 through a pertussis toxin-sensitive pathway. *J Immunol* 148:3216-20.

Castagna M., Takai Y., Kaibuchi K., Sano K., Kikkawa U., and Nishizuka Y. **(1982)**, Direct activation of calcium-activated, phospholipid-dependent protein kinase by tumor-promoting phorbol esters. *J Biol Chem* 257:7847-51.

Cedergren J., Forslund T., Sundqvist T., and Skogh T. **(2007)**, Intracellular oxidative activation in synovial fluid neutrophils from patients with rheumatoid arthritis but not from other arthritis patients. *J Rheumatol* 34:2162-70.

Cerhan J.R., Saag K.G., Merlino L.A., Mikuls T.R., and Criswell L.A. **(2003)**, Antioxidant micronutrients and risk of rheumatoid arthritis in a cohort of older women. *Am J Epidemiol* 157:345-54.

Cha H.S., Rosengren S., Boyle D.L., and Firestein G.S. **(2006)**, PUMA regulation and proapoptotic effects in fibroblast-like synoviocytes. *Arthritis Rheum* 54:587-92.

Chakravarti A., Raquil M.A., Tessier P., and Poubelle P.E. **(2009)**, Surface RANKL of Toll-like receptor 4-stimulated human neutrophils activates osteoclastic bone resorption. *Blood* 114:1633-44.

Channon J.Y., and Leslie C.C. **(1990)**, A calcium-dependent mechanism for associating a soluble arachidonoyl-hydrolyzing phospholipase A2 with membrane in the macrophage cell line RAW 264.7. *J Biol Chem* 265:5409-13.

Chen M., Lam B.K., Kanaoka Y., Nigrovic P.A., Audoly L.P., Austen K.F., and Lee D.M. **(2006a)**, Neutrophil-derived leukotriene B4 is required for inflammatory arthritis. *J Exp Med* 203:837-42.

Chen Q., Powell D.W., Rane M.J., Singh S., Butt W., Klein J.B., and McLeish K.R. **(2003)**, Akt phosphorylates p47phox and mediates respiratory burst activity in human neutrophils. *J Immunol* 170:5302-8.

Chen Y.F., Jobanputra P., Barton P., Jowett S., Bryan S., Clark W., Fry-Smith A., and Burls A. **(2006b)**, A systematic review of the effectiveness of adalimumab, etanercept and infliximab for the treatment of rheumatoid arthritis in adults and an economic evaluation of their cost-effectiveness. *Health Technol Assess* 10:iii-iv, xi-xiii, 1-229.

Chenevier-Gobeaux C., Lemarechal H., Bonnefont-Rousselot D., Poiraudeau S., Ekindjian O.G., and Borderie D. **(2006)**, Superoxide production and NADPH oxidase expression in human rheumatoid synovial cells: regulation by interleukin-1beta and tumour necrosis factor-alpha. *Inflamm Res* 55:483-90.

Cheng P., Corzo C.A., Luetteke N., Yu B., Nagaraj S., Bui M.M., Ortiz M., Nacken W., Sorg C., Vogl T., Roth J., and Gabrilovich D.I. **(2008)**, Inhibition of dendritic cell differentiation and accumulation of myeloid-derived suppressor cells in cancer is regulated by S100A9 protein. *J Exp Med* 205:2235-49.

Chessa T.A., Anderson K.E., Hu Y., Xu Q., Rausch O., Stephens L.R., and Hawkins P.T. **(2010)**, Phosphorylation of threonine 154 in p40phox is an important physiological signal for activation of the neutrophil NADPH oxidase. *Blood* 116:6027-36.

Chevrel G., Garnero P., and Miossec P. **(2002)**, Addition of interleukin 1 (IL1) and IL17 soluble receptors to a tumour necrosis factor alpha soluble receptor more effectively reduces the production of IL6 and macrophage inhibitory protein-3alpha and increases that of collagen in an in vitro model of rheumatoid synoviocyte activation. *Ann Rheum Dis* 61:730-3.

Choy E.H., and Panayi G.S. **(2001)**, Cytokine pathways and joint inflammation in rheumatoid arthritis. *N Engl J Med* 344:907-16.

Cimmino M.A., Salvarani C., Macchioni P., Montecucco C., Fossaluzza V., Mascia M.T., Punzi L., Davoli C., Filippini D., and Numo R. **(2000)**, Extra-articular manifestations in 587 Italian patients with rheumatoid arthritis. *Rheumatol Int* 19:213-7.

Clark J.D., Milona N., and Knopf J.L. **(1990)**, Purification of a 110-kilodalton cytosolic phospholipase A2 from the human monocytic cell line U937. *Proc Natl Acad Sci U S A* 87:7708-12.

Clegg P.D., and Carter S.D. **(1999)**, Matrix metalloproteinase-2 and -9 are activated in joint diseases. *Equine Vet J* 31:324-30.

Cotton D.J., Seligmann B., O'Brien W.F., and Gallin J.I. **(1983)**, Selective defect in human neutrophil superoxide anion generation elicited by the chemoattractant N-formylmethionylleucylphenylalanine in pregnancy. *J Infect Dis* 148:194-9.

Cross A.R., Heyworth P.G., Rae J., and Curnutte J.T. **(1995)**, A variant X-linked chronic granulomatous disease patient (X91+) with partially functional cytochrome b. *J Biol Chem* 270:8194-200.

Cross A.R., Noack D., Rae J., Curnutte J.T., and Heyworth P.G. **(2000)**, Hematologically important mutations: the autosomal recessive forms of chronic granulomatous disease (first update). *Blood Cells Mol Dis* 26:561-5.

Cross A.R., and Segal A.W. **(2004)**, The NADPH oxidase of professional phagocytes--prototype of the NOX electron transport chain systems. *Biochim Biophys Acta* 1657:1-22.

Cunnane G., FitzGerald O., Hummel K.M., Gay R.E., Gay S., and Bresnihan B. **(1999)**, Collagenase, cathepsin B and cathepsin L gene expression in the synovial membrane of patients with early inflammatory arthritis. *Rheumatology (Oxford)* 38:34-42.

Curnutte J.T., Erickson R.W., Ding J., and Badwey J.A. **(1994)**, Reciprocal interactions between protein kinase C and components of the NADPH oxidase complex may regulate superoxide production by neutrophils stimulated with a phorbol ester. *J Biol Chem* 269:10813-9.

Dacheux D., Toussaint B., Richard M., Brochier G., Croize J., and Attree I. **(2000)**, Pseudomonas aeruginosa cystic fibrosis isolates induce rapid, type III secretion-dependent, but ExoU-independent, oncosis of macrophages and polymorphonuclear neutrophils. *Infect Immun* 68:2916-24.

Dahinden C.A., Fehr J., and Hugli T.E. **(1983)**, Role of cell surface contact in the kinetics of superoxide production by granulocytes. *J Clin Invest* 72:113-21.

Dai L., Lamb D.J., Leake D.S., Kus M.L., Jones H.W., Morris C.J., and Winyard P.G. **(2000)**, Evidence for oxidised low density lipoprotein in synovial fluid from rheumatoid arthritis patients. *Free Radic Res* 32:479-86.

Dalle-Donne I., Rossi R., Giustarini D., Milzani A., and Colombo R. **(2003)**, Protein carbonyl groups as biomarkers of oxidative stress. *Clin Chim Acta* 329:23-38.

Damiano V.V., Kucich U., Murer E., Laudenslager N., and Weinbaum G. **(1988)**, Ultrastructural quantitation of peroxidase- and elastase-containing granules in human neutrophils. *Am J Pathol* 131:235-45.

Dana R., Leto T.L., Malech H.L., and Levy R. **(1998)**, Essential requirement of cytosolic phospholipase A2 for activation of the phagocyte NADPH oxidase. *J Biol Chem* 273:441-5.

Dang P.M., Babior B.M., and Smith R.M. **(1999a)**, NADPH dehydrogenase activity of p67PHOX, a cytosolic subunit of the leukocyte NADPH oxidase. *Biochemistry* 38:5746-53.

Dang P.M., Dewas C., Gaudry M., Fay M., Pedruzzi E., Gougerot-Pocidalo M.A., and El Benna J. **(1999b)**, Priming of human neutrophil respiratory burst by granulocyte/macrophage colony-stimulating factor (GM-CSF) involves partial phosphorylation of p47(phox). *J Biol Chem* 274:20704-8.

Dang P.M., Fontayne A., Hakim J., El Benna J., and Perianin A. **(2001)**, Protein kinase C zeta phosphorylates a subset of selective sites of the NADPH oxidase component p47phox and participates in formyl peptide-mediated neutrophil respiratory burst. *J Immunol* 166:1206-13.

Dang P.M., Johnson J.L., and Babior B.M. **(2000)**, Binding of nicotinamide adenine dinucleotide phosphate to the tetratricopeptide repeat domains at the N-terminus of p67PHOX, a subunit of the leukocyte nicotinamide adenine dinucleotide phosphate oxidase. *Biochemistry* 39:3069-75.

Dang P.M., Morel F., Gougerot-Pocidalo M.A., and El Benna J. **(2003)**, Phosphorylation of the NADPH oxidase component p67(PHOX) by ERK2 and P38MAPK: selectivity of phosphorylated sites and existence of an intramolecular regulatory domain in the tetratricopeptide-rich region. *Biochemistry* 42:4520-6.

Dang P.M., Raad H., Derkawi R.A., Boussetta T., Paclet M.H., Belambri S.A., Makni-Maalej K., Kroviarski Y., Morel F., Gougerot-Pocidalo M.A., and El-Benna J. **(2011)**, The NADPH oxidase cytosolic component p67phox is constitutively phosphorylated in human neutrophils: Regulation by a protein tyrosine kinase, MEK1/2 and phosphatases 1/2A. *Biochem Pharmacol* 82:1145-52.

Dang P.M., Stensballe A., Boussetta T., Raad H., Dewas C., Kroviarski Y., Hayem G., Jensen O.N., Gougerot-Pocidalo M.A., and El-Benna J. **(2006)**, A specific p47phox -serine phosphorylated by convergent MAPKs mediates neutrophil NADPH oxidase priming at inflammatory sites. *J Clin Invest* 116:2033-43.

Davies E.V., Williams B.D., and Campbell A.K. **(1990)**, Synovial fluid polymorphonuclear leucocytes from patients with rheumatoid arthritis have reduced MPO and NADPH-oxidase activity. *Br J Rheumatol* 29:415-21.

De Bandt M., Grossin M., Driss F., Pincemail J., Babin-Chevaye C., and Pasquier C. **(2002)**, Vitamin E uncouples joint destruction and clinical inflammation in a transgenic mouse model of rheumatoid arthritis. *Arthritis Rheum* 46:522-32.

De Seny D., Fillet M., Meuwis M.A., Geurts P., Lutteri L., Ribbens C., Bours V., Wehenkel L., Piette J., Malaise M., and Merville M.P. **(2005)**, Discovery of new rheumatoid arthritis biomarkers using the surface-enhanced laser desorption/ionization time-of-flight mass spectrometry ProteinChip approach. *Arthritis Rheum* 52:3801-12.

De Seny D., Fillet M., Ribbens C., Maree R., Meuwis M.A., Lutteri L., Chapelle J.P., Wehenkel L., Louis E., Merville M.P., and Malaise M. **(2008)**, Monomeric calgranulins measured by SELDI-TOF mass spectrometry and calprotectin measured by ELISA as biomarkers in arthritis. *Clin Chem* 54:1066-75.

DeChatelet L.R., McPhail L.C., Mullikin D., and McCall C.E. **(1974)**, Reduced nicotinamide adenine dinucleotide and reduced nicotinamide adenine dinucleotide phosphate diaphorase activity in human polymorphonuclear leukocytes. *Infect Immun* 10:528-34.

Dekker L.V., Leitges M., Altschuler G., Mistry N., McDermott A., Roes J., and Segal A.W. **(2000)**, Protein kinase C-beta contributes to NADPH oxidase activation in neutrophils. *Biochem J* 347:285-9.

Del Carlo M., Jr., and Loeser R.F. **(2002)**, Nitric oxide-mediated chondrocyte cell death requires the generation of additional reactive oxygen species. *Arthritis Rheum* 46:394-403.

DeLeo F.R., Burritt J.B., Yu L., Jesaitis A.J., Dinauer M.C., and Nauseef W.M. **(2000)**, Processing and maturation of flavocytochrome b_{558} include incorporation of heme as a prerequisite for heterodimer assembly. *J Biol Chem* 275:13986-93.

Depre C., Ponchaut S., Deprez J., Maisin L., and Hue L. **(1998)**, Cyclic AMP suppresses the inhibition of glycolysis by alternative oxidizable substrates in the heart. *J Clin Invest* 101:390-7.

Deprez J., Vertommen D., Alessi D.R., Hue L., and Rider M.H. **(1997)**, Phosphorylation and activation of heart 6-phosphofructo-2-kinase by protein kinase B and other protein kinases of the insulin signaling cascades. *J Biol Chem* 272:17269-75.

DerMardirossian C., Schnelzer A., and Bokoch G.M. **(2004)**, Phosphorylation of RhoGDI by Pak1 mediates dissociation of Rac GTPase. *Mol Cell* 15:117-27.

Derouazi M., Toussaint B., Quenee L., Epaulard O., Guillaume M., Marlu R., and Polack B. **(2008)**, High-yield production of secreted active proteins by the Pseudomonas aeruginosa type III secretion system. *Appl Environ Microbiol* 74:3601-4.

Didichenko S.A., Tilton B., Hemmings B.A., Ballmer-Hofer K., and Thelen M. **(1996)**, Constitutive activation of protein kinase B and phosphorylation of p47phox by a membrane-targeted phosphoinositide 3-kinase. *Curr Biol* 6:1271-8.

Didsbury J., Weber R.F., Bokoch G.M., Evans T., and Snyderman R. **(1989)**, rac, a novel ras-related family of proteins that are botulinum toxin substrates. *J Biol Chem* 264:16378-82.

Diebold B.A., and Bokoch G.M. **(2001)**, Molecular basis for Rac2 regulation of phagocyte NADPH oxidase. *Nat Immunol* 2:211-5.

Diez-Fraile A., Meyer E., and Burvenich C. **(2002)**, Regulation of adhesion molecules on circulating neutrophils during coliform mastitis and their possible immunomodulation with drugs. *Vet Immunol Immunopathol* 86:1-10.

Dihazi H., Kessler R., and Eschrich K. **(2003)**, Glucose-induced stimulation of the Ras-cAMP pathway in yeast leads to multiple phosphorylations and activation of 6-phosphofructo-2-kinase. *Biochemistry* 42:6275-82.

Djeu J.Y., Serbousek D., and Blanchard D.K. **(1990)**, Release of tumor necrosis factor by human polymorphonuclear leukocytes. *Blood* 76:1405-9.

Donato R. **(1999)**, Functional roles of S100 proteins, calcium-binding proteins of the EF-hand type. *Biochim Biophys Acta* 1450:191-231.

Donato R. **(2001)**, S100: a multigenic family of calcium-modulated proteins of the EF-hand type with intracellular and extracellular functional roles. *Int J Biochem Cell Biol* 33:637-68.

Doussière J., Bouzidi F., Poinas A., Gaillard J., and Vignais P.V. **(1999)**, Kinetic study of the activation of the neutrophil NADPH oxidase by arachidonic acid. Antagonistic effects of arachidonic acid and phenylarsine oxide. *Biochemistry* 38:16394-406.

Doussière J., Bouzidi F., and Vignais P.V. **(2002)**, The S100A8/A9 protein as a partner for the cytosolic factors of NADPH oxidase activation in neutrophils. *Eur J Biochem* 269:3246-55.

Doussière J., Gaillard J., and Vignais P.V. **(1996)**, Electron transfer across the O2- generating flavocytochrome b of neutrophils. Evidence for a transition from a low-spin state to a high-spin state of the heme iron component. *Biochemistry* 35:13400-10.

Dresch C., Najean Y., Bauchet J., and Bernard J. **(1972)**, [Hematologic abnormalities in evolutive chronic polyarthritis. Radioisotopic investigation]. *Nouv Presse Med* 1:163-70.

Drynda S., Ringel B., Kekow M., Kuhne C., Drynda A., Glocker M.O., Thiesen H.J., and Kekow J. **(2004)**, Proteome analysis reveals disease-associated marker proteins to differentiate RA patients from other inflammatory joint diseases with the potential to monitor anti-TNFalpha therapy. *Pathol Res Pract* 200:165-71.

Durand D., Vives C., Cannella D., Perez J., Pebay-Peyroula E., Vachette P., and Fieschi F. **(2010)**, NADPH oxidase activator p67(phox) behaves in solution as a multidomain protein with semi-flexible linkers. *J Struct Biol* 169:45-53.

Edmonds S.E., Winyard P.G., Guo R., Kidd B., Merry P., Langrish-Smith A., Hansen C., Ramm S., and Blake D.R. **(1997)**, Putative analgesic activity of repeated oral doses of vitamin E in the treatment of rheumatoid arthritis. Results of a prospective placebo controlled double blind trial. *Ann Rheum Dis* 56:649-55.

Eggleton P., Wang L., Penhallow J., Crawford N., and Brown K.A. **(1995)**, Differences in oxidative response of subpopulations of neutrophils from healthy subjects and patients with rheumatoid arthritis. *Ann Rheum Dis* 54:916-23.

El Benna J., Dang P.M., and Perianin A. **(2010)**, Peptide-based inhibitors of the phagocyte NADPH oxidase. *Biochem Pharmacol* 80:778-85.

El Benna J., Faust L.P., and Babior B.M. **(1994a)**, The phosphorylation of the respiratory burst oxidase component p47phox during neutrophil activation. Phosphorylation of sites recognized by protein kinase C and by proline-directed kinases. *J Biol Chem* 269:23431-6.

El Benna J., Faust R.P., Johnson J.L., and Babior B.M. **(1996a)**, Phosphorylation of the respiratory burst oxidase subunit p47phox as determined by two-dimensional phosphopeptide mapping. Phosphorylation by protein kinase C, protein kinase A, and a mitogen-activated protein kinase. *J Biol Chem* 271:6374-8.

El Benna J., Han J., Park J.W., Schmid E., Ulevitch R.J., and Babior B.M. **(1996b)**, Activation of p38 in stimulated human neutrophils: phosphorylation of the oxidase component p47phox by p38 and ERK but not by JNK. *Arch Biochem Biophys* 334:395-400.

El Benna J., Hayem G., Dang P.M., Fay M., Chollet-Martin S., Elbim C., Meyer O., and Gougerot-Pocidalo M.A. **(2002)**, NADPH oxidase priming and p47phox phosphorylation in neutrophils from synovial fluid of patients with rheumatoid arthritis and spondylarthropathy. *Inflammation* 26:273-8.

El Benna J., Ruedi J.M., and Babior B.M. **(1994b)**, Cytosolic guanine nucleotide-binding protein Rac2 operates in vivo as a component of the neutrophil respiratory burst oxidase. Transfer of Rac2 and the cytosolic

oxidase components p47phox and p67phox to the submembranous actin cytoskeleton during oxidase activation. *J Biol Chem* 269:6729-34.

El Benna J.E., Dang P.M., Gaudry M., Fay M., Morel F., Hakim J., and Gougerot-Pocidalo M.A. **(1997)**, Phosphorylation of the respiratory burst oxidase subunit p67(phox) during human neutrophil activation. Regulation by protein kinase C-dependent and independent pathways. *J Biol Chem* 272:17204-8.

Elbim C., Bailly S., Chollet-Martin S., Hakim J., and Gougerot-Pocidalo M.A. **(1994)**, Differential priming effects of proinflammatory cytokines on human neutrophil oxidative burst in response to bacterial N-formyl peptides. *Infect Immun* 62:2195-201.

Ellgaard L., and Helenius A. **(2003)**, Quality control in the endoplasmic reticulum. *Nat Rev Mol Cell Biol* 4:181-91.

Eshed I., Feist E., Althoff C.E., Hamm B., Konen E., Burmester G.R., Backhaus M., and Hermann K.G. **(2009)**, Tenosynovitis of the flexor tendons of the hand detected by MRI: an early indicator of rheumatoid arthritis. *Rheumatology (Oxford)* 48:887-91.

Faust L.R., el Benna J., Babior B.M., and Chanock S.J. **(1995)**, The phosphorylation targets of p47phox, a subunit of the respiratory burst oxidase. Functions of the individual target serines as evaluated by site-directed mutagenesis. *J Clin Invest* 96:1499-505.

Fava R.A., Olsen N.J., Postlethwaite A.E., Broadley K.N., Davidson J.M., Nanney L.B., Lucas C., and Townes A.S. **(1991)**, Transforming growth factor beta 1 (TGF-beta 1) induced neutrophil recruitment to synovial tissues: implications for TGF-beta-driven synovial inflammation and hyperplasia. *J Exp Med* 173:1121-32.

Filer A., Parsonage G., Smith E., Osborne C., Thomas A.M., Curnow S.J., Rainger G.E., Raza K., Nash G.B., Lord J., Salmon M., and Buckley C.D. **(2006)**, Differential survival of leukocyte subsets mediated by synovial, bone marrow, and skin fibroblasts: site-specific versus activation-dependent survival of T cells and neutrophils. *Arthritis Rheum* 54:2096-108.

Foell D., and Roth J. **(2004)**, Proinflammatory S100 proteins in arthritis and autoimmune disease. *Arthritis Rheum* 50:3762-71.

Foell D., Wittkowski H., Vogl T., and Roth J. **(2007)**, S100 proteins expressed in phagocytes: a novel group of damage-associated molecular pattern molecules. *J Leukoc Biol* 81:28-37.

Fontayne A., Dang P.M., Gougerot-Pocidalo M.A., and El-Benna J. **(2002)**, Phosphorylation of p47phox sites by PKC alpha, beta II, delta, and zeta: effect on binding to p22phox and on NADPH oxidase activation. *Biochemistry* 41:7743-50.

Forbes L.V., Truong O., Wientjes F.B., Moss S.J., and Segal A.W. **(1999)**, The major phosphorylation site of the NADPH oxidase component p67phox is Thr233. *Biochem J* 338:99-105.

Foubert T.R., Burritt J.B., Taylor R.M., and Jesaitis A.J. **(2002)**, Structural changes are induced in human neutrophil cytochrome b by NADPH oxidase activators, LDS, SDS, and arachidonate: intermolecular resonance energy transfer between trisulfopyrenyl-wheat germ agglutinin and cytochrome b_{558}. *Biochim Biophys Acta* 1567:221-31.

Francke U., Hsieh C.L., Foellmer B.E., Lomax K.J., Malech H.L., and Leto T.L. **(1990)**, Genes for two autosomal recessive forms of chronic granulomatous disease assigned to 1q25 (NCF2) and 7q11.23 (NCF1). *Am J Hum Genet* 47:483-92.

Freeman J.L., and Lambeth J.D. **(1996)**, NADPH oxidase activity is independent of p47phox in vitro. *J Biol Chem* 271:22578-82.

Frosch M., Strey A., Vogl T., Wulffraat N.M., Kuis W., Sunderkotter C., Harms E., Sorg C., and Roth J. **(2000)**, Myeloid-related proteins 8 and 14 are specifically secreted during interaction of phagocytes and activated endothelium and are useful markers for monitoring disease activity in pauciarticular-onset juvenile rheumatoid arthritis. *Arthritis Rheum* 43:628-37.

Fukuishi N., Sakaguchi M., Matsuura S., Nakagawa C., Akagi R., and Akagi M. **(1997)**, The mechanisms of compound 48/80-induced superoxide generation mediated by A-kinase in rat peritoneal mast cells. *Biochem Mol Med* 61:107-13.

Gabig T.G., Bearman S.I., and Babior B.M. **(1979)**, Effects of oxygen tension and pH on the respiratory burst of human neutrophils. *Blood* 53:1133-9.

Gadher S.J., Eyre D.R., Duance V.C., Wotton S.F., Heck L.W., Schmid T.M., and Woolley D.E. **(1988)**, Susceptibility of cartilage collagens type II, IX, X, and XI to human synovial collagenase and neutrophil elastase. *Eur J Biochem* 175:1-7.

Ganz T. **(1987)**, Extracellular release of antimicrobial defensins by human polymorphonuclear leukocytes. *Infect Immun* 55:568-71.

Gao J.X., Wilkins J., and Issekutz A.C. **(1995)**, Migration of human polymorphonuclear leukocytes through a synovial fibroblast barrier is mediated by both beta 2 (CD11/CD18) integrins and the beta 1 (CD29) integrins VLA-5 and VLA-6. *Cell Immunol* 163:178-86.

Garcia-Vicuna R., Gomez-Gaviro M.V., Dominguez-Luis M.J., Pec M.K., Gonzalez-Alvaro I., Alvaro-Gracia J.M., and Diaz-Gonzalez F. **(2004)**, CC and CXC chemokine receptors mediate migration, proliferation, and matrix metalloproteinase production by fibroblast-like synoviocytes from rheumatoid arthritis patients. *Arthritis Rheum* 50:3866-77.

Garcia R.C., and Segal A.W. **(1988)**, Phosphorylation of the subunits of cytochrome b-245 upon triggering of the respiratory burst of human neutrophils and macrophages. *Biochem J* 252:901-4.

Garofalo R.S., Orena S.J., Rafidi K., Torchia A.J., Stock J.L., Hildebrandt A.L., Coskran T., Black S.C., Brees D.J., Wicks J.R., McNeish J.D., and Coleman K.G. **(2003)**, Severe diabetes, age-dependent loss of adipose tissue, and mild growth deficiency in mice lacking Akt2/PKB beta. *J Clin Invest* 112:197-208.

Gartlehner G., Hansen R.A., Jonas B.L., Thieda P., and Lohr K.N. **(2006)**, The comparative efficacy and safety of biologics for the treatment of rheumatoid arthritis: a systematic review and metaanalysis. *J Rheumatol* 33:2398-408.

Gay S., Muller-Ladner U., and Gay R.E. **(1996)**, Molecular basis of rheumatoid joint destruction: analogies to the pathogenesis of autoimmunity in diabetes. *Diabetes Res Clin Pract* 30 Suppl:131-5.

Gebhardt C., Nemeth J., Angel P., and Hess J. **(2006)**, S100A8 and S100A9 in inflammation and cancer. *Biochem Pharmacol* 72:1622-31.

Geiszt M., Dagher M.C., Molnar G., Havasi A., Faure J., Paclet M.H., Morel F., and Ligeti E. **(2001)**, Characterization of membrane-localized and cytosolic Rac-GTPase-activating proteins in human neutrophil granulocytes: contribution to the regulation of NADPH oxidase. *Biochem J* 355:851-8.

Gottenberg J.E., Miceli-Richard C., Ducot B., Goupille P., Combe B., and Mariette X. **(2009)**, Markers of B-lymphocyte activation are elevated in patients with early rheumatoid arthritis and correlated with disease activity in the ESPOIR cohort. *Arthritis Res Ther* 11:R114.

Grange L., Nguyen M.V., Lardy B., Derouazi M., Campion Y., Trocme C., Paclet M.H., Gaudin P., and Morel F. **(2006)**, NAD(P)H oxidase activity of Nox4 in chondrocytes is both inducible and involved in collagenase expression. *Antioxid Redox Signal* 8:1485-96.

Gravallese E.M. **(2002)**, Bone destruction in arthritis. *Ann Rheum Dis* 61:84-6.

Grimbaldeston M.A., Geczy C.L., Tedla N., Finlay-Jones J.J., and Hart P.H. **(2003)**, S100A8 induction in keratinocytes by ultraviolet A irradiation is dependent on reactive oxygen intermediates. *J Invest Dermatol* 121:1168-74.

Gringhuis S.I., Papendrecht-van der Voort E.A., Leow A., Nivine Levarht E.W., Breedveld F.C., and Verweij C.L. **(2002)**, Effect of redox balance alterations on cellular localization of LAT and downstream T-cell receptor signaling pathways. *Mol Cell Biol* 22:400-11.

Groemping Y., and Rittinger K. **(2005)**, Activation and assembly of the NADPH oxidase: a structural perspective. *Biochem J* 386:401-16.

Grootveld M., Henderson E.B., Farrell A., Blake D.R., Parkes H.G., and Haycock P. **(1991)**, Oxidative damage to hyaluronate and glucose in synovial fluid during exercise of the inflamed rheumatoid joint. Detection of abnormal low-molecular-mass metabolites by proton-n.m.r. spectroscopy. *Biochem J* 273:459-67.

Guichard C., Pedruzzi E., Dewas C., Fay M., Pouzet C., Bens M., Vandewalle A., Ogier-Denis E., Gougerot-Pocidalo M.A., and Elbim C. **(2005)**, Interleukin-8-induced priming of neutrophil oxidative burst requires sequential recruitment of NADPH oxidase components into lipid rafts. *J Biol Chem* 280:37021-32.

Guignard F., and Markert M. **(1996)**, The nucleoside diphosphate kinase of human neutrophils. *Biochem J* 316:233-8.

Haataja L., Groffen J., and Heisterkamp N. **(1997)**, Characterization of RAC3, a novel member of the Rho family. *J Biol Chem* 272:20384-8.

Hagfors L., Leanderson P., Skoldstam L., Andersson J., and Johansson G. **(2003)**, Antioxidant intake, plasma antioxidants and oxidative stress in a randomized, controlled, parallel, Mediterranean dietary intervention study on patients with rheumatoid arthritis. *Nutr J* 2:5.

Hallows K.R., Alzamora R., Li H., Gong F., Smolak C., Neumann D., and Pastor-Soler N.M. **(2009)**, AMP-activated protein kinase inhibits alkaline pH- and PKA-induced apical vacuolar H+-ATPase accumulation in epididymal clear cells. *Am J Physiol Cell Physiol* 296:672-81.

Hamaguchi M., and Hanafusa H. **(1987)**, Association of p60src with Triton X-100-resistant cellular structure correlates with morphological transformation. *Proc Natl Acad Sci U S A* 84:2312-6.

Hamilton J.A., and Slywka J. **(1981)**, Stimulation of human synovial fibroblast plasminogen activator production by mononuclear cell supernatants. *J Immunol* 126:851-5.

Hammer H.B., Odegard S., Fagerhol M.K., Landewe R., van der Heijde D., Uhlig T., Mowinckel P., and Kvien T.K. **(2007)**, Calprotectin (a major leucocyte protein) is strongly and independently correlated with joint inflammation and damage in rheumatoid arthritis. *Ann Rheum Dis* 66:1093-7.

Hammer H.B., Odegard S., Syversen S.W., Landewe R., van der Heijde D., Uhlig T., Mowinckel P., and Kvien T.K. **(2008)**, Calprotectin (a major S100 leukocyte protein) predicts 10-year radiographic progression in patients with rheumatoid arthritis. *Ann Rheum Dis*.

Han C.H., Freeman J.L., Lee T., Motalebi S.A., and Lambeth J.D. **(1998)**, Regulation of the neutrophil respiratory burst oxidase. Identification of an activation domain in p67(phox). *J Biol Chem* 273:16663-8.

Han C.H., Nisimoto Y., Lee S.H., Kim E.T., and Lambeth J.D. **(2001)**, Characterization of the flavoprotein domain of gp91phox which has NADPH diaphorase activity. *J Biochem* 129:513-20.

Hansen T., Petrow P.K., Gaumann A., Keyszer G.M., Eysel P., Eckardt A., Brauer R., and Kriegsmann J. **(2000)**, Cathepsin B and its endogenous inhibitor cystatin C in rheumatoid arthritis synovium. *J Rheumatol* 27:859-65.

Haribabu B., Verghese M.W., Steeber D.A., Sellars D.D., Bock C.B., and Snyderman R. **(2000)**, Targeted disruption of the leukotriene B(4) receptor in mice reveals its role in inflammation and platelet-activating factor-induced anaphylaxis. *J Exp Med* 192:433-8.

Harrison C.A., Raftery M.J., Walsh J., Alewood P., Iismaa S.E., Thliveris S., and Geczy C.L. **(1999)**, Oxidation regulates the inflammatory properties of the murine S100 protein S100A8. *J Biol Chem* 274:8561-9.

Hashimoto S., Takahashi K., Amiel D., Coutts R.D., and Lotz M. **(1998)**, Chondrocyte apoptosis and nitric oxide production during experimentally induced osteoarthritis. *Arthritis Rheum* 41:1266-74.

Hashizume M., Hayakawa N., Suzuki M., and Mihara M. **(2009)**, IL-6/sIL-6R trans-signalling, but not TNF-alpha induced angiogenesis in a HUVEC and synovial cell co-culture system. *Rheumatol Int* 29:1449-54.

Haute Autorité de Santé **(2007)**, Polyarthrite rhumatoïde : Diagnostic et prise en charge initiale.

Hawkins D. **(1973)**, Neutrophilic leukocytes in immunologic reactions in vitro: effect of cytochalasin B. *J Immunol* 110:294-6.

Hegemann N., Wondimu A., Ullrich K., and Schmidt M.F. **(2003)**, Synovial MMP-3 and TIMP-1 levels and their correlation with cytokine expression in canine rheumatoid arthritis. *Vet Immunol Immunopathol* 91:199-204.

Heyworth P.G., and Badwey J.A. **(1990)**, Protein phosphorylation associated with the stimulation of neutrophils. Modulation of superoxide production by protein kinase C and calcium. *J Bioenerg Biomembr* 22:1-26.

Heyworth P.G., Bohl B.P., Bokoch G.M., and Curnutte J.T. **(1994)**, Rac translocates independently of the neutrophil NADPH oxidase components p47phox and p67phox. Evidence for its interaction with flavocytochrome b_{558}. *J Biol Chem* 269:30749-52.

Heyworth P.G., Curnutte J.T., Nauseef W.M., Volpp B.D., Pearson D.W., Rosen H., and Clark R.A. **(1991)**, Neutrophil nicotinamide adenine dinucleotide phosphate oxidase assembly. Translocation of p47-phox and p67-phox requires interaction between p47-phox and cytochrome b558. *J Clin Invest* 87:352-6.

Hiratsuka S., Watanabe A., Aburatani H., and Maru Y. **(2006)**, Tumour-mediated upregulation of chemoattractants and recruitment of myeloid cells predetermines lung metastasis. *Nat Cell Biol* 8:1369-75.

Hot A., and Miossec P. **(2011)**, Effects of interleukin (IL)-17A and IL-17F in human rheumatoid arthritis synoviocytes. *Ann Rheum Dis* 70:727-32.

Hu G., Ye R.D., Dinauer M.C., Malik A.B., and Minshall R.D. **(2008)**, Neutrophil caveolin-1 expression contributes to mechanism of lung inflammation and injury. *Am J Physiol Lung Cell Mol Physiol* 294:178-86.

Hu M.L., Louie S., Cross C.E., Motchnik P., and Halliwell B. **(1993)**, Antioxidant protection against hypochlorous acid in human plasma. *J Lab Clin Med* 121:257-62.

Huber L.C., Brock M., Hemmatazad H., Giger O.T., Moritz F., Trenkmann M., Distler J.H., Gay R.E., Kolling C., Moch H., Michel B.A., Gay S., Distler O., and Jungel A. **(2007)**, Histone deacetylase/acetylase activity in total synovial tissue derived from rheumatoid arthritis and osteoarthritis patients. *Arthritis Rheum* 56:1087-93.

Humby F., Bombardieri M., Manzo A., Kelly S., Blades M.C., Kirkham B., Spencer J., and Pitzalis C. **(2009)**, Ectopic lymphoid structures support ongoing production of class-switched autoantibodies in rheumatoid synovium. *PLoS Med* 6:59-75.

Hummel K.M., Petrow P.K., Franz J.K., Muller-Ladner U., Aicher W.K., Gay R.E., Bromme D., and Gay S. **(1998)**, Cysteine proteinase cathepsin K mRNA is expressed in synovium of patients with rheumatoid arthritis and is detected at sites of synovial bone destruction. *J Rheumatol* 25:1887-94.

Hunter M.J., and Chazin W.J. **(1998)**, High level expression and dimer characterization of the S100 EF-hand proteins, migration inhibitory factor-related proteins 8 and 14. *J Biol Chem* 273:12427-35.

Hwang T.L., Hung H.W., Kao S.H., Teng C.M., Wu C.C., and Cheng S.J. **(2003)**, Soluble guanylyl cyclase activator YC-1 inhibits human neutrophil functions through a cGMP-independent but cAMP-dependent pathway. *Mol Pharmacol* 64:1419-27.

Imaizumi T., Matsumiya T., Yoshida H., Naraoka T., Uesato R., Ishibashi Y., Ota K., Toh S., Fukuda S., and Satoh K. **(2009)**, Tumor-necrosis factor-alpha induces retinoic acid-inducible gene-I in rheumatoid fibroblast-like synoviocytes. *Immunol Lett* 122:89-93.

Ishida S., Yamane S., Nakano S., Yanagimoto T., Hanamoto Y., Maeda-Tanimura M., Toyosaki-Maeda T., Ishizaki J., Matsuo Y., Fukui N., Itoh T., Ochi T., and Suzuki R. **(2009)**, The interaction of monocytes with rheumatoid synovial cells is a key step in LIGHT-mediated inflammatory bone destruction. *Immunology* 128:315-24.

Ito T., Matsui Y., Ago T., Ota K., and Sumimoto H. **(2001)**, Novel modular domain PB1 recognizes PC motif to mediate functional protein-protein interactions. *Embo J* 20:3938-46.

Itou H., Yao M., Fujita I., Watanabe N., Suzuki M., Nishihira J., and Tanaka I. **(2002)**, The crystal structure of human MRP14 (S100A9), a Ca(2+)-dependent regulator protein in inflammatory process. *J Mol Biol* 316:265-76.

Iwanaga T., Shikichi M., Kitamura H., Yanase H., and Nozawa-Inoue K. **(2000)**, Morphology and functional roles of synoviocytes in the joint. *Arch Histol Cytol* 63:17-31.

Jagnandan D., Church J.E., Banfi B., Stuehr D.J., Marrero M.B., and Fulton D.J. **(2007)**, Novel mechanism of activation of NADPH oxidase 5. calcium sensitization via phosphorylation. *J Biol Chem* 282:6494-507.

Jay G.D., Fleming B.C., Watkins B.A., McHugh K.A., Anderson S.C., Zhang L.X., Teeple E., Waller K.A., and Elsaid K.A. **(2011)**, Prevention of cartilage degeneration and restoration of chondroprotection by lubricin tribosupplementation in the rat following anterior cruciate ligament transection. *Arthritis Rheum* 62:2382-91.

Jesaitis A.J., Tolley J.O., Painter R.G., Sklar L.A., and Cochrane C.G. **(1985)**, Membrane-cytoskeleton interactions and the regulation of chemotactic peptide-induced activation of human granulocytes: the effects of dihydrocytochalasin B. *J Cell Biochem* 27:241-53.

Jikko A., Wakisaka T., Iwamoto M., Hiranuma H., Kato Y., Maeda T., Fujishita M., and Fuchihata H. **(1998)**, Effects of interleukin-6 on proliferation and proteoglycan metabolism in articular chondrocyte cultures. *Cell Biol Int* 22:615-21.

Johansson A., Sarndahl E., Andersson T., Bengtsson T., Lundqvist H., and Dahlgren C. **(1995)**, Chemoattractant-induced NADPH oxidase activity in human monocytes is terminated without any association of receptor-ligand complex to cytoskeleton. *Inflammation* 19:179-91.

Johnson J.L., Park J.W., Benna J.E., Faust L.P., Inanami O., and Babior B.M. **(1998)**, Activation of p47(PHOX), a cytosolic subunit of the leukocyte NADPH oxidase. Phosphorylation of ser-359 or ser-370 precedes phosphorylation at other sites and is required for activity. *J Biol Chem* 273:35147-52.

Jones G., Halbert J., Crotty M., Shanahan E.M., Batterham M., and Ahern M. **(2003)**, The effect of treatment on radiological progression in rheumatoid arthritis: a systematic review of randomized placebo-controlled trials. *Rheumatology (Oxford)* 42:6-13.

Joosten L.A., and Netea M.G. **(2009)**, Interleukin-1 receptor-associated kinase 4 links innate immunity to the pathogenesis of rheumatoid arthritis. *Arthritis Rheum* 60:1571-4.

Kaipiainen-Seppanen O., Aho K., Isomaki H., and Laakso M. **(1996)**, Shift in the incidence of rheumatoid arthritis toward elderly patients in Finland during 1975-1990. *Clin Exp Rheumatol* 14:537-42.

Kaipiainen-Seppanen O., and Kautiainen H. **(2006)**, Declining trend in the incidence of rheumatoid factor-positive rheumatoid arthritis in Finland 1980-2000. *J Rheumatol* 33:2132-8.

Kanai F., Liu H., Field S.J., Akbary H., Matsuo T., Brown G.E., Cantley L.C., and Yaffe M.B. **(2001)**, The PX domains of p47phox and p40phox bind to lipid products of PI(3)K. *Nat Cell Biol* 3:675-8.

Kane D., Roth J., Frosch M., Vogl T., Bresnihan B., and FitzGerald O. **(2003)**, Increased perivascular synovial membrane expression of myeloid-related proteins in psoriatic arthritis. *Arthritis Rheum* 48:1676-85.

Karnovsky M.L. **(1968)**, The metabolism of leukocytes. *Semin Hematol* 5:156-65.

Karouzakis E., Gay R.E., Michel B.A., Gay S., and Neidhart M. **(2009)**, DNA hypomethylation in rheumatoid arthritis synovial fibroblasts. *Arthritis Rheum* 60:3613-22.

Kasama T., Strieter R.M., Lukacs N.W., Burdick M.D., and Kunkel S.L. **(1994)**, Regulation of neutrophil-derived chemokine expression by IL-10. *J Immunol* 152:3559-69.

Kaur H., Edmonds S.E., Blake D.R., and Halliwell B. **(1996)**, Hydroxyl radical generation by rheumatoid blood and knee joint synovial fluid. *Ann Rheum Dis* 55:915-20.

Kawahara T., Jackson H.M., Smith S.M., Simpson P.D., and Lambeth J.D. **(2011)**, Nox5 forms a functional oligomer mediated by self-association of its dehydrogenase domain. *Biochemistry* 50:2013-25.

Kawahara T., Ritsick D., Cheng G., and Lambeth J.D. **(2005)**, Point mutations in the proline-rich region of p22phox are dominant inhibitors of Nox1- and Nox2-dependent reactive oxygen generation. *J Biol Chem* 280:31859-69.

Kerkhoff C., Hofmann H.A., Vormoor J., Melkonyan H., Roth J., Sorg C., and Klempt M. **(2002)**, Binding of two nuclear complexes to a novel regulatory element within the human S100A9 promoter drives the S100A9 gene expression. *J Biol Chem* 277:41879-87.

Kerkhoff C., Klempt M., Kaever V., and Sorg C. **(1999)**, The two calcium-binding proteins, S100A8 and S100A9, are involved in the metabolism of arachidonic acid in human neutrophils. *J Biol Chem* 274:32672-9.

Kerkhoff C., Klempt M., and Sorg C. **(1998)**, Novel insights into structure and function of MRP8 (S100A8) and MRP14 (S100A9). *Biochim Biophys Acta* 1448:200-11.

Kerkhoff C., Nacken W., Benedyk M., Dagher M.C., Sopalla C., and Doussiere J. **(2005)**, The arachidonic acid-binding protein S100A8/A9 promotes NADPH oxidase activation by interaction with p67phox and Rac-2. *FASEB J* 19:467-9.

Khwaja A., Carver J.E., and Linch D.C. **(1992)**, Interactions of granulocyte-macrophage colony-stimulating factor (CSF), granulocyte CSF, and tumor necrosis factor alpha in the priming of the neutrophil respiratory burst. *Blood* 79:745-53.

Kindzelskii A.L., Ueki T., Michibata H., Chaiworapongsa T., Romero R., and Petty H.R. **(2004)**, 6-phosphogluconate dehydrogenase and glucose-6-phosphate dehydrogenase form a supramolecular complex in human neutrophils that undergoes retrograde trafficking during pregnancy. *J Immunol* 172:6373-81.

Kita H., Ohnishi T., Okubo Y., Weiler D., Abrams J.S., and Gleich G.J. **(1991)**, Granulocyte/macrophage colony-stimulating factor and interleukin 3 release from human peripheral blood eosinophils and neutrophils. *J Exp Med* 174:745-8.

Kitamura H., Okumura M., Sato F., Kimoto K., Kohama M., Hashimoto Y., Tagami M., and Iwanaga T. **(2001)**, Increased concentrations of protein gene product 9.5 in the synovial fluid from horses with osteoarthritis. *Jpn J Vet Res* 49:115-23.

Kitamura K., Kangawa K., Matsuo H., and Uyeda K. **(1988)**, Phosphorylation of myocardial fructose-6-phosphate,2-kinase: fructose-2,6-bisphosphatase by cAMP-dependent protein kinase and protein kinase C. Activation by phosphorylation and amino acid sequences of the phosphorylation sites. *J Biol Chem* 263:16796-801.

Klimiuk P.A., Yang H., Goronzy J.J., and Weyand C.M. **(1999)**, Production of cytokines and metalloproteinases in rheumatoid synovitis is T cell dependent. *Clin Immunol* 90:65-78.

Klingelhofer J., Senolt L., Baslund B., Nielsen G.H., Skibshoj I., Pavelka K., Neidhart M., Gay S., Ambartsumian N., Hansen B.S., Petersen J., Lukanidin E., and Grigorian M. **(2007)**, Up-regulation of metastasis-promoting S100A4 (Mts-1) in rheumatoid arthritis: putative involvement in the pathogenesis of rheumatoid arthritis. *Arthritis Rheum* 56:779-89.

Knaus U.G., Heyworth P.G., Evans T., Curnutte J.T., and Bokoch G.M. **(1991)**, Regulation of phagocyte oxygen radical production by the GTP-binding protein Rac 2. *Science* 254:1512-5.

Koch A.E., Kunkel S.L., Harlow L.A., Johnson B., Evanoff H.L., Haines G.K., Burdick M.D., Pope R.M., and Strieter R.M. **(1992)**, Enhanced production of monocyte chemoattractant protein-1 in rheumatoid arthritis. *J Clin Invest* 90:772-9.

Koga H., Terasawa H., Nunoi H., Takeshige K., Inagaki F., and Sumimoto H. **(1999)**, Tetratricopeptide repeat (TPR) motifs of p67(phox) participate in interaction with the small GTPase Rac and activation of the phagocyte NADPH oxidase. *J Biol Chem* 274:25051-60.

Korndorfer I.P., Brueckner F., and Skerra A. **(2007)**, The crystal structure of the human (S100A8/S100A9)2 heterotetramer, calprotectin, illustrates how conformational changes of interacting alpha-helices can determine specific association of two EF-hand proteins. *J Mol Biol* 370:887-98.

Koshkin V., Lotan O., and Pick E. **(1996)**, The cytosolic component p47(phox) is not a sine qua non participant in the activation of NADPH oxidase but is required for optimal superoxide production. *J Biol Chem* 271:30326-9.

Kramer I.M., van der Bend R.L., Verhoeven A.J., and Roos D. **(1988)**, The 47-kDa protein involved in the NADPH:O2 oxidoreductase activity of human neutrophils is phosphorylated by cyclic AMP-dependent protein kinase without induction of a respiratory burst. *Biochim Biophys Acta* 971:189-96.

Krey P.R., and Bailen D.A. **(1979)**, Synovial fluid leukocytosis. A study of extremes. *Am J Med* 67:436-42.

Kroger H., Miesel R., Dietrich A., Ohde M., Altrichter S., Braun C., and Ockenfels H. **(1997)**, Suppression of type II collagen-induced arthritis by N-acetyl-L-cysteine in mice. *Gen Pharmacol* 29:671-4.

Kurz B., Steinhagen J., and Schunke M. **(1999)**, Articular chondrocytes and synoviocytes in a co-culture system: influence on reactive oxygen species-induced cytotoxicity and lipid peroxidation. *Cell Tissue Res* 296:555-63.

Kvien T.K., Uhlig T., Odegard S., and Heiberg M.S. **(2006)**, Epidemiological aspects of rheumatoid arthritis: the sex ratio. *Ann N Y Acad Sci* 1069:212-22.

Kwoh C.K., Venglish C., Lynn A.H., Whitley D.M., Young E., and Chakravarti A. **(1996)**, Age, sex, and the familial risk of rheumatoid arthritis. *Am J Epidemiol* 144:15-24.

Kwong C.H., Malech H.L., Rotrosen D., and Leto T.L. **(1993)**, Regulation of the human neutrophil NADPH oxidase by rho-related G-proteins. *Biochemistry* 32:5711-7.

Laemmli U.K. **(1970)**, Cleavage of structural proteins during the assembly of the head of bacteriophage T4. *Nature* 227:680-5.

Lafyatis R., Thompson N.L., Remmers E.F., Flanders K.C., Roche N.S., Kim S.J., Case J.P., Sporn M.B., Roberts A.B., and Wilder R.L. **(1989)**, Transforming growth factor-beta production by synovial tissues from rheumatoid patients and streptococcal cell wall arthritic rats. Studies on secretion by synovial fibroblast-like cells and immunohistologic localization. *J Immunol* 143:1142-8.

Lapouge K., Smith S.J., Groemping Y., and Rittinger K. **(2002)**, Architecture of the p40-p47-p67phox complex in the resting state of the NADPH oxidase. A central role for p67phox. *J Biol Chem* 277:10121-8.

Lapouge K., Smith S.J., Walker P.A., Gamblin S.J., Smerdon S.J., and Rittinger K. **(2000)**, Structure of the TPR domain of p67phox in complex with Rac.GTP. *Mol Cell* 6:899-907.

Lee B.W., and Yap H.K. **(1994)**, Polyarthritis resembling juvenile rheumatoid arthritis in a girl with chronic granulomatous disease. *Arthritis Rheum* 37:773-6.

Lefevre S., Knedla A., Tennie C., Kampmann A., Wunrau C., Dinser R., Korb A., Schnaker E.M., Tarner I.H., Robbins P.D., Evans C.H., Sturz H., Steinmeyer J., Gay S., Scholmerich J., Pap T., Muller-Ladner U., and Neumann E. **(2009)**, Synovial fibroblasts spread rheumatoid arthritis to unaffected joints. *Nat Med* 15:1414-20.

Leino L., Forbes L., Segal A., and Cockcroft S. **(1999)**, Reconstitution of GTPgammaS-induced NADPH oxidase activity in streptolysin-O-permeabilized neutrophils by specific cytosol fractions. *Biochem Biophys Res Commun* 265:29-37.

Lemarie A., Bourdonnay E., Morzadec C., Fardel O., and Vernhet L. **(2008)**, Inorganic arsenic activates reduced NADPH oxidase in human primary macrophages through a Rho kinase/p38 kinase pathway. *J Immunol* 180:6010-7.

Lemmon M.A. **(2008)**, Membrane recognition by phospholipid-binding domains. *Nat Rev Mol Cell Biol* 9:99-111.

Leopoldt D., Hanck T., Exner T., Maier U., Wetzker R., and Nurnberg B. **(1998)**, Gbetagamma stimulates phosphoinositide 3-kinase-gamma by direct interaction with two domains of the catalytic p110 subunit. *J Biol Chem* 273:7024-9.

Lewis E.M., Sergeant S., Ledford B., Stull N., Dinauer M.C., and McPhail L.C. **(2010)**, Phosphorylation of p22phox on threonine 147 enhances NADPH oxidase activity by promoting p47phox binding. *J Biol Chem* 285:2959-67.

Li X., and Makarov S. **(2006a)**, An essenciatial role of NF-κb in the "tumor like" phenotype of arthritic synoviocytes. *Proc Natl Acad Sci* 103:17432-7.

Li Y., Brazzell J., Herrera A., and Walcheck B. **(2006b)**, ADAM17 deficiency by mature neutrophils has differential effects on L-selectin shedding. *Blood* 108:2275-9.

Lim S.Y., Raftery M., Cai H., Hsu K., Yan W.X., Hseih H.L., Watts R.N., Richardson D., Thomas S., Perry M., and Geczy C.L. **(2008)**, S-nitrosylated S100A8: novel anti-inflammatory properties. *J Immunol* 181:5627-36.

Lim S.Y., Raftery M.J., and Geczy C.L. **(2011)**, Oxidative Modifications of DAMPs Suppress Inflammation: The Case for S100A8 and S100A9. *Antioxid Redox Signal* 15:2235-48.

Lim S.Y., Raftery M.J., Goyette J., and Geczy C.L. **(2010)**, S-glutathionylation regulates inflammatory activities of S100A9. *J Biol Chem* 285:14377-88.

Lim S.Y., Raftery M.J., Goyette J., Hsu K., and Geczy C.L. **(2009)**, Oxidative modifications of S100 proteins: functional regulation by redox. *J Leukoc Biol* 86:577-87.

Lindemann A., Riedel D., Oster W., Meuer S.C., Blohm D., Mertelsmann R.H., and Herrmann F. **(1988)**, Granulocyte/macrophage colony-stimulating factor induces interleukin 1 production by human polymorphonuclear neutrophils. *J Immunol* 140:837-9.

Lindemann A., Riedel D., Oster W., Ziegler-Heitbrock H.W., Mertelsmann R., and Herrmann F. **(1989)**, Granulocyte-macrophage colony-stimulating factor induces cytokine secretion by human polymorphonuclear leukocytes. *J Clin Invest* 83:1308-12.

Linderkamp O., Ruef P., Brenner B., Gulbins E., and Lang F. **(1998)**, Passive deformability of mature, immature, and active neutrophils in healthy and septicemic neonates. *Pediatr Res* 44:946-50.

Lloyd P.G., and Hardin C.D. **(2001)**, Caveolae and the organization of carbohydrate metabolism in vascular smooth muscle. *J Cell Biochem* 82:399-408.

Lomax K.J., Leto T.L., Nunoi H., Gallin J.I., and Malech H.L. **(1989)**, Recombinant 47-kilodalton cytosol factor restores NADPH oxidase in chronic granulomatous disease. *Science* 245:409-12.

Lopes L.R., Dagher M.C., Gutierrez A., Young B., Bouin A.P., Fuchs A., and Babior B.M. **(2004)**, Phosphorylated p40PHOX as a negative regulator of NADPH oxidase. *Biochemistry* 43:3723-30.

Lu D.J., and Grinstein S. **(1990)**, ATP and guanine nucleotide dependence of neutrophil activation. Evidence for the involvement of two distinct GTP-binding proteins. *J Biol Chem* 265:13721-9.

Ma Y., and Pope R.M. **(2005)**, The role of macrophages in rheumatoid arthritis. *Curr Pharm Des* 11:569-80.

Maianski N.A., Geissler J., Srinivasula S.M., Alnemri E.S., Roos D., and Kuijpers T.W. **(2004)**, Functional characterization of mitochondria in neutrophils: a role restricted to apoptosis. *Cell Death Differ* 11:143-53.

Maianski N.A., Mul F.P., van Buul J.D., Roos D., and Kuijpers T.W. **(2002)**, Granulocyte colony-stimulating factor inhibits the mitochondria-dependent activation of caspase-3 in neutrophils. *Blood* 99:672-9.

Maillefert J.F., Combe B., Goupille P., Cantagrel A., and Dougados M. **(2003)**, Long term structural effects of combination therapy in patients with early rheumatoid arthritis: five year follow up of a prospective double blind controlled study. *Ann Rheum Dis* 62:764-6.

Mao G.D., and Poznansky M.J. **(1992)**, Electron spin resonance study on the permeability of superoxide radicals in lipid bilayers and biological membranes. *FEBS Lett* 305:233-6.

Marklund S.L. **(1982)**, Human copper-containing superoxide dismutase of high molecular weight. *Proc Natl Acad Sci U S A* 79:7634-8.

Marsin A.S., Bertrand L., Rider M.H., Deprez J., Beauloye C., Vincent M.F., Van den Berghe G., Carling D., and Hue L. **(2000)**, Phosphorylation and activation of heart PFK-2 by AMPK has a role in the stimulation of glycolysis during ischaemia. *Curr Biol* 10:1247-55.

Marsin A.S., Bouzin C., Bertrand L., and Hue L. **(2002)**, The stimulation of glycolysis by hypoxia in activated monocytes is mediated by AMP-activated protein kinase and inducible 6-phosphofructo-2-kinase. *J Biol Chem* 277:30778-83.

Martyn K.D., Frederick L.M., von Loehneysen K., Dinauer M.C., and Knaus U.G. **(2006)**, Functional analysis of Nox4 reveals unique characteristics compared to other NADPH oxidases. *Cell Signal* 18:69-82.

Matsumoto S., Muller-Ladner U., Gay R.E., Nishioka K., and Gay S. **(1996)**, Ultrastructural demonstration of apoptosis, Fas and Bcl-2 expression of rheumatoid synovial fibroblasts. *J Rheumatol* 23:1345-52.

Matute J.D., Arias A.A., Wright N.A., Wrobel I., Waterhouse C.C., Li X.J., Marchal C.C., Stull N.D., Lewis D.B., Steele M., Kellner J.D., Yu W., Meroueh S.O., Nauseef W.M., and Dinauer M.C. **(2009)**, A new genetic subgroup of chronic granulomatous disease with autosomal recessive mutations in p40 phox and selective defects in neutrophil NADPH oxidase activity. *Blood* 114:3309-15.

Matzinger P. **(2002a)**, The danger model: a renewed sense of self. *Science* 296:301-5.

Matzinger P. **(2002b)**, An innate sense of danger. *Ann N Y Acad Sci* 961:341-2.

Maxwell L., and Singh J.A. **(2009)**, Abatacept for rheumatoid arthritis. *Cochrane Database Syst Rev*CD007277.

McColl S.R., Beauseigle D., Gilbert C., and Naccache P.H. **(1990)**, Priming of the human neutrophil respiratory burst by granulocyte-macrophage colony-stimulating factor and tumor necrosis factor-alpha involves regulation at a post-cell surface receptor level. Enhancement of the effect of agents which directly activate G proteins. *J Immunol* 145:3047-53.

McCormick M.M., Rahimi F., Bobryshev Y.V., Gaus K., Zreiqat H., Cai H., Lord R.S., and Geczy C.L. **(2005)**, S100A8 and S100A9 in human arterial wall. Implications for atherogenesis. *J Biol Chem* 280:41521-9.

McPhail L.C., Shirley P.S., Clayton C.C., and Snyderman R. **(1985)**, Activation of the respiratory burst enzyme from human neutrophils in a cell-free system. Evidence for a soluble cofactor. *J Clin Invest* 75:1735-9.

Merkesdal S., Ruof J., Huelsemann J.L., Mittendorf T., Handelmann S., Mau W., and Zeidler H. **(2005)**, Indirect cost assessment in patients with rheumatoid arthritis (RA): comparison of data from the health economic patient questionnaire HEQ-RA and insurance claims data. *Arthritis Rheum* 53:234-40.

Merry P., Grootveld M., Lunec J., and Blake D.R. **(1991)**, Oxidative damage to lipids within the inflamed human joint provides evidence of radical-mediated hypoxic-reperfusion injury. *Am J Clin Nutr* 53:362S-369S.

Mertens M., and Singh J.A. **(2009)**, Anakinra for rheumatoid arthritis. *Cochrane Database Syst Rev*CD005121.

Mikuls T.R., Payne J.B., Reinhardt R.A., Thiele G.M., Maziarz E., Cannella A.C., Holers V.M., Kuhn K.A., and O'Dell J.R. **(2009)**, Antibody responses to Porphyromonas gingivalis (P. gingivalis) in subjects with rheumatoid arthritis and periodontitis. *Int Immunopharmacol* 9:38-42.

Miyazawa K., Mori A., and Okudaira H. **(1998)**, Establishment and characterization of a novel human rheumatoid fibroblast-like synoviocyte line, MH7A, immortalized with SV40 T antigen. *J Biochem* 124:1153-62.

Mizrahi A., Molshanski-Mor S., Weinbaum C., Zheng Y., Hirshberg M., and Pick E. **(2005)**, Activation of the phagocyte NADPH oxidase by Rac Guanine nucleotide exchange factors in conjunction with ATP and nucleoside diphosphate kinase. *J Biol Chem* 280:3802-11.

Mizuki K., Takeya R., Kuribayashi F., Nobuhisa I., Kohda D., Nunoi H., Takeshige K., and Sumimoto H. **(2005)**, A region C-terminal to the proline-rich core of p47phox regulates activation of the phagocyte NADPH oxidase by interacting with the C-terminal SH3 domain of p67phox. *Arch Biochem Biophys* 444:185-94.

Mohr W., Westerhellweg H., and Wessinghage D. **(1981)**, Polymorphonuclear granulocytes in rheumatic tissue destruction. III. an electron microscopic study of PMNs at the pannus-cartilage junction in rheumatoid arthritis. *Ann Rheum Dis* 40:396-9.

Momberger T.S., Levick J.R., and Mason R.M. **(2005)**, Hyaluronan secretion by synoviocytes is mechanosensitive. *Matrix Biol* 24:510-9.

Monod J., Wyman J., and Changeux J.P. **(1965)**, On the Nature of Allosteric Transitions: a Plausible Model. *J Mol Biol* 12:88-118.

Mora A., Davies A.M., Bertrand L., Sharif I., Budas G.R., Jovanovic S., Mouton V., Kahn C.R., Lucocq J.M., Gray G.A., Jovanovic A., and Alessi D.R. **(2003)**, Deficiency of PDK1 in cardiac muscle results in heart failure and increased sensitivity to hypoxia. *Embo J* 22:4666-76.

Morel F. **(2007)**, Molecular aspects of chronic granulomatous disease. "the NADPH oxidase complex". *Bull Acad Natl Med* 191:377-92.

Morel F., Dewald B., Berthier S., Zaoui P., Dianoux A.C., Vignais P.V., and Baggiolini M. **(1994)**, Further characterization of the gelatinase-containing particles of human neutrophils. *Biochim Biophys Acta* 1201:373-80.

Moulding D.A., Akgul C., Derouet M., White M.R., and Edwards S.W. **(2001)**, BCL-2 family expression in human neutrophils during delayed and accelerated apoptosis. *J Leukoc Biol* 70:783-92.

Mowat A.G. **(1976)**, Neutrophil chemotaxis in patients with rheumatoid arthritis: mechanisms responsible for impairment [Proceedings]. *Ann Rheum Dis* 35:286.

Mulherin D.M., Thurnham D.I., and Situnayake R.D. **(1996)**, Glutathione reductase activity, riboflavin status, and disease activity in rheumatoid arthritis. *Ann Rheum Dis* 55:837-40.

Muller-Ladner U., Kriegsmann J., Franklin B.N., Matsumoto S., Geiler T., Gay R.E., and Gay S. **(1996)**, Synovial fibroblasts of patients with rheumatoid arthritis attach to and invade normal human cartilage when engrafted into SCID mice. *Am J Pathol* 149:1607-15.

Muller-Ladner U., Ospelt C., Gay S., Distler O., and Pap T. **(2007)**, Cells of the synovium in rheumatoid arthritis. Synovial fibroblasts. *Arthritis Res Ther* 9:223.

Murphy G., Knauper V., Atkinson S., Butler G., English W., Hutton M., Stracke J., and Clark I. **(2002)**, Matrix metalloproteinases in arthritic disease. *Arthritis Res* 4:39-49.

Naccache P.H., Levasseur S., Lachance G., Chakravarti S., Bourgoin S.G., and McColl S.R. **(2000)**, Stimulation of human neutrophils by chemotactic factors is associated with the activation of phosphatidylinositol 3-kinase gamma. *J Biol Chem* 275:23636-41.

Nakamura R., Sumimoto H., Mizuki K., Hata K., Ago T., Kitajima S., Takeshige K., Sakaki Y., and Ito T. **(1998)**, The PC motif: a novel and evolutionarily conserved sequence involved in interaction between p40phox and p67phox, SH3 domain-containing cytosolic factors of the phagocyte NADPH oxidase. *Eur J Biochem* 251:583-9.

Nalefski E.A., Sultzman L.A., Martin D.M., Kriz R.W., Towler P.S., Knopf J.L., and Clark J.D. **(1994)**, Delineation of two functionally distinct domains of cytosolic phospholipase A2, a regulatory Ca(2+)-dependent lipid-binding domain and a Ca(2+)-independent catalytic domain. *J Biol Chem* 269:18239-49.

Narabayashi H., Lawson J.W., and Uyeda K. **(1985)**, Regulation of phosphofructokinase in perfused rat heart. Requirement for fructose 2,6-bisphosphate and a covalent modification. *J Biol Chem* 260:9750-8.

Nauseef W.M., Volpp B.D., McCormick S., Leidal K.G., and Clark R.A. **(1991)**, Assembly of the neutrophil respiratory burst oxidase. Protein kinase C promotes cytoskeletal and membrane association of cytosolic oxidase components. *J Biol Chem* 266:5911-7.

Navarro-Sarabia F., Ariza-Ariza R., Hernandez-Cruz B., and Villanueva I. **(2005)**, Adalimumab for treating rheumatoid arthritis. *Cochrane Database Syst Rev*CD005113.

Nebl T., Pestonjamasp K.N., Leszyk J.D., Crowley J.L., Oh S.W., and Luna E.J. **(2002)**, Proteomic analysis of a detergent-resistant membrane skeleton from neutrophil plasma membranes. *J Biol Chem* 277:43399-409.

Neidhart M., Seemayer C.A., Hummel K.M., Michel B.A., Gay R.E., and Gay S. **(2003)**, Functional characterization of adherent synovial fluid cells in rheumatoid arthritis: destructive potential in vitro and in vivo. *Arthritis Rheum* 48:1873-80.

Nicolas E., Ramus C., Berthier S., Arlotto M., Bouamrani A., Lefebvre C., Morel F., Garin J., Ifrah N., Berger F., Cahn J.Y., and Mossuz P. **(2011)**, Expression of S100A8 in leukemic cells predicts poor survival in de novo AML patients. *Leukemia* 25:57-65.

Nishimura K., Sugiyama D., Kogata Y., Tsuji G., Nakazawa T., Kawano S., Saigo K., Morinobu A., Koshiba M., Kuntz K.M., Kamae I., and Kumagai S. **(2007)**, Meta-analysis: diagnostic accuracy of anti-cyclic citrullinated peptide antibody and rheumatoid factor for rheumatoid arthritis. *Ann Intern Med* 146:797-808.

Nisimoto Y., Motalebi S., Han C.H., and Lambeth J.D. **(1999)**, The p67(phox) activation domain regulates electron flow from NADPH to flavin in flavocytochrome b_{558}. *J Biol Chem* 274:22999-3005.

Nisimoto Y., Ogawa H., Miyano K., and Tamura M. **(2004)**, Activation of the flavoprotein domain of gp91phox upon interaction with N-terminal p67phox (1-210) and the Rac complex. *Biochemistry* 43:9567-75.

Norgauer J., Kownatzki E., Seifert R., and Aktories K. **(1988)**, Botulinum C2 toxin ADP-ribosylates actin and enhances O2- production and secretion but inhibits migration of activated human neutrophils. *J Clin Invest* 82:1376-82.

Noss E.H., and Brenner M.B. **(2008)**, The role and therapeutic implications of fibroblast-like synoviocytes in inflammation and cartilage erosion in rheumatoid arthritis. *Immunol Rev* 223:252-70.

Nurmohamed M.T., and Dijkmans B.A. **(2005)**, Efficacy, tolerability and cost effectiveness of disease-modifying antirheumatic drugs and biologic agents in rheumatoid arthritis. *Drugs* 65:661-94.

Nuver-Zwart I., Schalkwijk J., Joosten L.A., van den Berg W.B., and van de Putte L.B. **(1988)**, Effects of synovial fluid and synovial fluid cells on chondrocyte metabolism in short term tissue culture. *J Rheumatol* 15:210-6.

Ospelt C., Brentano F., Jungel A., Rengel Y., Kolling C., Michel B.A., Gay R.E., and Gay S. **(2009)**, Expression, regulation, and signaling of the pattern-recognition receptor nucleotide-binding oligomerization domain 2 in rheumatoid arthritis synovial fibroblasts. *Arthritis Rheum* 60:355-63.

Ospelt C., Brentano F., Rengel Y., Stanczyk J., Kolling C., Tak P.P., Gay R.E., Gay S., and Kyburz D. **(2008)**, Overexpression of toll-like receptors 3 and 4 in synovial tissue from patients with early rheumatoid arthritis: toll-like receptor expression in early and longstanding arthritis. *Arthritis Rheum* 58:3684-92.

Ostrakhovitch E.A., and Afanas'ev I.B. **(2001)**, Oxidative stress in rheumatoid arthritis leukocytes: suppression by rutin and other antioxidants and chelators. *Biochem Pharmacol* 62:743-6.

Otsuki Y., Tanaka M., Yoshii S., Kawazoe N., Nakaya K., and Sugimura H. **(2001)**, Tumor metastasis suppressor nm23H1 regulates Rac1 GTPase by interaction with Tiam1. *Proc Natl Acad Sci U S A* 98:4385-90.

Pablos J.L., Santiago B., Galindo M., Torres C., Brehmer M.T., Blanco F.J., and Garcia-Lazaro F.J. **(2003)**, Synoviocyte-derived CXCL12 is displayed on endothelium and induces angiogenesis in rheumatoid arthritis. *J Immunol* 170:2147-52.

Paclet M.H., Berthier S., Kuhn L., Garin J., and Morel F. **(2007)**, Regulation of phagocyte NADPH oxidase activity: identification of two cytochrome b_{558} activation states. *Faseb J* 21:1244-55.

Paclet M.H., Coleman A.W., Burritt J., and Morel F. **(2001)**, NADPH oxidase of Epstein-Barr-virus immortalized B lymphocytes. Effect of cytochrome b_{558} glycosylation. *Eur J Biochem* 268:5197-208.

Paclet M.H., Coleman A.W., Vergnaud S., and Morel F. **(2000)**, P67-phox-mediated NADPH oxidase assembly: imaging of cytochrome b_{558} liposomes by atomic force microscopy. *Biochemistry* 39:9302-10.

Palacios F., Schweitzer J.K., Boshans R.L., and D'Souza-Schorey C. **(2002)**, ARF6-GTP recruits Nm23-H1 to facilitate dynamin-mediated endocytosis during adherens junctions disassembly. *Nat Cell Biol* 4:929-36.

Pap T., Muller-Ladner U., Gay R.E., and Gay S. **(2000)**, Fibroblast biology. Role of synovial fibroblasts in the pathogenesis of rheumatoid arthritis. *Arthritis Res* 2:361-7.

Pap T., Nawrath M., Heinrich J., Bosse M., Baier A., Hummel K.M., Petrow P., Kuchen S., Michel B.A., Gay R.E., Muller-Ladner U., Moelling K., and Gay S. **(2004)**, Cooperation of Ras- and c-Myc-dependent pathways in regulating the growth and invasiveness of synovial fibroblasts in rheumatoid arthritis. *Arthritis Rheum* 50:2794-802.

Park J.W., Ma M., Ruedi J.M., Smith R.M., and Babior B.M. **(1992)**, The cytosolic components of the respiratory burst oxidase exist as a M(r) approximately 240,000 complex that acquires a membrane-binding site during activation of the oxidase in a cell-free system. *J Biol Chem* 267:17327-32.

Patel S., Djerdjouri B., Raoul-Des-Essarts Y., Dang P.M., El-Benna J., and Perianin A. **(2010)**, Protein kinase B (AKT) mediates phospholipase D activation via ERK1/2 and promotes respiratory burst parameters in formylpeptide-stimulated neutrophil-like HL-60 cells. *J Biol Chem* 285:32055-63.

Pearse B.M., and Rosemeyer M.A. **(1974)**, The molecular weight and subunit structure of human erythrocyte 6-phosphogluconate dehydrogenase. *Eur J Biochem* 42:225-35.

Perlman H., and Pope R.M. **(2010)**, The synovial lining micromass system: toward rheumatoid arthritis in a dish? *Arthritis Rheum* 62:643-6.

Pessach I., Leto T.L., Malech H.L., and Levy R. **(2001)**, Essential requirement of cytosolic phospholipase A(2) for stimulation of NADPH oxidase-associated diaphorase activity in granulocyte-like cells. *J Biol Chem* 276:33495-503.

Peterson J.D., Herzenberg L.A., Vasquez K., and Waltenbaugh C. **(1998)**, Glutathione levels in antigen-presenting cells modulate Th1 versus Th2 response patterns. *Proc Natl Acad Sci U S A* 95:3071-6.

Petheo G.L., and Demaurex N. **(2005)**, Voltage- and NADPH-dependence of electron currents generated by the phagocytic NADPH oxidase. *Biochem J* 388:485-91.

Petrow P.K., Hummel K.M., Schedel J., Franz J.K., Klein C.L., Muller-Ladner U., Kriegsmann J., Chang P.L., Prince C.W., Gay R.E., and Gay S. **(2000)**, Expression of osteopontin messenger RNA and protein in rheumatoid arthritis: effects of osteopontin on the release of collagenase 1 from articular chondrocytes and synovial fibroblasts. *Arthritis Rheum* 43:1597-605.

Peveri P., Heyworth P.G., and Curnutte J.T. **(1992)**, Absolute requirement for GTP in activation of human neutrophil NADPH oxidase in a cell-free system: role of ATP in regenerating GTP. *Proc Natl Acad Sci U S A* 89:2494-8.

Polack B., Toussaint B., Quénée L., and inventors Outil de transfert et de production de protéines mettant en oeuvre le système de sécrétion de type III de Pseudomonas. Patent WO2005049644.

Polack B., Vergnaud S., Paclet M.H., Lamotte D., Toussaint B., and Morel F. **(2000)**, Protein delivery by Pseudomonas type III secretion system: Ex vivo complementation of p67(phox)-deficient chronic granulomatous disease. *Biochem Biophys Res Commun* 275:854-8.

Porter C.D., Kuribayashi F., Parkar M.H., Roos D., and Kinnon C. **(1996)**, Detection of gp91-phox precursor protein in B-cell lines from patients with X-linked chronic granulomatous disease as an indicator for mutations impairing cytochrome b_{558} biosynthesis. *Biochem J* 315:571-5.

Poubelle P.E., Chakravarti A., Fernandes M.J., Doiron K., and Marceau A.A. **(2007)**, Differential expression of RANK, RANK-L, and osteoprotegerin by synovial fluid neutrophils from patients with rheumatoid arthritis and by healthy human blood neutrophils. *Arthritis Res Ther* 9:R25.

Pouliot P., Plante I., Raquil M.A., Tessier P.A., and Olivier M. **(2008)**, Myeloid-related proteins rapidly modulate macrophage nitric oxide production during innate immune response. *J Immunol* 181:3595-601.

Pozuelo Rubio M., Peggie M., Wong B.H., Morrice N., and MacKintosh C. **(2003)**, 14-3-3s regulate fructose-2,6-bisphosphate levels by binding to PKB-phosphorylated cardiac fructose-2,6-bisphosphate kinase/phosphatase. *Embo J* 22:3514-23.

Pozzan T., Lew D.P., Wollheim C.B., and Tsien R.Y. **(1983)**, Is cytosolic ionized calcium regulating neutrophil activation? *Science* 221:1413-5.

Preston A. **(2002)**, Extracellular Matrix Proteases. *Calbiochem-Oncogen* 2:120.

Privat S.J., Oo A., and Waterbury L.D. **(2001)**, Production of interleukin-6, but not interleukin-8, induced by TNF-alpha or IL-1 beta in human fibroblast-like synoviocyte increases over cell passage. *Proc West Pharmacol Soc* 44:9-13.

Quenee L., Lamotte D., and Polack B. **(2005)**, Combined sacB-based negative selection and cre-lox antibiotic marker recycling for efficient gene deletion in pseudomonas aeruginosa. *Biotechniques* 38:63-7.

Quinn M.T., Mullen M.L., Jesaitis A.J., and Linner J.G. **(1992)**, Subcellular distribution of the Rap1A protein in human neutrophils: colocalization and cotranslocation with cytochrome b559. *Blood* 79:1563-73.

Quinn M.T., Parkos C.A., and Jesaitis A.J. **(1989)**, The lateral organization of components of the membrane skeleton and superoxide generation in the plasma membrane of stimulated human neutrophils. *Biochim Biophys Acta* 987:83-94.

Raad H., Paclet M.H., Boussetta T., Kroviarski Y., Morel F., Quinn M.T., Gougerot-Pocidalo M.A., Dang P.M., and El-Benna J. **(2009)**, Regulation of the phagocyte NADPH oxidase activity: phosphorylation of gp91phox/NOX2 by protein kinase C enhances its diaphorase activity and binding to Rac2, p67phox, and p47phox. *Faseb J* 23:1011-22.

Raftery M.J., Yang Z., Valenzuela S.M., and Geczy C.L. **(2001)**, Novel intra- and inter-molecular sulfinamide bonds in S100A8 produced by hypochlorite oxidation. *J Biol Chem* 276:33393-401.

Rammes A., Roth J., Goebeler M., Klempt M., Hartmann M., and Sorg C. **(1997)**, Myeloid-related protein (MRP) 8 and MRP14, calcium-binding proteins of the S100 family, are secreted by activated monocytes via a novel, tubulin-dependent pathway. *J Biol Chem* 272:9496-502.

Rat A.C., and Boissier M.C. **(2004)**, Rheumatoid arthritis: direct and indirect costs. *Joint Bone Spine* 71:518-24.

Ravasi T., Hsu K., Goyette J., Schroder K., Yang Z., Rahimi F., Miranda L.P., Alewood P.F., Hume D.A., and Geczy C. **(2004)**, Probing the S100 protein family through genomic and functional analysis. *Genomics* 84:10-22.

Rees M.D., Hawkins C.L., and Davies M.J. **(2004)**, Hypochlorite and superoxide radicals can act synergistically to induce fragmentation of hyaluronan and chondroitin sulphates. *Biochem J* 381:175-84.

Reeves E.P., Dekker L.V., Forbes L.V., Wientjes F.B., Grogan A., Pappin D.J., and Segal A.W. **(1999)**, Direct interaction between p47phox and protein kinase C: evidence for targeting of protein kinase C by p47phox in neutrophils. *Biochem J* 344:859-66.

Regier D.S., Greene D.G., Sergeant S., Jesaitis A.J., and McPhail L.C. **(2000)**, Phosphorylation of p22phox is mediated by phospholipase D-dependent and -independent mechanisms. Correlation of NADPH oxidase activity and p22phox phosphorylation. *J Biol Chem* 275:28406-12.

Reizer A., Deutscher J., Saier M.H., Jr., and Reizer J. **(1991)**, Analysis of the gluconate (gnt) operon of Bacillus subtilis. *Mol Microbiol* 5:1081-9.

Remijsen Q., Vanden Berghe T., Parthoens E., Asselbergh B., Vandenabeele P., and Willems J. **(2009)**, Inhibition of spontaneous neutrophil apoptosis by parabutoporin acts independently of NADPH oxidase inhibition but by lipid raft-dependent stimulation of Akt. *J Leukoc Biol* 85:497-507.

Reparon-Schuijt C.C., van Esch W.J., van Kooten C., Rozier B.C., Levarht E.W., Breedveld F.C., and Verweij C.L. **(2000)**, Regulation of synovial B cell survival in rheumatoid arthritis by vascular cell adhesion molecule 1 (CD106) expressed on fibroblast-like synoviocytes. *Arthritis Rheum* 43:1115-21.

Rider M.H., Bertrand L., Vertommen D., Michels P.A., Rousseau G.G., and Hue L. **(2004)**, 6-phosphofructo-2-kinase/fructose-2,6-bisphosphatase: head-to-head with a bifunctional enzyme that controls glycolysis. *Biochem J* 381:561-79.

Rider M.H., and Hue L. **(1986)**, Phosphorylation of purified bovine heart and rat liver 6-phosphofructo-2-kinase by protein kinase C and comparison of the fructose-2,6-bisphosphatase activity of the two enzymes. *Biochem J* 240:57-61.

Rider M.H., van Damme J., Lebeau E., Vertommen D., Vidal H., Rousseau G.G., Vandekerckhove J., and Hue L. **(1992a)**, The two forms of bovine heart 6-phosphofructo-2-kinase/fructose-2,6-bisphosphatase result from alternative splicing. *Biochem J* 285:405-11.

Rider M.H., van Damme J., Vertommen D., Michel A., Vandekerckhove J., and Hue L. **(1992b)**, Evidence for new phosphorylation sites for protein kinase C and cyclic AMP-dependent protein kinase in bovine heart 6-phosphofructo-2-kinase/fructose-2,6-bisphosphatase. *FEBS Lett* 310:139-42.

Ritchie D.M., Boyle J.A., McInnes J.M., Jasani M.K., Dalakos T.G., Grieveson P., and Buchanan W.W. **(1968)**, Clinical studies with an articular index for the assessment of joint tenderness in patients with rheumatoid arthritis. *Q J Med* 37:393-406.

Rosengren S., Corr M., and Boyle D.L. **(2010)**, Platelet-derived growth factor and transforming growth factor beta synergistically potentiate inflammatory mediator synthesis by fibroblast-like synoviocytes. *Arthritis Res Ther* 12:R65.

Roth J., Burwinkel F., van den Bos C., Goebeler M., Vollmer E., and Sorg C. **(1993)**, MRP8 and MRP14, S-100-like proteins associated with myeloid differentiation, are translocated to plasma membrane and intermediate filaments in a calcium-dependent manner. *Blood* 82:1875-83.

Roth J., Vogl T., Sorg C., and Sunderkotter C. **(2003)**, Phagocyte-specific S100 proteins: a novel group of proinflammatory molecules. *Trends Immunol* 24:155-8.

Roux C.H., Saraux A., Le Bihan E., Fardellone P., Guggenbuhl P., Fautrel B., Masson C., Chary-Valckenaere I., Cantagrel A., Juvin R., Flipo R.M., Euller-Ziegler L., Coste J., and Guillemin F. **(2007)**, Rheumatoid arthritis and spondyloarthropathies: geographical variations in prevalence in France. *J Rheumatol* 34:117-22.

Royer-Pokora B., Kunkel L.M., Monaco A.P., Goff S.C., Newburger P.E., Baehner R.L., Cole F.S., Curnutte J.T., and Orkin S.H. **(1986)**, Cloning the gene for an inherited human disorder--chronic granulomatous disease--on the basis of its chromosomal location. *Nature* 322:32-8.

Rucks E.A., and Olson J.C. **(2005)**, Characterization of an ExoS Type III translocation-resistant cell line. *Infect Immun* 73:638-43.

Ryckman C., Gilbert C., de Medicis R., Lussier A., Vandal K., and Tessier P.A. **(2004)**, Monosodium urate monohydrate crystals induce the release of the proinflammatory protein S100A8/A9 from neutrophils. *J Leukoc Biol* 76:433-40.

Ryckman C., McColl S.R., Vandal K., de Medicis R., Lussier A., Poubelle P.E., and Tessier P.A. **(2003a)**, Role of S100A8 and S100A9 in neutrophil recruitment in response to monosodium urate monohydrate crystals in the air-pouch model of acute gouty arthritis. *Arthritis Rheum* 48:2310-20.

Ryckman C., Vandal K., Rouleau P., Talbot M., and Tessier P.A. **(2003b)**, Proinflammatory activities of S100: proteins S100A8, S100A9, and S100A8/A9 induce neutrophil chemotaxis and adhesion. *J Immunol* 170:3233-42.

Sarfstein R., Gorzalczany Y., Mizrahi A., Berdichevsky Y., Molshanski-Mor S., Weinbaum C., Hirshberg M., Dagher M.C., and Pick E. **(2004)**, Dual role of Rac in the assembly of NADPH oxidase, tethering to the membrane and activation of p67phox: a study based on mutagenesis of p67phox-Rac1 chimeras. *J Biol Chem* 279:16007-16.

Sato H., Takino T., Okada Y., Cao J., Shinagawa A., Yamamoto E., and Seiki M. **(1994)**, A matrix metalloproteinase expressed on the surface of invasive tumour cells. *Nature* 370:61-5.

Savina A., Jancic C., Hugues S., Guermonprez P., Vargas P., Moura I.C., Lennon-Dumenil A.M., Seabra M.C., Raposo G., and Amigorena S. **(2006)**, NOX2 controls phagosomal pH to regulate antigen processing during crosspresentation by dendritic cells. *Cell* 126:205-18.

Sbarra A.J., and Karnovsky M.L. **(1959)**, The biochemical basis of phagocytosis. I. Metabolic changes during the ingestion of particles by polymorphonuclear leukocytes. *J Biol Chem* 234:1355-62.

Scheibner K.A., Lutz M.A., Boodoo S., Fenton M.J., Powell J.D., and Horton M.R. **(2006)**, Hyaluronan fragments act as an endogenous danger signal by engaging TLR2. *J Immunol* 177:1272-81.

Schellekens G.A., Visser H., de Jong B.A., van den Hoogen F.H., Hazes J.M., Breedveld F.C., and van Venrooij W.J. **(2000)**, The diagnostic properties of rheumatoid arthritis antibodies recognizing a cyclic citrullinated peptide. *Arthritis Rheum* 43:155-63.

Schenten V., Brechard S., Plancon S., Melchior C., Frippiat J.P., and Tschirhart E.J. **(2010)**, iPLA2, a novel determinant in Ca2+- and phosphorylation-dependent S100A8/A9 regulated NOX2 activity. *Biochim Biophys Acta* 1803:840-7.

Schenten V., Melchior C., Steinckwich N., Tschirhart E.J., and Brechard S. **(2011)**, Sphingosine kinases regulate NOX2 activity via p38 MAPK-dependent translocation of S100A8/A9. *J Leukoc Biol* 89:587-96.

Schraufstatter I.U., Browne K., Harris A., Hyslop P.A., Jackson J.H., Quehenberger O., and Cochrane C.G. **(1990)**, Mechanisms of hypochlorite injury of target cells. *J Clin Invest* 85:554-62.

Schurigt U., Stopfel N., Huckel M., Pfirschke C., Wiederanders B., and Brauer R. **(2005)**, Local expression of matrix metalloproteinases, cathepsins, and their inhibitors during the development of murine antigen-induced arthritis. *Arthritis Res Ther* 7:174-88.

Scialom C., Najean Y., and Bernard J. **(1966)**, [Congenital nonspherocytic hemolytic anemia with incomplete deficiency of 6-phosphogluconate dehydrogenase]. *Nouv Rev Fr Hematol* 6:452-7.

Segal A.W. **(1987)**, Absence of both cytochrome b-245 subunits from neutrophils in X-linked chronic granulomatous disease. *Nature* 326:88-91.

Servant G., Weiner O.D., Herzmark P., Balla T., Sedat J.W., and Bourne H.R. **(2000)**, Polarization of chemoattractant receptor signaling during neutrophil chemotaxis. *Science* 287:1037-40.

Shao D., Segal A.W., and Dekker L.V. **(2003)**, Lipid rafts determine efficiency of NADPH oxidase activation in neutrophils. *FEBS Lett* 550:101-6.

Shao D., Segal A.W., and Dekker L.V. **(2010)**, Subcellular localisation of the p40phox component of NADPH oxidase involves direct interactions between the Phox homology domain and F-actin. *Int J Biochem Cell Biol* 42:1736-43.

Sharma A., Sharma A.K., Madhunapantula S.V., Desai D., Huh S.J., Mosca P., Amin S., and Robertson G.P. **(2009)**, Targeting Akt3 signaling in malignant melanoma using isoselenocyanates. *Clin Cancer Res* 15:1674-85.

Shigeyama Y., Pap T., Kunzler P., Simmen B.R., Gay R.E., and Gay S. **(2000)**, Expression of osteoclast differentiation factor in rheumatoid arthritis. *Arthritis Rheum* 43:2523-30.

Shikichi M., Kitamura H.P., Yanase H., Konno A., Takahashi-Iwanaga H., and Iwanaga T. **(1999)**, Three-dimensional ultrastructure of synoviocytes in the horse joint as revealed by the scanning electron microscope. *Arch Histol Cytol* 62:219-29.

Shiose A., and Sumimoto H. **(2000)**, Arachidonic acid and phosphorylation synergistically induce a conformational change of p47phox to activate the phagocyte NADPH oxidase. *J Biol Chem* 275:13793-801.

Shirafuji N., Matsuda S., Ogura H., Tani K., Kodo H., Ozawa K., Nagata S., Asano S., and Takaku F. **(1990)**, Granulocyte colony-stimulating factor stimulates human mature neutrophilic granulocytes to produce interferon-alpha. *Blood* 75:17-9.

Shmelzer Z., Haddad N., Admon E., Pessach I., Leto T.L., Eitan-Hazan Z., Hershfinkel M., and Levy R. **(2003)**, Unique targeting of cytosolic phospholipase A2 to plasma membranes mediated by the NADPH oxidase in phagocytes. *J Cell Biol* 162:683-92.

Shmelzer Z., Karter M., Eisenstein M., Leto T.L., Hadad N., Ben-Menahem D., Gitler D., Banani S., Wolach B., Rotem M., and Levy R. **(2008)**, Cytosolic phospholipase A2alpha is targeted to the p47phox-PX domain of the assembled NADPH oxidase via a novel binding site in its C2 domain. *J Biol Chem* 283:31898-908.

Simard J.C., Girard D., and Tessier P.A. **(2010)**, Induction of neutrophil degranulation by S100A9 via a MAPK-dependent mechanism. *J Leukoc Biol* 87:905-14.

Simard J.C., Simon M.M., Tessier P.A., and Girard D. **(2011)**, Damage-associated molecular pattern S100A9 increases bactericidal activity of human neutrophils by enhancing phagocytosis. *J Immunol* 186:3622-31.

Singh J.A., Christensen R., Wells G.A., Suarez-Almazor M.E., Buchbinder R., Lopez-Olivo M.A., Tanjong Ghogomu E., and Tugwell P. **(2009)**, Biologics for rheumatoid arthritis: an overview of Cochrane reviews. *Cochrane Database Syst Rev*CD007848.

Singh K., Colmegna I., He X., Weyand C.M., and Goronzy J.J. **(2008)**, Synoviocyte stimulation by the LFA-1-intercellular adhesion molecule-2-Ezrin-Akt pathway in rheumatoid arthritis. *J Immunol* 180:1971-8.

Skapenko A., Leipe J., Lipsky P.E., and Schulze-Koops H. **(2005)**, The role of the T cell in autoimmune inflammation. *Arthritis Res Ther* 7:4-14.

Skoldstam L., Hagfors L., and Johansson G. **(2003)**, An experimental study of a Mediterranean diet intervention for patients with rheumatoid arthritis. *Ann Rheum Dis* 62:208-14.

Smith C.W. **(1993)**, Endothelial adhesion molecules and their role in inflammation. *Can J Physiol Pharmacol* 71:76-87.

Smith R.M., Connor J.A., Chen L.M., and Babior B.M. **(1996)**, The cytosolic subunit p67phox contains an NADPH-binding site that participates in catalysis by the leukocyte NADPH oxidase. *J Clin Invest* 98:977-83.

Smith R.M., Curnutte J.T., Mayo L.A., and Babior B.M. **(1989)**, Use of an affinity label to probe the function of the NADPH binding component of the respiratory burst oxidase of human neutrophils. *J Biol Chem* 264:12243-8.

Smith R.S., Smith T.J., Blieden T.M., and Phipps R.P. **(1997)**, Fibroblasts as sentinel cells. Synthesis of chemokines and regulation of inflammation. *Am J Pathol* 151:317-22.

Smith S.C., Folefac V.A., Osei D.K., and Revell P.A. **(1998)**, An immunocytochemical study of the distribution of proline-4-hydroxylase in normal, osteoarthritic and rheumatoid arthritic synovium at both the light and electron microscopic level. *Br J Rheumatol* 37:287-91.

Smolen J.E., Korchak H.M., and Weissmann G. **(1980)**, Increased levels of cyclic adenosine-3',5'-monophosphate in human polymorphonuclear leukocytes after surface stimulation. *J Clin Invest* 65:1077-85.

Sopalla C., Leukert N., Sorg C., and Kerkhoff C. **(2002)**, Evidence for the involvement of the unique C-tail of S100A9 in the binding of arachidonic acid to the heterocomplex S100A8/A9. *Biol Chem* 383:1895-905.

Sorsa T., Konttinen Y.T., Lindy O., Ritchlin C., Saari H., Suomalainen K., Eklund K.K., and Santavirta S. **(1992)**, Collagenase in synovitis of rheumatoid arthritis. *Semin Arthritis Rheum* 22:44-53.

Sroussi H.Y., Lu Y., Zhang Q.L., Villines D., and Marucha P.T. **(2010)**, S100A8 and S100A9 inhibit neutrophil oxidative metabolism in-vitro: involvement of adenosine metabolites. *Free Radic Res* 44:389-96.

Stanczyk J., Pedrioli D.M., Brentano F., Sanchez-Pernaute O., Kolling C., Gay R.E., Detmar M., Gay S., and Kyburz D. **(2008)**, Altered expression of MicroRNA in synovial fibroblasts and synovial tissue in rheumatoid arthritis. *Arthritis Rheum* 58:1001-9.

Stasia M.J., Brion J.P., Boutonnat J., and Morel F. **(2003)**, Severe clinical forms of cytochrome b-negative chronic granulomatous disease (X91-) in 3 brothers with a point mutation in the promoter region of CYBB. *J Infect Dis* 188:1593-604.

Stasia M.J., Cathebras P., Lutz M.F., and Durieu I. **(2009)**, Chronic-granulomatous disease. *Rev Med Interne* 30:221-32.

Steenvoorden M.M., Bank R.A., Ronday H.K., Toes R.E., Huizinga T.W., and DeGroot J. **(2007a)**, Fibroblast-like synoviocyte-chondrocyte interaction in cartilage degradation. *Clin Exp Rheumatol* 25:239-45.

Steenvoorden M.M., Toes R.E., Ronday H.K., Huizinga T.W., and Degroot J. **(2007b)**, RAGE activation induces invasiveness of RA fibroblast-like synoviocytes in vitro. *Clin Exp Rheumatol* 25:740-2.

Steinckwich N., Schenten V., Melchior C., Brechard S., and Tschirhart E.J. **(2011)**, An essential role of STIM1, Orai1, and S100A8-A9 proteins for Ca2+ signaling and FcgammaR-mediated phagosomal oxidative activity. *J Immunol* 186:2182-91.

Stephens L., Smrcka A., Cooke F.T., Jackson T.R., Sternweis P.C., and Hawkins P.T. **(1994)**, A novel phosphoinositide 3 kinase activity in myeloid-derived cells is activated by G protein beta gamma subunits. *Cell* 77:83-93.

Stralin P., and Marklund S.L. **(2000)**, Multiple cytokines regulate the expression of extracellular superoxide dismutase in human vascular smooth muscle cells. *Atherosclerosis* 151:433-41.

Streicher W.W., Lopez M.M., and Makhatadze G.I. **(2010)**, Modulation of quaternary structure of S100 proteins by calcium ions. *Biophys Chem* 151:181-6.

Strupat K., Rogniaux H., Van Dorsselaer A., Roth J., and Vogl T. **(2000)**, Calcium-induced noncovalently linked tetramers of MRP8 and MRP14 are confirmed by electrospray ionization-mass analysis. *J Am Soc Mass Spectrom* 11:780-8.

Sugiyama D., Nishimura K., Tamaki K., Tsuji G., Nakazawa T., Morinobu A., and Kumagai S. **(2010)**, Impact of smoking as a risk factor for developing rheumatoid arthritis: a meta-analysis of observational studies. *Ann Rheum Dis* 69:70-81.

Suh Y.A., Arnold R.S., Lassegue B., Shi J., Xu X., Sorescu D., Chung A.B., Griendling K.K., and Lambeth J.D. **(1999)**, Cell transformation by the superoxide-generating oxidase Mox1. *Nature* 401:79-82.

Sumimoto H., Kage Y., Nunoi H., Sasaki H., Nose T., Fukumaki Y., Ohno M., Minakami S., and Takeshige K. **(1994)**, Role of Src homology 3 domains in assembly and activation of the phagocyte NADPH oxidase. *Proc Natl Acad Sci U S A* 91:5345-9.

Sumimoto H., Sakamoto N., Nozaki M., Sakaki Y., Takeshige K., and Minakami S. **(1992)**, Cytochrome b_{558}, a component of the phagocyte NADPH oxidase, is a flavoprotein. *Biochem Biophys Res Commun* 186:1368-75.

Sunahori K., Yamamura M., Yamana J., Takasugi K., Kawashima M., Yamamoto H., Chazin W.J., Nakatani Y., Yui S., and Makino H. **(2006)**, The S100A8/A9 heterodimer amplifies proinflammatory cytokine production by macrophages via activation of nuclear factor kappa B and p38 mitogen-activated protein kinase in rheumatoid arthritis. *Arthritis Res Ther* 8:R69.

Sung J.Y., Hong J.H., Kang H.S., Choi I., Lim S.D., Lee J.K., Seok J.H., Lee J.H., and Hur G.M. **(2000)**, Methotrexate suppresses the interleukin-6 induced generation of reactive oxygen species in the synoviocytes of rheumatoid arthritis. *Immunopharmacology* 47:35-44.

Suzuki Y., and Lehrer R.I. **(1980)**, NAD(P)H oxidase activity in human neutrophils stimulated by phorbol myristate acetate. *J Clin Invest* 66:1409-18.

Tamura M., Kanno M., and Endo Y. **(2000)**, Deactivation of neutrophil NADPH oxidase by actin-depolymerizing agents in a cell-free system. *Biochem J* 349:369-75.

Tamura M., Kanno M., and Kai T. **(2001)**, Destabilization of neutrophil NADPH oxidase by ATP and other trinucleotides and its prevention by Mg(2+). *Biochim Biophys Acta* 1510:270-7.

Tamura M., Shiozaki I., Ono S., Miyano K., Kunihiro S., and Sasaki T. **(2007)**, p40phox as an alternative organizer to p47phox in Nox2 activation: a new mechanism involving an interaction with p22phox. *FEBS Lett* 581:4533-8.

Tang W., Lu Y., Tian Q.Y., Zhang Y., Guo F.J., Liu G.Y., Syed N.M., Lai Y., Lin E.A., Kong L., Su J., Yin F., Ding A.H., Zanin-Zhorov A., Dustin M.L., Tao J., Craft J., Yin Z., Feng J.Q., Abramson S.B., Yu X.P., and Liu C.J. **(2011)**, The growth factor progranulin binds to TNF receptors and is therapeutic against inflammatory arthritis in mice. *Science* 332:478-84.

Taura M., Miyano K., Minakami R., Kamakura S., Takeya R., and Sumimoto H. **(2009)**, A region N-terminal to the tandem SH3 domain of p47phox plays a crucial role in the activation of the phagocyte NADPH oxidase. *Biochem J* 419:329-38.

Taylor W.R., Jones D.T., and Segal A.W. **(1993)**, A structural model for the nucleotide binding domains of the flavocytochrome b-245 beta-chain. *Protein Sci* 2:1675-85.

Teigelkamp S., Bhardwaj R.S., Roth J., Meinardus-Hager G., Karas M., and Sorg C. **(1991)**, Calcium-dependent complex assembly of the myeloic differentiation proteins MRP-8 and MRP-14. *J Biol Chem* 266:13462-7.

Teitelbaum S.L. **(2000)**, Bone resorption by osteoclasts. *Science* 289:1504-8.

Theron A.J., Steenkamp K.J., and Anderson R. **(1994)**, NADPH-oxidase activity of stimulated neutrophils is markedly increased by serum. *Inflammation* 18:459-67.

Tilleman K., Van Beneden K., Dhondt A., Hoffman I., De Keyser F., Veys E., Elewaut D., and Deforce D. **(2005)**, Chronically inflamed synovium from spondyloarthropathy and rheumatoid arthritis investigated by protein expression profiling followed by tandem mass spectrometry. *Proteomics* 5:2247-57.

Tirone F., Radu L., Craescu C.T., and Cox J.A. **(2010)**, Identification of the binding site for the regulatory calcium-binding domain in the catalytic domain of NOX5. *Biochemistry* 49:761-71.

Tolboom T.C., Pieterman E., van der Laan W.H., Toes R.E., Huidekoper A.L., Nelissen R.G., Breedveld F.C., and Huizinga T.W. **(2002)**, Invasive properties of fibroblast-like synoviocytes: correlation with growth characteristics and expression of MMP-1, MMP-3, and MMP-10. *Ann Rheum Dis* 61:975-80.

Towbin H., Staehelin T., and Gordon J. **(1979)**, Electrophoretic transfer of proteins from polyacrylamide gels to nitrocellulose sheets: procedure and some applications. *Proc Natl Acad Sci U S A* 76:4350-4.

Trabandt A., Aicher W.K., Gay R.E., Sukhatme V.P., Nilson-Hamilton M., Hamilton R.T., McGhee J.R., Fassbender H.G., and Gay S. **(1990)**, Expression of the collagenolytic and Ras-induced cysteine proteinase cathepsin L and proliferation-associated oncogenes in synovial cells of MRL/I mice and patients with rheumatoid arthritis. *Matrix* 10:349-61.

Treves S., Di Virgilio F., Vaselli G.M., and Pozzan T. **(1987)**, Effect of cytochalasins on cytosolic-free calcium concentration and phosphoinositide metabolism in leukocytes. *Exp Cell Res* 168:285-98.

Trocmé C., Marotte H., Baillet A., Pallot-Prades B., Garin J., Grange L., Miossec P., Tebib J., Berger F., Nissen M.J., Juvin R., Morel F., and Gaudin P. **(2008)**, Apolipoprotein A-I and platelet factor 4 are biomarkers for Infliximab response in rheumatoid arthritis. *Ann Rheum Dis*.

Ueyama T., Tatsuno T., Kawasaki T., Tsujibe S., Shirai Y., Sumimoto H., Leto T.L., and Saito N. **(2007)**, A regulated adaptor function of p40phox: distinct p67phox membrane targeting by p40phox and by p47phox. *Mol Biol Cell* 18:441-54.

Ugolev Y., Molshanski-Mor S., Weinbaum C., and Pick E. **(2006)**, Liposomes comprising anionic but not neutral phospholipids cause dissociation of Rac(1 or 2) x RhoGDI complexes and support amphiphile-independent NADPH oxidase activation by such complexes. *J Biol Chem* 281:19204-19.

Valentin F., Bueb J., Capdeville-Atkinson C., and Tschirhart E. **(2001)**, Rac-1-mediated O2- secretion requires Ca2+ influx in neutrophil-like HL-60 cells. *Cell Calcium* 29:409-15.

Van den Bos C., Roth J., Koch H.G., Hartmann M., and Sorg C. **(1996)**, Phosphorylation of MRP14, an S100 protein expressed during monocytic differentiation, modulates Ca(2+)-dependent translocation from cytoplasm to membranes and cytoskeleton. *J Immunol* 156:1247-54.

Van der Veen R.C., Dietlin T.A., Hofman F.M., Pen L., Segal B.H., and Holland S.M. **(2000)**, Superoxide prevents nitric oxide-mediated suppression of helper T lymphocytes: decreased autoimmune

encephalomyelitis in nicotinamide adenine dinucleotide phosphate oxidase knockout mice. *J Immunol* 164:5177-83.

Van Lent P.L., Grevers L., Blom A.B., Sloetjes A., Mort J.S., Vogl T., Nacken W., van den Berg W.B., and Roth J. **(2008a)**, Myeloid-related proteins S100A8/S100A9 regulate joint inflammation and cartilage destruction during antigen-induced arthritis. *Ann Rheum Dis* 67:1750-8.

Van Lent P.L., Grevers L.C., Blom A.B., Arntz O.J., van de Loo F.A., van der Kraan P., Abdollahi-Roodsaz S., Srikrishna G., Freeze H., Sloetjes A., Nacken W., Vogl T., Roth J., and van den Berg W.B. **(2008b)**, Stimulation of chondrocyte-mediated cartilage destruction by S100A8 in experimental murine arthritis. *Arthritis Rheum* 58:3776-87.

Vanhaesebroeck B., and Alessi D.R. **(2000)**, The PI3K-PDK1 connection: more than just a road to PKB. *Biochem J* 346 Pt 3:561-76.

Vankemmelbeke M.N., Ilic M.Z., Handley C.J., Knight C.G., and Buttle D.J. **(1999)**, Coincubation of bovine synovial or capsular tissue with cartilage generates a soluble "Aggrecanase" activity. *Biochem Biophys Res Commun* 255:686-91.

Venkatraman J.T., and Chu W.C. **(1999)**, Effects of dietary omega-3 and omega-6 lipids and vitamin E on serum cytokines, lipid mediators and anti-DNA antibodies in a mouse model for rheumatoid arthritis. *J Am Coll Nutr* 18:602-13.

Vergnaud S., Paclet M.H., El Benna J., Pocidalo M.A., and Morel F. **(2000)**, Complementation of NADPH oxidase in p67-phox-deficient CGD patients p67-phox/p40-phox interaction. *Eur J Biochem* 267:1059-67.

Vignais P.V. **(2002)**, The superoxide-generating NADPH oxidase: structural aspects and activation mechanism. *Cell Mol Life Sci* 59:1428-59.

Vilhardt F., and van Deurs B. **(2004)**, The phagocyte NADPH oxidase depends on cholesterol-enriched membrane microdomains for assembly. *Embo J* 23:739-48.

Villiger P.M., Terkeltaub R., and Lotz M. **(1992)**, Monocyte chemoattractant protein-1 (MCP-1) expression in human articular cartilage. Induction by peptide regulatory factors and differential effects of dexamethasone and retinoic acid. *J Clin Invest* 90:488-96.

Vincent F., Brun H., Clain E., Ronot X., and Adolphe M. **(1989)**, Effects of oxygen-free radicals on proliferation kinetics of cultured rabbit articular chondrocytes. *J Cell Physiol* 141:262-6.

Visser K., Goekoop-Ruiterman Y.P., de Vries-Bouwstra J.K., Ronday H.K., Seys P.E., Kerstens P.J., Huizinga T.W., Dijkmans B.A., and Allaart C.F. **(2010)**, A matrix risk model for the prediction of rapid radiographic progression in patients with rheumatoid arthritis receiving different dynamic treatment strategies: post hoc analyses from the BeSt study. *Ann Rheum Dis* 69:1333-7.

Vives Corrons J.L., Colomer D., Pujades A., Rovira A., Aymerich M., Merino A., and Aguilar i Bascompte J.L. **(1996)**, Congenital 6-phosphogluconate dehydrogenase (6PGD) deficiency associated with chronic hemolytic anemia in a Spanish family. *Am J Hematol* 53:221-7.

Vogl T., Ludwig S., Goebeler M., Strey A., Thorey I.S., Reichelt R., Foell D., Gerke V., Manitz M.P., Nacken W., Werner S., Sorg C., and Roth J. **(2004)**, MRP8 and MRP14 control microtubule reorganization during transendothelial migration of phagocytes. *Blood* 104:4260-8.

Vogl T., Tenbrock K., Ludwig S., Leukert N., Ehrhardt C., van Zoelen M.A., Nacken W., Foell D., van der Poll T., Sorg C., and Roth J. **(2007)**, Mrp8 and Mrp14 are endogenous activators of Toll-like receptor 4, promoting lethal, endotoxin-induced shock. *Nat Med* 13:1042-9.

Voss A., Bode G., Sopalla C., Benedyk M., Varga G., Bohm M., Nacken W., and Kerkhoff C. **(2011)**, Expression of S100A8/A9 in HaCaT keratinocytes alters the rate of cell proliferation and differentiation. *FEBS Lett* 585:440-6.

Wallach T.M., and Segal A.W. **(1996)**, Stoichiometry of the subunits of flavocytochrome b_{558} of the NADPH oxidase of phagocytes. *Biochem J* 320:33-8.

Ward R.A., Nakamura M., and McLeish K.R. **(2000)**, Priming of the neutrophil respiratory burst involves p38 mitogen-activated protein kinase-dependent exocytosis of flavocytochrome b_{558}-containing granules. *J Biol Chem* 275:36713-9.

Wardman P., and Candeias L.P. **(1996)**, Fenton chemistry: an introduction. *Radiat Res* 145:523-31.

Warstat K., Hoberg M., Rudert M., Tsui S., Pap T., Angres B., Essl M., Smith T.J., Cruikshank W.W., Klein G., Gay S., and Aicher W.K. **(2011)**, Transforming growth factor beta1 and laminin-111 cooperate in the induction of interleukin-16 expression in synovial fibroblasts from patients with rheumatoid arthritis. *Ann Rheum Dis* 69:270-5.

Wijnands M.J., Nuver-Zwart I.H., van Riel P.L., van 't Hof M.A., Gribnau F.W., and van De Putte L.B. **(1991)**, Hemolysis during low-dose sulfasalazine treatment in rheumatoid arthritis patients. *Scand J Rheumatol* 20:52-7.

Wilson P.D., Rustin G.J., and Peters T.J. **(1981)**, The ultrastructural localization of human neutrophil alkaline phosphatase in normal individuals during pregnancy and in patients with chronic granulocytic leukaemia. *Histochem J* 13:31-43.

Winkelstein J.A., Marino M.C., Johnston R.B., Jr., Boyle J., Curnutte J., Gallin J.I., Malech H.L., Holland S.M., Ochs H., Quie P., Buckley R.H., Foster C.B., Chanock S.J., and Dickler H. **(2000)**, Chronic granulomatous disease. Report on a national registry of 368 patients. *Medicine (Baltimore)* 79:155-69.

Wipke B.T., and Allen P.M. **(2001)**, Essential role of neutrophils in the initiation and progression of a murine model of rheumatoid arthritis. *J Immunol* 167:1601-8.

Wittkowski H., Foell D., af Klint E., De Rycke L., De Keyser F., Frosch M., Ulfgren A.K., and Roth J. **(2007)**, Effects of intra-articular corticosteroids and anti-TNF therapy on neutrophil activation in rheumatoid arthritis. *Ann Rheum Dis* 66:1020-5.

Wright G.L., Maroulakou I.G., Eldridge J., Liby T.L., Sridharan V., Tsichlis P.N., and Muise-Helmericks R.C. **(2008)**, VEGF stimulation of mitochondrial biogenesis: requirement of AKT3 kinase. *Faseb J* 22:3264-75.

Wright H.L., Moots R.J., Bucknall R.C., and Edwards S.W. **(2010)**, Neutrophil function in inflammation and inflammatory diseases. *Rheumatology (Oxford)* 49:1618-31.

Wulffraat N.M., Haas P.J., Frosch M., De Kleer I.M., Vogl T., Brinkman D.M., Quartier P., Roth J., and Kuis W. **(2003)**, Myeloid related protein 8 and 14 secretion reflects phagocyte activation and correlates with disease activity in juvenile idiopathic arthritis treated with autologous stem cell transplantation. *Ann Rheum Dis* 62:236-41.

Wurtele M., Wolf E., Pederson K.J., Buchwald G., Ahmadian M.R., Barbieri J.T., and Wittinghofer A. **(2001)**, How the Pseudomonas aeruginosa ExoS toxin downregulates Rac. *Nat Struct Biol* 8:23-6.

Xia Y., Pauza M.E., Feng L., and Lo D. **(1997)**, RelB regulation of chemokine expression modulates local inflammation. *Am J Pathol* 151:375-87.

Yang L., Anderson D.E., Baecher-Allan C., Hastings W.D., Bettelli E., Oukka M., Kuchroo V.K., and Hafler D.A. **(2008)**, IL-21 and TGF-beta are required for differentiation of human T(H)17 cells. *Nature* 454:350-2.

Yasuda T. **(2006)**, Cartilage destruction by matrix degradation products. *Mod Rheumatol* 16:197-205.

Yoshida L.S., Saruta F., Yoshikawa K., Tatsuzawa O., and Tsunawaki S. **(1998)**, Mutation at histidine 338 of gp91(phox) depletes FAD and affects expression of cytochrome b_{558} of the human NADPH oxidase. *J Biol Chem* 273:27879-86.

Yu L., DeLeo F.R., Biberstine-Kinkade K.J., Renee J., Nauseef W.M., and Dinauer M.C. **(1999)**, Biosynthesis of flavocytochrome b558 . gp91(phox) is synthesized as a 65-kDa precursor (p65) in the endoplasmic reticulum. *J Biol Chem* 274:4364-9.

Yu L., Zhen L., and Dinauer M.C. **(1997)**, Biosynthesis of the phagocyte NADPH oxidase cytochrome b558. Role of heme incorporation and heterodimer formation in maturation and stability of gp91phox and p22phox subunits. *J Biol Chem* 272:27288-94.

Yuzawa S., Ogura K., Horiuchi M., Suzuki N.N., Fujioka Y., Kataoka M., Sumimoto H., and Inagaki F. **(2004)**, Solution structure of the tandem Src homology 3 domains of p47phox in an autoinhibited form. *J Biol Chem* 279:29752-60.

Zhan S., Vazquez N., Zhan S., Wientjes F.B., Budarf M.L., Schrock E., Ried T., Green E.D., and Chanock S.J. **(1996)**, Genomic structure, chromosomal localization, start of transcription, and tissue expression of the human p40-phox, a new component of the nicotinamide adenine dinucleotide phosphate-oxidase complex. *Blood* 88:2714-21.

Zhang S.L., Yu Y., Roos J., Kozak J.A., Deerinck T.J., Ellisman M.H., Stauderman K.A., and Cahalan M.D. **(2005)**, STIM1 is a Ca2+ sensor that activates CRAC channels and migrates from the Ca2+ store to the plasma membrane. *Nature* 437:902-5.

Zhao X., Xu B., Bhattacharjee A., Oldfield C.M., Wientjes F.B., Feldman G.M., and Cathcart M.K. **(2005)**, Protein kinase Cdelta regulates p67phox phosphorylation in human monocytes. *J Leukoc Biol* 77:414-20.

Zreiqat H., Howlett C.R., Gronthos S., Hume D., and Geczy C.L. **(2007)**, S100A8/S100A9 and their association with cartilage and bone. *J Mol Histol* 38:381-91.

Zucker-Franklin D. **(1968)**, Electron microscopic studies of human granulocytes: structural variations related to function. *Semin Hematol* 5:109-33.

ANNEXES

Annexe 1 : Liste des publications et des communications en congrès

Les articles publiés dans des revues avec comité de lecture sont figurés ci-dessous :

2011

- **Baillet A,** Vaillant M, Guinot M, Juvin R, Gaudin P. Efficacy of resistance exercises in Rheumatoid Arthritis : Meta-analysis of randomized controlled trials. Rheumatology (Oxford) 2011 *sous presse.*
- **Baillet A,** Xu R, Berthier S, Grichine A, Morel F, Paclet MH. Coupling of 6-phosphogluconate dehydrogenase with NADPH oxidase in neutrophils: NOX2 activity regulation by NADPH availability. *FASEB J* 2011;25:2333-43.
- Roncoroni C, **Baillet A**, Durand M, Juvin R, Gaudin P. Efficacy and tolerance of systemic steroids in acute sciatica : a Systematic Review and Meta-Analysis. *Rheumatology* 2011;50:1603-11.
- **Baillet A,** Gaujoux-Viala C, Mouterde G, Pham T, Tebib J, Saraux A, Fautrel B, Cantagrel A, Le Loët X, Gaudin P. Comparison of the Efficacy of Sonography, Magnetic Resonance Imaging and Conventional Radiography for the Detection of Bone Erosions in Rheumatoid Arthritis Patients: a Systematic Review and Meta-Analysis. *Rheumatology* 2011;50:1137-47.

2010

- **Baillet A**, Trocmé C, Berthier S, Arlotto M, Grange L, Chenau J, Quétant S, Sève M, Berger F, Juvin R, Morel F, Gaudin P. Synovial fluid proteomic fingerprint: S100A8, S100A9 and S100A12 proteins discriminate rheumatoid arthritis from other inflammatory joint diseases. *Rheumatology* 2010;49:671-82.
- **Baillet A**, Zeboulon N, Gossec L, Combescure C, Bodin A, Juvin R, Dougados M, Gaudin P. Efficacy of cardio-respiratory aerobic exercise in Rheumatoid Arthritis: Meta-analysis of randomized controlled trials. *Arthritis Care Res* 2010;62:984-92.
- **Baillet A,** Chanteperdrix V, Trocmé C, Casez P, Garrel C, Besson G. The Role of Oxidative Stress in Amyotrophic Lateral Sclerosis and Parkinson's Disease. *Neurochem Res.* 2010;10:1530-1537.
- **Baillet A**. S100A8, S100A9 and S100A12 proteins in rheumatoid arthritis. *Rev Med Interne*. 2010;3:458-61.

2009

- **Baillet A,** Payraud E, Niderprim VA, Nissen MJ, Allenet B, François P, Grange L, Casez P, Juvin R, Gaudin P. A dynamic exercise program to improve patients' disability in Rheumatoid Arthritis: a prospective randomized controlled trial. *Rheumatology* 2009;48:410–415.
- Trocme C, Marotte H, **Baillet A,** Pallot-Prades B, Garin J, Grange L, et al. Apolipoprotein A-I and platelet factor 4 are biomarkers for infliximab response in rheumatoid arthritis. *Ann Rheum Dis* 2009;68:1328-33.
- Berthier S, **Baillet A**, Paclet MH, Gaudin P and Morel F. How important are S100A8/S100A9 Calcium Binding Proteins for the Activation of Phagocyte NADPH Oxidase, NOX2. *Anti-Inflammatory & Anti-Allergy Agents in Medicinal Chemistry* 2009;8:282-284.
- Campion Y, Jesaitisb A, Nguyen MVC, Grichine A, Herenger Y, **Baillet A**, Berthier S, Morel F, Paclet MH. New p22-phox monoclonal antibodies: identification of a conformational probe for cytochrome b_{558}. *J Innate Immun* 2009;1:556-569.

Les communications lors de congrès scientifiques sont figurées ci-dessous :

Invitation conférences

2011

- **Baillet A,** Trocmé C, Gaudin P. Le protéome en Rhumatologie : intérêt diagnostique, pronostique et théranostique. EMPREINTE (8 et 9 avril 2011, Paris).

Communications orale

2011

- **Baillet A,** Paclet MH, Xu R, Hograindleur MA, Berthier S et Morel F. Régulation de l'activité NADPH oxydase phagocytaire : Rôle de la 6-phosphogluconate déshydrogénase et de la 6-phosphofructokinase 2 (Club Oxydase 2011, CRSSA Grenoble).

2010

- Roncoroni C, Durand M, **Baillet A,** Gaudin P, Juvin R. Efficacité et tolérance des glucocorticoïdes par voie systémique dans la lombosciatique aiguë. (SFR 2010, *Revue du Rhumatisme* 2010;77 :A55)

2009

- **Baillet A**, Zeboulon N, Gossec L, Combescure C, Juvin R, Dougados M, Gaudin P. Physical exercise improves disability and quality of life in Rheumatoid Arthritis (RA): Meta analysis of randomized controlled trials. (EULAR 2009 *Ann Rheum Dis* 2009;68S3:106)
- **Baillet A**, Paclet MH, Rang Xu, BerthierS, et Morel F. Régulation de la NADPH oxydase phagocytaire : identification de nouveaux effecteurs de régulation (Club Oxydase 2009, Paris FIAP)

Communications par affiche (comme premier auteur)

2011

- **Baillet A,** Paclet MH, Grichine A, Berthier S, Gaudin P et Morel F. Modulation de l'activité de la NADPH oxydase des neutrophiles par des enzymes du métabolisme énergétique. (Journée médicale de la recherche 2011 CHU Grenoble)

2010

- **Baillet A**, Paclet MH, Berthier S, et Morel F. Régulation de la NADPH oxydase phagocytaire par les protagonistes du métabolisme du glucose : 6-phosphogluconate déshydrogénase et la 6-phosphofructokinase 2. (Journée médicale de la recherche 2010 CHU Grenoble)

Annexe 2

How important are S100A8/S100A9 Calcium Binding Proteins for the Activation of Phagocyte NADPH Oxidase, NOX2

How Important are S100A8/S100A9 Calcium Binding Proteins for the Activation of Phagocyte NADPH Oxidase, Nox2

Berthier Sylvie[1], Baillet Athan[1,2], Paclet Marie-Hélène[1], Gaudin Philippe[1,2] and Morel Françoise[1]

[1]*GREPI TIMC-Imag, UMR 5525 CNRS -Université de Grenoble, 38043 Grenoble-France;* [2]*Clinic of Rheumatology, CHU Hôpital Sud. 38434 Echirolles Cedex – France*

Abstract: S100A8 and S100A9 are two soluble calcium-binding proteins highly expressed in myeloid cells, mainly neutrophils (45% of cytosolic proteins) or monocytes (1-5%) and also early differentiated macrophages. In neutrophils, they are believed to be expressed as a 1/1 non covalent heterodimer; the process of dimer and mainly tetramer formation is calcium dependent. The S100A8/S100A9 calcium loaded complex binds arachidonic acid and shuttles between cytosol and plasma membrane upon neutrophil stimulation.

Neutrophils display, upon stimulation, a respiratory burst in which the cells catalyze NADPH oxidase activity through a redox membrane hemoprotein, cytochrome b_{558}, which is constituted of 2 subunits: gp91-phox, the redox core and p22-phox the stabilizing partner. In neutrophils, this activity is transitory: to be active, regulatory cytosolic factors, p67-phox, p47-phox, p40-phox and Rac1/2 assemble with membrane cytochrome b_{558}.

Both S100A8 and S100A9 were recently introduced as partners for NADPH oxidase activation and associate with the cytosolic activating factors especially p67-phox and Rac1/2. Moreover, S100A8/S100A9 potentiates NADPH oxidase activity. This was observed *ex vivo* after co-transfection of genes encoding both S100A8 and S100A9 in B lymphocytes that express all the components of the phagocyte oxidase, but display a very low NADPH oxidase activity (in these cells, S100A8 and S100A9 are not present endogenously). In the biological function of S100A8/S100A9, S100A8 is a strategic protein that needs to be active *in vivo* as *in vitro*, its specific partner S100A9. New data introduce S100A8 and S100A9 as positive effectors in allosteric regulation of phagocyte NADPH oxidase activity.

Keywords: NADPH oxidase, S100A8 protein, S100A9 protein, neutrophils, cytochrome b_{558}.

INTRODUCTION

The innate immune system represents the first line of defense against invading pathogens; it is involved in the initiation and amplification of inflammatory response [1]. Upon stimulation by a variety of endogenous or exogenous signals, phagocytes, mainly neutrophils, become capable of activating a respiratory burst and the synthesis of superoxide anion $O_2^{\cdot -}$ by a specific NADPH oxidase system. Reactive oxygen species (ROS) are generated from $O_2^{\cdot -}$; they participate in both the destruction of pathogens and the development of inflammation. In chronic granulomatous disease (CGD), ROS are not synthesized due to a defective NADPH oxidase activity; the patients are submitted to recurrent and often fatal infections because of the absence of bactericidal tools [2]**.** Myeloid-related proteins MRP8 (S100A8) and MRP14 (S100A9) are two calcium-binding proteins of a family named S100 due to their solubility in 100% ammonium sulfate. Specifically linked to innate immune function [3], they are expressed in cells of myeloid origin such as neutrophils; overexpression of both proteins was reported at local sites of inflammation, in neoplastic tumor cells and in skin pathology [4-6]. S100A8 and S100A9 proteins play a pivotal role through independent intra- and extracellular effects: in response to inflammatory stimuli, they are released in the extracellular medium via an alternative pathway bypassing the classical Golgi-route and they behave as a crucial danger signal during inflammatory process associated with infections, autoimmunity and cancer [1]. At the intracellular level, they were recently introduced as novel partners of NADPH oxidase family. In this respect, they potentiate activation of $O_2^{\cdot -}$-generating NADPH oxidase (Nox) and ROS production [7-9]. Moreover, recent data demonstrated that S100A8/S100A9 is an endogenous ligand of Toll-like receptor 4 and promotes lethal endotoxin-induced shock [10].

This review focuses on recent advances in understanding the function of S100A8 and S100A9 proteins as partners of NADPH oxidase in neutrophils.

NADPH OXIDASE OF PHAGOCYTES

NADPH oxidase of phagocytes (phox) is the prototype of a Nox family coming from an ancestral Nox that appears through evolution before the separation into animals, plants and fungi [11]. Seven Nox-Duox were characterized in human [12]. NADPH oxidase of neutrophils is an essential actor of the host defense against microbial agents. It is involved in shaping the cellular response to many physiological and pathological signals. Neutrophil NADPH oxidase catalyzes a transitory respiratory burst (Fig. (**1A**)) that is abolished in Chronic Granulomatous Disease (CGD) [2].

*Address correspondence to this author at the GREPI Enzymology laboratory – CHU Grenoble; BP217 38043 Grenoble Cedex, France; Tel: 33 (0)4 76 76 57 52; Fax: 33 (0)4 76 76 56 08;
E-mail: FrMorel.enzymo@chu-grenoble.fr

1871-5230/09 $55.00+.00

Epstein-Barr-Virus immortalized (EBV) B lymphocytes that express all the components of phagocyte NADPH oxidase, display contrary to neutrophils, a weak oxidase activity that may be due to a low expression of cytochrome b_{558} and different stoichiometry of the constituents compared to hemoprotein, or to different mechanisms of regulation [13, 14]. NADPH oxidase synthesizes superoxide anions that give ROS. While these derivatives are essential tools for killing during phagocytosis, they are also involved in signaling; in contrast, overexpression may trigger inflammatory reactions or ageing.

NADPH oxidase of neutrophils is unassembled and inactive in resting cells. Activation is initiated upon soluble (inflammatory mediators) or particulate (phagocytosis of microorganisms) stimulation, by phosphorylation of phox proteins which is believed to induce intra- and intermolecular rearrangements affecting the p40-p47-p67 phox complex. These events lead to the translocation of the complex to plasma membrane and association with Rac1/2-GTP and cytochrome b_{558} in order to form the active enzyme (Fig. (**1B**)). Cytochrome b_{558} is the anchorage site for the biological complex that is stabilized at the membrane level through many protein/protein or protein/lipid interactions. It consists of two transmembrane subunits whereby gp91-phox or Nox2 (β subunit) mediates NADPH oxidase catalysis while maturation and integrity of cytochrome b_{558} require the presence of p22-phox (α subunit). Both Rac1/2 and p47-phox facilitate a specific interface of p67-phox with gp91-phox: this initiates activation and the electron transfer [9]. Gp91-phox is the redox core of NADPH oxidase: its oxidase activity is cyanide-insensitive. Opposite to the mitochondrial respiratory chain, the unique protein, gp91-phox, contains all the prosthetic groups necessary for electron transfer from NADPH to oxygen. Upon assembly, cytochrome b_{558} changes its conformation as illustrated by atomic force microscopy [15]. Purified cytochrome b_{558} was incorporated into L-α-phosphatidylcholine liposomes and incubated with recombinant cytosolic factors, rp67-phox and rp47-phox, in the presence of arachidonic acid (AA) and Rac1/2. The difference in liposome size and bell shape profiles before and after activation illustrate the oxidase assembly and the size of the assembled complex was calculated and assumed to be approximately 4 nm.

All members of the Nox family are isoenzymes that catalyze the same reaction. As they originate from an ancestral gene that evolved differently, the Nox isoforms differ according to tissue expression, subcellular localization or partner of activation. Moreover, oxidase activity can be low and constitutive in non-phagocytic cells or inducible as in neutrophils where stimulation triggers a transitory respiratory burst.

Role of S100A8 and S100A9 Calcium-Binding Proteins in Neutrophils

S100A8 and S100A9 are two proteins of the myeloid-related S100 family that participate in neutrophil migration, phagocytosis and activation [1, 5, 16]. The S100 family comprises more than 20 members including S100A8 and S100A9 which are directly linked to the innate immune system and represent ~45 % of the cytosolic proteins in neutrophils *versus* 1-5% in monocytes. Their expression is restricted to a specific stage of myeloid differentiation and is probably driven by a recently characterized regulatory element [17].

The S100A8/S100A9 protein complex (S100A8/S100A9) is a unique AA-binding complex in human neutrophils: it is the intracellular AA reservoir and proceeds in a calcium dependent manner [18]. The unique cytosolic tail of S100A9 contains 3 consecutive histidine residues (His103-His105) which represent the region to which carboxyl-groups of fatty acids bind. Each S100 protein binds calcium through two EF-hands containing classical helix-loop-helix motifs but displaying high and low affinities for calcium; they are connected by a central hinge region [19]. The estimated calcium concentration required to induce fatty acid binding is within the physiological range. S100A8/S100A9 heterodimer (termed calprotectin) seems to be strongly favored *in vivo* and represents the basic structure of both proteins but the calcium-dependent formation of tetramers is essential for biological function [20]. In neutrophils, S100A8 and S100A9 are distributed between cytosol and gelatinase-granules [21, 22]. In the presence of calcium, S100A8/S100A9 interacts with actin filaments of cytoskeleton and promotes tubulin polymerization. This interaction depends on formation of the tetramer complex and on phosphorylation of S100A9 [1]. Various phosphorylation states of S100A8 and S100A9 proteins may discriminate their subcellular compartmentalization whereby different isoforms were also identified [9]. The S100A8/S100A9 heterodimer binds and sequesters zinc through a HXXXH motif of S100A8 that was shown in all crystal structures and located at the interface between the respective S100A8 and S100A9 subunits [19]. Thus they inhibit matrix metalloproteinases and interfere with microbial growth.

Strong evidence indicates that active non classical secretion rather passive release from necrotic cells is the major physiological source for extracellular S100A8 and S100A9 which are secreted from neutrophils stimulated by inflammatory mediators or by the contact with activated endothelium. The release of gelatinase-granule content is favored by chemotactic signals during neutrophils recruitment [21].

S100A8/S100A9 plays a prominent role in autocrine and paracrine regulation of inflammatory process and immune response [1]. They serve as markers of inflammation in rheumatoid arthritis [23] or other inflammatory diseases. S100A8 and S100A9 act as strong chemoattractants for monocytes and neutrophils [24, 25] but the recruitment of tumor cells responding to both proteins was recently reported in the lung [26]. S100A8/S100A9 can inactivate casein kinase II and thereby prevents oncoprotein E7 activation [27].

S100A8/S100A9 CONTROLS NADPH OXIDASE ACTIVATION

In stimulated neutrophils, huge amounts of $O_2^{\cdot -}$ and ROS are used for killing microorganisms but an overproduction is injurious to the tissues suggesting the necessity for a strict control of NADPH oxidase activity; S100A8/S100A9 is directly involved in regulation.

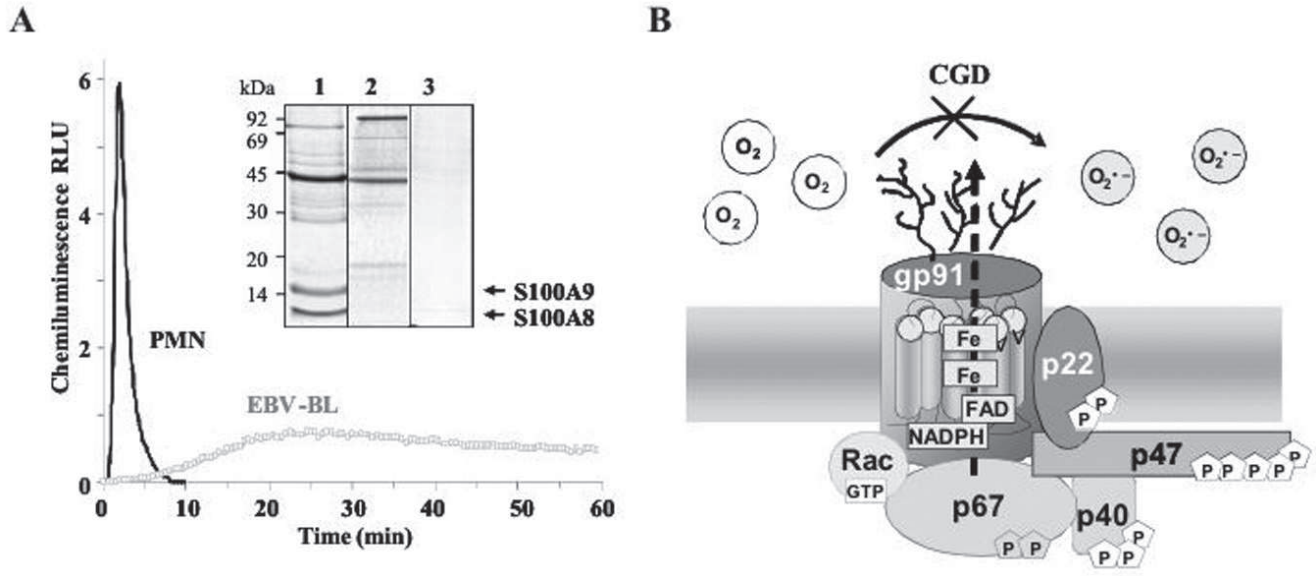

Fig. (1). Regulation of the phagocytic NADPH oxidase activity. Characterization of S100A8/A9 association with NADPH oxidase cytosolic proteins.

A- Differential regulation of NADPH oxidase activity in PMN and EBV-B lymphocytes. NADPH oxidase activity was measured in PMN and EBV-B cells by chemiluminescence. PMN (2×10^5) and EBV-B lymphocytes (EBV-BL) (1×10^6), washed twice with PBS and resuspended in 50 µl of PBS were incubated with 200 µl of the reaction medium containing 0.9 mM $CaCl_2$, 0.5 mM $MgCl_2$, 20 mM glucose, 20 µM luminol and 10 U/ml Horseradish peroxidase. Superoxide production was measured by chemiluminescence after cell stimulation with 130 nM PMA. Photon emission, expressed as Relative Luminescence Unit (RLU), was recorded at 37 °C for 1 h with a Luminoscan (Labsystem, Pontoise, France). **Inset. Association of S100A8/S100A9 with the cytosolic regulatory factors of NADPH oxidase activity in PMN.** The isolation of oxidase cytosolic factors as a complex was carried out on a specific anti-p47-phox affinity matrix (Carbolink™). Cytosol (50-100mg) of PMN, EBV-BL or p47-phox-deficient EBV-B lymphocytes was loaded successively on an uncoupled matrix, a non-specific immunoglobulin coupled matrix, and on the specific anti-p47-phox immunoglobulin coupled matrix overnight. After extensive washings, proteins bound to the specific anti-p47-phox coupled matrix were eluted with 0.1 M glycine pH3, immediately buffered with 1 M Tris-HCl pH 8.5: the eluted protein fractions were called cytosolic oxidase complex. The cytosolic oxidase complex (10-15 µg) isolated from cytosol of PMN (lane 1), EBV-BL (lane 2) and p47-phox-deficient EBV-BL (lane3) was analyzed after protein separation on a 11% SDS-PAGE and Coomassie Blue protein staining [9]. **B- NADPH oxidase activation model.** Following cell stimulation, cytosolic factors (p47-phox, p40-phox and p67-phox) are phosphorylated and translocate to the membrane cytochrome b_{558}, the catalytic core of the enzyme composed of gp91-phox and p22-phox. At the same time, Rac1/2 translocates independently to the membrane and associates with both p67-phox and cytochrome b_{558}. The assembly of cytosolic factors with cytochrome b_{558} induces a cytochrome b_{558} conformation change leading to an electron transfer from NADPH to oxygen *via* FAD and hemes. This process generates superoxide anions involved in bacterial killing. The defect of NADPH oxidase activity is responsible for CGD.

S100A8/S100A9 Activates NADPH Oxidase

S100A8 and S100A9 were isolated from human neutrophils with cytosolic activating factors in a complex that bound to an anti-p47-phox affinity matrix (Fig. (**1A**) inset lane 1). Both S100A8 and S100A9 were identified in the eluted fraction that contained p40-phox, p67-phox and p47-phox by MALDI TOF mass spectrometry [9].

The specificity of bound proteins was confirmed by isolating oxidase cytosolic factors from cytosol of p47-phox deficient (Fig. (**1A**) inset lane 3) *versus* control EBV-B lymphocytes (Fig. (**1A**) inset lane 2). There was neither S100A8 nor S100A9 in the isolated complex from EBV-B cell cytosol. A preferential interaction between the S100A8/S100A9 complex and p67-phox was proposed in resting neutrophils with S100A8 as the privileged interaction partner since it binds to p67-phox and Rac1/2. These observations suggest a co-translocation mechanism to membrane of cytosolic factors and S100A8/S100A9 proteins upon stimulation of neutrophils [28].

NADPH oxidase of neutrophils can be activated *in vitro* by native or recombinant S100A8/S100A9 that increases the affinity of p67-phox for cytochrome b_{558} synergistically with p47-phox (Fig. (**2**)). Moreover S100A8/S100A9 is also able to induce on its own oxidase activation of cytochrome b_{558} in a calcium-dependent interaction, as shown by atomic force microscopy and a structure/function relationship [9] (Fig. (**2**)). The impaired NADPH oxidase activity in neutrophils from $S100A9^{-/-}$ mice (compared with wild-type mice) or the reduced NADPH oxidase activity in neutrophil-like NB4 cells after specific blockage of S100A9 point out the physiological role of S100A8/S100A9 in NADPH oxidase activation [28]. These observations were confirmed *ex vivo* upon transfection in EBV-B lymphocytes that do not contain S100 proteins, with plasmids encoding S100A8 and (or) S100A9 [9]. Coexpression of both proteins is required for enhancing NADPH oxidase activity.

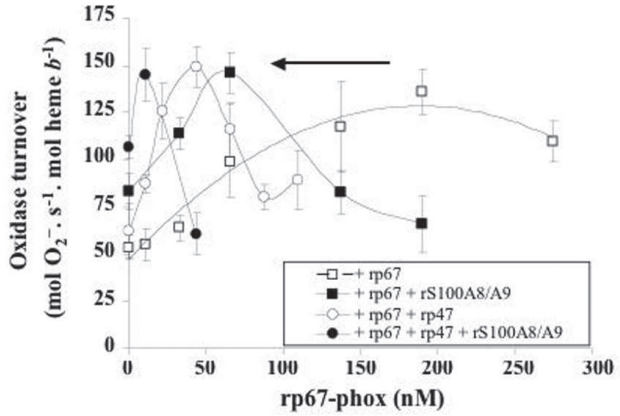

Fig. (2). Effect of S100A8 and S100A9 on the NADPH oxidase turnover in a semi-recombinant system [9].

The NADPH oxidase activity was reconstituted in a cell free system with purified cytochrome b_{558} (2.15 nM), increasing concentration of recombinant p67-phox (0-300 nM) and rRac(100 nM) in PBS buffer containing 10 µM FAD, 5 mM GTPγS and 5 mM $MgCl_2$. NADPH oxidase activity was measured after addition of arachidonic acid (1 mM) and NADPH (150 µM) by evaluating the cytochrome *c* reduction sensitive to superoxide dismutase (white squares). In some experiments, NADPH oxidase activity was reconstituted in the presence of p47-phox (185 nM) (white circles), or/and purified S100A8/S100A9 (300 nM) loaded with 500 nM Ca^{2+} (black squares and black circles respectively).

Arachidonic Acid-Dependent Activation of NADPH Oxidase

AA enhances NADPH oxidase activity both *in vitro* and *in vivo*: *in vitro*, it induces a significant conformation change of cytochrome b_{558} [29-31] upon assembly of the oxidase complex [15]. Interestingly, AA is indispensable for *in vivo* NADPH oxidase activation as reported by the effect of invalidation of the cytosolic phospholipase A2, enzyme that catalyzes AA release, and by the total restoration of activity after addition of exogenous fatty acid [32]. *In vitro*, activation of NADPH oxidase in a cell-free assay requires micromolar concentrations of AA [33]. *In vivo*, the binding of AA to S100A9 and assembly of S100A8/S100A9 at the membrane level may raise its local concentration and facilitate specific interaction with cytochrome b_{558}. So upon assembly of the oxidase complex, AA may directly take part in oxidase activation favoring the change of cytochrome b_{558} conformation that initiates the electron transfer [9, 34].

S100A8/S100A9 is a Regulatory Effector of NADPH Oxidase: Interaction with Cytochrome b_{558}.

The phagocyte oxidase complex was isolated for the first time, from stimulated neutrophils in an active state upon assembly onto a heparin-affinity matrix (Fig. (**3**)); the recovered complex required only the substrate, NADPH, to produce superoxide anion at a maximum rate, in the absence of any stimulation (Fig. (**4A**)). This constitutive NADPH oxidase activity remained constant for at least 30 days indicating a stable association between regulatory proteins, especially p67-phox, and cytochrome b_{558}. The data indicate that

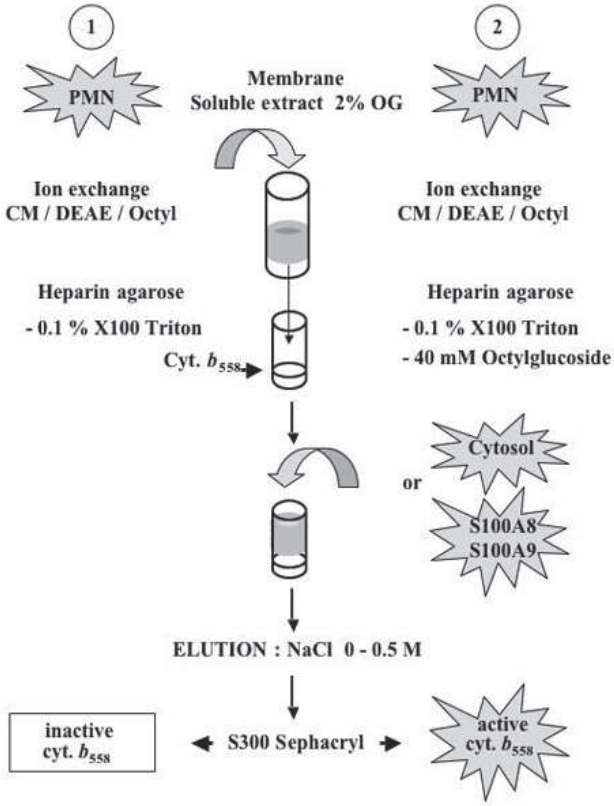

Fig. (3). Procedure for isolating cytochrome b_{558} alone or the whole NADPH oxidase complex [34].

Cytochrome b_{558} and whole NADPH oxidase complexes were prepared from activated cells [15, 34]. PMN purified from human buffy coats were stimulated 10 min at 37 °C with 0.8 µM PMA in the presence of 5 µM cytochalasin B in PBS supplemented with 0.9 mM $CaCl_2$, 0.5 mM $MgCl_2$. After cell sonication and ultracentrifugation at 200,000 × g for 1h at 4°C, membranes were collected [13] and solubilized in presence of 2% (w/v) n-octylglucoside for 20 min at 4°C. The membrane soluble extract was loaded on an ion exchange column prepared with a mixture (1v/1v/1v) CM-Sepharose, DEAE-Sepharose and N-amino-octyl-Sepharose and equilibrated with the purification buffer (100 mM HEPES pH 7.2, 100 mM KCl, 10 mM NaCl, 1 mM EDTA, 0.1 mM DTT, 20% (v/v) glycerol) containing 0.1% (v/v) Triton X100. The flow through containing cytochrome b_{558} was directly applied to a Heparin agarose matrix where cytochrome b_{558} bound. At this stage, Triton X100 was replaced by 40 mM n-octyl-glucoside in the purification buffer for complex isolation (panel 2). After an extensive washing of the column, cytosol from stimulated PMN (25 mg) or a mixture of recombinant S100A8 and S100A9 preloaded with 500 nM Ca^{2+} was applied to the matrix [34]. For cytochrome b_{558} purification (panel 1), the buffer was unchanged. Cytochrome b_{558} alone (panel 1) or the whole oxidase complex (panel 2) was eluted from the heparin agarose matrix by a NaCl gradient 0-0.5 M. Cytochrome b_{558}-containing fractions were pooled and purified on gel filtration (Sephacryl S300). The presence of cytochrome b_{558} was detected by measuring the "reduced minus oxidized" differential spectrum. Isolated oxidase complexes displayed a constitutive oxidase activity while purified cytochrome b_{558} did not.

NADPH oxidase complex assembles onto the matrix; cytochrome b_{558} becomes active and able to transfer electrons in

the absence of AA that is normaly required in cell-free assay to reconstitute high level of active NADPH oxidase. In the isolated phox complex, the level of constitutive NADPH oxidase activity depends on the source of cytosol that is used for incubation: it is maximum with neutrophil cytosol (120 s^{-1}) or intermediate (50 s^{-1}) with that of B lymphocytes as shown on Fig. (**4A**) and Fig. (**4B**); AA alone has no effect, but a combination of S100A8/S100A9 with the phospholipid, restores a total oxidase activity (Fig (**4B**)). Moreover, there is no oxidase activity of the purified fraction when cytosol of EBV-B lymphocytes originates from p47-phox deficient patients (Fig. (**4A**) and (**4B**)).

Finally, a mixture of rS100A8 and rS100A9 preloaded with calcium and added on the matrix instead of cytosol, was shown to induce a direct activation of cytochrome b_{558}. The resulting cytochrome b_{558}/S100A8/S100A9 complex was able to transfer electrons at a rate significantly higher than that of cytochrome b_{558} alone: oxidase turnover is low but significant (Fig (**4C**)). These observations that heparin-bound cytochrome b_{558} can be partially activated by recombinant S100A8/S100A9 in the absence of cytosolic factors and AA, confirm a direct interaction of S100 proteins with cytochrome b_{558}.

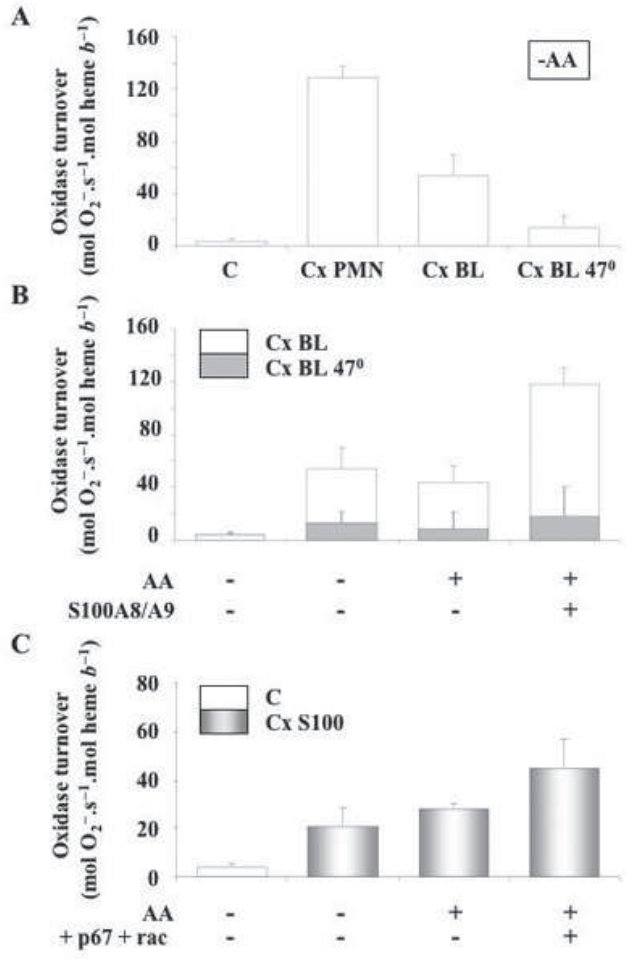

Fig. (4). Constitutive NADPH oxidase activity of isolated oxidase complexes: effect of S100A8 and S100A9 [34].

The constitutive NADPH oxidase activity was measured after mixing purified oxidase complex (0.2 pmol cytochrome b_{558}/assay) with 10 μM FAD, 40 μM GTPγS, and 5 mM $MgCl_2$ in a final volume of 100 μl PBS and adding 150 μM NADPH (final concentrations). NADPH oxidase activity was estimated by measuring the superoxide dismutase-sensitive cytochrome *c* reduction at 550 nm ($\varepsilon_{550\ nm}$=21.1 $mM^{-1}.cm^{-1}$) and expressed as turnover, mol $O_2^{\cdot-}$. s^{-1}. mol heme b^{-1}. **A- Constitutive oxidase activity of various "phox"complexes.** Constitutive oxidase activity was measured in complexes prepared with cytosol from neutrophils (Cx PMN), control EBV-B lymphocytes (Cx BL) or p47-phox –deficient EBV-B cells (Cx BL 47^0) or in absence of cytosol (C). **B- Enhancement of the NADPH oxidase activity of EBV-B lymphocyte complex by S100A8/S100A9.** S100A8/A9 (0.78 μg) purified from PMN cytosol and preincubated with 500 nM Ca^{2+} [9] was added to the control B lymphocyte complex (Cx BL –open bars) (0.2 pmol) or to the p47-phox-deficient complex (Cx BL 47^0-grey bars). Oxidase activity was measured in presence of AA (1 mM). **C- Constitutive activity of the Cx S100: effect of p67-phox and Rac on this activity.** The constitutive activity of the oxidase complex prepared by loading Ca^{2+}-loaded recombinant S100A8/S100A9 (120 nmol each) (Cx S100) instead of cytosol onto the heparin column was measured. A significant constitutive turnover was detected in absence of stimulus as compared to the cytochrome b_{558} activity (C). Recombinant p67-phox (33 nM) and Rac (100 nM) were added to the Cx S100 and the oxidase activity was then measured in presence of AA (1 mM).

CONCLUSION

The data presented in Table **1** summarize essential properties of S100A8 and S100A9 myeloid-related proteins in their specific interface with NADPH oxidase of phagocytes.

In neutrophils, after inflammatory stimuli, the elevated concentration of calcium initiates a reaction cascade beginning in cytosol with phosphorylation of oxidase cytosolic factors, mainly p47-phox but also p67-phox, p40-phox and S100A9. S100 proteins associate in a calcium-dependent non-covalent oligomeric S100A8/S100A9 structure (heterodimer or tetramer) and translocate with p67-phox to plasma membrane. At the membrane level, AA released *in situ* from phospholipase A2 activity and (or) cotransported with cytosolic factors, induces the assembly of NADPH oxidase complex on cytochrome b_{558}. In this biological assembly, gp91-phox/Nox2 stabilized by p22-phox catalyzes NADPH oxidase activity: the change in cytochrome b_{558} conformation due to molecular interaction(s) with p67-phox initiates the electron transfer. The presence of other factors is essential *in vivo* as they are regulatory effectors or adaptors as p47-phox that may position p67-phox on cytochrome b_{558} in order to give an optimum binding and oxidase activity. S100A8 and S100A9 calcium binding proteins are introduced as limitant molecules and new positive effectors of oxidase regulation.

The specificity of S100A8/S100A9 interaction with cytochrome b_{558} and that of p67-phox point out the existence of different consensus sites on the hemoprotein. Both S100A8/S100A9 and p67-phox are required to give a fully active cytochrome b_{558} conformation as shown in neutrophils and contrary to EBV-B lymphocytes that do not contain

Table 1. S100A8/S100A9 Potentiates NADPH Oxidase Activity of Phagocytes

NADPH oxidase activity *: in vivo* and *ex vivo*	**Ref**
$S100A9^{-/-}$ mice: no expression of S100A8, decrease in NADPH oxidase activity	[28]
Invalidation of S100A9 gene in NB4 differentiated cells: decrease in NADPH oxidase activity	[28]
S100A8/A9 gene transfection in EBV-B lymphocytes: increase in NADPH oxidase activity	[9]
Translocation of cytosolic activating factors and assembly	
Requirement of S100A9 for S100A8 effect	[7, 9, 28]
Phosphorylation of S100A9 upon PMN stimulation	[35, 36]
Association of S100A8/S100A9 with oxidase cytosolic factors	[8, 9]
Interaction S100A8/p67-phox for translocation	[7, 28]
NADPH oxidase activation : regulation *in vitro*	
Ca^{2+} involvement for S100A8/S100A9 action on NADPH oxidase activation	[7, 9, 28]
Increase in the affinity of p67-phox for cytochrome b_{558} by S100A8/S100A9	[9]
Specific interaction of S100A8/ S100A9 with cytochrome b_{558}	[9, 34]
S100A8/S100A9: mediator of cytochrome b_{558} conformation change correlated to activation	[9, 34]
S100A8/S100A9: allosteric effector	[9, 34]

S100 proteins (Fig. (**5**)). Identification of consensus sites is a subject of further investigation. A molecular mechanism is suggested *in vitro* in a cell free assay, by atomic force microscopy or upon the direct activation of cytochrome b_{558} by S100 proteins. It favors the idea that S100A8 and S100A9 proteins potentiate oxidase activation by mediating enhancement of p67-phox affinity for cytochrome b_{558} in synergy, *in vivo*, with p47-phox, p40-phox and Rac1/2. The effects of S100A8/S100A9 favor an allosteric regulation of NADPH oxidase activity. Respective function of S100A8 and S100A9 has to be determined; while S100A8 is strategic, efficiency of NADPH oxidase regulation depends on the presence of both S100A8 and S100A9 proteins.

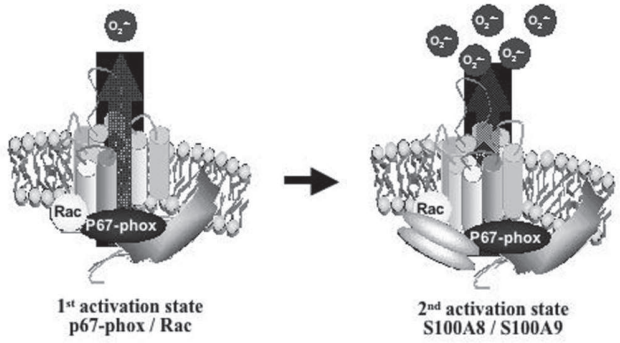

Fig. (5). Identification of two cytochrome b_{558} activation states.
The study of isolated "phox" complex suggests at least two activation states for cytochrome b_{558}: the first one is dependent on the interaction of p67-phox and Rac1/2 with cytochrome b_{558} leading to a first conformation change. This is correlated to a partial activation of cytochrome b_{558} and to an intermediate superoxide anion production (left panel). A second activation state is obtained in presence of S100A8/S100A9 in neutrophils leading to a fully active cytochrome b_{558} and to a maximum NADPH oxidase turnover (right panel).

ACKNOWLEDGEMENTS

The authors thank Anna Reinicke for linguistic corrections of the manuscript. This work was supported by grants from the « ministère de l'Enseignement Supérieur de la Recherche et Technologie, Paris », the « UFR de Médecine, Université Joseph Fourier, Grenoble », the « Région Rhône-Alpes, programme Emergence 2003 », the «Association Nationale de Défense contre L'Arthrite Rhumatoïde», the «Groupement des Entreprises Françaises dans la lutte contre le Cancer, délégation de Grenoble », the « Société Française de Rhumatologie » and the « Délégation Régionale de la Recherche Clinique, CHU Grenoble ».

ABBREVIATIONS

AA	=	Arachidonic Acid
CGD	=	Chronic Granulomatous Disease
DTT	=	Dithiothreitol
EBV	=	Epstein-Barr-virus
EDTA		Ethylene Diamine Tetraacetic Acid
FAD	=	Flavin Adenine Dinucleotide
GTP	=	Guanosine triphosphate
MALDI TOF	=	Matrix Assisted Laser Desorption/Ionization-Time Of Flight
MRP14	=	Myeloid-Related Protein 14 (S100A9)
MRP8	=	Myeloid-Related Protein 8 (S100A8)
NADPH		Nicotinamide Adenine Dinucleotide Phosphate
Nox	=	NADPH oxidase
$O_2^{\cdot-}$	=	Superoxide anion
PBS	=	Phosphate Buffer Saline
PMA	=	Phorbol 12-myristate 13-acetate
PMN	=	PolyMorphonuclear Neutrophils
ROS	=	Reactive Oxygen Species
RLU	=	Relative Luminescence Unit

REFERENCES

[1] Ehrchen, J. M.; Sunderkotter, C.; Foell, D.; Vogl, T.; Roth, J. The endogenous Toll-like receptor 4 agonist S100A8/S100A9 (calprotectin) as innate amplifier of infection, autoimmunity, and cancer. *J. Leukoc. Biol.,* **2009,** *86*, 557-566.

[2] Morel, F. [Molecular aspects of chronic granulomatous disease. "the NADPH oxidase complex". *Bull. Acad. Natl. Med.,* **2007,** *191*, 377-392.

[3] Nacken, W.; Roth, J.; Sorg, C.; Kerkhoff, C. S100A9/S100A8: Myeloid representatives of the S100 protein family as prominent players in innate immunity. *Microsc. Res. Tech.,* **2003,** *60*, 569-580.

[4] Gebhardt, C.; Nemeth, J.; Angel, P.; Hess, J. S100A8 and S100A9 in inflammation and cancer. *Biochem. Pharmacol.,* **2006,** *72*, 1622-1631.

[5] Foell, D.; Wittkowski, H.; Vogl, T.; Roth, J. S100 proteins expressed in phagocytes: a novel group of damage-associated molecular pattern molecules. *J. Leukoc. Biol.,* **2007,** *81*, 28-37.

[6] Benedyk, M.; Sopalla, C.; Nacken, W.; Bode, G.; Melkonyan, H.; Banfi, B.; Kerkhoff, C. HaCaT keratinocytes overexpressing the S100 proteins S100A8 and S100A9 show increased NADPH oxidase and NF-kappaB activities. *J. Invest. Dermatol.,* **2007,** *127*, 2001-2011.

[7] Bouzidi, F.; Doussiere, J. Binding of arachidonic acid to myeloid-related proteins (S100A8/A9) enhances phagocytic NADPH oxidase activation. *Biochem. Biophys. Res. Commun.,* **2004,** *325*, 1060-1065.

[8] Doussiere, J.; Bouzidi, F.; Vignais, P. V. The S100A8/A9 protein as a partner for the cytosolic factors of NADPH oxidase activation in neutrophils. *Eur. J. Biochem.,* **2002,** *269*, 3246-3255.

[9] Berthier, S.; Paclet, M. H.; Lerouge, S.; Roux, F.; Vergnaud, S.; Coleman, A. W.; Morel, F. Changing the conformation state of cytochrome b558 initiates NADPH oxidase activation: MRP8/MRP14 regulation. *J. Biol. Chem.,* **2003,** *278*, 25499-25508.

[10] Vogl, T.; Tenbrock, K.; Ludwig, S.; Leukert, N.; Ehrhardt, C.; van Zoelen, M. A.; Nacken, W.; Foell, D.; van der Poll, T.; Sorg, C.; Roth, J. Mrp8 and Mrp14 are endogenous activators of Toll-like receptor 4, promoting lethal, endotoxin-induced shock. *Nat. Med.,* **2007,** *13*, 1042-1049.

[11] Bedard, K.; Lardy, B.; Krause, K. H. NOX family NADPH oxidases: not just in mammals. *Biochimie,* **2007,** *89*, 1107-1112.

[12] Bedard, K.; Krause, K. H. The NOX family of ROS-generating NADPH oxidases: physiology and pathophysiology. *Physiol. Rev.,* **2007,** *87*, 245-313.

[13] Batot, G.; Paclet, M. H.; Doussiere, J.; Vergnaud, S.; Martel, C.; Vignais, P. V.; Morel, F. Biochemical and immunochemical properties of B lymphocyte cytochrome b558. *Biochim. Biophys. Acta,* **1998,** *1406*, 188-202.

[14] Paclet, M. H.; Coleman, A. W.; Burritt, J.; Morel, F. NADPH oxidase of Epstein-Barr-virus immortalized B lymphocytes. Effect of cytochrome b(558) glycosylation. *Eur. J. Biochem.,* **2001,** *268*, 5197-5208.

[15] Paclet, M. H.; Coleman, A. W.; Vergnaud, S.; Morel, F. P67-phox-mediated NADPH oxidase assembly: imaging of cytochrome b558 liposomes by atomic force microscopy. *Biochemistry,* **2000,** *39*, 9302-9310.

[16] Roth, J.; Vogl, T.; Sorg, C.; Sunderkotter, C. Phagocyte-specific S100 proteins: a novel group of proinflammatory molecules. *Trends Immunol.,* **2003,** *24*, 155-158.

[17] Kerkhoff, C.; Hofmann, H. A.; Vormoor, J.; Melkonyan, H.; Roth, J.; Sorg, C.; Klempt, M. Binding of two nuclear complexes to a novel regulatory element within the human S100A9 promoter drives the S100A9 gene expression. *J. Biol. Chem.,* **2002,** *277*, 41879-4187.

[18] Sopalla, C.; Leukert, N.; Sorg, C.; Kerkhoff, C. Evidence for the involvement of the unique C-tail of S100A9 in the binding of arachidonic acid to the heterocomplex S100A8/A9. *Biol. Chem.,* **2002,** *383*, 1895-1905.

[19] Korndorfer, I. P.; Brueckner, F.; Skerra, A. The crystal structure of the human (S100A8/S100A9)2 heterotetramer, calprotectin, illustrates how conformational changes of interacting alpha-helices can determine specific association of two EF-hand proteins. *J. Mol. Biol.,* **2007,** *370*, 887-898.

[20] Leukert, N.; Vogl, T.; Strupat, K.; Reichelt, R.; Sorg, C.; Roth, J. Calcium-dependent tetramer formation of S100A8 and S100A9 is essential for biological activity. *J. Mol. Biol.,* **2006,** *359*, 961-972.

[21] Morel, F.; Dewald, B.; Berthier, S.; Zaoui, P.; Dianoux, A. C.; Vignais, P. V.; Baggiolini, M. Further characterization of the gelatinase-containing particles of human neutrophils. *Biochim. Biophys. Acta,* **1994,** *1201*, 373-380.

[22] Stroncek, D. F.; Shankar, R. A.; Skubitz, K. M. The subcellular distribution of myeloid-related protein 8 (MRP8) and MRP14 in human neutrophils. *J. Transl. Med.,* **2005,** *3*, 36.

[23] Baillet, A.; Trocmé, C.; Berthier, S.; Arlotto, M.; Grange, L.; Quétant, S.; Sève, M.; Berger, F.; Juvin, R.; Morel, F.; Gaudin, P. Synovial fluid proteomic fingerprint: S100A8, S100A9 and S100A12 proteins discriminate rheumatoid arthritis from other inflammatory joint diseases. *Rheumatology (Oxford),* **2009,** *[under revision].*

[24] Passey, R. J.; Xu, K.; Hume, D. A.; Geczy, C. L. S100A8: emerging functions and regulation. *J. Leukoc. Biol.,* **1999,** *66*, 549-556.

[25] Vandal, K.; Rouleau, P.; Boivin, A.; Ryckman, C.; Talbot, M.; Tessier, P. A. Blockade of S100A8 and S100A9 suppresses neutrophil migration in response to lipopolysaccharide. *J. Immunol.,* **2003,** *171*, 2602-2609.

[26] Hiratsuka, S.; Watanabe, A.; Aburatani, H.; Maru, Y. Tumour-mediated upregulation of chemoattractants and recruitment of myeloid cells predetermines lung metastasis. *Nat. Cell. Biol.,* **2006,** *8*, 1369-1375.

[27] Tugizov, S.; Berline, J.; Herrera, R.; Penaranda, M. E.; Nakagawa, M.; Palefsky, J. Inhibition of human papillomavirus type 16 E7 phosphorylation by the S100 MRP-8/14 protein complex. *J. Virol.,* **2005,** *79*, 1099-1112.

[28] Kerkhoff, C.; Nacken, W.; Benedyk, M.; Dagher, M. C.; Sopalla, C.; Doussiere, J. The arachidonic acid-binding protein S100A8/A9 promotes NADPH oxidase activation by interaction with p67phox and Rac-2. *Faseb J.,* **2005,** *19*, 467-469.

[29] Foubert, T. R.; Burritt, J. B.; Taylor, R. M.; Jesaitis, A. J. Structural changes are induced in human neutrophil cytochrome b by NADPH oxidase activators, LDS, SDS, and arachidonate: intermolecular resonance energy transfer between trisulfopyrenyl-wheat germ agglutinin and cytochrome b(558). *Biochim. Biophys. Acta,* **2002,** *1567*, 221-231.

[30] Doussiere, J.; Gaillard, J.; Vignais, P. V. Electron transfer across the O2- generating flavocytochrome b of neutrophils: evidence for a transition from a low-spin state to a high-spin state of the heme iron component. *Biochemistry,* **1996,** *35*, 13400-13410.

[31] Doussiere, J.; Bouzidi, F.; Poinas, A.; Gaillard, J.; Vignais, P. V. Kinetic study of the activation of the neutrophil NADPH oxidase by arachidonic acid. Antagonistic effects of arachidonic acid and phenylarsine oxide. *Biochemistry,* **1999,** *38*, 16394-16406.

[32] Dana, R.; Leto, T. L.; Malech, H. L.; Levy, R. Essential requirement of cytosolic phospholipase A2 for activation of the phagocyte NADPH oxidase. *J. Biol. Chem.,* **1998,** *273*, 441-445.

[33] Brash, A. R. Arachidonic acid as a bioactive molecule. *J. Clin. Invest.,* **2001,** *107*, 1339-1345.

[34] Paclet, M. H.; Berthier, S.; Kuhn, L.; Garin, J.; Morel, F. Regulation of phagocyte NADPH oxidase activity: identification of two cytochrome b558 activation states. *Faseb J.,* **2007,** *21*, 1244-1255.

[35] van den Bos, C.; Roth, J.; Koch, H. G.; Hartmann, M.; Sorg, C. Phosphorylation of MRP14, an S100 protein expressed during monocytic differentiation, modulates Ca(2+)-dependent translocation from cytoplasm to membranes and cytoskeleton. *J. Immunol.,* **1996,** *156*, 1247-1254.

[36] Guignard, F.; Mauel, J.; Markert, M. Phosphorylation of myeloid-related proteins MRP-14 and MRP-8 during human neutrophil activation. *Eur. J. Biochem.,* **1996,** *241*, 265-271.

Received: ?????????????? **Revised:** ?????????????? **Accepted:** ??????????????

Annexe 3

Analyse protéomique en rhumatologie : implication dans la prise en charge des rhumatismes inflammatoires

Revue du Rhumatisme 78 (2011) S187-S190

Analyse protéomique en rhumatologie : implication dans la prise en charge des rhumatismes inflammatoires

Athan Baillet[1,3*], Candice Trocmé[2], Philippe Gaudin[1,3]

[1] *Clinique de rhumatologie, pôle locomotion rééducation et physiologie, CHU Grenoble, hôpital Sud, Avenue de Kimberley, BP 338,38434 Echirolles, France*
[2] *Laboratoire de biochimie des enzymes et des protéines, institut de biologie et pathologie, CHU Albert Michallon, BP 217, 38043 Grenoble cedex 9, France*
[3] *GREPI FRE3405 – AGIM – CNRS, Université Joseph Fourier, EPHE, CHU Albert Michallon, BP 217, 38043 Grenoble cedex 9, France*

Mots clés :
Biomarqueurs
Analyse protéomique
Polyarthrite rhumatoïde
SELDI-TOF
Protéines S100

RÉSUMÉ

La mise sur le marché de nouvelles thérapeutiques dans le traitement des rhumatismes inflammatoires chroniques, dont il est difficile à priori de prédire l'efficacité à l'échelon individuel, illustre parfaitement le besoin de développer une médecine personnalisée pour offrir une prise en charge adaptée à chaque patient. Des techniques d'analyse du protéome de plus en plus discriminantes permettent d'isoler les profils protéiques spécifiques de pathologies, de prédire l'évolution de certains rhumatismes inflammatoires ainsi que leurs réponses aux traitements. Les études protéomiques ont permis de caractériser des biomarqueurs qui seront probablement utiles aux cliniciens prenant en charge les rhumatismes inflammatoires comme aux chercheurs examinant les mécanismes physiopathologiques en œuvre dans ces pathologies. Cependant des essais incluant un plus grand nombre de patients sont nécessaires pour valider des biomarqueurs d'intérêt avant de les utiliser en pratique courante.

1. Introduction

Le protéome est l'ensemble des protéines produites par un génome particulier et exprimées par des cellules, tissus ou organes à un moment donné, avec un historique donné, dans un environnement et des conditions donnés. Ainsi, le protéome peut être assimilé à une empreinte d'une condition particulière pathologique ou non. L'analyse protéomique consiste à caractériser, quantifier, identifier toutes les protéines présentes dans un milieu biologique. Les informations données par l'analyse du génome et du transcriptome et par l'analyse du protéome ne sont pas nécessairement redondantes. Ce sont, au contraire, des outils complémentaires pour la prise en charge des patients.

C'est en cancérologie que la recherche de biomarqueurs par analyse protéomique a initialement été conduite. De nombreux biomarqueurs ont ainsi été mis en évidence dans le cadre du cancer de l'ovaire [1], du cancer colorectal [2], du lymphome non Hodgkinien [3]. Ces nouveaux biomarqueurs, découverts par des approches de plus en plus efficaces, avaient un intérêt supérieur aux marqueurs classiquement utilisés [1,4].

Depuis quelques années la recherche de biomarqueurs a fait l'objet d'un nombre grandissant d'études dans le champ de la rhumatologie, particulièrement dans le cadre des rhumatismes inflammatoires. Plusieurs étapes sont nécessaires entre la découverte d'un potentiel biomarqueur et son utilisation en pratique courante. Après avoir détecté une protéine d'intérêt au moyen d'une technique permettant le criblage de l'ensemble du protéome d'un milieu biologique, les résultats doivent être confirmés dans une cohorte indépendante comprenant un nombre important de patients [5] en utilisant volontiers une approche protéomique plus ciblée. Il faut ensuite procéder au développement du test diagnostique au moyen d'une méthode permettant son utilisation et sa commercialisation pour une utilisation clinique.

* Auteur correspondant.
Adresse e-mail : ABaillet@chu-grenoble.fr (A. Baillet).

2. Analyse protéomique des rhumatismes inflammatoires

La comparaison de l'empreinte protéomique de liquide biologique est une formidable opportunité pour caractériser de nouveaux biomarqueurs utiles au diagnostic de rhumatismes inflammatoires, à l'évaluation du pronostic ou de la réponse au traitement. Ainsi on peut identifier une protéine prédictive de telle ou telle pathologie, ou spécifiquement exprimée chez des patients avec un mauvais pronostic ou une faible probabilité de réponse au traitement.

2.1. Intérêt de l'analyse protéomique dans le diagnostic de rhumatisme inflammatoire

L'intérêt d'un traitement précoce de patients souffrant de polyarthrite rhumatoïde (PR) n'est plus à démontrer [6]. De nombreux efforts doivent donc être portés pour mettre au point de nouveaux outils le permettant. L'outil protéomique est extrêmement intéressant car il parvient à déceler des protéines spécifiquement exprimées dans une condition pathologique dans différents milieux biologiques.

2.1.1. Étude protéomique du sérum

Après avoir montré par chromatographie 2D, que la protéine S100A9 est surexprimée dans le liquide synovial de Drynda et al. ont caractérisé la surexpression de l'hétéro-complexe S100A8/S100A9 dans le plasma de 23 PR [7]. L'étude par chromatographie liquide HPLC (*high-performance liquid chromatography*) du plasma d'un nombre plus restreint de patients souffrant de PR a confirmé la possibilité d'utiliser les protéines de la famille S100 comme biomarqueurs diagnostiques de PR [8]. La technique SELDI-TOF (*Surface-enhanced laser desorption/ionization - time of flight*), plus adaptée à l'analyse d'un nombre important de patients, suggère que la protéine S100A8 offre une sensibilité de que 75 % pour une spécificité de 85 % pour le diagnostic de PR [9]. Dans une autre étude, Liu et al. montrent qu'un algorithme combinant 4 biomarqueurs détectés par cette même technique offre une sensibilité de 90 % et une spécificité de 92 % pour le diagnostique de PR [10]. Cependant les auteurs se sont contentés de caractériser les biomarqueurs par leurs masses moléculaires sans aller jusqu'à l'identification par séquençage du biomarqueur.

2.1.2. Étude protéomique du liquide synovial et de la salive

Le sang circulant offre l'avantage d'être facilement accessible pour l'ensemble des patients. Cependant l'analyse du protéome d'autres liquides biologiques permet de s'affranchir de certains problèmes techniques liés aux protéines majoritaires ou à la dilution des protéines d'intérêts dans le sérum (Fig. 1). Certains milieux biologiques peuvent présenter l'intérêt de porter l'empreinte de la réaction inflammatoire. Par exemple, le liquide synovial reflète de manière plus fine la synovite rhumatoïde tout comme la salive l'atteinte des glandes salivaires du syndrome de Gougerot-Sjögren (GS).

Une étude a comparé le protéome du liquide synovial de PR à celui d'arthrose et d'arthrite non rhumatoïde [11]. Parmi les 74 pics protéiques du liquide synovial dont l'intensité est statistiquement différente entre le groupe PR et arthrose et les 27 pics dont le signal diffère dans le liquide synovial de PR et de synovite non rhumatoïde, les trois biomarqueurs les plus surexprimés dans le groupe PR sont les protéines S100A8, S100A12 et S100A9. La protéine S100A8, dont expression est dix à quinze fois plus importante dans le liquide synovial de PR, offre une sensibilité de 91 % et une spécificité de 75 % pour le diagnostique de PR devant une arthrite inflammatoire.

Le syndrome de GS, fréquemment associé à la PR, peut parfois poser des problèmes diagnostiques. Des études protéomiques de la salive de patients souffrant de cette pathologie ont révélé la surexpression de β_2-microglobuline et d'IgGκ [12,13]. Cependant certaines protéines salivaires, comme l'amylase, sont surexprimées dans une étude [12] mais sous-exprimées dans une autre étude [13]. Ces résultats discordants peuvent s'expliquer par des différences entre les 2 essais en termes de caractéristiques démographiques et de durée d'évolution de la maladie.

2.2. Intérêt de l'analyse protéomique dans le pronostic du rhumatisme inflammatoire

L'évolution structurale, prédictive du handicap à moyen et long terme [14], est un critère d'évaluation primordial de la PR. Malheureusement les performances de l'imagerie demeurent imparfaites [15]. La présence d'auto-anticorps et d'un syndrome inflammatoire important sont notoirement corrélés à une évolution péjorative sur le plan structural [16]. L'analyse protéomique du liquide synovial de 15 PR érosives, 15 PR non érosives et 15 patients sains a suggéré que 6 protéines de la famille S100 dont S100A8, S100A9 et S100A12 étaient présents chez les patients avec des destructions articulaires [17]. Une étude transversale a pu valider ces résultats dans une plus grande cohorte de 145 patients [18] au moyen d'un dosage ELISA. De manière encore plus intéressante, une étude prospective incluant 124 PR [19] souligne que le dosage initial de certains de ces biomarqueurs est prédictif de l'évolution structurale à 10 ans.

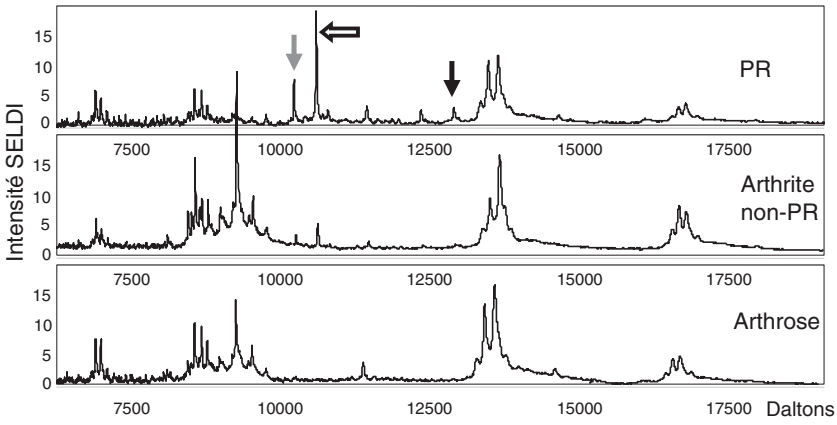

Figure 1. Protéome du liquide synovial de patient souffrant de polyarthrite rhumatoïde (PR), d'arthrite non rhumatoïde et d'arthrose par technique SELDI-TOF. Les protéines S100A8 (flèche blanche), S100A9 (flèche noire) et S100A12 (flèche grise) sont surexprimées dans le liquide synovial de PR.

2.3. Intérêt de l'analyse protéomique dans la réponse au traitement par anti-TNFα

L'analyse du protéome peut être appréhendée de plusieurs manières différentes dans le contexte de l'évaluation de la réponse au traitement. Certaines études comparent le protéome avant et après le début d'un traitement afin d'analyser les variations spécifiques de réponse ou de non-réponse thérapeutique. D'autres équipes adoptent une autre approche qui consiste à déterminer des facteurs prédictifs de réponse avant le début du traitement chez des patients suivis de manière prospective.

Drynda et al. [7] ont analysé le plasma de 40 PR traitées par étanercept (2 × 25 mg/semaine). Une association entre l'efficacité à 3 mois de l'étanercept et la diminution des protéines S100A8/S100A9 était constatée chez les patients répondeurs DAS28. Une étude récente a montré, à partir du sérum de seulement 10 PR traitées par infliximab avec une bonne réponse EULAR, la présence de 30 protéines dont l'expression était modifiée après 12 semaines. Une diminution significative chez les répondeurs de CRP, C3, C5, C1inh, ApoA1, Serpines, S100A8 a été notée.

Le profil cytokinique sérique peut également nous apporter des renseignements intéressant. La concentration de 12 cytokines, IL-1α, IL-1β, IL-6, IL-2, IL-8, IL-4, IL-10, TNFα, INFγ, MCP-1 (*monocyte chemoattractant protein-1*), EGF (*epithelial growth factor*), VEGF (*vascular endothelial growth factor*) a été dosée chez 33 PR au début puis après 3 mois d'un traitement par etanercept (25 mg × 2/semaine), date à laquelle il existait 24 répondeurs et 9 non-répondeurs. Un taux initial élevé de MCP-1, EGF et CRP était associé à une bonne réponse thérapeutique avec une sensibilité de 87 % et une spécificité de 75 % [14]. La même équipe a conduit une étude chez 46 patients traités par rituximab (1000 mg J1-J14). Les répondeurs avaient une concentration de MCP-1 et d'EGF supérieure à trois mois par rapport aux non répondeurs, mais aucune cytokine ne permettait initialement de discriminer les répondeurs des non répondeurs [20].

Trocmé et al. [21] ont analysé par technique SELDI-TOF le plasma de 60 patients souffrant de PR juste avant le traitement par infliximab. Après 30 semaines, 28 patients étaient non répondeurs (ACR20 négatifs) alors que 32 patients avaient une bonne réponse à l'infliximab (ACR70 positifs). Les protéines apolipoprotéine A1 (Apo-A1) et *Platelet Factor 4* (PF4) étaient surexprimées respectivement dans le groupe avec une bonne et mauvaise réponse. De plus l'analyse combinée de 5 marqueurs protéiques dont PF4 et Apo-A1 a permis de différencier les patients répondeurs et non répondeurs avec une sensibilité et une spécificité de plus de 97 %.

3. Conclusion

L'analyse du profil protéique permet d'isoler des marqueurs pouvant améliorer le diagnostic, déterminer le pronostic et orienter le traitement des patients atteints de PR. Des techniques extrêmement sensibles sont récemment apparues permettant de conduire des études avec un nombre limité de patients. Il est néanmoins indispensable de confirmer ces résultats dans des cohortes plus importantes [5]. Cette étape réduit beaucoup le nombre de biomarqueurs d'intérêt qui doivent ensuite être soumis au filtre OMERACT [22]. L'analyse protéomique dépasse le cadre de la polyarthrite rhumatoïde pour intéresser d'autres rhumatismes inflammatoires tels que les rhumatismes idiopathiques juvéniles [23] ou la spondylarthrite [24] mais également des pathologies cartilagineuses fréquentes telles que l'arthrose [25-27] ou moins connues comme la maladie de Kashin-Beck [28]. Cette approche a également concerné la mise en évidence de biomarqueurs dans l'ostéoporose tant au niveau du modèle murin [29] que chez la femme ménopausée [30]. Le tableau 1 résume les différents marqueurs protéiques identifiés par technique protéomique dans diverses pathologies rhumatismales [31].

Tableau 1
Différents marqueurs protéiques identifiés par technique protéomique dans diverses pathologies rhumatismales (d'après [31]).

Pathologie	Échantillon	Biomarqueurs confirmés
Polyarthrite rhumatoïde	sérum	AAT, CRP, SAA, protéines S100A8/A9
	plasma	Apolipoprotéine, COLT1, SAA, PF4
	liquide ou membrane synoviale	Aldolase A, annexine, protéines S100A8/A9, cathepsine D, CRP, ENOA, Ig k-chain, MnSOD, NGAL, PRDX2, PRDX4, SOD2, TPI, TXNDC5
	salive	6-PGDH, protéines 14-3-3, apolipoprotéine A, protéines S100A8/A9, E-FABP, GRP78/BiP, PRDX5
Arthrose	membrane synoviale, cartilage ou chondrocytes en culture	ANNX-1, COLL-I and VI, Hsp 27, HtrA1, ROS, SOD2, TRAP1, vimentine
Spondylarthrite	sérum	Précurseur de l'haptoglobine
	leucocytes	SOD
Lupus	urine	Hepcidine-20 et -25, PGD2, rénine, SAP, SOD
Gougerot-Sjögren	salive	α-amylase, α-defensine, β-active, protéines S100A8/A9, anhydrase carbonique, précurseur de cystatine, kéraline
	glande salivaire	α-défensine, calmoduline

6-PGDH : 6-phosophogluconate dehydrogenase ; AAT : alpha 1-antitrypsin ; ANNX-1 : annexin-1 ; COLL-I : collagen type I ; COLT1, coactosin-like 1 ; CRP : C-reactive protein ; E-FABP : epidermal fatty-acid binding protein ; ENOA : alpha enolase ; GRP78/BiP : 78-kDa glucose-regulated protein precursor (also known as binding immunoglobulin protein) ; Ig k-chain : immunoglobulin kappa chain ; LEI ; MnSOD : manganese superoxide dismutase ; MRP8 : myloid-related protein 8 ; NGAL : neutrophil gelatinase-associated lipocalin ; PF4 : platelet factor 4 ; PRDX2 : peroxiredoxin-2 ; SAA : serum amyloid A ; SAP, SOD, :superoxide dismutase ; TPI : triose phosphate isomerase ; TRAP1 : tumor necrosis factor receptor-associated protein 1 ; TXNDC5 : thioredoxin domain-containing protein 5.

Remerciements

Les auteurs remercient la Société Française de Rhumatologie et la Délégation à la Recherche Clinique et à l'Innovation du CHU de Grenoble pour leurs soutiens financiers.

Déclarations d'intérêts

A. Baillet : interventions ponctuelles : activités de conseil (Abbott) ; conférences : invitations en qualité d'intervenant (Abbott, BMS, Roche) et en qualité d'auditeur (Abbott, Wyeth, Schering Plough).

C. Trocmé : essais cliniques : en qualité de co-investigateur, expérimentateur non principal, collaborateur à l'étude (BMS) ; conférences : invitations en qualité d'intervenant (Roche).

Ph. Gaudin : conférences : invitations en qualité d'intervenant (Roche).

Références

[1] Petricoin EF, Ardekani AM, Hitt BA, et al. Use of proteomic patterns in serum to identify ovarian cancer. Lancet 2002;359:572-7.
[2] Smith FM, Gallagher WM, Fox E, et al. Combination of SELDI-TOF-MS and data mining provides early-stage response prediction for rectal tumors undergoing multimodal neoadjuvant therapy. Ann Surg 2007;245:259-66.
[3] Zhang X, Wang B, Zhang XS, et al. Serum diagnosis of diffuse large B-cell lymphomas and further identification of response to therapy using SELDI-TOF-MS and tree analysis patterning. BMC Cancer 2007;7:235.
[4] Check E. Proteomics and cancer: running before we can walk? Nature 2004;429:496-7.
[5] Ruiz-Romero C, Blanco FJ. Proteomics role in the search for improved diagnosis, prognosis and treatment of osteoarthritis. Osteoarthritis Cartilage 2010;18:500-9.
[6] Finckh A, Liang MH, van Herckenrode CM, et al. Long-term impact of early treatment on radiographic progression in rheumatoid arthritis: a meta-analysis. Arthritis Rheum 2006;55:864-72.
[7] Drynda S, Ringel B, Kekow M, et al. Proteome analysis reveals disease-associated marker proteins to differentiate RA patients from other inflammatory joint diseases with the potential to monitor anti-TNFalpha therapy. Pathol Res Pract 2004;200:165-71.
[8] Zheng X, Wu SL, Hincapie M, et al. Study of the human plasma proteome of rheumatoid arthritis. J Chromatogr A 2009;1216:3538-45.
[9] de Seny D, Fillet M, Meuwis MA, et al. Discovery of new rheumatoid arthritis biomarkers using the surface-enhanced laser desorption/ionization time-of-flight mass spectrometry ProteinChip approach. Arthritis Rheum 2005;52:3801-12.
[10] Liu W, Li X, Ding F, et al. Using SELDI-TOF MS to identify serum biomarkers of rheumatoid arthritis. Scand J Rheumatol 2008;37:94-102.
[11] Baillet A, Trocme C, Berthier S, et al. Synovial fluid proteomic fingerprint: S100A8, S100A9 and S100A12 proteins discriminate rheumatoid arthritis from other inflammatory joint diseases. Rheumatology (Oxford) 2010;49:671-82.
[12] Hu S, Wang J, Meijer J, et al. Salivary proteomic and genomic biomarkers for primary Sjogren's syndrome. Arthritis Rheum 2007;56:3588-600.
[13] Ryu OH, Atkinson JC, Hoehn GT, et al. Identification of parotid salivary biomarkers in Sjogren's syndrome by surface-enhanced laser desorption/ionization time-of-flight mass spectrometry and two-dimensional difference gel electrophoresis. Rheumatology (Oxford) 2006;45:1077-86.
[14] Maillefert JF, Combe B, Goupille P, et al. The 5-yr HAQ-disability is related to the first year's changes in the narrowing, rather than erosion score in patients with recent-onset rheumatoid arthritis. Rheumatology (Oxford) 2004;43:79-84.
[15] Baillet A, Gaujoux-Viala C, Mouterde G, et al. Comparison of the efficacy of sonography, magnetic resonance imaging and conventional radiography for the detection of bone erosions in rheumatoid arthritis patients: a systematic review and meta-analysis. Rheumatology (Oxford) 2011;50:1137-47.
[16] Visser K, Goekoop-Ruiterman YP, de Vries-Bouwstra JK, et al. A matrix risk model for the prediction of rapid radiographic progression in patients with rheumatoid arthritis receiving different dynamic treatment strategies: post hoc analyses from the BeSt study. Ann Rheum Dis 2010;69:1333-7.
[17] Liao H, Wu J, Kuhn E, et al. Use of mass spectrometry to identify protein biomarkers of disease severity in the synovial fluid and serum of patients with rheumatoid arthritis. Arthritis Rheum 2004;50:3792-803.
[18] Hammer HB, Odegard S, Fagerhol MK, et al. Calprotectin (a major leucocyte protein) is strongly and independently correlated with joint inflammation and damage in rheumatoid arthritis. Ann Rheum Dis 2007;66:1093-7.
[19] Hammer HB, Odegard S, Syversen SW, et al. Calprotectin (a major S100 leucocyte protein) predicts 10-year radiographic progression in patients with rheumatoid arthritis. Ann Rheum Dis 2010;69:150-4.
[20] Fabre S, Guisset C, Tatem L, et al. Protein biochip array technology to monitor rituximab in rheumatoid arthritis. Clin Exp Immunol 2009;155:395-402.
[21] Trocme C, Marotte H, Baillet A, et al. Apolipoprotein A-I and platelet factor 4 are biomarkers for infliximab response in rheumatoid arthritis. Ann Rheum Dis 2009;68:1328-33.
[22] Maksymowych WP, Landewe R, Tak PP, et al. Reappraisal of OMERACT 8 draft validation criteria for a soluble biomarker reflecting structural damage endpoints in rheumatoid arthritis, psoriatic arthritis, and spondyloarthritis: the OMERACT 9 v2 criteria. J Rheumatol 2009;36:1785-91.
[23] Gibson DS, Blelock S, Curry J, et al. Comparative analysis of synovial fluid and plasma proteomes in juvenile arthritis--proteomic patterns of joint inflammation in early stage disease. J Proteomics 2009;72:656-76.
[24] Tilleman K, Van Beneden K, Dhondt A, et al. Chronically inflamed synovium from spondyloarthropathy and rheumatoid arthritis investigated by protein expression profiling followed by tandem mass spectrometry. Proteomics 2005;5:2247-57.
[25] Guo D, Tan W, Wang F, et al. Proteomic analysis of human articular cartilage: identification of differentially expressed proteins in knee osteoarthritis. Joint Bone Spine 2008;75:439-44.
[26] Wu J, Liu W, Bemis A, et al. Comparative proteomic characterization of articular cartilage tissue from normal donors and patients with osteoarthritis. Arthritis Rheum 2007;56:3675-84.
[27] Gobezie R, Kho A, Krastins B, et al. High abundance synovial fluid proteome: distinct profiles in health and osteoarthritis. Arthritis Res Ther 2007;9:R36.
[28] Wang S, Guo X, Tan WH, et al. Detection of serum proteomic changes and discovery of serum biomarkers for Kashin-Beck disease using surface-enhanced laser desorption ionization mass spectrometry (SELDI-TOF MS). J Bone Miner Metab 2008;26:385-93.
[29] Fan Y, Liu J, Wang S, et al. Functional proteome of bones in rats with osteoporosis following ovariectomy. Life Sci 2005;76:2893-901.
[30] Bhattacharyya S, Siegel ER, Achenbach SJ, et al. Serum biomarker profile associated with high bone turnover and BMD in postmenopausal women. J Bone Miner Res 2008;23:1106-17.
[31] Vanarsa K., Mohan C. Proteomics in rheumatology: the dawn of a new era. F1000 Medicine Reports 2010;2:1-5.